UNIVERSITÀ DEGLI STUDI DI PALERMO

Dottorato di Ricerca in Ingegneria Elettrica, Elettronica e
delle Telecomunicazioni, Matematica e Automatica.
INDIRIZZO: Matematica ed Automatica per l'innovazione scientifica e tecnologica.
Dipartimento di Energia, ingegneria dell'Informazione e modelli Matematici.
Settore Scientifico Disciplinare – MAT07

HEAT FLUX IN SUPERFLUID TRANSITION AND IN TURBULENT HELIUM COUNTERFLOW

IL DOTTORE
Lidia Saluto

IL COORDINATORE
Prof. Francesco Alonge

IL TUTOR
Prof.ssa Maria Stella Mongiovì

CICLO XXV
ANNO CONSEGUIMENTO TITOLO 2015

Contents

List of symbols

h	Planck's constant
m_4	mass of helium atom
^{3}He and ^{4}He	isotopes of helium atom
T	temperature
p	pressure
T_λ	critical temperature for phase transition of helium ($T_\lambda = 1.7\,\mathrm{K}$ for liquid ^{4}He)
He I	normal state of liquid ^{4}He (normal viscous fluid)
He II	superfluid state of liquid ^{4}He
$\mathbf{v}_n$	velocity of the normal component of He II in the two-fluid model
$\mathbf{v}_s$	velocity of the superfluid component of He II in the two-fluid model
ρ_n	density of the normal component of He II
ρ_s	density of the superfluid component of He II
$\rho = \rho_n + \rho_s$	total mass density of the fluid
$\mathbf{q}$	heat flux
s	specific entropy per unit mass
s_n	specific entropy of the normal component of He II
s_s	specific entropy of the superfluid component of He II
$S = \rho s$	entropy of the fluid
ψ	complex wave function describing the quantum coherent aspect of superfluid
f	order parameter that describes the transition between normal and superfluid state, defined by $f^2 = \rho m_4 \lvert\psi\rvert^2 = \rho\rho_s$
ϵ	specific internal energy per unit mass
$E = \rho\epsilon$	internal energy density per unit volume
$\mathbf{v}$	velocity of the fluid
L	vortex line length density (average length of vortex line per unit volume), having dimension (length)$^{-2}$, briefly called "vortex line density"
$\mathbf{J}^{\mathbf{v}} = (\mathbf{J}^{\mathbf{v}})_{ij}$	stress tensor
$\mathbf{J}^f$	flux of the order parameter

$\mathbf{J^q} = (\mathbf{J^q})_{ij}$	flux of the heat flux
$\mathbf{J}^S$	entropy flux density
$\mathbf{J}^L$	flux of the vortex line density
σ^f	production term in the equation for the order parameter
$\sigma^{\mathbf{q}}$	production term in the equation for the heat flux
σ^L	production term in the equation for the vortex line density
Λ^ρ	Lagrange multiplier related to the balance equation of the mass
$\mathbf{\Lambda^v}$	Lagrange multiplier related to the balance equation of the momentum
Λ^E	Lagrange multiplier related to the balance equation of the energy
Λ^f	Lagrange multiplier related to the equation for the order parameter f
$\mathbf{\Lambda^q}$	Lagrange multiplier related to the equation for the heat flux $\mathbf{q}$
Λ^L	Lagrange multiplier related to the equation for the vortex line density L
$\mathbf{U}$	unit tensor
μ or μ_ρ	mass chemical potential
μ_L	chemical potential of quantized vortex line
θ	generalized temperature
$G = E - TS$	free energy
w_2	second sound velocity
ζ	non negative coefficient linked to the second sound velocity by the relation $w_2^2 = \zeta/\rho c_V$
c_V	constant-volume specific heat
c_p	constant-pressure specific heat
τ, τ_0, τ_2	relaxation times
τ_1	relaxation time of heat flux in He II
λ_0	bulk viscosity of He II
λ_1	heat conductivity of He II
λ_2	shear viscosity of He II, that can be identified with the viscosity of a normal fluid η
η	viscosity of a normal fluid
ν	kinematic viscosity of a normal fluid
k	thermal conductivity of a normal fluid
$\mathbf{m} = (m_{ij})$	non-equilibrium stress
p_V	non-equilibrium pressure or bulk viscous pressure
$m_{<ij>}$	shear viscous stress
β and β'	coefficients appearing in the entropy flux expression in Extended Irreversible Thermodynamics
$\mathbf{v}_{ns} = \mathbf{v}_n - \mathbf{v}_s$	microscopic counterflow velocity in the two-fluid model
$\mathbf{V}_{ns} = \langle \mathbf{v}_n - \mathbf{v}_s \rangle$	counterflow velocity in the two-fluid model, evaluated in a volume sufficiently small with respect to the sizes of the channel

$V_{ns} = \overline{\mathbf{V}}_{ns}$	counterflow velocity in the two-fluid model averaged over a transversal section of the channel and defined by $\overline{\mathbf{v}}_n - \overline{\mathbf{v}}_s$
$\mathbf{u}^{(n)}$	velocity of the normal component in the one-fluid model
$\mathbf{u}^{(s)}$	velocity of the superfluid component in the one-fluid model
$U_{ns} = \overline{\mathbf{U}}_{ns}$	relative velocity in the one-fluid model averaged over a transversal section of the channel and defined by $\overline{\mathbf{u}}^{(n)} - \overline{\mathbf{u}}^{(s)}$
κ	quantum of vorticity, defined by h/m_4 ($\kappa \simeq 9.97 \cdot 10^{-4}$ cm^2/s)
α_V and β_V	coefficients of Vinen equation, that describe the formation and destruction of vortex line
$\mathbf{F}_{ns}$	mutual friction force between normal and superfluid components
B_{HV} and B'_{HV}	Hall-Vinen coefficients appearing in the expression of the mutual friction
$\mathbf{I}$ and $\mathbf{J}$	vectors related to the polarization of the vortex tangle
$\mathbf{\Pi}$	tensor related to anisotropy of the vortex tangle
$\mathbf{T}$	vortex tension force
$\mathbf{s}(\xi)$	position vector that localize a point of a quantized vortex line (being ξ the arc-length)
$\mathbf{s}'(\xi)$	tangent unit vector to the quantized vortex line
$\mathbf{s}''(\xi)$	local curvature of the quantized vortex line
$\mathbf{v}_i$	self-induced velocity
ϵ_V	energy per unit length of quantized vortex line
$\mathbf{W} = (\mathbf{W})_{ijk}$	Ricci tensor
Rey	Reynold number
Rey_q	quantum Reynold number
λ_{eff}	effective thermal conductivity
l	length of the channel
ℓ	mean free path of phonons
$L_{entrance}$	length of the entrance region
D	coefficient that describes the diffusion of vortices
$J_n(x)$	Bessel function of first kind and order n
$Y_n(x)$	Bessel function of second kind and order n
$I_n(x)$	modified Bessel function of first kind and order n
$K_n(x)$	modified Bessel function of second kind and order n

Introduction

Low-temperature phenomena are a very active frontier of physics, in superfluidity, superconductivity, Bose-Einstein condensates, laser-induced lowering of temperatures and in the search for quantum computers. These topics have been recognized with several Nobel awards in the last two decades, have revealed new aspects of quantum physics at the macroscopic level, and have opened new technological alleys, as production of high magnetic fields, transport of electricity with extremely low dissipation, high precision measurement of time, and construction of several quantum logic gates for future quantum computers. Collective excitations in those systems, and in particular quantized vortices is superfluids, superconductors, and Bose-Einstein condensates, are an expecially exciting challenge.

The analysis of liquid helium — liquid helium 4, but also liquid helium 3, which needs much lower temperatures and has a much richer and complex phenomenology than helium 4 — is one of the basic grounds for research in the field of low-temperatures, because of its own interest as well as because helium 4, also called helium II, is used as a cryogenic fluid at low temperatures, below 2 K. Furthermore, for many years it has been known that liquid helium 4 has many unusual properties, which may be explained only on the grounds of collective quantum effects.

The behavior of liquid helium, below the *lambda*-point ($T_\lambda = 2.17$ K), is very different from that of ordinary fluids. One example of non-classical behavior is the possibility to propagate the second sound, a wave motion in which temperature and entropy oscillate. A second example of non-classical behavior is heat transfer in counterflow experiments. Using an ordinary fluid (such as helium I) for which is valid the Fourier's law, a temperature gradient can be measured along the channel, which indicates the existence of a finite thermal conductivity. If helium II is used, and the heat flux inside the channel is not too high, the temperature gradient is so small that it cannot be measured, so indicating that the liquid has an extremely high thermal conductivity (three million times larger than that of helium I). This is confirmed by the fact that helium II is unable to boil. This effect explains the remarkable ability of helium II to remove heat and makes it important in engineering applications: for example, liquid helium is often used in the aerospace industry as refrigerant of highly sensitive detectors in order to minimize thermal noise, as for instance in the exploration of the minute fluctuations of the intensity of the cosmic background microwave radiation, or in the future search of gravitational waves. Furthermore, it is used at CERN for the refrigeration of large

magnets required to provide the suitable curvature of the trajectories of extremely fast particles.

In addition to the above described properties of He II related to heat transfer, there are other features in the transport properties. For instance the thermomechanical phenomena in which a pressure difference corresponds to a temperature difference, and *vice-versa*. The most typical is the well known *fountain effect*, whose name is due to the fact that in the experimantal apparatus the pressure difference is able to produce a jet of helium similar to a fountain.

When the heat flux exceeds the critical value q_c one observes the formation of microscopic quantized vortices which imply a big decrease of the thermal conductivity of the superfluid, because of the internal friction produced by these vortices on the normal component (Barenghi et al., 2001; Donnelly, 1991; Nemirovskii, 2013; Tsubota et al., 2012). Therefore, an important problem to be addressed in cryogenic refrigeration is the onset of quantized vortices. This situation is known as superfluid turbulence and was discovered in the 50s of the last century. Note that the vortices themselves are quantum entities, and they have quantized vorticity. This means that the line integral of the superfluid velocity along any closed line around the core of the vortex is equal to h/m_4, h being Planck's constant and m_4 the mass of a helium atom. This condition is analogous to Bohr quantization condition in the electronic orbits in atomic physics, where $2\pi rmv = nh$, where r is the radius of the orbit, m the electron mass and n a natural number. In superfluids, only the situation with $n = 1$ is found, because it requires less energy to elongate a vortex line keeping $n = 1$ than keeping the length of a vortex line but changing from $n = 1$ to $n = 2$. We have commented this point to emphasize that the analysis of quantum vortices is a very interesting topic, at the interface of quantum physics and physics of fluids.

Superfluid behaviour — both laminar and turbulent — may be described from two different models: two-fluid model, where the fluid is assumed to be a mixture of a normal and a superfluid component, each with its own density and velocity (Khalatnikov, 1989; Landau and Lifshitz, 1987); and one-fluid model, with the heat flux as a vectorial internal variable. These two models will be explained and compared in Chapter 2. These problems have already been addressed in (Jou et al., 2002; Mongiovì and Jou, 2007), where a hydrodynamical model for turbulent helium II has been proposed, by using Extended Thermodynamics (E.T.) (Jou et al., 2011a; Lebon et al., 2008; Mongiovì, 1993; Muller and Ruggeri, 1998) where dissipative terms are introduced, dependent on the gradients of velocity and heat flux.

Analogously to the situation found in heat transfer, many experimental results have been reported in helium superfluid flows along capillary channels and narrow slits, where they flow with almost no viscous effects. The first analysis dealts with laminar flow, but it was realized that turbulence appears when the velocity exceeds some critical values v_c. Also in this case, a tangle of quantized vortices appears which contributes to friction against the barycentric motion, in a similar way to what happens for heat flux higher than q_c.

The analysis of quantized vortices and of quantum turbulence in helium — as well

as that of quantized vortices in Bose-Einstein condensates, or of electric current vortices in superconductors — is an active topic of research, because it reveals new coherent collective behaviors in quantum fluids, and because of the practical interest to control quantum vortices in superconductors, in which pinned vortices represent an unwanted source of dissipation. Amongst the problems in this field are the knowledge of how the vortex line density L depends on the heat flux — or the current flux in superconductors — and on the boundary conditions, or the comparison between quantum and classical turbulence.

Indeed, the main topic of this thesis is the mesoscopic structure of quantum turbulence in three main aspects:

1. the velocity profiles of normal and superfluid component;

2. the structure of inhomogeneous and anisotropic tangles;

3. the mutual interaction between these two aspects in different flow geometries.

After many years of focusing the interest on the quantized vortices, one of the current topics of research in superfluid turbulence is the dynamical behavior of the normal component. For instance, it is not completely known whether the normal component is itself in a turbulent state or whether it remains in a laminar flow, in contrast to the turbulent superfluid component. In particular, counterflow situations — in which the barycentric velocity of the total fluid is zero, because of suitable opposite flows of the normal and superfluid components — have been examined in much detail, either theoretically and experimentally. This is a particular example of a more general and active topic, the comparison of classical and quantum turbulence.

The spatial aspects of the interaction between the vortices and the heat flux are another interesting topic of research which has not yet been fully explored. Some questions are, for instance, the behaviour of the heat profile near the walls, a region which may be a specially active source of vorticity. Another question is the curvature — or lack of curvature — of the heat profile in the center of the channel, which is another specially sensitive region allowing the possibility to explore whether the flow of the normal component is laminar (and has a typical parabolic velocity profile corresponding to a Poiseuille flow) or turbulent (and has a flat profile in the central region). Furthermore, the description of inhomogeneous and anisotropic vortex tangles is another important topic, because recent simulations and experiments have revealed that the usual hypothesis of homogeneous and isotropic tangle is too simplistic. Exploring these aspects requires a detailed knowledge of the mathematical consequences of the corresponding field equations.

The aim of this thesis is the detailed mathematical study of heat flow in superfluids. First of all we report in Chapter 1 the derivation of a phase field model for *lambda*-transition from He I to He II, when the liquid is subject to pressure and heat flux. Besides its original aspects, this chapter is useful as an introduction to the quantum microscopic aspects of superfluidity. In Chapter 2 we provide a general presentation

of the equations used in the following chapters, and introduce the essential physical concepts, from a macroscopic perspective. The other three chapters explore the profiles of the heat flux, of the pressure and of the vortex line density in the following characteristic flows: fully developed flow along a cylindrical channel or a slit (Chapter 3), entrance flow in a cylindrical channel or a slit (Chapter 4), axial flow of superfluid between two concentric cylinders or flow in convergent or divergent channels (Chapter 5).

In the introduction of each chapter we explain the specific motivations for such analysis, and we discuss the state of the art in research; at the end of each chapter we make some remarks, that are recalled in the final discussions of this thesis.

Acknowledgments

I wish to thank my tutor, Prof.ssa Maria Stella Mongiovì to put his experience and knowledge at my disposal, for enlightening discussions about the arguments of this thesis and for the constant support over these three years.

Furthermore I wish to especially thank Prof. David Jou, for his continuous stimulus and suggestions to research, for his hospitality during the months I spent at the Universitat Autònoma de Barcelona, for putting at my disposal his immense knowledge, for his stories and beautiful walks and chats.

I also thank my husband Michele to believe in me and for his constant support, always given in our life together and in particular in these three years. And at last, but not at least, I'd like to thank my little daughter Giorgia and the forthcoming one because their existence and smiles have allowed me to overcome the difficulties.

Chapter 1

Superfluid phase transition in the presence of a heat flux

Helium is one of the most unique and interesting elements in physics. The helium atom occurs in nature in two stable isotopes, ^{3}He and ^{4}He. In this chapter, we will report some results on transition to superfluidity in liquid ^{4}He, as well as an original investigation on the influence of a heat flux on the mentioned transition.

The critical temperature of ^{4}He is about 5.2 K at 1 atmosphere; above this critical temperature it cannot exist as a liquid irrespective of the external pressure. Actually, the interatomic (van der Waals) forces are too weak for liquid ^{4}He to solidify at 0.1 MPa (1 atm) pressure even at the lowest temperatures which have been attained. The phase diagram of ^{4}He is shown schematically in Figure 1.1. Besides the vapour to liquid, and liquid to solid, phase transition, The solid phase appears only for pressures above 2.5 MPa.

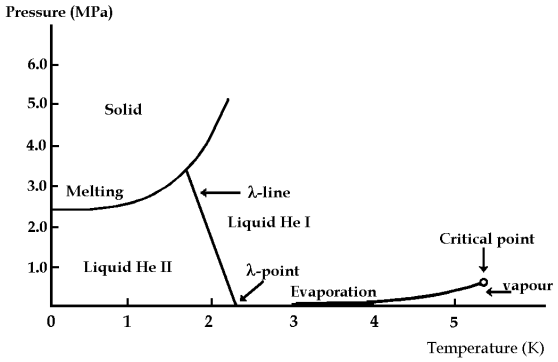

Figure 1.1: Phase diagram of ^{4}He.

Liquid ^{4}He exhibits a transition from normal liquid ^{4}He (known as liquid helium I) to superfluid liquid ^{4}He (known as liquid helium II) when the liquid is cooled below a critical temperature T_λ, which is $T_\lambda = 2.17$ K at vapour pressure. The solid phase appears only for pressures above 2.5 MPa.

Apart from its very low mass density, liquid He I is a normal viscous liquid, instead, liquid He II has some remarkable and unusual properties. For example, its viscosity is extremely small and its thermal conductivity extremely high (three million times larger than that of helium I). This new phase of ^{4}He is similar to the superconducting state of metals: the vanishing ohmic resistance in the motion of conduction electrons is similar to the frictionless motion of atoms in superfluid He II.

In order to describe the behaviour of the superfluid state discovered in the 1930's; In (London, 1954) the author associated this liquid with the quantum properties of an ideal Boson gas close to its ground state. Indeed, it is known that in a non-interacting Boson gas the Bose-Einstein condensation takes place, as the temperature is lowered below a critical one. This is an unusual kind of condensation in the configurational space: the atoms condense to their common ground state, i.e. a macroscopic fraction of the atoms occupies in a coherent collective way the same quantum state, which is the state of minimum energy. These considerations led Tisza to build up the famous two-fluid model having as the basis the condensate fraction as one fluid and the excited fraction as another fluid, intimately mixed with each other (Tisza, 1938).

A more detailed physical basis for the two-fluid model was developed in (Landau, 1941). Noting that He II is a complicated system of strongly interacting particles, Landau argued that superfluid helium cannot be considered an ideal gas, and based his arguments on the character of the low-energy spectrum of the excitations of the system, the so-called quasiparticles (rotons and phonons). According to Landau, He II corresponds to a potential flowing ground state in which quasiparticles move. The quanta of these collective modes of the ground state form a rarefied gas which is responsible for the thermal and viscous effects ascribed to the presence of the normal component. The motion of the quasiparticle gas produces the normal-superfluid counterflow, the relative motion of the "normal component" with respect to the ground state. The condensed phase corresponds to a macroscopically occupied quantum state and can be described by a complex macroscopic wave function ψ. In this model the overall fluid is assumed as a mixture of normal and superfluid components with respective densities ρ_n and ρ_s and velocities $\mathbf{v_n}$ and $\mathbf{v_s}$ (the total density is $\rho = \rho_n + \rho_s$).

Another macroscopic model to describe the anomalous behaviour of liquid helium II is the one-fluid model (Mongiovì, 1993, 1994, 2000a, 2001) derived by Extended Thermodynamics (E.T.) (Jou et al., 2011a, 2010; Lebon et al., 2008; Muller and Ruggeri, 1993, 1998). In this model the relative motion between normal and superfluid components is described by an internal variable, that macroscopically can be related

to the heat flux. Indeed, the two different components (normal and superfluid) are not directly observed, but velocity and heat flux are. Usually, the thermodynamics of He II are determined experimentally through the measurements of the sound velocities (Maynard, 1976), that determine directly the thermodynamic derivatives which can be integrated to give the temperature and pressure dependence of the thermodynamic quantities ρ, S, ρ_n/ρ. From these quantities, using the relations of the two-fluid model, the velocities of the normal and superfluid components are also derived. Thus, the one-fluid proposal is clarely related to observations, without need of an *a priori* microscopic interpretation.

As the normal liquid He I is cooled, a line of *lambda*-points appears at about 2 K; indeed, the temperature at which this line occurs depends on the pressure, in the absence of heat current. But, when an external heat flux is imposed, the temperature at which the transition occurs is lower than in the absence of it (Weichman et al., 2001). The appearance of the critical points (a surface in the space of the variables p, T, q^2, where p is the pressure, T the temperature and q the modulus of the heat flux) is indicative of a continuous symmetry-breaking phase transition that occurs. This situation is characteristic of a second order phase transition.

Second-order phase transitions can be regarded as going from an ordered to a disordered state and can be macroscopically described introducing a parameter called the order parameter. Examples of second-order phase transitions are the ferromagnetic transition, the superconducting transition (Berti and Fabrizio, 2007a,b; Tilley and Tilley, 1990), and the superfluid transition (Fabrizio, 2010; Fabrizio and Mongiovì, 2013a,b; Tilley and Tilley, 1990). From a theoretical perspective, order parameters arise from symmetry breaking. In such cases one must introduce one or more extra variables to describe the state of the system. In some systems the order parameter is a real number (e.g. the magnetization in ferromagnetic materials), in other systems is a vector (e.g. the direction in liquid-crystal phases (Berti et al., 2013)), or a complex number, as in superconductors and superfluids.

The Landau theory of second-order phase transitions (Ginzburg and Landau, 1950; Tilley and Tilley, 1990) is a macroscopic theory that describes transformations which involve a broken symmetry and a continuous change in the free energy. This theory was applied to liquid ^{4}He near the *lambda*-point in (Ginzburg and Pitaevskii, 1958). They used as order parameter the macroscopic coherent wave function of the condensate $\psi(\mathbf{x}, t)$, that they assumed linked to the superfluid density by the relation

$$\rho_s(\mathbf{x}, t) = m_4 |\psi(\mathbf{x}, t)|^2, \tag{1.1}$$

where m_4 is the mass of a helium atom.

However, Ginzburg and Pitaevskii studied only stationary situations, in an inertial frame, and did not consider the influence on the transition of the pressure and of the

heat flux. Our aim, in this chapter, will be to build up a thermodynamic model of ^{4}He able to describe the *lambda*-transition in this liquid, also in non stationary and inhomogeneous situations under pressure and in the presence of heat flux.

For this reason in this chapter, following previous results (Fabrizio and Mongiovì, 2013a,b; Mongiovì and Saluto, 2014), a phase field model is built to describe the *lambda*-transition, under pressure and in the presence of heat current. The model chooses as fundamental fields the density, the temperature, the velocity, the heat flux and a phase field scalar function, that is the order parameter that controls the transition. Indeed, following Landau, the transition from the liquid He I (normal state) to the liquid He II (superfluid state) induces a change in the internal structure order. The field that describes the structure order and controls the transition is linked to the modulus of the collective wave function describing the quantum coherent aspects of the fluid $|\psi(x)|$ by the relation

$$f^2(\mathbf{x},t) = \rho m_4 |\psi(x)|^2 = \rho\rho_s, \tag{1.2}$$

where ρ is the total mass density of the liquid helium. Hence the phase field $f = 0$ denotes the normal state, while $f \neq 0$ describes a superfluid state. Note that this change of structure is related to a purely quantum feature, namely, the coherent of the ground state.

As in (Fabrizio and Mongiovì, 2013b), in this study we consider the dependence of the superfluid transition on the heat flux. This is important, because the presence of the heat flux involves a change in transition temperature, in agreement with the well known analogy between superconductivity and superfluidity (Tilley and Tilley, 1990; Tinkham, 1996).

Indeed, for type II superconductors, a high magnetic field destroys superconductivity and generates magnetic vortices. In fact, in a type-II superconductor there are two critical values H_{c1} and H_{c2} of the magnetic field. For applied field intensity less than H_{c1}, superconductor exhibits the usual Meissner effect; for an applied field strength higher than H_{c2} superconductivity is destroyed. In between H_{c1} and H_{c2} the superconductor allows partial penetration of the magnetic field, in the form of an Abrikosov vortex lattice (Abrikosov, 1957); this state is called a mixed-state vortex lattice. Each vortex carries a quantum of magnetic field. The supercurrent circulates around the normal (i.e. non-superconducting) core of the vortex. Abrikosov vortices tend to arrange themselves in a flux-line (usually) triangular lattice, which however can be perturbed by material inhomogeneities (defects/dislocations) that pin the flux lines (Maruszewski, 2008a,b; Maruszewski and Restuccia, 1999; Tilley and Tilley, 1990; Tinkham, 1996).

Similarly, the presence of heat current can generate an analogous phenomenon: for applied heat flux less that q_{c1} the superfluid is in the laminar regime; for a heat flux higher that q_{c2} superfluidity is destroyed, i.e. the liquid helium is in the normal phase

He I. In between q_{c1} and q_{c2} the superfluid is in the turbulent regime, in which a tangle of quantized vortices is present.

1.1 Evolution equations of Liquid ^{4}He describing the transition from He I to He II

In this section a phase field model will be built to describe the *lambda*-transition, under pressure and in the presence of heat current. The model chooses as fundamental fields (state vector):

mass density	ρ
velocity	$\mathbf{v}$
temperature	T
phase field function	f
heat flux	$\mathbf{q}$

For these fields, we consider a general set of evolution equations, adding to the balance equations of mass, momentum and energy two additional balance equations for the order parameter f and for the vector field $\mathbf{q}$. Then we will particularize the constitutive relations for the fields in order to describe the material in consideration.

1.1.1 Balance equations

The starting point will be the following general set of balance equations for the density ρ, the baricentric velocity $\mathbf{v}$, the internal energy E, the order parameter f and the heat flux $\mathbf{q}$:

$$\begin{cases} \dot{\rho}(\mathbf{x},t) + \rho(\mathbf{x},t)\nabla\cdot\mathbf{v}(\mathbf{x},t) = 0, \\ \rho(\mathbf{x},t)\dot{\mathbf{v}}(\mathbf{x},t) + \nabla\cdot\mathbf{J}^{\mathbf{v}}(\mathbf{x},t) = 0, \\ \dot{E}(\mathbf{x},t) + E(\mathbf{x},t)\,\nabla\cdot\mathbf{v}(\mathbf{x},t) + \nabla\cdot\mathbf{q}(\mathbf{x},t) + \mathbf{J}^{\mathbf{v}}(\mathbf{x},t) : \nabla\mathbf{v}(\mathbf{x},t) = 0, \\ \dot{f}(\mathbf{x},t) + f(\mathbf{x},t)\,\nabla\cdot\mathbf{v}(\mathbf{x},t) + \nabla\cdot\mathbf{J}^{f}(\mathbf{x},t) = \sigma^{f}(\mathbf{x},t), \\ \dot{\mathbf{q}}(\mathbf{x},t) + \mathbf{q}(\mathbf{x},t)\,\nabla\cdot\mathbf{v}(\mathbf{x},t) + \nabla\cdot\mathbf{J}^{\mathbf{q}}(\mathbf{x},t) = \sigma^{\mathbf{q}}(\mathbf{x},t). \end{cases} \tag{1.3}$$

In these equations $E = \rho\epsilon$ is the internal energy density, $\mathbf{J}^{\mathbf{v}}$ is the stress tensor, $\mathbf{J}^{f}$ the flux of the order parameter f, $\mathbf{J}^{\mathbf{q}}$ the flux of the heat flux; σ^{f} and $\sigma^{\mathbf{q}}$ are terms describing the net supplies of the two fields f and $\mathbf{q}$; in the following we will write constitutive relations for these fields adding to those for the entropy S and the entropy flux $\mathbf{J}^{S}$. In system (1.3) an upper dot denotes the material time derivative, while the colon denotes the double scalar product, i.e. $\mathbf{J}^{\mathbf{v}} : \nabla\mathbf{v} = \Sigma_{i,j}[\mathbf{J}^{\mathbf{v}}]_{ij}[\nabla\mathbf{v}]_{ji}$.

Note that if one wants to describe with this set of equations both liquid helium I and liquid helium II, these equations must reduce to the classical equations of a normal viscous fluid above the *lambda*-line, while sufficiently below this line they must reduce to a system of field equations describing the superfluid liquid helium II.

We will determine restrictions on the fluxes by using the material objectivity principle and the second law of thermodynamics. The second law of thermodynamics states that the rate of entropy production per unit volume, σ^S, is a positive definite quantity. Accordingly, there exists a convex function S, the entropy per unit volume, and a vector function $\mathbf{J}^S$, the entropy flux density, such that the rate of production of entropy σ^S is non-negative

$$Q^S = \dot{S} + S\nabla\cdot\mathbf{v} + \nabla\cdot\mathbf{J}^S \geq 0. \tag{1.4}$$

In principle, also entropy S and entropy flux $\mathbf{J}^S$ may depend on the gradients of the basic quantities. However, we may directly exclude the terms in $\nabla\rho$, ∇E, ∇f, $\nabla\mathbf{v}$ and $\nabla\mathbf{q}$ from S, because we are not considering an evolution equation for the gradients themselves, and in this case the entropy does not depend on the gradients, as it will be shown in equations (1.13) — see also (Cimmelli, 2009; Cimmelli and Frischmuth, 2007; Van, 2003) —.

We assume for S and $\mathbf{J}^S$ approximate constitutive relations to second order in $\mathbf{q}$ and in the derivative of the fundamental variables, satisfying the material objectivity principle (Muller and Ruggeri, 1998), i.e.

$$S = S(\rho, E, f, q^2), \tag{1.5}$$

$$\begin{aligned}\mathbf{J}^s = {} & \phi_0\mathbf{q} + \phi_1\nabla\rho + \phi_2\nabla E + \phi_3\nabla f + \\ & \phi_4\left(\nabla\cdot\mathbf{v}\right)\mathbf{q} + \phi_5\left(\nabla\cdot\mathbf{q}\right)\,\mathbf{q} + \phi_6\,\mathbf{q}\cdot\langle\nabla\mathbf{v}\rangle + \phi_7\,\mathbf{q}\cdot\langle\nabla\mathbf{q}\rangle,\end{aligned} \tag{1.6}$$

where $\phi_h = \phi_h(\rho, E, f)$.

Note that inequality (1.4) does not hold for any value of the fundamental variables, but only for the thermodynamic processes, i.e., only for those values which are solution of the system (1.3). This means that we can consider the equations (1.3) as constraints for the entropy inequality to hold. A way to take these constraints into account was proposed in (Liu, 1972). He showed that the entropy inequality becomes valid for totally arbitrary values of the basic variables provided that one complements it by the evolution equations for the fields ρ, $\mathbf{v}$, E, f and $\mathbf{q}$ affected by multiplying factors Λ^ρ, $\mathbf{\Lambda}^\mathbf{v}$, Λ^E, Λ^f and $\mathbf{\Lambda}^\mathbf{q}$, that are also supposed objective functions of the fundamental fields. He called these factors Lagrange multipliers, in analogy with the extremization problems in the presence of constraints, which is a typical situation in information theoretical approach to equilibrium statistical mechanics.

Because our aim is to write a weakly non local model of *lambda*-transition, we will choose for the fluxes the following constitutive expressions, compatible with the

material objectivity principle, i.e.

$$\mathbf{J}^{\mathbf{v}} = (p - \alpha_1 \nabla\cdot\mathbf{v} - \alpha_2 \nabla\cdot\mathbf{q})\mathbf{U} - \eta_1\langle\nabla\mathbf{v}\rangle - \eta_2\langle\nabla\mathbf{q}\rangle, \tag{1.7}$$

$$\mathbf{J}^{\mathbf{q}} = (\beta_0 - \beta_1 \nabla\cdot\mathbf{v} - \beta_2 \nabla\cdot\mathbf{q})\mathbf{U} - \xi_1\langle\nabla\mathbf{v}\rangle - \xi_2\langle\nabla\mathbf{q}\rangle, \tag{1.8}$$

$$\mathbf{J}^{f} = \delta_0\mathbf{q} + \delta_1\nabla\rho + \delta_2\nabla E + \delta_3\nabla f, \tag{1.9}$$

where $\mathbf{U}$ is the unit matrix and angular brackets denote the deviatoric part of the tensors $\nabla\mathbf{v}$ and $\nabla\mathbf{q}$ (for example, $\frac{\partial q_{<i}}{\partial x_{j>}} = \frac{1}{2}\frac{\partial q_i}{\partial x_j} + \frac{1}{2}\frac{\partial q_j}{\partial x_i} - \frac{1}{3}\frac{\partial q_k}{\partial x_k}\delta_{ij}$). These constitutive equations introduce new terms in the balance equations (1.3) with respect to the previous model (Fabrizio and Mongiovì, 2013a). Coefficients p, β_0 and δ_0 are assumed dependent on all the field variables. The coefficients α_h, η_h, β_h, ξ_h and δ_h are assumed dependent on ρ, E and f. Moreover, the coefficients α_h, η_h, β_h and ξ_h must reduce to the viscosity coefficients of liquid helium I when f goes to zero, i.e. in the normal phase; instead, in the superfluid phase they must reduce to coefficients appearing in the model proposed in (Mongiovì, 1993) for describing helium II (described in more detail in the next chapter), as we will show in (1.58), (1.59), (1.61) and (1.62).

After introducing the Lagrange multipliers, one obtains from (1.4) the following inequality, which is satisfied for arbitrary values of the field variables

$$\begin{aligned}\dot{S} + S\,\nabla\cdot\mathbf{v} + \nabla\cdot\mathbf{J}^S &- \Lambda^\rho\left[\dot\rho + \rho\,\nabla\cdot\mathbf{v}\right] - \mathbf{\Lambda}^{\mathbf{v}}\cdot\left[\rho\dot{\mathbf{v}} + \nabla\cdot\mathbf{J}^{\mathbf{v}}\right]\\ &- \Lambda^E\left[\dot E + E\,\nabla\cdot\mathbf{v} + \nabla\cdot\mathbf{q} + \mathbf{J}^{\mathbf{v}} : \nabla\mathbf{v}\right]\\ &- \Lambda^f\left[\dot f + f\,\nabla\cdot\mathbf{v} + \nabla\cdot\mathbf{J}^f - Q^f\right]\\ &- \mathbf{\Lambda}^{\mathbf{q}}\cdot\left[\dot{\mathbf{q}} + \mathbf{q}\,\nabla\cdot\mathbf{v} + \nabla\cdot\mathbf{J}^{\mathbf{q}} - \mathbf{Q}^{\mathbf{q}}\right] \geq 0.\end{aligned} \tag{1.10}$$

In the following subsections the consequences of inequality (1.10) on the constitutive relations will be exploited and a set of field equations compatible with the second law will be written.

1.1.2 Restrictions imposed by the entropy principle

The constitutive theory is obtained substituting (1.5) and (1.6) in (1.10), taking into account (1.3), (1.7), (1.8) and (1.9), and imposing that the coefficients of all derivatives must vanish. In order to consider the derivatives with respect to time, we obtain $\frac{\partial S}{\partial \mathbf{v}} = \Lambda^{\mathbf{v}} = 0$ and

$$\frac{\partial S}{\partial \rho} = \Lambda^\rho, \quad \frac{\partial S}{\partial E} = \Lambda^E, \quad \frac{\partial S}{\partial f} = \Lambda^f, \quad \frac{\partial S}{\partial \mathbf{q}} = \Lambda^{\mathbf{q}}, \tag{1.11}$$

from which we can write

$$dS = \Lambda^\rho d\rho + \Lambda^E dE + \Lambda^f df + \lambda\mathbf{q}\cdot d\mathbf{q}, \tag{1.12}$$

where we have put $\mathbf{\Lambda}^q = \lambda \mathbf{q}$. Note that if we had *ab initio* assumed S dependent also on the gradient of the field variables, we would have obtained

$$\frac{\partial S}{\partial \nabla \rho} = 0, \qquad \frac{\partial S}{\partial \nabla E} = 0, \qquad \frac{\partial S}{\partial \nabla f} = 0, \qquad \frac{\partial S}{\partial \nabla \mathbf{q}} = 0. \tag{1.13}$$

This justifies, *a posteriori*, our assumption that S does not depend on the gradient of the basic variables.

Concerning the fluxes, we obtain

$$\nabla \cdot \mathbf{J}^S = \Lambda^E \left[\nabla \cdot \mathbf{q} + \mathbf{J}^{\mathbf{v}} : \nabla \mathbf{v}\right] + \Lambda^f \left[\nabla \cdot \mathbf{J}^f\right] + \mathbf{\Lambda}^{\mathbf{q}} \cdot \left[\nabla \cdot \mathbf{J}^{\mathbf{q}}\right], \tag{1.14}$$

imposing the coefficients of space derivatives of velocity to be zero, we obtain

$$S - \rho \Lambda^\rho - \Lambda^E (E + p) - \Lambda^f f - \mathbf{\Lambda}^{\mathbf{q}} \cdot \mathbf{q} = 0, \tag{1.15}$$

imposing that the coefficients of the linear terms in the spatial derivatives of ρ, E, f and $\mathbf{q}$ have to be zero, we get

$$\phi_0 = \Lambda^E + \Lambda^f \delta_0, \qquad d\phi_0 = \lambda d\beta_0 + \Lambda^f d\delta_0, \tag{1.16}$$

and vanishing the coefficients of the spatial derivatives of the second order, we obtain

$$\phi_1 = \Lambda^f \delta_1, \qquad \phi_2 = \Lambda^f \delta_2, \qquad \phi_3 = \Lambda^f \delta_3, \tag{1.17}$$

$$\phi_4 = -\lambda \beta_1, \qquad \phi_5 = -\lambda \beta_2, \qquad \phi_6 = -\lambda \xi_1, \qquad \phi_7 = -\lambda \xi_2. \tag{1.18}$$

It remains from (1.10) the following inequality

$$\begin{array}{c} \Lambda^E \alpha_1 (\nabla \cdot \mathbf{v})^2 + (\Lambda^E \alpha_2 + \phi_4)(\nabla \cdot \mathbf{v})(\nabla \cdot \mathbf{q}) + \phi_5 (\nabla \cdot \mathbf{q})^2 + \Lambda^E \eta_1 \langle \nabla \mathbf{v} \rangle : \langle \nabla \mathbf{v} \rangle \\ + (\Lambda^E \eta_2 + \phi_6) \langle \nabla \mathbf{v} \rangle : \langle \nabla \mathbf{q} \rangle + \phi_7 \langle \nabla \mathbf{q} \rangle : \langle \nabla \mathbf{q} \rangle + \lambda \mathbf{q} \cdot \mathbf{Q}^{\mathbf{q}} + \Lambda^f Q^f \geq 0. \end{array} \tag{1.19}$$

1.1.3 Physical meaning of the constitutive equations and of the Lagrange multipliers

Analyze now in detail the relations obtained in the previous section. Consider first equations (1.12) and (1.15). When we put in them $f = 0$ and $\mathbf{q} = 0$, they reduce to

$$dS_I = \Lambda_I^\rho d\rho + \Lambda_I^E dE, \tag{1.20}$$

$$S_I - \rho \Lambda_I^\rho - \Lambda_I^E [E + p] = 0, \tag{1.21}$$

where we have put $S_I = S(\rho, E, 0, 0)$, $\Lambda_I^\rho = \Lambda^\rho(\rho, E, 0, 0)$, $\Lambda_I^E = \Lambda^E(\rho, E, 0, 0)$. So, if we identify $1/\Lambda_I^E$ and $-\Lambda_I^\rho / \Lambda_I^E$ as the temperature T_I and the mass chemical potential μ_I of the normal liquid helium I

$$\Lambda_I^E(\rho, T) = \left[\frac{\partial S_I}{\partial E}\right]_\rho = \frac{1}{T_I}, \qquad -\frac{\Lambda_I^\rho(\rho, E)}{\Lambda_I^E(\rho, E)} = \left[\frac{\partial S_I}{\partial \rho}\right]_E = \mu_I, \tag{1.22}$$

equations (1.20) and (1.21) become the well known Gibbs equations of thermostatics of liquid helium I:

$$T_I dS_I = dE - \mu_I d\rho, \tag{1.23}$$

$$\rho\mu_I = E - T_I S_I + p, \tag{1.24}$$

We will suppose now $f \neq 0$. Introducing the temperature of liquid helium (in the normal and in the superfluid phase) as the reciprocal of the first-order part of the Lagrange multiplier of the energy

$$\Lambda^E = \left[\frac{\partial S}{\partial E}\right]_{\rho,f,q^2} = \frac{1}{T}, \tag{1.25}$$

we can write equations (1.12) and (1.15) in the following form

$$TdS = dE + T\Lambda^\rho d\rho + T\Lambda^f df + T\mathbf{\Lambda^q}\cdot d\mathbf{q}, \tag{1.26}$$

$$TS = E + p + T\rho\Lambda^\rho + Tf\Lambda^f + T\lambda q^2. \tag{1.27}$$

Note that, because we have assumed a weakly non-local model where the entropy S is independent of the gradients of field variables, from equation (1.26) we deduce that also the Lagrange multipliers do not depend on the gradients. When we perform a change of variables, substituting the temperature T to the energy density E, using equation (1.25), we conclude that also the energy density E is independent of the gradients, in this model. More general models where the energy and the entropy depend on the gradients of the field variables can be built up (see the Remarks of this chapter), but they are beyond our aim.

Introducing the free energy $G = E - TS$, from (1.26) we obtain

$$dG = -SdT - T\Lambda^\rho d\rho - T\Lambda^f df - \frac{1}{2}T\lambda dq^2, \tag{1.28}$$

from which we get:

$$\begin{array}{ll} \left[\frac{\partial G}{\partial T}\right]_{\rho,f,q^2} = -S, & \left[\frac{\partial G}{\partial \rho}\right]_{T,f,q^2} = -T\Lambda^\rho, \\ \left[\frac{\partial G}{\partial f}\right]_{\rho,T,q^2} = -T\Lambda^f, & \left[\frac{\partial G}{\partial q^2}\right]_{\rho,T,f} = -\frac{1}{2}\lambda T. \end{array} \tag{1.29}$$

Consider now the consequences of equations (1.16). Using definitions (1.25), we get

$$\lambda d\beta_0 = d\left(\frac{1}{T}\right) + \delta_0 d\Lambda^f. \tag{1.30}$$

Defining:

$$\varphi = \frac{f^2}{\rho^2}\frac{\partial\beta_0}{\partial\rho} = \frac{\delta_0 f^2}{\lambda\rho^2}\frac{\partial\Lambda^f}{\partial\rho}, \qquad \zeta = \frac{f^2}{\rho^2}\frac{\partial\beta_0}{\partial T} = -\frac{f^2}{\lambda\rho^2 T^2} + \frac{\delta_0 f^2}{\lambda\rho^2}\frac{\partial\Lambda^f}{\partial T}, \tag{1.31}$$

$$\chi = \frac{f^2}{\rho^2}\frac{\partial\beta_0}{\partial f} = \frac{\delta_0 f^2}{\lambda\rho^2}\frac{\partial\Lambda_f}{\partial f}, \qquad \xi = \frac{f^2}{\rho^2}\frac{\partial\beta_0}{\partial q^2} = \frac{\delta_0 f^2}{\lambda\rho^2}\frac{\partial\Lambda_f}{\partial q^2}, \tag{1.32}$$

equation (1.30) is written

$$\frac{f^2}{\rho^2} d\beta_0 = \varphi d\rho + \zeta dT + \chi df + \xi dq^2. \tag{1.33}$$

Note that above the *lambda*-line, where $f = 0$, all coefficients φ, ζ, χ and ξ vanish.

In particular, if we assume that coefficient δ_0 vanishes, it results $\partial\beta_0/\partial\rho = 0$, $\partial\beta_0/\partial f = 0$, $\partial\beta_0/\partial q^2 = 0$ and coefficient ζ assumes the simple expression

$$\zeta = -\frac{f^2}{\lambda\rho^2 T^2}. \tag{1.34}$$

It remains to determine the expressions of the production terms Q^f and $\mathbf{Q^q}$ of the two fields f and $\mathbf{q}$.

1.1.4 Determination of the source terms

A Ginzburg-Landau type equation for the order parameter

As we have said, in this model, the entropy and the energy are objective functions of the fundamental fields and do not depend on their gradients. To write an evolution equation for the order parameter f, we start supposing that the free energy density G has the simple expression

$$G = G_1 + G^f = G_1 + \frac{1}{2}\tilde{a} f^2 + \frac{1}{4}\tilde{b} f^4, \tag{1.35}$$

where $G_1 = G_1(\rho, T)$ is the free-energy density of He I, and coefficients $\tilde{a}$ and $\tilde{b}$ are general functions of the field variables:

$$\tilde{a} = \tilde{a}(\rho, T, q^2), \qquad \tilde{b} = \tilde{b}(\rho, T, q^2). \tag{1.36}$$

In Subsection 1.2.2 we will compare the equation for the order parameter, obtained in what follows, with that obtained from the usual Ginzburg-Landau model.

Now, following Landau, we will assume that the stable stationary state of the system is that which minimizes the free energy, with respect to the order parameter f. One obtains from (1.35) the simple equation:

$$\frac{\partial G}{\partial f} = \tilde{a}(\rho, T, q^2) f + \tilde{b}(\rho, T, q^2) f^3 = 0. \tag{1.37}$$

Our aim, is to write an evolution equation for the phase field f that reduces to equation (1.37) in homogeneous stationary states. Therefore, we will assume that the production term in the equation of the order parameter is proportional to $\partial G/\partial f$ and we get

$$Q^f = -K\frac{\partial G}{\partial f} = -K\left[\tilde{a}(\rho, T, q^2) f + \tilde{b}(\rho, T, q^2) f^3\right], \tag{1.38}$$

where K is a positive constant. Recalling equation $(1.29)_c$, we see that with this choice, the Lagrange multiplier Λ^f of the field f is proportional to Q^f. This result will be useful in the exploration of the residual inequality (1.19), where the product $\Lambda^f Q^f$ appears.

We consider now the balance equation (1.3_d) for the field f and substitute in it relations (1.9) and (1.38), we get:

$$\dot{f}+f\nabla\cdot\mathbf{v}+\nabla\cdot(\delta_0\mathbf{q}+\delta_1\nabla\rho+\delta_2\nabla E+\delta_3\nabla f) = -K\left[\tilde{a}(\rho,T,q^2)f+\tilde{b}(\rho,T,q^2)f^3\right]. \quad (1.39)$$

To describe *lambda*-transition in liquid helium, now we determine some constrains for coefficients $\tilde{a}$ and $\tilde{b}$. The first observation is that the stationary solutions of equation (1.39), neglecting spatial inhomogeneities of the field variables, are:

$$f = 0 \qquad \text{and} \qquad f^2 = -\frac{\tilde{a}(\rho,T,q^2)}{\tilde{b}(\rho,T,q^2)}. \quad (1.40)$$

The first of them describes the normal phase, and therefore this solution must be stable for T higher than a critical temperature T_c; instead, the second stationary solution describes the superfluid phase, and must be stable for $T < T_c$.

As usual in the thermodynamics of liquid helium, in the following, we will assume the pressure p as independent variable instead of the density ρ. Further, we will suppose that $\tilde{a}$ depends on p, q^2 and on the critical temperature T_c, while $\tilde{b}$ is independent of the temperature, then we assume

$$\tilde{a} = \mathcal{A}(p,q^2)(T-T_c) \quad \text{and} \quad \tilde{b} = \mathcal{B}(p,q^2), \quad (1.41)$$

with $\mathcal{A}$ and $\mathcal{B}$ positive quantities. With this choice, $f = 0$ is stable (i.e. $\partial^2 G/\partial f^2 > 0$) for $T > T_c$, and $f \neq 0$ is stable for $T < T_c$. Experiments show that the critical temperature T_c depends on the pressure and on the heat current. So we have:

$$T_c = T_c(p,q^2). \quad (1.42)$$

Therefore, in the space of the thermodynamic variables (p,T,q^2) we will have a surface of *lambda*-points, of equation $T = T_c(p,q^2)$. The equation of this surface can be obtained by using experimental data. First, we observe that in the absence of heat flux the equation (1.42) must reduce to:

$$T_c(p,0) = T_\lambda(1-ap), \quad (1.43)$$

where a is the slope of the line of critical points, the so-called *lambda*-line of Figure 1.1. A glance to Figure 1.1 shows that coefficient a is positive. If we suppose q not too high, equation (1.42) can be approximated by

$$T_c = T_c(p,q^2) \simeq T_\lambda\left[1-ap-bq^2\right], \quad (1.44)$$

where b can be determined from experimental data. Noting that the presence of the heat flux can create vortices, so destroying superfluidity, we deduce that also coefficient b is a positive coefficient, i.e. the presence of $\mathbf{q}$ reduces the critical temperature T_λ. Equation (1.44) represents a plane of critical points in the space of the variables p, q^2 and T, that we will call *lambda*-plane.

Recalling the microscopic meaning of the order parameter f ($f^2 = \rho\rho_s$), we can determine the link between coefficients $\mathcal{A}$ and $\mathcal{B}$. In fact, with the assumptions (1.41) for $\tilde{a}$ and $\tilde{b}$, if we neglect spatial inhomogeneities of the field variables, the non-zero stationary solution of equation (1.39) is

$$f^2 = \frac{\mathcal{A}(p,q^2)}{\mathcal{B}(p,q^2)}\left(T_c(p,q^2) - T\right). \tag{1.45}$$

Since $\rho_s/\rho \to 1$, when $T \to 0$, then f must be equal to ρ when $T \to 0$. So we infer that

$$\mathcal{B} = \frac{\mathcal{A}T_c}{\rho^2}. \tag{1.46}$$

Finally, putting:

$$\delta_1\frac{\partial\rho}{\partial p} + \delta_2\frac{\partial E}{\partial p} = \tilde{\delta}_1, \tag{1.47}$$

$$\delta_1\frac{\partial\rho}{\partial T} + \delta_2\frac{\partial E}{\partial T} = \tilde{\delta}_2, \tag{1.48}$$

$$\delta_1\frac{\partial\rho}{\partial f} + \delta_2\frac{\partial E}{\partial f} + \delta_3 = \tilde{\delta}_3, \tag{1.49}$$

we obtain the following evolution equation for f:

$$\begin{aligned} \dot{f} \;&+\; f\nabla\cdot\mathbf{v} + \nabla\cdot(\delta_0\mathbf{q} + \tilde{\delta}_1\nabla p + \tilde{\delta}_2\nabla T + \tilde{\delta}_3\nabla f) = \\ &=\; -K\left[\mathcal{A}(p,q^2)\left(T - T_c(p,q^2)\right)f + \frac{1}{\rho^2}\mathcal{A}(p,q^2)T_c(p,q^2)f^3\right]. \end{aligned} \tag{1.50}$$

Using relations (1.41) and (1.46), the free energy G becomes:

$$G(\mathbf{x},t) = G_1 + \frac{1}{2}\mathcal{A}(T - T_c)f^2 + \frac{1}{4\rho^2}\mathcal{A}T_c f^4. \tag{1.51}$$

This choice of G allows us to obtain the expressions for the entropy density S^f and the energy density E^f, that depend on the order parameter,

$$S^f = -\frac{\partial G}{\partial T} = -\frac{1}{2}\mathcal{A}f^2, \qquad E^f = G^f + TS^f = \mathcal{A}T_c\left(\frac{1}{4\rho^2}f^4 - \frac{1}{2}f^2\right). \tag{1.52}$$

Intuitively, it is logical that the entropy of liquid helium II is lower than that of liquid helium I, because it is microscopically more ordered, because of the quantum coherence of the particles condensed in the fundamental state.

Further, from equations (1.29), we get the following expressions of the Lagrange multipliers:

$$\begin{aligned}
\Lambda^{\rho} &= -\tfrac{1}{T}\left[\tfrac{\partial G_1}{\partial \rho} + \tfrac{1}{2}Tf^2\tfrac{\partial \mathcal{A}}{\partial \rho} + \tfrac{\partial}{\partial \rho}\left(\left(\tfrac{1}{4\rho^2}f^4 - \tfrac{1}{2}f^2\right)\mathcal{A}T_c\right)\right], \\
\Lambda^{f} &= -\tfrac{1}{T}\left[\mathcal{A}(T-T_c)f + \tfrac{1}{\rho^2}\mathcal{A}T_c f^3\right], \\
\mathbf{\Lambda^{q}} &= \lambda\mathbf{q} = -\tfrac{2}{T}\left[\tfrac{1}{2}Tf^2\tfrac{\partial \mathcal{A}}{\partial q^2} + \left(\tfrac{1}{4\rho^2}f^4 - \tfrac{1}{2}f^2\right)\tfrac{\partial(\mathcal{A}T_c)}{\partial q^2}\right]\mathbf{q}.
\end{aligned} \tag{1.53}$$

A generalized Cattaneo equation for the heat flux

Following (Fabrizio and Mongiovì, 2013a), for the production terms $\mathbf{Q^q}$ in the equation for the heat flux, we will choose the expression

$$\mathbf{Q^q} = -\frac{1}{\tau_q(\rho, f)}\mathbf{q}, \tag{1.54}$$

with $\tau_q(\rho, f)$ a scalar coefficient of the dimension of time, that can be interpreted as relaxation time of $\mathbf{q}$. This coefficient depends on the order parameter f, and it results zero above the *lambda*-line, while it becomes extremely high below it. As in (Fabrizio and Mongiovì, 2013a), in the following we will choose for τ_q the simple expression

$$\tau_q(\rho, f) = \tau\frac{f^2}{\rho^2 - f^2}, \tag{1.55}$$

where τ is a constant having the dimension of time. In this way the evolution equation for the heat flux is:

$$\dot{\mathbf{q}} + \mathbf{q}\nabla\cdot\mathbf{v} + \nabla\cdot[(\beta_0 - \beta_1\nabla\cdot\mathbf{v} - \beta_2\nabla\cdot\mathbf{q})\mathbf{U} - \xi_1\langle\nabla\mathbf{v}\rangle - \xi_2\langle\nabla\mathbf{q}\rangle] = -\frac{\rho^2 - f^2}{\tau f^2}\mathbf{q}. \tag{1.56}$$

If one assumes coefficient $\delta_0 = 0$, it results $\nabla\beta_0 = \zeta(\rho^2/f^2)\nabla T$ and eq. (1.56) reduces to

$$\begin{aligned}
\mathbf{q} = &-\frac{\tau\rho^2}{\rho^2 - f^2}\zeta\nabla T \\
&-\frac{\tau f^2}{\rho^2 - f^2}\left\{\dot{\mathbf{q}} + \mathbf{q}\nabla\cdot\mathbf{v} - \nabla\cdot[(\beta_1\nabla\cdot\mathbf{v} + \beta_2\nabla\cdot\mathbf{q})\mathbf{U} + \xi_1\langle\nabla\mathbf{v}\rangle + \xi_2\langle\nabla\mathbf{q}\rangle]\right\}.
\end{aligned} \tag{1.57}$$

We will choose for the coefficients of the nonlocal terms in this equation the following expressions:

$$\beta_1 = -\lambda_0\beta' T^2\zeta, \qquad \beta_2 = \lambda_0\frac{f^2}{\rho^2}\beta'^2 T^3\zeta, \tag{1.58}$$

$$\xi_1 = -2\lambda_2\beta T^2\zeta, \qquad \xi_2 = 2\lambda_2\frac{f^2}{\rho^2}\beta^2 T^3\zeta. \tag{1.59}$$

In this way, in the superfluid phase, the coefficients of equation (1.57) reduce to the coefficients used in the following chapters to describe He II as in (Mongiovì, 1993), that are described in more detail in the next chapter.

Coefficient ζ in equation (1.57) is a nonnegative coefficient (as it will be shown in Subsection 1.1.7). In fact, when $f = 0$, i.e. in the normal phase, from (1.57) one gets $\mathbf{q} = -\tau\zeta\nabla T$, from which we deduce that $\tau\zeta$ must be identified with the heat conductivity k of He I. Indeed, because both k and τ are nonnegative coefficients, also ζ is nonnegative. While in the superfluid state this positive coefficient is linked to the velocity of the second sound, as proved in (Mongiovì, 1993), by the relation $w_2^2 = \zeta/(\rho c_V)$, with c_V the constant-volume specific heat.

1.1.5 The motion equation

We consider now the balance equation for the momentum (1.3_b), that, using the constitutive relation (1.7), is written as

$$\rho\dot{\mathbf{v}} + \nabla p - \nabla\cdot[(\alpha_1\nabla\cdot\mathbf{v} + \alpha_2\nabla\cdot\mathbf{q})\mathbf{U} + \eta_1\langle\nabla\mathbf{v}\rangle + \eta_2\langle\nabla\mathbf{q}\rangle] = 0. \tag{1.60}$$

This equation must reduce to the classical motion equation of a normal viscous fluid above the *lambda*-line. Simple expressions for these coefficients that satisfy this assumption are:

$$\alpha_1 = \lambda_0, \qquad \alpha_2 = -\frac{f^2}{\rho^2}\lambda_0\beta' T, \tag{1.61}$$

$$\eta_1 = 2\lambda_2, \qquad \eta_2 = -2\frac{f^2}{\rho^2}\lambda_2\beta T. \tag{1.62}$$

Note that λ_0 and λ_2 correspond to the bulk and shear viscosity, whereas α_2 and η_2 relate dissipation to the inhomogeneities of the heat flux and are typical of the superfluid. They are null for usual viscous fluids, in which dissipation is related to velocity gradients. With this choice, equation (1.60) becomes

$$\rho\dot{\mathbf{v}}+\nabla p-\nabla\cdot\left[\left(\lambda_0\nabla\cdot\mathbf{v} - \frac{f^2}{\rho^2}\lambda_0\beta' T\nabla\cdot\mathbf{q}\right)\mathbf{U} + 2\lambda_2\langle\nabla\mathbf{v}\rangle - 2\frac{f^2}{\rho^2}\lambda_2\beta T\langle\nabla\mathbf{q}\rangle\right] = 0. \tag{1.63}$$

1.1.6 The temperature equation

The energy balance equation (1.3_c), using the constitutive relation (1.7), can be written as

$$\rho\dot{\epsilon} + \nabla\cdot\mathbf{q} + p\nabla\cdot\mathbf{v} - \alpha_1(\nabla\cdot\mathbf{v})^2 - \alpha_2(\nabla\cdot\mathbf{q})(\nabla\cdot\mathbf{v}) - \eta_1\langle\nabla\mathbf{v}\rangle : \langle\nabla\mathbf{v}\rangle - \eta_2\langle\nabla\mathbf{q}\rangle : \langle\nabla\mathbf{v}\rangle = 0. \tag{1.64}$$

The equation for the temperature T is then obtained assuming that $\epsilon = \epsilon(p, T, f, q^2)$. Taking in mind relations (1.61), (1.62), one gets the following equation

$$\rho c_p \dot{T} + \rho \epsilon_p \dot{p} + \rho \epsilon_f \dot{f} + 2\rho \epsilon_{q^2} \mathbf{q} \cdot \dot{\mathbf{q}} = -\nabla \cdot \mathbf{q} - p \nabla \cdot \mathbf{v} + \lambda_0 (\nabla \cdot \mathbf{v})^2$$
$$-\frac{f^2}{\rho^2} \lambda_0 \beta' T (\nabla \cdot \mathbf{q})(\nabla \cdot \mathbf{v}) + 2\lambda_2 \langle \nabla \mathbf{v} \rangle : \langle \nabla \mathbf{v} \rangle - 2\frac{f^2}{\rho^2} \lambda_2 \beta T \langle \nabla \mathbf{q} \rangle : \langle \nabla \mathbf{v} \rangle, \quad (1.65)$$

where $c_p = \epsilon_T$ is the constant-pressure specific heat of helium, whose plot is shown in Figure 1.2; near the *lambda*-point it takes very high values and can be approximated by $c_p = c_0 |T - T_\lambda|^{-\alpha}$, with $\alpha = 0.0127 \pm 0.0003$ (Lipa et al., 2003). Incidentally, it is precisely this peculiar form of c_p as a function of T near T_λ the origin of the name *lambda*-temperature, because it has the form of a Greek lambda. This divergence of c_p when $T \to T_\lambda$ is typical of second-order transitions. A tentative expression for c_V under pressure and in the presence of heat flux could be $c_V = c_0 \left|T - T_c\right|^{-\alpha} \simeq c_0 \left|T - T_\lambda (1 - ap - bq^2)\right|^{-\alpha}$.

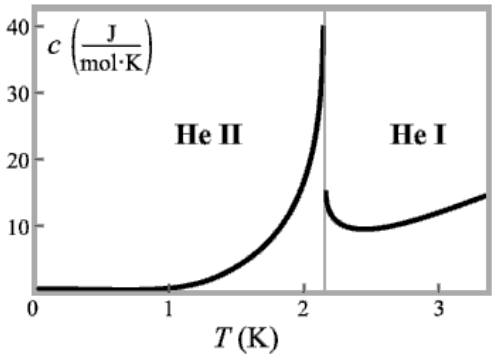

Figure 1.2: The specific heat of liquid ^{4}He vs the temperature.

1.1.7 Entropy inequality

We will consider finally the residual inequality (1.19). Using definition (1.25) and relations (1.18), (1.58), (1.59), (1.61), (1.62), it can be written in the following way:

$$\frac{1}{T} \lambda_0 (\nabla \cdot \mathbf{v})^2 - \lambda_0 \beta' \left(\frac{f^2}{\rho^2} - \lambda \zeta T^2 \right) (\nabla \cdot \mathbf{v}) (\nabla \cdot \mathbf{q}) - \frac{f^2}{\rho^2} \lambda \lambda_0 \beta'^2 T^3 \zeta (\nabla \cdot \mathbf{q})^2$$
$$+ \frac{2}{T} \lambda_2 \langle \nabla \mathbf{v} \rangle : \langle \nabla \mathbf{v} \rangle - 2\lambda_2 \beta \left(\frac{f^2}{\rho^2} - \lambda \zeta T^2 \right) \langle \nabla \mathbf{v} \rangle : \langle \nabla \mathbf{q} \rangle$$
$$-2\frac{f^2}{\rho^2} \lambda \lambda_2 \beta^2 T^3 \zeta \langle \nabla \mathbf{q} \rangle : \langle \nabla \mathbf{q} \rangle + \lambda \mathbf{q} \cdot \mathbf{Q}^{\mathbf{q}} + \Lambda^f Q^f \geq 0. \quad (1.66)$$

Let's denote:

$$N_1 = \tfrac{1}{T}\lambda_0(\nabla\cdot\mathbf{v})^2 - \lambda_0\beta'\left(\tfrac{f^2}{\rho^2} - \lambda\zeta T^2\right)(\nabla\cdot\mathbf{v})(\nabla\cdot\mathbf{q}) - \tfrac{f^2}{\rho^2}\lambda\lambda_0\beta'^2T^3\zeta(\nabla\cdot\mathbf{q})^2$$

$$N_2 = \tfrac{2}{T}\lambda_2\langle\nabla\mathbf{v}\rangle : \langle\nabla\mathbf{v}\rangle - 2\lambda_2\beta\left(\tfrac{f^2}{\rho^2} - \lambda\zeta T^2\right)\langle\nabla\mathbf{v}\rangle : \langle\nabla\mathbf{q}\rangle - 2\tfrac{f^2}{\rho^2}\lambda\lambda_2\beta^2T^3\zeta\langle\nabla\mathbf{q}\rangle : \langle\nabla\mathbf{q}\rangle$$

$$N_3 = \Lambda^f Q^f + \lambda\mathbf{q}\cdot\mathbf{Q}^{\mathbf{q}}$$

Recalling definitions $(1.31)_b$, we have:

$$\lambda = -\frac{f^2}{\rho^2}\frac{1}{\zeta T^2}\left(1 - \delta_0 T^2\frac{\partial\Lambda^f}{\partial T}\right). \tag{1.67}$$

We consider first the case $\delta_0 = 0$. In this case $\lambda = -\frac{f^2}{\rho^2}\frac{1}{\zeta T^2}$ and one sees that:

$$N_1 = \tfrac{1}{T}\lambda_0\left[\nabla\cdot\mathbf{v} - \tfrac{f^2}{\rho^2}\beta' T\nabla\cdot\mathbf{q}\right]^2,$$

$$N_2 = \tfrac{2}{T}\lambda_2\left[\langle\nabla\mathbf{v}\rangle - \tfrac{f^2}{\rho^2}\beta T\langle\nabla\mathbf{q}\rangle\right] : \left[\langle\nabla\mathbf{v}\rangle - \tfrac{f^2}{\rho^2}\beta T\langle\nabla\mathbf{q}\rangle\right],$$

$$N_3 = \lambda\mathbf{q}\cdot\mathbf{Q}^{\mathbf{q}} + \Lambda^f Q^f.$$

Being N_1 and N_2 nonnegative expressions, the entropy inequality is satisfied if it results also $N_3 \geq 0$.

In the case $\delta_0 \neq 0$, the entropy inequality (1.66) will be verified if any N_i is semidefinite positive. Therefore the matrices

$$\begin{bmatrix} \frac{1}{T}\lambda_0 & \frac{-\lambda_0\beta'}{2}(\frac{f^2}{\rho^2} - \lambda\zeta T^2) \\ \frac{-\lambda_0\beta'}{2}(\frac{f^2}{\rho^2} - \lambda\zeta T^2) & -\frac{f^2}{\rho^2}\lambda\lambda_0\beta'^2\zeta T^3 \end{bmatrix} \text{ and } \begin{bmatrix} \frac{2}{T}\lambda_2 & \lambda_2\beta(\frac{f^2}{\rho^2} - \lambda\zeta T^2) \\ \lambda_2\beta(\frac{f^2}{\rho^2} - \lambda\zeta T^2) & -2\frac{f^2}{\rho^2}\lambda\lambda_2\beta^2\zeta T^3 \end{bmatrix}$$

must be semidefinite positive. Both the determinants of these matrices are negative quantities, independent of the value of the coefficients appearing in them. Then, the compatibility of this model with the second law of thermodynamics imposes the vanishing of the coefficient δ_0.

We will consider finally the residual inequality

$$N_3 = \Lambda^f Q^f + \lambda\mathbf{q}\cdot\mathbf{Q}^{\mathbf{q}} \geq 0. \tag{1.68}$$

Recalling that $\Lambda^f = -\frac{1}{T}\frac{\partial G}{\partial f}$ (equation $(1.29)_c$) and that in (1.38) we have assumed $Q^f = -K\frac{\partial G}{\partial f}$, we have that the first term in N_3 is positive (because $K > 0$). Using relations (1.54), (1.55) and (1.67) with $\delta_0 = 0$, inequality (1.68) can be written:

$$\tfrac{K}{T}\left[\tfrac{\partial G}{\partial f}\right]^2 + \tfrac{f^2}{\rho^2\zeta T^2}\tfrac{\rho^2 - f^2}{\tau f^2}q^2 \geq 0, \tag{1.69}$$

and it is always verified because it results $\tau > 0$, $K > 0$ and $f^2 \leq \rho^2$.

Moreover, because $\mathbf{Q^q}$ is negative, also λ must be negative in order to have $N_3 > 0$, and then $\zeta = -\frac{f^2}{\rho^2}\frac{1}{\lambda T^2}$ must be nonnegative. This is consistent with the identification of $\tau\zeta$ as the thermal conductivity of liquid helium I (see paragraph below (1.59)).

1.2 Field equations and comparison with Ginzburg-Landau model

In this section we summarize the main field equations obtained in this chapter and we compare the evolution equation for the order parameter with that obtained from the usual Ginzburg-Landau model.

1.2.1 Evolution equations for the field variables

Summarizing, we have obtained the following system of evolution equations for the field variables ρ, $\mathbf{v}$, T, f and $\mathbf{q}$, able to describe both liquid helium I and liquid helium II:

$$\begin{cases} \rho_p\dot{p} + \rho_T\dot{T} + \rho_f\dot{f} + \rho\nabla\cdot\mathbf{v} = 0 \\ \rho\dot{\mathbf{v}} + \nabla p - \nabla\left[\lambda_0\left(\nabla\cdot\mathbf{v} - \frac{f^2}{\rho^2}\beta' T\nabla\cdot\mathbf{q}\right)\right] - \nabla\cdot\left[2\lambda_2\left(\langle\nabla\mathbf{v}\rangle - \frac{f^2}{\rho^2}\beta T\langle\nabla\mathbf{q}\rangle\right)\right] = 0 \\ \rho c_p\dot{T} + \rho\epsilon_p\dot{p} + \rho\epsilon_f\dot{f} + 2\rho\epsilon_{q^2}\mathbf{q}\cdot\dot{\mathbf{q}} + \nabla\cdot\mathbf{q} - p\nabla\cdot\mathbf{v} - \lambda_0(\nabla\cdot\mathbf{v})^2 - 2\lambda_2\langle\nabla\mathbf{v}\rangle : \langle\nabla\mathbf{v}\rangle \\ \qquad + \frac{f^2}{\rho^2}\lambda_0\beta' T(\nabla\cdot\mathbf{q})(\nabla\cdot\mathbf{v}) - 2\frac{f^2}{\rho^2}\lambda_2\beta T\langle\nabla\mathbf{q}\rangle : \langle\nabla\mathbf{v}\rangle = 0 \\ \dot{f} + f\nabla\cdot\mathbf{v} + \nabla\cdot(\tilde{\delta}_1\nabla p + \tilde{\delta}_2\nabla T + \tilde{\delta}_3\nabla f) + K\left[\mathcal{A}(T - T_c)f + \frac{1}{\rho^2}\mathcal{A}T_c f^3\right] = 0 \\ \dot{\mathbf{q}} + \mathbf{q}\nabla\cdot\mathbf{v} + \frac{\rho^2}{f^2}\zeta\nabla T + \nabla\left[\lambda_0\beta' T^2\zeta\left(\nabla\cdot\mathbf{v} - \frac{f^2}{\rho^2}\beta' T\nabla\cdot\mathbf{q}\right)\right] \\ \qquad + \nabla\cdot\left[2\lambda_2\beta T^2\zeta\left(\langle\nabla\mathbf{v}\rangle - \frac{f^2}{\rho^2}\beta T\langle\nabla\mathbf{q}\rangle\right)\right] + \frac{\rho^2 - f^2}{\tau f^2}\mathbf{q} = 0 \end{cases} \tag{1.70}$$

This system of field equations is obtained starting from a general set of balance equations by using Liu procedure and the production term in the equation of the order parameter is obtained from the simple expression (1.35) for the free energy density. In the next subsection we will point out how a similar evolution equation for the order parameter f (the fourth equation above) can be obtained starting with a generalized Ginzburg-Landau expression for the free energy density.

1.2.2 Comparison with the GL equation for the order parameter

In the model of *lambda*-transition in liquid helium proposed in (Ginzburg and Pitaevskii, 1958), one supposes that the free-energy density G can be expanded in powers of f^2 and $|\nabla f|^2$ in the following way:

$$G(\mathbf{x},t) = G_1 + G^f = G_1 + \frac{1}{2}\tilde{a}f^2 + \frac{1}{4}\tilde{b}f^4 + \frac{1}{2}\alpha|\nabla f|^2. \tag{1.71}$$

Considering the fluid at rest and following the Ginzburg-Landau (GL) general theory of second-order phase transitions, they assumed that the stable stationary state of the system is that which minimizes the total free energy with respect to the phase field f, obtaining an equation for the order parameter of the type

$$\partial_t f = -A\frac{\delta G}{\delta f} = -A\left[\tilde{a}f + \tilde{b}f^3 + \alpha\nabla^2 f\right] \tag{1.72}$$

Note that if one chooses for the free energy the following more general expression

$$G = G_1 + G^f = G_1 + \frac{1}{2}\tilde{a}f^2 + \frac{1}{4}\tilde{b}f^4 + \frac{1}{2}\left|\alpha_1\nabla p + \alpha_2\nabla T + \alpha_3\nabla f\right|^2, \tag{1.73}$$

and one minimizes it in a steady-state with respect to the order parameter f, one obtains for f the following equation:

$$\partial_t f = -A\frac{\delta G}{\delta f} = -A\left[\tilde{a}f + \tilde{b}f^3 + \nabla\cdot\left[\alpha_3(\alpha_1\nabla p + \alpha_2\nabla T + \alpha_3\nabla f)\right]\right]. \tag{1.74}$$

To compare this result with that obtained in our work, we note that if the fluid is at rest equation (1.70_d) becomes:

$$\partial_t f = -\nabla\cdot(\tilde{\delta}_1\nabla p + \tilde{\delta}_2\nabla T + \tilde{\delta}_3\nabla f) - K\left[\mathcal{A}(T-T_c)f + \frac{1}{\rho^2}\mathcal{A}T_c f^3\right]. \tag{1.75}$$

This equation is identical with equation (1.74), if one assumes $A\tilde{a} = K\mathcal{A}(p,q^2)(T-T_c)$, $A\tilde{b} = K\mathcal{B}(p,q^2)$ and $\tilde{\delta}_h = A\alpha_3\alpha_h$ (with A a constant quantity).

1.3 Remarks

In this chapter, we have build up a macroscopic model able to describe the behaviour of liquid ^{4}He above and below the *lambda*-line, under pressure and in the presence of heat flux. We have worked in a non-equilibrium thermodynamic framework, choosing as fundamental fields the heat flux $\mathbf{q}$ in addition to the mass, momentum and energy densities, and introducing as a new internal variable a scalar function f, linked to the modulus of the wave function of the condensate by the equation (1.2) and whose physical

mean is the geometrical mean between the total density of the fluid and that of the superfluid component. This internal variable is the order parameter that controls the phase transition. To determine the restrictions by the second law of thermodynamics on the constitutive quantities we have used the Liu procedure, that uses the Lagrange multipliers.

This model describes the behaviour of liquid helium I, when $f = 0$, while it reduces to the one-fluid model of liquid helium II deduced from E.T, when f/ρ goes to 1, as we will see in the following chapter.

Other models were build up over the years, that reduce to the two-fluid model, when the order parameter goes to 1. Among these we recall the model proposed in (Fabrizio, 2010) and recently in the paper (Berti and Berti, 2013). The model proposed here is a macroscopic one and the variables used can be directly measured; in contrast, the models formulated in (Fabrizio, 2010) and (Berti and Berti, 2013) use as fundamental variables the velocities of normal and superfluid components, that are only indirectly measured, through measures of $\mathbf{v}$ and $\mathbf{q}$. It could be of interest to compare the results of these two different points of view.

In the future it would be of interest to generalize the model presented in this chapter, to describe also phenomena as the vortex formation when the imposed heat flux is sufficiently high (Donnelly, 1991) and the successive establishment of superfluid turbulence (Ardizzone et al., 2009). It is known indeed that a sufficiently high value of the heat flux $\mathbf{q}$ destroys superfluidity, i.e. determines a shift of the transition, by creating a high number of quantized vortices, in analogy with what happens in a superconductor when a magnetic field higher than a critical value H_{c2} is applied (Tilley and Tilley, 1990; Tinkham, 1996).

Another factor which could modify the superfluid transition is a rotation of the fluid. If helium I is in a cylindrical container rotating with angular velocity Ω, the *lambda*-temperature would also be lowered. In fact, there is a strong analogy between Ω in a superfluid and H in a superconductor (even stronger than the analogy between $\mathbf{q}$ and H, bacause Ω produces ordered vortices, as it will be discussed in next chapters). An analogous analysis to that carried out here in the presence of $\mathbf{q}$ could be carried out for Ω, but we will not do it here, because we will focus our thesis on the role of heat flux.

In the following chapters we will consider liquid helium sufficiently below the transition temperature, in such a way that it is possible to assume the order parameter closer or equal to density ρ of the helium II.

- The model presented in this chapter is published in:
  M.S. Mongiovì and L. Saluto, *A model of λ transition in liquid ^4He*,
  Meccanica **49** 2125–2137 (2014), DOI 10.1007/s11012-014-9922-0

Chapter 2

Basic equations of He II: hydrodynamics, thermodynamics, and vortex dynamics

In the previous chapter we have build up a macroscopic model to describe the behaviour of liquid ^{4}He above and below the *lambda*-transition line, under pressure and in the presence of heat flux. In the following chapters we plan to study superfluid helium (i.e. we consider liquid helium sufficiently below the transition temperature), in such a way that the order parameter can be assumed constant and closer or equal to the density ρ of the helium. For this reason, we don't need to consider the equation for the order parameter.

There are two frameworks to study the motion of superfluid helium: the well known and much used two-fluid model of Tisza, Landau and Khalatnikov (Khalatnikov, 1989; Landau, 1941; London, 1954; Mendelsohn, 1956; Tisza, 1938), inspired on quantum microscopic grounds, and the one-fluid model with heat flux as an internal variable (Mongiovì, 1991, 1993), derived from Extended Thermodynamics (Jou et al., 2011a, 2010; Lebon et al., 2008; Muller and Ruggeri, 1993, 1998). In this chapter we present and compare both models, their physical assumptions and mathematical formulations, and we establish the set of equations which will be the basis of our analysis along the next chapters. Our aim is to obtain evolution equations for E, $\mathbf{v}$, $\mathbf{q}$ and L on macroscopic grounds. We will assume that the fluxes of the fundamental fields in these equations depend on the gradient of the same fields and then we will use the term "hydrodynamics equations" for the obtained evolution equations. We will try to give to the discussion a wide scope to get rather general forms, which will be simplified in the next chapters, according to the particular physical situations which will be considered in them.

2.1 Hydrodynamic equations in the two-fluid model

The two-fluid model assumes that the overall fluid is composed of normal and superfluid components with respective densities ρ_n and ρ_s and velocities $\mathbf{v_n}$ and $\mathbf{v_s}$. The total density is $\rho = \rho_n + \rho_s$, and the barycentric velocity is

$$\mathbf{v} = \frac{\rho_n}{\rho}\mathbf{v}_n + \frac{\rho_s}{\rho}\mathbf{v}_s. \tag{2.1}$$

The slope of ρ_n/ρ and ρ_s/ρ under the *lambda*-temperature T_λ in shown in Figure 2.1. It is assumed that the superfluid component corresponds to a Bose-Einstein condensate

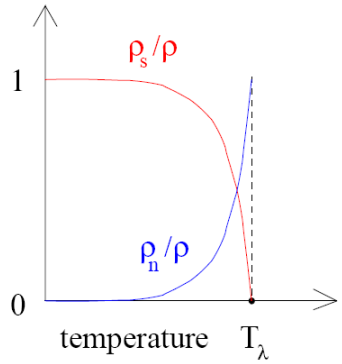

Figure 2.1: Slope of ρ_n/ρ and ρ_s/ρ

with strong mutual interactions, and that it is characterized by a macroscopic coherent wave function. Instead, the normal component is formed of excitations (phonons, rotons) flowing in the background of the superfluid component. The superfluid component is assumed to have zero entropy and zero viscosity, and the normal component has non-vanishing entropy and viscosity. In this model, heat flow is, therefore, a motion of the normal component with respect to superfluid component.

The densities $\rho_s(T)$ and $\rho_n(T)$ change with temperature as

$$\frac{\rho_s(T)}{\rho} = 1 - \frac{\rho_n(T)}{\rho} = \left(\frac{T_\lambda - T}{T_\lambda}\right)^{\frac{1}{2}}. \tag{2.2}$$

At $T = 0$ K, the normal component disappears and the whole system is superfluid. Equation (2.2) indicates that just at $T = T_\lambda$ practically the whole fluid is formed by the normal component, whereas at $T = 0$ K, the normal component has disappeared and all the fluid is in the form of the superfluid component.

Following the two-fluid model, the heat flux would be $\mathbf{q} = \rho_n s_n T(\mathbf{v}_n - \mathbf{v})$, if the intrinsic thermal conductivity is ignored. Here s_n is the entropy of the normal component

per unit mass of the normal component. By using (2.1) for $\mathbf{v}$, $\mathbf{q}$ may be rewritten as $\mathbf{q} = \frac{\rho_n s_n T \rho_s}{\rho}(\mathbf{v}_n - \mathbf{v}_s)$. If one defines $\rho_n s_n = \rho s$, this is rewritten as $\mathbf{q} = \rho_s T s(\mathbf{v}_n - \mathbf{v}_s)$, where s is the entropy per unit mass referred to the total mass of the fluid (i.e. both the mass of the normal component and the mass of the superfluid component). Thus, if one also takes into account a non-vanishing thermal conductivity k of the mixture, the heat flux $\mathbf{q}$ is given by the relation

$$\mathbf{q} = \mathbf{q}^{(tf)} = \rho_s T s(\mathbf{v}_n - \mathbf{v}_s) - k\nabla T, \tag{2.3}$$

where the superscript *(tf)* in $\mathbf{q}^{(tf)}$ indicates the two-fluid model. We note that, as a consequence of (2.3), if one assumes that the liquid helium is globally at rest ($\mathbf{v} = 0$), the heat flux $\mathbf{q}^{(tf)}$ is directly linked to the velocity of the normal component as

$$\mathbf{v}_n = (\mathbf{q}^{(tf)} + k\nabla T)(\rho T s)^{-1}. \tag{2.4}$$

To relate (2.3) and (2.4) it has been taken into account that $\mathbf{v} = 0$ implies, according to (2.1), either $\mathbf{v}_n = \mathbf{v}_s = 0$, or $\rho_s \mathbf{v}_s = -\rho_n \mathbf{v}_n$ (the so-called counterflow situation). For $\mathbf{v}_s = \mathbf{v}_n = 0$, the heat flux (2.3) reduces to Fourier's law, but in general, heat transport will be due essentially to the relative motion $\mathbf{v}_n - \mathbf{v}_s$, in such a way that the term in $k\nabla T$ is often neglected in (2.3). A brief discussion considering the possibility of a nonvanishing entropy of the superfluid component s_s to the total entropy, namely, $\rho s = \rho_n s_n + \rho_s s_s$, but with $s_s \ll s_n$, will be presented in Section 3.4, in a discussion of heat flow in very narrow channels.

On the other side, if one works in the framework of the one-fluid model, the velocity $\mathbf{v}$ and the heat flux $\mathbf{q}$, the density ρ and the temperature T are chosen as fundamental variables. Thus, the heat flux $\mathbf{q}$ plays the role of an independent variable, with a long relaxation time. The conceptual advantage of the one-fluid model is that, in fact, from the purely macroscopic point of view one sees only a single fluid, rather than two physically different fluids. Indeed the variables $\mathbf{v}$ and $\mathbf{q}$ used in E.T. are directly measurable, whereas the variables $\mathbf{v}_n$ and $\mathbf{v}_s$ are only indirectly measured, usually from the measurements of $\mathbf{q}$ and $\mathbf{v}$. The internal degree of freedom arising from the relative motion of the two fluids is here taken into account by the heat flux. In contrast, the two-fluid model directly provides a very appealing image of the microscopic helium behavior, and therefore is the most widely known.

In the next sections, the hydrodynamic equations of the one-fluid model are presented and compared with those of the two-fluid model, and their thermodynamic implications are emphasized with special attention to on the one-fluid model.

2.2 Hydrodynamic equations in the one-fluid model

Extended Thermodynamics (E.T.) has been applied to formulate a one-fluid model of liquid helium II. We recall briefly here the model formulated in (Mongiovì, 1993), modifying it to take into account the presence of a turbulent vortex tangle. In Section 2.4 we will go to deeper detail.

2.2.1 Basic equations

The fundamental fields in the E.T. are the mass density ρ, the barycentric velocity $\mathbf{v} = (v_i)$, the temperature T, the non-equilibrium stress $\mathbf{m} = (m_{ij})$, and the heat flux $\mathbf{q} = (q_i)$. In the following, we assume the non-equilibrium part of the stress decomposed into its trace p_V (non-equilibrium pressure) or bulk viscous pressure, and its deviator $m_{<ij>}$, that is $m_{ij} = p_V \delta_{ij} + m_{<ij>}$. For the purpose of this thesis, it is sufficient to consider equations in which only linear terms are retained. The corresponding evolution equations are, on the one side, the balance equations of mass, momentum and internal energy (Jou et al., 2010), i.e.

$$\begin{cases} \dot{\rho} + \rho \frac{\partial v_j}{\partial x_j} = 0 \\ \rho \dot{v}_i + \frac{\partial}{\partial x_j}[(p + p_V)\delta_{ij} + m_{<ij>}] = 0 \\ \rho \dot{\epsilon} + \frac{\partial q_j}{\partial x_j} + [(p + p_V)\delta_{ij} + m_{<ij>}]\frac{\partial v_i}{\partial x_j} = 0 \end{cases} \tag{2.5}$$

where ϵ is the specific internal energy and p the thermostatic pressure.

These equations have a general form which does not depend on the material. In them, the unknown quantities q_i, p_V and $m_{<ij>}$ (heat flux, bulk and shear viscous stress) appear. Therefore, other three equations are needed, to close the system. In classical irreversible thermodynamics, constitutive equations for the fluxes q_i, p_V and $m_{<ij>}$ are chosen, relating them to the density ρ and the temperature T and their gradients (de Groot and Mazur, 1962; Lebon et al., 2008). Instead, in the E.T. framework, these fluxes are considered independent fields, and three evolution equations for them are written. This view is especially useful when the relaxation times of such fluxes are long, in such a way that the fluxes are not completely determined by the gradients of the classical variables.

Neglecting non linear terms, these equations for the fluxes are:

$$\begin{cases} \tau_0 \dot{p}_V + \lambda_0 \frac{\partial v_j}{\partial x_j} - \beta' T \lambda_0 \frac{\partial q_j}{\partial x_j} = -p_V \\ \\ \tau_2 \dot{m}_{<ik>} + 2\lambda_2 \frac{\partial v_{<i}}{\partial x_{k>}} - 2\beta T \lambda_2 \frac{\partial q_{<i}}{\partial x_{k>}} = -m_{<ik>} \\ \\ \tau_1 \dot{q}_i + \lambda_1 \frac{\partial T}{\partial x_i} - \beta' T^2 \lambda_1 \frac{\partial p_V}{\partial x_i} - \beta T^2 \lambda_1 \frac{\partial m_{<ij>}}{\partial x_j} = -q_i \end{cases} \tag{2.6}$$

in these equations τ_0, τ_2 and τ_1 are the relaxation times of the non-equilibrium pressure, stress deviator and heat flux, respectively; λ_0, λ_2 and λ_1 are the coefficients which (in a normal fluid) can be identified respectively with the bulk viscosity, shear viscosity and heat conductivity. Finally, β and β' are coefficients which can be related to the moments of fluctuations (Jou et al., 2010), or to nonclassical contributions to the entropy flux.

Experiments (Mendelsohn, 1956) show that in liquid helium II the relaxation time τ_1 of heat flux is very long comparable to the evolution times of the usual conserved variables, while the relaxation times τ_0 and τ_2 of the stress (trace and deviator) are extremely small. Further, at the *lambda*-point and below, the heat conductivity λ_1 of liquid helium becomes extremely high. This is confirmed by the fact that helium II is unable to boil when it is heated because it diffuses efficiently the received heat instead of accumulating it.

As a consequence, the fundamental fields needed to describe the dynamical behavior of this quantum fluid are the two scalar fields ρ and T and the two vector fields v_i and q_i, as mentioned in the previous section. Constitutive relations for the trace p_V and for the deviator $m_{<ij>}$ of the non-equilibrium stress, depending on the derivatives of the fundamental fields, are determined by taking in the field equations (2.6_a) and (2.6_b) the relaxation times τ_0 and τ_2 equal to zero. One gets:

$$p_V = -\lambda_0 \frac{\partial v_j}{\partial x_j} + \beta' T \lambda_0 \frac{\partial q_j}{\partial x_j}, \tag{2.7}$$

$$m_{<ik>} = -2\lambda_2 \frac{\partial v_{<i}}{\partial x_{k>}} + 2\beta T \lambda_2 \frac{\partial q_{<i}}{\partial x_{k>}}, \tag{2.8}$$

Equations (2.7) and (2.8) contain, in addition to terms proportional to the velocity gradient, typical of usual Newtonian fluids, terms depending on the gradient of the heat flux. The first ones are responsible for dissipation of mechanical origin, the second ones for dissipation of thermal origin.

The field equations of helium II in the presence of dissipation are then obtained by substituting relations (2.7) and (2.8) into the field equations (2.5_b), (2.5_c) and (2.6_c).

The following linearized system of equations is obtained:

$$\begin{cases} \frac{\partial \rho}{\partial t} + \rho \frac{\partial v_j}{\partial x_j} = 0 \\ \\ \frac{\partial v_i}{\partial t} + \frac{1}{\rho}\frac{\partial p}{\partial x_i} - \frac{\lambda_0}{\rho}\frac{\partial}{\partial x_i}\left[\frac{\partial v_j}{\partial x_j} - \beta' T \frac{\partial q_j}{\partial x_j}\right] - \frac{\lambda_2}{\rho}\frac{\partial}{\partial x_j}\left[2\frac{\partial v_{<j}}{\partial x_{i>}} - 2\beta T \frac{\partial q_{<j}}{\partial x_{i>}}\right] = 0 \\ \\ \frac{\partial T}{\partial t} + \frac{1}{\rho c_V}\frac{\partial q_j}{\partial x_j} = 0 \\ \\ \frac{\partial q_i}{\partial t} + \zeta \frac{\partial T}{\partial x_i} + \lambda_0 \beta' T^2 \zeta \frac{\partial}{\partial x_i}\left[\frac{\partial v_j}{\partial x_j} - \beta' T \frac{\partial q_j}{\partial x_j}\right] + \lambda_2 \beta T^2 \zeta \frac{\partial}{\partial x_j}\left[2\frac{\partial v_{<j}}{\partial x_{i>}} - 2\beta T \frac{\partial q_{<j}}{\partial x_{i>}}\right] = \sigma_i^q \end{cases} \tag{2.9}$$

where we have put $\zeta = \frac{\lambda_1}{\tau_1}$ (the quantities λ_1 and τ_1 are very high, but their ratio is finite). As proved in (Mongiovì, 1993), this positive coefficient is linked to the velocity of the second sound w_2 by the relation $w_2^2 = \zeta/\rho c_V$, with c_V the constant-volume specific heat, as we said in the previous chapter.

The production term σ_i^q, in the equation of the heat flux, can be supposed zero in the laminar regime, while it depends on the imposed heat flux in the presence of a disordered superfluid vortex tangle (if $q > q_c$); this situation, different by classical turbulence, is known as *quantum turbulence*.

2.2.2 Comparison with two-fluid model

A detailed comparison between the one-fluid model and the two-fluid model by Landau and Khalatnikov (Khalatnikov, 1989) was made in (Mongiovì, 1993). The main difference between the one-fluid and the two-fluid models is that, while the mechanical dissipation is described in the same way in both models, the dissipation associated with heat transfer is described and interpreted in a different way. Incidentally, we observe that the terms heat flux and thermal conductivity have a slightly different meaning in the two-fluid theory and in the extended one. In fact in the former, the heat flux is the second term in the right hand side of (2.3), and the small parameter k is the thermal conductivity of the mixture, which, in the two-fluid model of helium II, is supposed similar to that of a normal fluid. In the extended theory, which is a monofluid one, the energy flux is instead identified with the heat flux. The parameter λ_1, appearing in the third equation in (2.6), can be identified with the thermal conductivity only in a normal fluid, where, being zero the relaxation time τ_1, and also the non classical contribution to the entropy flux ($\beta = \beta' = 0$), one arrives at a constitutive equation for $\mathbf{q}$ of the Fourier type. In contrast, in the extended model of helium II, the relaxation time τ_1 cannot be neglected, and the heat flux $\mathbf{q}$ is an independent variable, so the parameter λ_1, which is extremely high, and which we call still (extended) thermal conductivity, has nothing to bear with the small parameter k of the two-fluid model.

In fact, in (Mongiovì, 2001), in order to put into evidence the difference between the extended one-fluid and the two-fluid model, the transverse modes were analyzed. This study leads to define, in a natural way, two vectorial fields $\mathbf{u}^{(n)} = (u_i^{(n)})$ and $\mathbf{u}^{(s)} = (u_i^{(s)})$, that have the dimension of velocity, and that exhibit deeply different behaviors in the transverse modes, namely:

$$\mathbf{u}^{(n)} = \mathbf{v} - \beta T \mathbf{q}, \tag{2.10}$$

$$\mathbf{u}^{(s)} = \mathbf{v} + \frac{\beta T}{P-1}\mathbf{q}, \tag{2.11}$$

where $P = 1 + \rho\beta^2 T^3 \zeta$. Indeed, in (Mongiovì, 2001) it was shown that, while an initial transversal perturbation of $\mathbf{u}^{(s)}$ is almost stationary, the penetration depth of a harmonic transversal perturbation of $\mathbf{u}^{(n)}$ is almost zero. As shown in (Mongiovì, 2001), under the hypothesis $\beta = -1/(ST^2)$ (where $S = \rho s$ is the entropy of liquid helium II), no entropy transfer is associated to the field $\mathbf{u}^{(s)}$, and if one assumes $\beta' = \beta$ all the dissipative phenomena, both of mechanical and thermal origin are associated only to the field $\mathbf{u}^{(n)}$. Using the standard terminology of the two-fluid model, $\mathbf{u}^{(s)}$ and $\mathbf{u}^{(n)}$ can be interpreted as the velocities of the superfluid and normal component respectively, but this interpretation is not needed in the one-fluid model, where $\mathbf{u}^{(n)}$ and $\mathbf{u}^{(s)}$ appear in a natural way according to purely macroscopic dynamical behaviour.

The above considerations suggested that no tangential boundary condition must be imposed on $\mathbf{u}^{(s)}$, owing to its nondissipative nature, while the following boundary condition for $\mathbf{u}^{(n)}$ was postulated in (Mongiovì, 2001): *On the walls of a container, the tangential component of the vector field* $\mathbf{u}^{(n)}$ *is zero.* In terms of the variables $\mathbf{v}$ and $\mathbf{q}$, we can write

$$u_t^{(n)} = v_t - \beta T q_t = 0, \tag{2.12}$$

where the underscript t denotes the tangential component of the vectors.

In the following we will assume that $\mathbf{u}^{(s)}$ does not produce dissipation, while $\mathbf{u}^{(n)}$ behaves as an ordinary fluid, subject to dissipation. As we have said, this happens under the hypothesis

$$\beta = \beta' = -\frac{1}{ST^2}, \tag{2.13}$$

with this assumption, the evolution equation for the heat flux in system (2.9) is written:

$$\frac{\partial q_i}{\partial t} + \zeta\frac{\partial T}{\partial x_i} - \lambda_0\frac{\zeta}{S}\frac{\partial}{\partial x_i}\left[\frac{\partial v_j}{\partial x_j} + \frac{1}{TS}\frac{\partial q_j}{\partial x_j}\right] - \lambda_2\frac{\zeta}{S}\frac{\partial}{\partial x_j}\left[2\frac{\partial v_{<j}}{\partial x_{i>}} + \frac{2}{TS}\frac{\partial q_{<j}}{\partial x_{i>}}\right] = \sigma_i^q. \tag{2.14}$$

In (Mongiovì, 2001), two scalar fields, $\rho^{(s)}$ and $\rho^{(n)}$, associated with $\mathbf{u}^{(s)}$ and $\mathbf{u}^{(n)}$, where also introduced, which can be interpreted as the "densities" of the superfluid and normal components in helium II. They are:

$$\frac{\rho^{(s)}}{\rho} = \frac{P-1}{P} = \frac{\zeta}{\zeta + \rho s^2 T}, \qquad \frac{\rho^{(n)}}{\rho} = \frac{1}{P} = \frac{\rho s^2 T}{\zeta + \rho s^2 T}. \tag{2.15}$$

With this interpretation, one sees that:

$$\mathbf{v} = \frac{\rho^{(n)}}{\rho}\mathbf{u}^{(n)} + \frac{\rho^{(s)}}{\rho}\mathbf{u}^{(s)}. \tag{2.16}$$

It is to note that the two fields $\mathbf{u}^{(n)}$ and $\mathbf{u}^{(s)}$ cannot be directly identified with the velocities $\mathbf{v}_n$ and $\mathbf{v}_s$ introduced in the dissipative two-fluid model by Landau and Khalatnikov (Khalatnikov, 1989), indeed while in the two-fluid model the objective part of the energy flux is expressed by equation (2.3), in the one-fluid model it is linked to the velocities $\mathbf{u}^{(n)}$ and $\mathbf{u}^{(s)}$ by the equation

$$\mathbf{q} = -\frac{P-1}{P}\frac{1}{ST}\left(\mathbf{u}^{(n)} - \mathbf{u}^{(s)}\right) = -\rho^{(s)}Ts\left(\mathbf{u}^{(n)} - \mathbf{u}^{(s)}\right). \tag{2.17}$$

Because, as shown in (Mongiovì, 2001), the field $\mathbf{u}^{(s)}$ does not produce dissipation, from this equation we deduce that in the one-fluid model the dissipation of thermal origin, that is due to the presence of the elementary excitations (phonons and rotons), is associated only to the field $\mathbf{u}^{(n)}$. On the contrary, in the two-fluid model, by inversion of the equations (2.1) and (2.3), one has:

$$\mathbf{v}_n = \mathbf{v} + \frac{1}{\rho Ts}(\mathbf{q}^{(tf)} + k\nabla T), \tag{2.18}$$

$$\mathbf{v}_s = \mathbf{v} - \frac{\rho_n}{\rho_s}\frac{1}{\rho Ts}(\mathbf{q}^{(tf)} + k\nabla T), \tag{2.19}$$

therefore, velocity field $\mathbf{v}_n$ is not associated to the dissipation of thermal origin, that in this model is expressed by $-k\nabla T$. This is in contrast with the two-fluid model assumption that the field $\mathbf{v}_n$ takes into account of the presence of the thermal excitations. We conclude that the one-fluid model appears to better describe the dissipative phenomena of thermal origin.

2.3 Formation of vortex filament in superfluid helium

It is known that the presence of a heat flow in superfluid helium II if higher than a critical value causes the formation of quantized vortex lines, which move inside the superfluid until a stationary situation is reached, and whose presence is usually investigated by second sound waves (Barenghi et al., 2001; Donnelly, 1991; Nemirovskii and Fiszdon, 1995). The main attractive issue of this situation, known as superfluid turbulence, are quantized vortices, which are filamentous vortices, whose core dimension is of the order of the atomic diameter of the helium atom, of the order of 1 Å, due to the rotational of superfluid component whose circulation is quantized.

From a microscopic point of view, they are described by specifying the whole detailed curve of each vortex line, but from a macroscopic perspective this detailed description is lost and it is usually reduced simply to a scalar quantity L, the *vortex line length density*, i.e.the average length of vortex line per unit volume, having units of $(\text{length})^{-2}$.

Quantized vortices in superfluids have been mainly studied in two typical situations: rotating superfluids and counterflow experiments, the latter meaning the presence of a heat flux, but with zero barycentric motion. In these situations the vortices are modeled, respectively, as an array of parallel rectilinear vortices or as an almost isotropic tangle. In both cases, the mutual force between the normal component and the superfluid due to the presence of vortex lines is well known, and the so-called vortex line tension, due to the curvature of vortex line, is zero (Barenghi et al., 2001; Donnelly, 1991; Nemirovskii and Fiszdon, 1995; Vinen and Niemela, 2002).

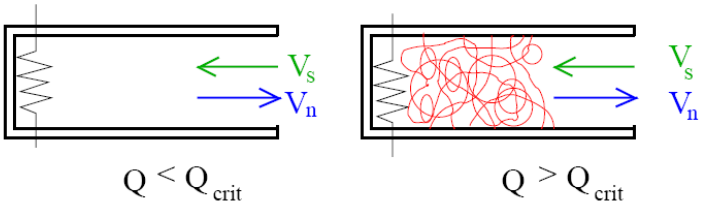

Figure 2.2: Counterflow experiment

When the heat flux inside the channel exceeds a typical heat flux q_c, one observes an extra attenuation of second sound, and this attenuation grows with the square of the heat flux. This attenuation is due to the presence of a damping force, known as *mutual friction*, that finds its origin in the interaction between the flow of excitations and a chaotic tangle of quantized vortex filaments, of equal circulation κ, the so-called *quantum of vorticity* and is given by $\kappa = h/m_4$, with h the Planck constant, and m_4 the mass of ^{4}He atom; it results $\kappa \simeq 9.97\ 10^{-4}\text{cm}^2/\text{s}$.

In order to describe the superfluid turbulence one must introduce a new independent variable L, describing the total vortex line length per unit volume, which has its own evolution equation. More detailed descriptions accounting for anisotropy and polarization of the vortices will be discussed in Section 2.5. The evolution equation for L under constant values of the counterflow velocity $\mathbf{V}_{ns} = \langle \mathbf{v}_n - \mathbf{v}_s \rangle$, (evaluated in a volume small with respect to the channle's dimensions and being $\mathbf{v}_n$ and $\mathbf{v}_s$ the velocities of the normal and superfluid components) and in the absence of inhomogeneities and of rotation was formulated by Vinen. In the simplest case, one takes the so-called

Vinen equation:

$$\frac{\partial L}{\partial t} = \alpha_V \mathbf{V}_{ns} L^{\frac{3}{2}} - \beta_V \kappa L^2, \tag{2.20}$$

with α_V and β_V being the Vinen coefficient (which are functions of T and ρ), that describe the rate of formation and destruction of vortex lines respectively. Equation (2.20) was proposed in (Vinen, 1957), by combining dimensional analysis and physical arguments. More general equations for dL/dt including the influence of the walls, the rotation velocity, or a velocity gradient have been proposed in (Mongiovì and Jou, 2007). Other generalizations will be proposed in this thesis, for inhomogeneous tangles and for convergent (or divergent) channels, in Chapter 5.

To take into account the presence of vortices, neglecting inhomogeneities in the vortex tangle, following (Jou et al., 2002; Mongiovì and Jou, 2007), we choose in the heat flux equation in system (2.9) for the production term σ_i^q the simple expression

$$\sigma_i^q = -KLq_i \qquad \text{with} \qquad K = \frac{1}{3}\kappa B_{HV}, \tag{2.21}$$

where B_{HV} is the dissipative coefficient of the Hall-Vinen mutual friction between the normal and superfluid components, introduced in (Hall and Vinen, 1956). Note that, in this macroscopic hydrodynamical model, a fluid particle is considered to be a small but mesoscopic region threaded by vortex lines.

2.4 Thermodynamic basis and nonlocal model

Often one assumes that the vortex tangle is homogeneous and isotropic, and that it can be described by introducing the scalar quantity L, the average vortex line length per unit volume. In the one-fluid model, this may be imagined as a further independent internal variable, additional to the heat flux, mentioned before, but having a different topological character: a scalar instead of a vector. The isotropy hypothesis is no longer tenable in situations involving counterflow and rotation, or when the influence of the walls becomes important, as for example in flow in small channels. In this case to describe vortex tangle one must consider a tensorial variable, as we will show in Section 2.5. On the other side, also some experiments (Wang et al., 1987) and simulations (Schwarz, 1985, 1988) show that the vortex tangle is always anisotropic. Since the aim of this thesis is the mesoscopic structure of superfluid turbulence, we need equations able to deal with inhomogeneous and anisotropic tangles. Therefore, we must generalize the set of equations (2.9) and (2.20).

A first study of this inhomogeneous and anisotropic vortex tangles using extended thermodynamics was made in (Jou et al., 2002). In that work, the presence of vortices was modeled through a tensor for which a constitutive relation was written. In succes-

sive works (Ardizzone et al., 2009; Mongiovì and Jou, 2007), a model of inhomogeneous superfluid turbulence was formulated, both in the linear and in the nonlinear regime.

In the hydrodynamical model proposed in (Ardizzone et al., 2009, 2011, 2013; Mongiovì and Jou, 2007) the vortex line density L is an independent field, with its own evolution equation. However in (Ardizzone et al., 2009, 2011, 2013; Mongiovì and Jou, 2007) the presence of the viscous forces was neglected and only the friction with vortex lines was considered. Because, in our study, the presence of these forces cannot be omitted, we will use here the system of field equations (2.9) and (2.20) and give some generalizations.

2.4.1 Hydrodynamical model of turbulent superfluids accounting for nonlocal effects

Here we formulate a more general model of superfluid turbulence that takes into account also non local contributions. In particular, we want to deal with inhomogeneous vortex tangles, and to consider tangle diffusion from zones with higher L to lower L, and some other effects. As in (Mongiovì and Jou, 2007), we choose as fundamental fields the density ρ, the velocity $\mathbf{v}$, the energy density $E = \rho\epsilon$, the heat flux $\mathbf{q}$, and the averaged vortex line length per unit volume L.

The starting point is a general set of balance equations for the fields ρ, $\rho\mathbf{v}$, $E = \rho\epsilon + \frac{1}{2}\rho v^2$, $\mathbf{q}$ and L that are written as:

$$\begin{cases} \dot{\rho} + \rho\,\nabla\cdot\mathbf{v} = 0 \\ \rho\dot{\mathbf{v}} + \nabla\cdot\mathbf{J}^{\mathbf{v}} = 0 \\ \dot{E} + E\,\nabla\cdot\mathbf{v} + \nabla\cdot\mathbf{q} + \mathbf{J}^{\mathbf{v}}\cdot\nabla\mathbf{v} = 0 \\ \dot{\mathbf{q}} + \mathbf{q}\,\nabla\cdot\mathbf{v} + \nabla\cdot\mathbf{J}^{\mathbf{q}} = \sigma^{\mathbf{q}} \\ \dot{L} + L\,\nabla\cdot\mathbf{v} + \nabla\cdot\mathbf{J}^{L} = \sigma^{L} \end{cases} \tag{2.22}$$

where $\mathbf{J}^{\mathbf{v}}$ is the stress tensor, $\mathbf{J}^{\mathbf{q}}$ the flux of the heat flux, and $\mathbf{J}^{L}$ the flux of vortex lines. In this system, an upper dot denotes the material time derivative. In (2.22) $\sigma^{\mathbf{q}}$ and σ_L are terms describing the net production of heat flux and vortices (though the flux of vortex lines has a direct and intuitive meaning, the flux of the heat flux is more formal and less intuitive, but it is often used in non-local formulations of heat transfer (Jou et al., 2010); for instance, in ideal gases it is related to the fourth-order moments of the velocity distribution function with respect to the molecular velocity; in phenomenological theories, it may be often expressed in terms of the gradient of the heat flux, as it will be done in (5.5), with measurable coefficients).

This system is analogous to (2.5), (2.6) and (2.20), but with the following differences: **a)** the pressure tensor is called $\mathbf{J^v}$ instead of $\mathbf{m}$, and it is not assumed to be an independent quantity, **b)** the evolution equation for the heat flux and that for the vortex line density contain additional terms in the fluxes $\mathbf{J^q}$ and $\mathbf{J}^L$, which are introduced to describe non-local effects (in other words, typical effects arising in inhomogeneous tangles).

To describe such nonlocal effects, the constitutive equations for the fluxes are assumed to depend not only on the fundamental fields, but also on their first spatial derivative. As a consequence of the material objectivity principle (Muller and Ruggeri, 1998), the expressions of the fluxes are:

$$\mathbf{J^v} = (p - \alpha_1 \nabla \cdot \mathbf{v} - \alpha_2 \nabla \cdot \mathbf{q})\mathbf{U} - \eta_1 \langle \nabla \mathbf{v} \rangle - \eta_2 \langle \nabla \mathbf{q} \rangle, \tag{2.23}$$

$$\mathbf{J^q} = (\beta_0 - \beta_1 \nabla \cdot \mathbf{v} - \beta_2 \nabla \cdot \mathbf{q})\mathbf{U} - \xi_1 \langle \nabla \mathbf{v} \rangle - \xi_2 \langle \nabla \mathbf{q} \rangle, \tag{2.24}$$

$$\mathbf{J}^L = \nu \mathbf{q} + \nu_1 \nabla \rho + \nu_2 \nabla E + \nu_3 \nabla L, \tag{2.25}$$

where p, β_0 and ν are functions of ρ, E and L. For the sake of simplicity here the coefficients α_h, η_h, β_h, ξ_h, and ν_h are assumed constant and they have expressions (1.58), (1.59), (1.61) and (1.62) (with $f^2/\rho^2 = 1$)), relating these coefficient with λ_0, λ_2, β and β' of system (2.9). Angular brackets denote the deviatoric part of the tensors $\nabla \mathbf{v}$ and $\nabla \mathbf{q}$. These constitutive equations introduce new terms in the balance equations (2.22) with respect to the previous models (Ardizzone et al., 2009; Mongiovì and Jou, 2007).

Note that this model, in principle, is similar to that one presented in Chapter 1, but here we have another variable, i.e. L, that describes the superfluid turbulence, instead of the order parameter f, that we assume constant because we are considering that the temperature is sufficiently below the transition temperature. Though f itself may depend on T, on macroscopic grounds ($f = \sqrt{\rho \rho_s}$) this will be reflected trough the dependence of ρ_n and ρ_s on T.

In the following of this chapter we use still the Liu method of Lagrange multipliers, as in the previous chapter, in order to obtain some restriction on the fields equations and to explain the meaning of the Lagrange multipliers. The method retraces the same general steps but the details are different.

2.4.2 Restrictions imposed by the entropy principle

Restrictions on the constitutive equations (2.23), (2.24) and (2.25) for the fluxes can be obtained imposing the validity of the second law of thermodynamics, which states that the rate of entropy production per unit volume is a positive definite quantity, i.e. there exists a convex function S, the entropy per unit volume, and a vector function $\mathbf{J}^S$, the entropy flux density, such that the rate of production of entropy is non-negative.

As in the previous chapter, following the Liu method of Lagrange multipliers, we can consider the equations (2.22) as constraints for the entropy inequality to hold. In the present case, the evolution equations for the fields ρ, $\mathbf{v}$, E, L and $\mathbf{q}$ are affected by multiplying factors Λ^ρ, $\mathbf{\Lambda^v}$, Λ^E, Λ^L and $\mathbf{\Lambda^q}$.

In order to make the theory internally consistent, we must consider for S and $\mathbf{J}^S$ approximate constitutive relations to second order in $\mathbf{q}$ and in the gradients of the fundamental variables:

$$\begin{aligned} S &= S(\rho, E, L, q^2, && (2.26)\\ \mathbf{J}^s &= \phi\mathbf{q} + \phi_1\nabla\rho + \phi_2\nabla E + \phi_3\nabla L + \phi_4\left(\nabla\cdot\mathbf{v}\right)\mathbf{q} \\ &\quad +\phi_5\left(\nabla\cdot\mathbf{q}\right)\,\mathbf{q} + \phi_6\,\mathbf{q}\cdot\langle\nabla\mathbf{v}\rangle + \phi_7\,\mathbf{q}\cdot\langle\nabla\mathbf{q}\rangle, && (2.27)\end{aligned}$$

where $\phi = \phi(\rho, E, L)$ and the other ϕ_h are assumed constant.

Following Liu procedure one obtains the following inequality, which is satisfied for arbitrary values of the field variables,

$$\begin{aligned} \dot{S} &+ S\,\nabla\cdot\mathbf{v} + \nabla\cdot\mathbf{J}^S - \Lambda^\rho\left[\dot\rho + \rho\nabla\cdot\mathbf{v}\right] - \Lambda^{\mathbf{v}}\cdot\left[\rho\dot{\mathbf{v}} + \nabla\cdot\mathbf{J}^{\mathbf{v}}\right] \\ &- \Lambda^E\left[\dot E + E\,\nabla\cdot\mathbf{v} + \nabla\cdot\mathbf{q} + \mathbf{J}^{\mathbf{v}}\cdot\nabla\mathbf{v}\right] - \Lambda^{\mathbf{q}}\cdot\left[\dot{\mathbf{q}} + \mathbf{q}\,\nabla\cdot\mathbf{v} + \nabla\cdot\mathbf{J}^{\mathbf{q}} - \sigma^{\mathbf{q}}\right] \\ &- \Lambda^L\left[\dot L + L\,\nabla\cdot\mathbf{v} + \nabla\cdot\mathbf{J}^L - \sigma^L\right] \geq 0. \qquad (2.28)\end{aligned}$$

In this expression the Lagrange multipliers are supposed objective functions of the fundamental fields and of their first spatial derivatives.

2.4.3 Constitutive restrictions for the fluxes

The constitutive theory is obtained substituting (2.27) in (2.28), taking into account (2.23), (2.24) and (2.25), and imposing that the coefficients of all derivatives must vanish. After some lengthy calculations, in order to consider the derivatives with respect to time, one must have

$$\dot S - \Lambda^\rho\dot\rho - \Lambda^{\mathbf{v}}\rho\dot{\mathbf{v}} - \Lambda^E\dot E - \Lambda^{\mathbf{q}}\cdot\dot{\mathbf{q}} - \Lambda^L\dot L = 0. \qquad (2.29)$$

Because $\dot S = \frac{\partial S}{\partial\rho}\dot\rho + \frac{\partial S}{\partial E}\dot E + \frac{\partial S}{\partial L}\dot L + \frac{\partial S}{\partial q^2}2\mathbf{q}\cdot\dot{\mathbf{q}}$, we obtain the following relations:

$$\Lambda^{\mathbf{v}} = 0, \qquad \frac{\partial S}{\partial\rho} = \Lambda^\rho, \qquad \frac{\partial S}{\partial E} = \Lambda^E, \qquad \frac{\partial S}{\partial L} = \Lambda^L, \qquad \frac{\partial S}{\partial q^2} = \frac{\lambda}{2}, \qquad (2.30)$$

where we have considered the Lagrange multiplier $\mathbf{\Lambda^q}$ proportional to $\mathbf{q}$: $\mathbf{\Lambda^q} = \lambda\mathbf{q}$. Then, we can write the differential of entropy as

$$dS = \Lambda^\rho d\rho + \Lambda^E dE + \Lambda^L dL + \lambda\mathbf{q}\cdot d\mathbf{q}. \qquad (2.31)$$

This is analogous to (1.12), but here we have L instead of the order parameter f as a variable.

Imposing the coefficients of space derivatives of velocity to be zero, we obtain

$$S - \rho\Lambda^{\rho} - \Lambda^{E}(E+p) - \Lambda^{L}L - \mathbf{\Lambda}^{\mathbf{q}} \cdot \mathbf{q} = 0, \tag{2.32}$$

while with respect to the coefficients of space derivatives of $\mathbf{q}$ one has

$$\phi - \Lambda^{E} - \Lambda^{L}\nu = 0. \tag{2.33}$$

Let′s consider now the linear terms in $\mathbf{q}$, and we obtain

$$\frac{\partial \phi}{\partial \rho} = -\lambda \frac{\partial \beta_0}{\partial \rho} - \Lambda^{L}\frac{\partial \nu}{\partial \rho}, \tag{2.34}$$

$$\frac{\partial \phi}{\partial E} = -\lambda \frac{\partial \beta_0}{\partial E} - \Lambda^{L}\frac{\partial \nu}{\partial E}, \tag{2.35}$$

$$\frac{\partial \phi}{\partial L} = -\lambda \frac{\partial \beta_0}{\partial L} - \Lambda^{L}\frac{\partial \nu}{\partial L}, \tag{2.36}$$

i.e.:

$$d\phi = \lambda d\beta_0 + \Lambda^{L} d\nu. \tag{2.37}$$

In the next section, we will determine the implications on the constitutive quantities imposed by relations (2.31) and (2.37). Vanishing the coefficients of the spatial derivatives of the second order of ρ, E, L and $\mathbf{q}$ we still get:

$$\phi_1 = \Lambda^{L}\nu_1, \qquad \phi_2 = \Lambda^{L}\nu_2, \qquad \phi_3 = \Lambda^{L}\nu_3 \tag{2.38}$$

$$\phi_4 = -\lambda\beta_1, \qquad \phi_5 = -\lambda\beta_2, \qquad \phi_6 = -\lambda\xi_1, \qquad \phi_7 = -\lambda\xi_2. \tag{2.39}$$

Using previous relations, we obtain the following expression for the entropy flux density

$$\begin{aligned} \mathbf{J}^{s} = {} & (\Lambda^{E} + \Lambda^{L}\nu)\mathbf{q} + \Lambda^{L}(\nu_1 \nabla\rho + \nu_2 \nabla E + \nu_3 \nabla L) \\ & -\lambda\left[\beta_1 \nabla\cdot\mathbf{v} + \beta_2 \nabla\cdot\mathbf{q} + \xi_1\langle\nabla\mathbf{v}\rangle + \xi_2\langle\nabla\mathbf{q}\rangle\right]\cdot\mathbf{q} \end{aligned} \tag{2.40}$$

Therefore it remains the following inequality

$$\begin{aligned} &\Lambda^{E}\alpha_1(\nabla\cdot\mathbf{v})^2 + (\Lambda^{E}\alpha_2 + \phi_4)(\nabla\cdot\mathbf{v})(\nabla\cdot\mathbf{q}) + \phi_5(\nabla\cdot\mathbf{q})^2 + \Lambda^{E}\eta_1\langle\nabla\mathbf{v}\rangle : \langle\nabla\mathbf{v}\rangle \\ &+(\Lambda^{E}\eta_2 + \phi_6)\langle\nabla\mathbf{v}\rangle : \langle\nabla\mathbf{q}\rangle + \phi_7\langle\nabla\mathbf{q}\rangle : \langle\nabla\mathbf{q}\rangle + \lambda\mathbf{q}\cdot\sigma^{\mathbf{q}} + \Lambda^{L}\sigma^{L} \geq 0, \end{aligned} \tag{2.41}$$

where the colon denotes the double scalar product, i.e. $\langle\nabla\mathbf{q}\rangle : \langle\nabla\mathbf{v}\rangle = \Sigma_{i,j}\langle\nabla\mathbf{q}\rangle_{ij}\langle\nabla\mathbf{v}\rangle_{ji}$. Let's denote in analogy with our analysis in Subsection 1.1.7:

$$A_1 = \Lambda^{E}\alpha_1(\nabla\cdot\mathbf{v})^2 + (\Lambda^{E}\alpha_2 + \phi_4)(\nabla\cdot\mathbf{v})(\nabla\cdot\mathbf{q}) + \phi_5(\nabla\cdot\mathbf{q})^2, \tag{2.42}$$

$$A_2 = \Lambda^{E}\eta_1\langle\nabla\mathbf{v}\rangle : \langle\nabla\mathbf{v}\rangle + (\Lambda^{E}\eta_2 + \phi_6)\langle\nabla\mathbf{v}\rangle : \langle\nabla\mathbf{q}\rangle + \phi_7\langle\nabla\mathbf{q}\rangle : \langle\nabla\mathbf{q}\rangle, \tag{2.43}$$

$$A_3 = \lambda\mathbf{q}\cdot\sigma^{\mathbf{q}} + \Lambda^{L}\sigma^{L}. \tag{2.44}$$

If any A_i is semi-definite positive, the inequality (2.41) is verified, therefore the matrices

$$\begin{bmatrix} \Lambda^E\alpha_1 & \frac{\Lambda^E\alpha_2+\phi_4}{2} \\ \frac{\Lambda^E\alpha_2+\phi_4}{2} & \phi_5 \end{bmatrix} \quad \text{and} \quad \begin{bmatrix} \Lambda^E\eta_1 & \frac{\Lambda^E\eta_2+\phi_6}{2} \\ \frac{\Lambda^E\eta_2+\phi_6}{2} & \phi_7 \end{bmatrix} \tag{2.45}$$

must be semidefinite positive.

Because $\Lambda^E = \frac{dS}{dE} \geq 0$, this implies for A_1:

$$\begin{aligned} &\alpha_1 > 0 \\ &4\Lambda^E\alpha_1\phi_5 - \left(\Lambda^E\alpha_2 + \phi_4\right)^2 \geq 0 \\ &\phi_5 > 0 \end{aligned} \tag{2.46}$$

and for A_2:

$$\begin{aligned} &\eta_1 > 0 \\ &4\Lambda^E\eta_1\phi_7 - \left(\Lambda^E\eta_2 + \phi_6\right)^2 \geq 0 \\ &\phi_7 > 0 \end{aligned} \tag{2.47}$$

Finally, it must be:

$$A_3 = \lambda\mathbf{q}\cdot\sigma^{\mathbf{q}} + \Lambda^L\sigma^L \geq 0 \tag{2.48}$$

The restrictions obtained here are similar to those obtained in the previous chapter, but with L instead of f, which makes that the physical meaning of Λ^L is new, as compared to the previous chapter. For this reason, in the following section we want to explain the physical interpretation of them.

2.4.4 Physical interpretation of the Lagrange multipliers

In this section we analyze the relations obtained in the previous section, in order to single out the physical meaning of the constitutive quantities and of the Lagrange multipliers.

Constitutive relations near equilibrium

We denote with Υ any of the scalar quantities S, Λ^ρ, Λ^E, λ and make the position

$$\Upsilon_0(\rho, E, 0, 0) = \Upsilon_0(\rho, E), \tag{2.49}$$

then, from (2.31), (2.32), (2.33) and (2.37) we obtain:

$$dS_0 = \Lambda_0^\rho d\rho + \Lambda_0^E dE, \tag{2.50}$$

$$S_0 = \rho\Lambda_0^\rho + \Lambda_0^E(E+p), \tag{2.51}$$

$$\phi = \Lambda_0^E, \tag{2.52}$$

$$d\phi = \lambda_0 d\beta_0. \tag{2.53}$$

In this way, if we can identify the reciprocal of Λ_0^E with the thermostatics temperature, we can identify equation (2.50) as the classical Gibbs equation of thermostatics, when $-\frac{\Lambda_0^\rho}{\Lambda_0^E}$ is identified with the "mass chemical potential", μ_0^ρ, i.e.

$$\Lambda_0^E = \left[\frac{\partial S_0}{\partial E}\right]_\rho = \frac{1}{T}, \qquad \text{and} \qquad \mu_0^\rho = -\frac{\Lambda_0^\rho}{\Lambda_0^E} = -T\left[\frac{\partial S_0}{\partial \rho}\right]_E. \tag{2.54}$$

With this assumptions, one can write equations (2.50) and (2.51) in the following form

$$dS_0 = \frac{1}{T}dE - \frac{\mu_0^\rho}{T}d\rho, \tag{2.55}$$

$$\rho\mu_0^\rho = E - TS_0 + p. \tag{2.56}$$

Now we want to show how the presence of vortices modifies the energy density E, and the chemical potential μ_0^ρ, and introduce a new chemical potential linked to the vortex line.

Constitutive relations in the presence of heat flux and vortices

In this subsection the complete mathematical expressions far from equilibrium of the constitutive functions and of the Lagrange multipliers will be analyzed.

First, we introduce the following quantity

$$\theta = \frac{1}{\Lambda_E(\rho, E, L, q^2)}, \tag{2.57}$$

which is a "generalized temperature", that at equilibrium ($L = 0$, $\mathbf{q} = 0$) can be identified with the local equilibrium absolute temperature T, as in the previous subsection. In the following we will choose as fundamental field the quantity θ, instead of the internal energy density E. In agreement with (Jou et al., 2011a), we will call θ "non-equilibrium temperature". In (Jou and Restuccia, 2013) a detailed discussion on different definitions of non-equilibrium temperature in systems with internal variables have been made, because in equilibrium states, all the different definitions of temperature lead to the same value, but in non-equilibrium they lead to different values.

In (Mongiovì and Jou, 2007) it was shown that, near equilibrium (i.e. neglecting terms of second order in $\mathbf{q}$), the quantities $-\Lambda^\rho/\Lambda^E$ and $-\Lambda^L/\Lambda^E$ can be interpreted as the equilibrium mass chemical potential and the equilibrium vortex line density chemical potential. Also in this nonlocal model we define as non-equilibrium chemical potentials the quantities

$$\mu_\rho = -\frac{\Lambda_\rho}{\Lambda_E}, \qquad \text{and} \qquad \mu_L = -\frac{\Lambda_L}{\Lambda_E}, \tag{2.58}$$

respectively the "mass chemical potential" and the "chemical potential of vortex line density". For them, we can take the expression

$$\mu_\rho(T,C) = \mu_{\rho 0} + KT\ln\left(\frac{\alpha_C}{C^*}\right) \qquad \text{and} \qquad \mu_L(T,L) = \mu_{L0} + \epsilon_V \ln\left(\frac{L}{L^*}\right), \tag{2.59}$$

where C^* and L^* are a reference mass density and vortex line density. The latter, L^*, defined as the average length $< l >$ of the vortex loops composing the tangle, divided by the volume of the system, namely $L^* = \frac{<l>}{V}$, then $\ln\left(\frac{L}{L^*}\right)$ vanishes when there is only one vortex loop in the whole volume, and ϵ_V is the energy per unit length of the vortex line, defined as $\epsilon_V = \rho_s \frac{\kappa^2}{4\pi} \ln\left(\frac{c}{a_0 L^{\frac{1}{2}}}\right)$, with a_0 the radius of vortex core and c a constant of order 1. Usually one takes ϵ_V as constant, because its dependence on L is very mild. The coefficient α_C in (2.59_a) is 1 for ideal systems, and it is called the "activity" coefficient $\alpha(T,C)$ in non-ideal systems. The term $\mu_{\rho 0}$ depends only on temperature. Note that KT is related to the average thermal energy per particle, whereas ϵ_V is the energy per unit length of vortex line. Thus, they play analogous roles in (2.59).

Introducing in equations (2.31), (2.32), (2.33) and (2.37) the non-equilibrium quantities (2.58), one obtains:

$$\theta dS = dE - \mu_\rho d\rho - \mu_L dL + \frac{1}{2}\theta\lambda dq^2, \tag{2.60}$$

$$\theta S = E + p - \rho\mu_\rho - L\mu_L + \theta\lambda q^2, \tag{2.61}$$

$$\phi = \frac{1}{\theta} - \frac{\mu_L}{\theta}\nu, \tag{2.62}$$

$$d\phi = \lambda d\beta_0 - \frac{\mu_L}{\theta} d\nu. \tag{2.63}$$

From equations (2.60) and (2.61), denoting with $\tilde{s} = S/\rho$ the non-equilibrium entropy per unit mass, one deduces that the non-equilibrium chemical potentials μ_ρ and μ_L must satisfy the relation

$$\rho\mu_\rho + L\mu_L = \rho\epsilon - \theta\rho\tilde{s} + p + \theta\lambda q^2. \tag{2.64}$$

Then, the complete expression of the non-equilibrium Gibbs equation becomes

$$\theta d\tilde{s} = d\epsilon - \frac{1}{\rho^2}\left(p - \mu_L - \theta\lambda q^2\right) d\rho - \frac{\mu_L}{\rho} dL + \frac{\theta\lambda}{2\rho} dq^2. \tag{2.65}$$

From equations (2.60) or (2.65) one can obtain the conditions on the non-equilibrium chemical potentials and on the derivative of energy density. From (2.60) we have

$$dS = \frac{1}{\theta}(E_\rho - \mu_\rho)d\rho + \frac{1}{\theta}E_\theta d\theta + \frac{1}{\theta}(E_L - \mu_L)dL + \left(\frac{1}{\theta}E_{q^2} + \frac{1}{2}\lambda\right) dq^2 \tag{2.66}$$

and then the following relations must be verified for it to be an exact differential,

$$\frac{\partial}{\partial\theta}\left(\frac{E_\rho}{\theta}-\frac{\mu_\rho}{\theta}\right)=\frac{\partial}{\partial\rho}\left(\frac{E_\theta}{\theta}\right) \qquad \Rightarrow \qquad E_\rho=\mu_\rho-\theta\frac{\partial\mu_\rho}{\partial\theta} \tag{2.67}$$

$$\frac{\partial}{\partial L}\left(\frac{E_\rho}{\theta}-\frac{\mu_\rho}{\theta}\right)=\frac{\partial}{\partial\rho}\left(\frac{E_L}{\theta}-\frac{\mu_L}{\theta}\right) \qquad \Rightarrow \qquad \frac{\partial\mu_\rho}{\partial L}=\frac{\partial\mu_L}{\partial\rho} \tag{2.68}$$

$$\frac{\partial}{\partial q^2}\left(\frac{E_\rho}{\theta}-\frac{\mu_\rho}{\theta}\right)=\frac{\partial}{\partial\rho}\left(\frac{E_{q^2}}{\theta}+\frac{1}{2}\lambda\right) \qquad \Rightarrow \qquad \frac{\partial\mu_\rho}{\partial q^2}=0 \tag{2.69}$$

$$\frac{\partial}{\partial L}\left(\frac{E_\theta}{\theta}\right)=\frac{\partial}{\partial\theta}\left(\frac{E_L}{\theta}-\frac{\mu_L}{\theta}\right) \qquad \Rightarrow \qquad E_L=\mu_L-\theta\frac{\partial\mu_L}{\partial\theta} \tag{2.70}$$

$$\frac{\partial}{\partial q^2}\left(\frac{E_\theta}{\theta}\right)=\frac{\partial}{\partial\theta}\left(\frac{E_{q^2}}{\theta}+\frac{1}{2}\lambda\right) \qquad \Rightarrow \qquad E_{q^2}=0 \tag{2.71}$$

$$\frac{\partial}{\partial q^2}\left(\frac{E_L}{\theta}-\frac{\mu_L}{\theta}\right)=\frac{\partial}{\partial L}\left(\frac{E_{q^2}}{\theta}+\frac{1}{2}\lambda\right) \qquad \Rightarrow \qquad \frac{\partial\mu_L}{\partial q^2}=0 \tag{2.72}$$

In particular, (2.68) shows that μ_ρ and μ_L must be mutually coupled, in such a way that expressions (2.59) should be generalized to exibit this coupling. For instance, the functions $\mu_{\rho 0}(T)$ and $\mu_{L0}(T)$ could become $\mu_{\rho 0}(T,L)$ and $\mu_{L0}(T,\rho)$.

Finally, we consider the consequences of equations (2.62) and (2.63) which concerns the expressions of the fluxes. Using definitions (2.57) and (2.58_b), we get

$$\lambda d\beta_0=d\left(\frac{1}{\theta}\right)-\nu d\left(\frac{\mu_L}{\theta}\right). \tag{2.73}$$

It is useful to make the following positions:

$$\gamma = \frac{\partial\beta_0}{\partial\rho}=-\frac{\nu}{T\lambda}\frac{\partial\mu_L}{\partial\rho} \tag{2.74}$$

$$\zeta = \frac{\partial\beta_0}{\partial\theta}=-\frac{1}{\theta^2\lambda}\left[1+\nu\theta^2\frac{\partial}{\partial\theta}\left(\frac{\mu_L}{\theta}\right)\right], \tag{2.75}$$

$$\chi = \frac{\partial\beta_0}{\partial L}=-\frac{\nu}{\theta\lambda}\frac{\partial\mu_L}{\partial L}. \tag{2.76}$$

The following relation must be verified too:

$$\frac{\partial\gamma}{\partial L}=\frac{\partial\chi}{\partial\rho} \qquad \Rightarrow \qquad \frac{\partial\nu}{\partial L}\frac{\partial\mu_L}{\partial\rho}=\frac{\partial\nu}{\partial\rho}\frac{\partial\mu_L}{\partial L} \tag{2.77}$$

$$\frac{\partial\gamma}{\partial\theta}=\frac{\partial\zeta}{\partial\rho} \qquad \Rightarrow \qquad \frac{\partial\nu}{\partial\theta}\frac{\partial\mu_L}{\partial\rho}=\frac{\partial\nu}{\partial\rho}\left(\frac{\partial\mu_L}{\partial\theta}-\frac{\mu_L}{\theta}\right) \tag{2.78}$$

$$\frac{\partial\zeta}{\partial L}=\frac{\partial\chi}{\partial\theta} \qquad \Rightarrow \qquad \frac{\partial\nu}{\partial\theta}\frac{\partial\mu_L}{\partial L}=\frac{\partial\nu}{\partial L}\left(\frac{\partial\mu_L}{\partial\theta}-\frac{\mu_L}{\theta}\right) \tag{2.79}$$

Note that, if $\nu=0$, one gets $\chi=0$ too, and

$$\zeta=-\frac{1}{\theta^2\lambda}, \tag{2.80}$$

and this expression is identical to that found in (Mongiovì, 2000a) in the study of laminar flows of non viscous fluids in the presence of heat flux near equilibrium.

The coefficient λ may be interpreted as

$$\lambda = -\frac{\tau}{k\theta^2}, \tag{2.81}$$

with τ the relaxation time of the heat flux and k the thermal conductivity, these quantities can be identified with τ_1 and λ_1 for He II, introduced in (2.6_c), and their ratio is finite. Expression (2.81) is also found in extended irreversible thermodynamics of usual fluids and solids (Jou et al., 2011a; Lebon et al., 2008), and therefore is more general than for superfluids.

2.4.5 Field equations

Introducing in system (2.22) the expressions for the fluxes (2.23), (2.24) and (2.25) and using the new variable θ, we obtain:

$$\begin{cases} \dot{\rho} + \rho\,\nabla\cdot\mathbf{v} = 0 \\ \\ \rho\dot{\mathbf{v}} + \nabla\cdot[(p - \alpha_1\nabla\cdot\mathbf{v} - \alpha_2\nabla\cdot\mathbf{q})\mathbf{U} - \eta_1\langle\nabla\mathbf{v}\rangle - \eta_2\langle\nabla\mathbf{q}\rangle] = 0 \\ \\ \frac{\partial E}{\partial\theta}\dot{\theta} + \frac{\partial E}{\partial\rho}\dot{\rho} + \frac{\partial E}{\partial L}\dot{L} + E\,\nabla\cdot\mathbf{v} + \nabla\cdot\mathbf{q} + \\ \qquad + [(p - \alpha_1\nabla\cdot\mathbf{v} - \alpha_2\nabla\cdot\mathbf{q})\mathbf{U} - \eta_1\langle\nabla\mathbf{v}\rangle - \eta_2\langle\nabla\mathbf{q}\rangle]\cdot\nabla\mathbf{v} = 0 \\ \\ \dot{\mathbf{q}} + \mathbf{q}\,\nabla\cdot\mathbf{v} + \nabla\cdot[(\beta_0 - \beta_1\nabla\cdot\mathbf{v} - \beta_2\nabla\cdot\mathbf{q})\mathbf{U} - \xi_1\langle\nabla\mathbf{v}\rangle - \xi_2\langle\nabla\mathbf{q}\rangle] = \sigma^{\mathbf{q}} \\ \\ \dot{L} + L\,\nabla\cdot\mathbf{v} + \nabla\cdot[\nu\mathbf{q} + \nu_1\nabla\rho + \nu_2\nabla E + \nu_3\nabla L] = \sigma^{L} \end{cases} \tag{2.82}$$

These are the most general evolution equations accounting for nonlocal effects, compatible with the second law of thermodynamics, once $\sigma^{\mathbf{q}}$ and σ^{L} obeying the restriction (2.48) are choosen.

Choice of the source terms $\sigma^{\mathbf{q}}$ and σ^{L}

As production terms in the equations for the heat flux $\mathbf{q}$ and vortex line density L in (2.22_c) and (2.22_d), we choose the following expressions:

$$\sigma^{\mathbf{q}} = -N_1 L\boldsymbol{\Pi}\cdot\mathbf{q} + N_2 L^{3/2}\left(B\mathbf{I} + B''\mathbf{J}\right), \tag{2.83}$$

$$\sigma^{L} = \tilde{\gamma}_1 L^{3/2}\left(B\mathbf{I} + B''\mathbf{J}\right)\cdot\mathbf{q} - \gamma_2 L^2, \tag{2.84}$$

where coefficients B, B'', N_1, N_2, $\tilde{\gamma}_1$ and γ_2, vectors $\mathbf{I}$ and $\mathbf{J}$ (Donnelly, 1991; Schwarz, 1988), related to the polarization of the tangle, and tensor $\boldsymbol{\Pi}$, related to anisotropy of the tangle, will be defined in Section 2.5, where a detailed microscopic motivation of

this choice can be found. Let us emphasize that (2.84) combining with (2.22_e) yields a generalization of the Vinen equation for anisotropic tangles of vortices. Expressions (2.83) and (2.84) of the production terms can be written in the matrix form as

$$\begin{bmatrix} \sigma^{\mathbf{q}} \\ \\ \sigma^{L} \end{bmatrix} = L \begin{bmatrix} -\frac{N_1}{\lambda}\mathbf{\Pi} & \frac{N_2}{\Lambda_L} L^{\frac{1}{2}} \left(B\mathbf{I} + B''\mathbf{J}\right) \\ \\ \frac{\tilde{\gamma}_1}{\lambda} L^{\frac{1}{2}} \left(B\mathbf{I} + B''\mathbf{J}\right) & -\frac{\gamma_2}{\Lambda^L} L \end{bmatrix} \begin{bmatrix} \lambda\mathbf{q} \\ \\ \Lambda^L \end{bmatrix} \tag{2.85}$$

where, as a consequence of the Onsager reciprocity relations, it must be:

$$\Lambda^L \tilde{\gamma}_1 = \lambda N_2.$$

Let′s consider the quantity A_3, defined in (2.44) and (2.48), that is written, according to (2.85) as

$$A_3 = L\left[-N_1\lambda\mathbf{q}\cdot\mathbf{\Pi}\cdot\mathbf{q} + (\lambda N_2 + \Lambda_L\tilde{\gamma}_1)L^{1/2}\left(B\mathbf{I} + B''\mathbf{J}\right)\cdot\mathbf{q} - \Lambda^L\gamma_2 L\right] \geq 0, \tag{2.86}$$

and we determine some conditions under particular hypotheses. We will suppose $\mathbf{\Pi}$ to be the unit matrix $\mathbf{U}$ (isotropic tangle). Assume further that vector $\mathbf{I}$ is collinear with $\mathbf{q}$ ($B\mathbf{I} = H\hat{\mathbf{q}}$) and $\mathbf{J} = 0$ (non-polarized tangle). Under these assumptions, $\sigma^{\mathbf{q}}$ and σ^L simplify as

$$\sigma^{\mathbf{q}} = -N_1 L\mathbf{q} + N_2 H L^{3/2}\frac{\mathbf{q}}{|\mathbf{q}|}, \tag{2.87}$$

$$\sigma^{L} = \tilde{\gamma}_1 H L^{3/2}|\mathbf{q}| - \gamma_2 L^2. \tag{2.88}$$

Then (2.88) coincides with (2.20) and the first term in (2.87) coincides with (2.21). In this case the quantity A_3 is written

$$A_3 = L\left[-N_1\lambda q^2 + H(\lambda N_2 + \Lambda_L\tilde{\gamma}_1)L^{1/2}|q| - \Lambda^L\gamma_2 L\right] \geq 0. \tag{2.89}$$

This quantity is non negative *iff* the matrix

$$\begin{bmatrix} -\lambda N_1 & \frac{1}{2}H\left(\lambda N_2 + \Lambda^L\tilde{\gamma}_1\right) \\ \\ \frac{1}{2}H\left(\lambda N_2 + \Lambda^L\tilde{\gamma}_1\right) & -\Lambda^L\gamma_2 \end{bmatrix} \tag{2.90}$$

is semidefinite positive. Being positive the coefficients N_1, N_2, $\tilde{\gamma}_1$, γ_2, this implies $\lambda \leq 0$, $\Lambda^L \leq 0$ and $4\lambda\Lambda^L N_1\gamma_2 - H^2\left(\lambda N_2 + \Lambda^L\tilde{\gamma}_1\right)^2 \geq 0$.

Evolution equations for q and L

Introducing the source terms (2.83) and (2.84) in the evolution equations for $\mathbf{q}$ and L in (2.82), which are the basic equations to be explored along this thesis in different

physical situations, we obtain:

$$\begin{aligned}\dot{\mathbf{q}} &+ \mathbf{q}\nabla\cdot\mathbf{v} + \nabla\beta_0 - \nabla\cdot[(\beta_1\nabla\cdot\mathbf{v} + \beta_2\nabla\cdot\mathbf{q})\mathbf{U} + \xi_1\langle\nabla\mathbf{v}\rangle + \xi_2\langle\nabla\mathbf{q}\rangle] = \\ &= -N_1 L\mathbf{\Pi}\cdot\mathbf{q} + N_2 L^{3/2}\left(B\mathbf{I} + B''\mathbf{J}\right), \qquad (2.91)\\ \dot{L} &+ L\nabla\cdot\mathbf{v} + \nabla\cdot(\nu\mathbf{q} + \nu_1\nabla\rho + \nu_2\nabla E + \nu_3\nabla L) = \\ &= \tilde{\gamma}_1 L^{3/2}\left(B\mathbf{I} + B''\mathbf{J}\right)\cdot\mathbf{q} - \gamma_2 L^2. \qquad (2.92)\end{aligned}$$

These are the most general evolution equations for $\mathbf{q}$ and L, compatible with the second law of thermodynamics. Here, they have a very formal aspect, but we will explore in detail the physical meaning and consequences of each term in Section 2.5, and we will become fully acquainted with them.

2.5 Microscopic derivation of the source terms

To determine the expressions of the source terms (2.83)–(2.84) we recall that they are a consequence, at a microscopic level, of the interaction between the superfluid vortices and the elementary excitations; the latter, in the terminology of the two-fluid model, constitute the normal component. These interactions lead to a force $\mathbf{F}_{ns}$, named mutual friction force, but also an additional term $\mathbf{T}$ tied to the vortex tension, is present.

As shown in (Donnelly, 1991; Jou et al., 2002), the microscopic expression of the mutual friction force per unit length of the vortex is

$$\mathbf{f}_{MF} = \alpha\rho_s\kappa\mathbf{s}'\times[\mathbf{s}'\times(\mathbf{v}_{ns} - \mathbf{v}_\mathbf{i})] + \alpha'\rho_s\kappa\mathbf{s}'\times(\mathbf{v}_{ns} - \mathbf{v}_\mathbf{i}), \qquad (2.93)$$

where $\mathbf{s}'$ is the tangent unit vector to the position vector $\mathbf{s}(\xi)$ of the quantized vortex line (being ξ the arc-length), α and α' are dimensionless, temperature dependent coefficients, $\mathbf{v}_{ns} = \mathbf{v}_n - \mathbf{v}_s$ is the microscopic counterflow velocity, $\mathbf{v}_\mathbf{i}$ the self-induced velocity, that can be described in the "local induction approximation", that is, ignoring contributions coming from the nonlocal portion of the vortex, (Donnelly, 1991)

$$\mathbf{v}_\mathbf{i} \simeq \mathbf{v}_\mathbf{i}^{(loc)} = \tilde{\beta}\left[\mathbf{s}'\times\mathbf{s}''\right], \qquad (2.94)$$

where $\mathbf{s}''$ is the curvature of the quantized vortex line described by $\mathbf{s}(\xi)$, and $\tilde{\beta}$ is the vortex tension parameter, that is linked to the energy per unit length of vortex line ϵ_V by the relation (Donnelly, 1991)

$$\epsilon_V = \kappa\rho_s\tilde{\beta}. \qquad (2.95)$$

The intensity of $\mathbf{v}_\mathbf{i}$ is $|\mathbf{v}_\mathbf{i}| \simeq \tilde{\beta}/R$, with R the curvature radius of the vortex line. The self-induced velocity is zero if the vortices are straight lines (namely, if $\mathbf{s}'' = 0$).

In the evolution equations for the averaged velocities of normal and superfluid components (that we will denote with capital letters), the "macroscopic" mutual friction

force $\mathbf{F}_{ns}$ per unit volume which superfluid and normal components mutually exert, is obtained by averaging (2.93) over a small volume Λ and multiplying by L. One obtains

$$\mathbf{F}_{ns} = L\langle \mathbf{f}_{MF} \rangle = \alpha \rho_s \kappa L \langle \mathbf{s}' \times [\mathbf{s}' \times (\mathbf{v}_{ns} - \mathbf{v_i})] \rangle + \alpha' \rho_s \kappa L \langle \mathbf{s}' \times (\mathbf{v}_{ns} - \mathbf{v_i}) \rangle, \tag{2.96}$$

where angular brackets denote average. The macroscopic vortex tension force $\mathbf{T}$ is expressed as (Donnelly, 1991; Jou et al., 2010)

$$\mathbf{T} = \kappa L \langle \mathbf{v_i} \times \mathbf{s}' \rangle. \tag{2.97}$$

Note that for straight vortex lines $\mathbf{T} = 0$, because for them the induced velocity $\mathbf{v_i}$, (2.94) is zero. Using the local-induction approximation and neglecting the fluctuations of the relative velocity $\mathbf{V}_{ns}$, see (Jou et al., 2010), we deduce that $\mathbf{F}_{ns}$ and $\mathbf{T}$ can be written

$$\mathbf{F}_{ns} = L\left[-\frac{2}{3}\alpha \rho_s \kappa \mathbf{\Pi} \cdot \mathbf{V}_{ns} + \epsilon_V c_1 L^{1/2} \left(\alpha \mathbf{I} + \alpha' \mathbf{J} \right) \right], \tag{2.98}$$

$$\rho_s \mathbf{T} = \rho_s \kappa \tilde{\beta} L^{3/2} c_1 \mathbf{J} = \epsilon_V c_1 L^{3/2} \mathbf{J}, \tag{2.99}$$

where we have introduced the tensor $\mathbf{\Pi} = \mathbf{\Pi}^s + \mathbf{\Pi}^a$ (Jou and Mongiovì, 2006), with

$$\mathbf{\Pi}^s \equiv \frac{3}{2} < \mathbf{U} - \mathbf{s}'\mathbf{s}' >, \qquad \mathbf{\Pi}^a \equiv \frac{3}{2}\frac{\alpha'}{\alpha} < \mathbf{W} \cdot \mathbf{s}' >, \tag{2.100}$$

with $\mathbf{U}$ the unit matrix, $\mathbf{s}'\mathbf{s}'$ the diadic product, and $\mathbf{W}$ the Ricci tensor (a completely antisymmetric third-order tensor such that $\mathbf{W} \cdot \mathbf{s}' \cdot \mathbf{V}_{ns} = -\mathbf{s}' \times \mathbf{V}_{ns}$). The vectors $\mathbf{I}$ and $\mathbf{J}$ are defined as (Donnelly, 1991; Schwarz, 1988)

$$\mathbf{I} \equiv \frac{\int \mathbf{s}' \times \mathbf{s}'' d\xi}{\int |\mathbf{s}''| d\xi}, \qquad \mathbf{J} \equiv \frac{\int \mathbf{s}'' d\xi}{\int |\mathbf{s}''| d\xi}, \tag{2.101}$$

and $c_1 = \frac{1}{\Lambda L^{3/2}} \int |\mathbf{s}''| d\xi$.

Observe again that the tension of the vortex line is zero in pure rotation with parallel straight vortex lines and in isotropic tangles, but it is not so in the presence of simultaneous counterflow and rotation (Jou and Mongiovì, 2004; Mongiovì and Jou, 2005c) or in the first stages of the turbulence (Mongiovì and Jou, 2005b) or in the transient states after sudden acceleration in plane Couette and Poiseuille flow (Jou et al., 2008).

In homogeneous situations, the dynamical equations for the average normal and superfluid velocities, in an inertial frame, are:

$$\rho_n \frac{d\mathbf{V}_n}{dt} = \mathbf{F}_{ns}, \qquad \rho_s \frac{d\mathbf{V}_s}{dt} = -\mathbf{F}_{ns} - \rho_s \mathbf{T}. \tag{2.102}$$

The evolution equation for the counterflow velocity $\mathbf{V}_{ns}$ is

$$\rho_s \frac{d\mathbf{V}_{ns}}{dt} = \frac{\rho}{\rho_n} \mathbf{F}_{ns} + \rho_s \mathbf{T}, \tag{2.103}$$

and can be written, using the expressions (2.98) and (2.99) for $\mathbf{F}_{ns}$ and $\mathbf{T}$ and taking in mind the relations $\alpha = B(\rho_n/2\rho)$, $\alpha' = B'(\rho_n/2\rho)$, where B_{HV} and B'_{HV} are the Hall-Vinen coefficients (Donnelly, 1991)

$$\rho_s \frac{d\mathbf{V}_{ns}}{dt} = L\left[-\frac{1}{3}\rho_s B_{HV}\kappa\mathbf{\Pi}\cdot\mathbf{V}_{ns} + \frac{1}{2}\epsilon_V c_1 L^{1/2}\left(B_{HV}\mathbf{I} + B'_{HV}\mathbf{J}\right)\right] + \epsilon_V L^{3/2} c_1 \mathbf{J}. \tag{2.104}$$

The evolution equation for the heat flux $\mathbf{q}$ ($\mathbf{q} = \rho_s T s \mathbf{V}_{ns}$), neglecting nonlinear contributions and assuming a homogeneous situation, is therefore

$$\frac{d\mathbf{q}}{dt} = L\left[-\frac{1}{3}\kappa B_{HV}\mathbf{\Pi}\cdot\mathbf{q} + \frac{1}{2}Ts\epsilon_V c_1 L^{1/2}\left(B_{HV}\mathbf{I} + B''\mathbf{J}\right)\right] \tag{2.105}$$

where we have put $B'' = B'_{HV} + 2$. Here we will choose as source terms in the evolution equation for the heat flux the right-hand side of equation (2.105).

In order to determine the source term in the evolution equation for L, we consider the following extension of Vinen equation, proposed in (Mongiovì et al., 2007), where the authors were interested to study wall effects on the evolution of L,

$$\frac{dL}{dt} = c_1 L^{3/2}\left(\alpha\mathbf{I} + \alpha'\mathbf{J}\right)\cdot\mathbf{V}_{ns} - \alpha\tilde{\beta}c_2 L^2, \tag{2.106}$$

with c_1, $\mathbf{I}$ and $\mathbf{J}$ defined in equations (2.101), c_1 in the line below (2.101), and $c_2 = \frac{1}{\Lambda L^2}\int |\mathbf{s}''|^2 d\xi$. Equation (2.106), using the variable $\mathbf{q}$ instead of the variable $\mathbf{V}_{ns}$, is written

$$\frac{dL}{dt} = \frac{s}{2\zeta^*} c_1 L^{3/2}\left(B_{HV}\mathbf{I} + B'_{HV}\mathbf{J}\right)\cdot\mathbf{q} - \frac{Ts^2}{2\zeta^*}\frac{\epsilon_V}{\kappa} B_{HV} c_2 L^2, \tag{2.107}$$

where we have put:

$$\zeta^* = \frac{\rho\rho_s T s^2}{\rho_n}. \tag{2.108}$$

As shown in (Mongiovì, 1993, 2001), the coefficient ζ^* determines the second sound velocity (in the laminar regime).

Now, we will show that a modification of this equation is necessary to insure the thermodynamic consistency of the evolution equations for L and for $\mathbf{q}$, according to the formalism of linear irreversible thermodynamics (de Groot and Mazur, 1962; Jou and Mongiovì, 2005; Lebon et al., 2008). We analyze the consequences of the Onsager-Casimir reciprocity relations on the evolution equations of $\mathbf{q}$ and L, showing that an additional term linked to the tension of vortices must be added in the evolution equation for vortex line density. Accordingly the evolution equations for $\mathbf{q}$ and L must be written in terms of $\Lambda^{\mathbf{q}} = \lambda\mathbf{q}$ and Λ^L in matrix form, in the following way

$$\begin{bmatrix} \frac{d\mathbf{q}}{dt} \\ \\ \frac{dL}{dt} \end{bmatrix} = L \begin{bmatrix} -\frac{1}{3\lambda}\kappa B_{HV}\mathbf{\Pi} & \frac{Ts\epsilon_V}{2\Lambda^L} c_1 L^{1/2}\left(B_{HV}\mathbf{I} + B''\mathbf{J}\right) \\ \\ \frac{s}{2\lambda\zeta^*} c_1 L^{1/2}\left(B_{HV}\mathbf{I} + B''\mathbf{J}\right) & \frac{T s^2}{2\zeta^*\Lambda^L}\frac{\epsilon_V}{\kappa} c_2 L \end{bmatrix} \begin{bmatrix} \lambda\mathbf{q} \\ \\ \Lambda^L \end{bmatrix} \tag{2.109}$$

Further, to satisfy the Onsager-Casimir reciprocity relations, it must be:

$$\frac{T\epsilon_V}{\Lambda^L} = \frac{1}{\lambda\zeta^*} \qquad \rightarrow \qquad \lambda = \frac{\Lambda^L}{T\epsilon_V\zeta^*}. \tag{2.110}$$

So, the evolution equation for the vortex line density L must be modified in

$$\frac{dL}{dt} = \frac{s}{2\zeta^*}c_1 L^{3/2}\left(B_{HV}\mathbf{I} + (B'_{HV}+2)\mathbf{J}\right)\cdot\mathbf{q} - \frac{T\,s^2}{2\zeta^*}\frac{\epsilon_V}{\kappa}B_{HV}c_2L^2, \tag{2.111}$$

We choose finally, as production terms in the evolution equations for $\mathbf{q}$ and L, the following quantities:

$$\sigma^{\mathbf{q}} = -N_1 L\boldsymbol{\Pi}\cdot\mathbf{q} + N_2 L^{3/2}\left(B_{HV}\mathbf{I} + B''\mathbf{J}\right) \tag{2.112}$$

$$\sigma^{L} = \tilde{\gamma}_1 L^{3/2}\left(B_{HV}\mathbf{I} + B''\mathbf{J}\right)\cdot\mathbf{q} - \gamma_2 L^2, \tag{2.113}$$

where we have put:

$$N_1 = \frac{1}{3}\kappa B_{HV}, \qquad N_2 = \frac{Ts\epsilon_V}{2}c_1, \qquad \tilde{\gamma}_1 = \frac{s}{2\zeta^*}c_1, \qquad \gamma_2 = \frac{T\,s^2}{2\zeta^*}\frac{\epsilon_V}{\kappa}c_2B_{HV}.$$

These expressions coincide with (2.83) and (2.84) but they provide microscopic interpretations, for the corresponding coefficients. The expressions of the production terms, written in matrix form, are:

$$\begin{bmatrix} \sigma^{\mathbf{q}} \\ \\ \sigma^{L} \end{bmatrix} = L \begin{bmatrix} -\frac{N_1}{\lambda}\boldsymbol{\Pi} & \frac{N_2}{\Lambda_L}L^{\frac{1}{2}}\left(B_{HV}\mathbf{I} + B''\mathbf{J}\right) \\ \\ \frac{\tilde{\gamma}_1}{\lambda}L^{\frac{1}{2}}\left(B_{HV}\mathbf{I} + B''\mathbf{J}\right) & -\frac{\gamma_2}{\Lambda^L}L \end{bmatrix} \begin{bmatrix} \lambda\mathbf{q} \\ \\ \Lambda^L \end{bmatrix} \tag{2.114}$$

2.6 Remarks

In this chapter we recalled the basic equations for the study of superfluid helium in presence of turbulence in the two frameworks of the two-fluid model and of the one-fluid model, comparing the two models.

Furthermore, we have reexamined and generalized a previous thermodynamic derivation of non-local effects in inhomogeneous vortex tangles (Mongiovì and Jou, 2007) to get expressions for $\dot{E}$, $\dot{\mathbf{v}}$, $\dot{\mathbf{q}}$ and $\dot{L}$. The main contributions have been the incorporation of non-local terms in the evolution equation for the heat flux, namely, the terms in ξ_1 and β_1, and a detailed discussion of the physical meaning of the several terms, also from a microscopic point of view.

- Some results are published in:
  L. Saluto *Nonlocal model of Superfluid Turbulence: Constitutive Theory*,
  Bollettino di Matematica Pura e Applicata **Vol. V** 165–175 (2013), Aracne Ed.

In (2.91) and (2.92) we have incorporated a way to describe the effects of quantization, anisotropy and inhomogeneity of the vortex tangle on the evolution equations for $\mathbf{q}$ and L. Finally we have provided a microscopic interpretation of the quantities appearing in the source terms of the evolution equations for $\mathbf{q}$ and L.

2.7 Appendix 2.A: Comments on the entropy and entropy flux

In this appendix we discuss the form of the entropy and the entropy flux obtained in (2.31) and (2.40) as compared with the expressions obtained from microscopic arguments based on information theory, and also some additional aspects of the physical meaning of the Lagrange multipliers. In particular, the discussion on Λ^E lead us to discuss two different contributions to the internal energy and entropy of the system: that of the thermal motions of normal and superfluid components, and that of the tangle, related to the kinetic energy of the rotating superfluid around the vortex core. This is helpful to have a microscopic understanding of the several terms and a wider view on several thermodynamic formalisms.

If we choose $\beta_0 = \beta_1 = \nu_1 = \xi_1 = 0$ in (2.24), the expression for the entropy flux (2.40) is written

$$\mathbf{J}^S = (\Lambda^E + \Lambda^L \nu)\mathbf{q} + \Lambda^L(\nu_2 \nabla E + \nu_3 \nabla L) + \lambda \mathbf{q}\left(-\beta_2 \nabla \cdot \mathbf{q} - \xi_2 \langle \nabla \mathbf{q} \rangle\right), \tag{2.115}$$

and $\mathbf{J}^{\mathbf{q}}$ is

$$\mathbf{J}^{\mathbf{q}} = -\beta_2 (\nabla \cdot \mathbf{q})\mathbf{U} - \xi_2 \langle \nabla \mathbf{q} \rangle. \tag{2.116}$$

Furthermore, if we consider ρ constant, $\mathbf{J}^L$ is written

$$\mathbf{J}^L = \nu \mathbf{q} + \nu_2 \nabla E + \nu_3 \nabla L, \tag{2.117}$$

and expression (2.31) for the entropy differential becomes

$$dS = \Lambda^E dE + \Lambda^L dL + \lambda \mathbf{q} \cdot d\mathbf{q}. \tag{2.118}$$

It is interesting to compare the expression for the entropy flux (2.115) with those obtained from microscopic arguments based on maximun-entropy formalism (Domínguez-Cascante and Jou, 1998; Luzzi et al., 2001, 2002). One can observe that considering (2.116) and (2.117), (2.115) may be written in a more compact form as

$$\mathbf{J}^S = \Lambda^E \mathbf{q} + \Lambda^L \mathbf{J}^L + \Lambda^{\mathbf{q}} \cdot \mathbf{J}^{\mathbf{q}}. \tag{2.119}$$

Here we want comment the microscopic origin of (2.119).

In information theory one obtains the distribution function by maximizing the entropy under the constraint of given average values of some quantities (in our case, E, L and $\mathbf{q}$). Then, one maximizes the combination

$$-\kappa_B \int f \log f d\Gamma - \Lambda^E \int \hat{E} f d\Gamma - \Lambda^L \int \hat{L} f d\Gamma - \Lambda^{\mathbf{q}} \cdot \int \hat{\mathbf{q}} f d\Gamma \tag{2.120}$$

Here, $\hat{E}$, $\hat{L}$ and $\hat{\mathbf{q}}$ are the respective microscopic physical quantities, f is the distribution function, and $d\Gamma$ the volume differential of the phase space of the system. In (2.120) Λ^E, Λ^L and $\Lambda^{\mathbf{q}}$ are Lagrange multipliers accounting for the constraints on the average values for the mentioned variables. The role of these coefficients is here related to steady state values, instead to dynamical conditions (balance laws), as in (2.28). For ideal gases, in (Dreyer, 1987), the author compared the role of Lagrange multipliers in information theory and in Liu's formalism and showed their mutual consistency. Here we do so for superfluid turbulence.

The result for the f maximizing (2.120) is

$$f = z^{-1} \exp\left[-\Lambda^E \hat{E} - \Lambda^L \hat{L} - \Lambda^{\mathbf{q}} \cdot \hat{\mathbf{q}}\right], \tag{2.121}$$

with z the partition function related to the normalization of the distribution function, given by

$$z = \int \exp\left[-\Lambda^E \hat{E} - \Lambda^L \hat{L} - \Lambda^{\mathbf{q}} \cdot \hat{\mathbf{q}}\right] d\Gamma. \tag{2.122}$$

As a consequence of (2.121), the expression for the Gibbs relation is exactly (2.31) with $d\rho = 0$ (i.e. ρ constant), and the entropy flux is found to have the form (Domínguez-Cascante and Jou, 1998; Luzzi et al., 2002)

$$\mathbf{J}^S = \Lambda^E \mathbf{q} + \Lambda^L \mathbf{J}^L + \Lambda^{\mathbf{q}} \cdot \mathbf{J}^{\mathbf{q}}. \tag{2.123}$$

Expression (2.123) has an appealing meaning, as it is related to the expression for the entropy differential (where the Lagrange multipliers are the conjugate variables to the independent variables E, L and $\mathbf{q}$) with the expression for the entropy flux, where the Lagrange multipliers multiply the respective fluxes of E, L and $\mathbf{q}$. By combining (2.116) and (2.117) it is seen that (2.115) may be written in exactly the same form as (2.123).

The treatment of the entropy flux is different in the several thermodynamic formalisms going beyond local-equilibrium approximation. For instance, in EIT (Jou et al., 2010) one directly assumes that $\mathbf{J}^S$ is a combination of $\mathbf{q}$, $\mathbf{J}^L$ and $\mathbf{J}^{\mathbf{q}}$, with respective coefficients which are not a priori identified with the Lagrange multipliers, but identified with them a posteriori after a full identification of the coefficients appearing in the transport equations. Instead, in RET (Muller and Ruggeri, 1998), with Liu procedure one must consider for $\mathbf{J}^S$ a form like (2.27), because the fluxes $\mathbf{J}^L$ and $\mathbf{J}^{\mathbf{q}}$ are not taken directly as independent variables, but they are given as constitutive quantities in (2.116) and (2.27). Eventually, both formalisms lead to the same entropy flux, but since (2.115) — the flux in RET — and (2.123) — the flux in EIT — are apparently so different, one could have the impression that RET and EIT were giving different results for the entropy flux (Jou et al., 2004). Here we have shown that this is

not so in the nonlocal model considered here. As far as we know, this is the first time this is explicitly shown, as previous comparisons between both formalisms (Jou et al., 2010) did not pay enough attention to the entropy flux, but focused on entropy and on transport equations.

Expressions (2.118) and (2.123), for the entropy differential and for the entropy flux, contain the Lagrange multipliers. Their physical meaning is made more intuitive if we introduce, as in (Mongiovì and Jou, 2007), a "generalized temperature" as the reciprocal of the Lagrange multiplier of the energy as in Section 2.4.4

In terms of these form of Lagrange multipliers, (2.123) could be written as

$$\mathbf{J}^S = \frac{1}{\theta}\mathbf{q} - \frac{\mu_L}{\theta}\mathbf{J}^L + \Lambda^{\mathbf{q}} \cdot \mathbf{J}^{\mathbf{q}}, \tag{2.124}$$

whose two first terms are analogous to those of the classical theory of systems with flow of mass (Jou et al., 2010), except for the part that θ and μ_L are those defined in (2.57) and (2.58_b) and they may also depend on $\mathbf{q}$, in contrast to the local-equilibrium version.

Note, also, that identification of temperature in (2.124) is relatively ambiguous. It is not clearly seen whether it is the temperature of the superfluid, or whether it refers to a temperature characterizing only the tangle, as it has been proposed in (Mongiovì et al., 2007). This question depends on the meaning of E, which may be the energy of the fluid, or the energy of the turbulent vortex tangle. The most suitable possibility would be to consider $E = E_f + E_t$, with E_f the energy of the fluid and E_t that of the tangle, each of them with their respective absolute temperatures.

In this case, the differential of the entropy would be

$$dS = \frac{1}{\theta_f}dE_f + \frac{1}{\theta_t}dE_t - \frac{\mu^L}{\theta}dL + \lambda\mathbf{q} \cdot d\mathbf{q}, \tag{2.125}$$

with θ_f and θ_t the respective temperature of the fluid and of the tangle, and E_f and E_t the respective energies. But the temperature of the tangle (Mongiovì et al., 2007) is much higher than that of the fluid, and the term in $\theta_t^{-1}dE_t$ may be neglected as compared with $\theta_f^{-1}dE_f$. Thus, the energy E appearing here could be taken equal to that of the fluid.

The energy of the tangle is, in fact, the kinetic energy of the superfluid component rotating around the central line of the vortex. From a microscopic perspective it is a considerably ordered energy, but, from a macroscopic perspective, it is a considerably disordered energy, because the vortex lines are very disordered. The temperature related to the tangle is much higher than that of the fluid itself because of two reasons: **a)** it is related to much higher energies than the disordered atomic energy, and **b)** it is much more ordered than the random atomistic motion (Mongiovì et al., 2007), implying that the tangle energy has a relatively small contribution to the entropy.

- The considerations of this appendix are reported in:
  L. Saluto, D. Jou and M. S. Mongiovì, *Thermodynamic approach to vortex production and diffusion in inhomogeneous superfluid turbulence*,
  Physica A **406** 272–280 (2014), DOI 10.1016/j.physa.2014.03.062

Chapter 3

Longitudinal flows: well-developed flow in long channels

In this chapter we study the simplest flow situation, namely, the well-developed velocity profile along cylindrical channels or along flat channels between two parallel plates. We focus our attention on counterflow situation. In principle, this is motivated by the experiments in turbulent counterflow, although, as we will see in the next chapter, a more realistic analysis requires considering finite channels, and the role of the entry region. One of the motivations of this analysis is the evaluation of the effective thermal conductivity and the influence on it of the presence of the normal component, in channels filled with superfluid helium, connecting a warmer system to a cooler system. This is in fact one of the most complex problems in heat transport, because it does not follow the usual Fourier's law. Indeed, the heat flux produces a vortex tangle which, in turn, has a deep influence on the thermal resistance because of two different reasons: the mutual friction between the normal component and the vortex lines, and the modification of the velocity profile of the normal component.

Though this topic has been considered many times in the literature, rigorous analyses of the influence of vortices on the form of the normal component velocity profile have not been done in detail, because they are not strictly necessary for a practical analysis of heat transport, since the mutual friction with the vortex lines is, by far, the dominating factor. However, from a conceptual perspective there is much interest in exploring in which circumstances the flow of the normal component may be turbulent, adding in this way its turbulent effects to the peculiar quantum turbulence of the superfluid component. The analyses of this chapter are motivated by this central topic.

The aim of this chapter is to find out some relevant stationary solutions of the system (2.9), describing the heat transfer in counterflow experiments in a long (semi-

infinite) cylindrical channel filled with turbulent superfluid helium. In particular, we will explore the influence of the vortex lines on the radial distribution of the heat flow. This is a problem which has not yet been considered with sufficient depth in the previous analyses, and which has much interest, however, because this spatial dependence may provide additional information about the interaction between heat flux and vortex lines.

3.1 Stationary equations in cylindrical coordinates

In stationary situations, the set (2.9) of evolution equations neglecting non linear terms in the derivative of the field variables, can be written as:

$$\begin{cases} \frac{\partial v_j}{\partial x_j} = 0 \\ \\ \frac{\partial q_j}{\partial x_j} = 0 \\ \\ \frac{\partial p}{\partial x_i} - \lambda_2 \frac{\partial^2 v_i}{\partial x_j \partial x_j} + \lambda_2 \beta T \frac{\partial^2 q_i}{\partial x_j \partial x_j} = 0 \\ \\ \frac{\partial T}{\partial x_i} + \lambda_2 \beta T^2 \frac{\partial^2 v_i}{\partial x_j \partial x_j} - \lambda_2 \beta^2 T^3 \frac{\partial^2 q_i}{\partial x_j \partial x_j} = -\frac{K}{\zeta} L_0 q_i \end{cases} \tag{3.1}$$

where we have used equation (2.21) for $\sigma_i^{\mathbf{q}}$.

As we have said, we want to determine a solution of (3.1) in a semi-infinite cylindrical channel subject to a longitudinal heat flux (Saluto et al., 2014). We will look for solutions of system (3.1) under the simplified hypothesis that the superfluid is at rest, i.e. $\mathbf{v} = 0$ anywhere in the channel, which is a strong version of the condition of counterflow (a less stringent version is that $\mathbf{v}$ is zero on the average, but not locally at each point of the fluid) (Sciacca and Galantucci, 2015; Sciacca et al., 2014a,b). Under this hypothesis, boundary condition (2.12) postulated in (Mongiovì, 2001), implies that also the component of the heat flux $\mathbf{q}$ vanishes on the walls of the channel, i.e.

$$q_t = 0. \tag{3.2}$$

Note that this condition is not too restrictive, as the hydrodynamical model used here does not give informations on microscopic level, but allows us only to study what happens at an intermediate level; indeed in this hydrodynamical model a fluid particle is a small but mesoscopic region where both the normal and superfluid components (i.e. quasi-particles and ground state) are present. Anyway, the possibility of a heat slip flow along the walls will be also examined in Section 3.4, for the sake of completeness, and because this contribution may be relevant in very narrow channels.

Under the hypothesis $\mathbf{v} = 0$, system (3.1) reduces to:

$$\begin{cases} \frac{\partial q_j}{\partial x_j} = 0 \\ \\ \frac{\partial p}{\partial x_i} + \lambda_2 \beta T \frac{\partial^2 q_i}{\partial x_j \partial x_j} = 0 \\ \\ \frac{\partial T}{\partial x_i} - \lambda_2 \beta^2 T^3 \frac{\partial^2 q_i}{\partial x_j \partial x_j} = -\frac{K}{\zeta} L_0 q_i \end{cases} \tag{3.3}$$

From the second and third equations of (3.3) follows that the pressure gradient $\frac{\partial p}{\partial x_i}$ is given by the relation

$$\frac{\partial p}{\partial x_i} = -\frac{1}{\beta T^2} \left(\frac{\partial T}{\partial x_i} + \frac{K}{\zeta} L_0 q_i \right). \tag{3.4}$$

Because of the geometry of the problems we will consider, we use cylindrical coordinates (x, r, θ). If isotropy with respect to θ is assumed, the fundamental fields depend on the only variables (x, r), and the system (3.3) can be rewritten more explicitly as

$$\begin{cases} \frac{\partial q_x}{\partial x} + \frac{1}{r} \frac{\partial}{\partial r}(r q_r) = 0 \\ \\ \frac{\partial p}{\partial x} - \lambda_2 \beta T \frac{1}{r} \frac{\partial}{\partial r} \left(r \frac{\partial q_x}{\partial r} \right) = 0 \\ \\ \frac{\partial T}{\partial x} - \lambda_2 \beta^2 T^3 \frac{1}{r} \frac{\partial}{\partial r} \left(r \frac{\partial q_x}{\partial r} \right) = -\frac{K}{\zeta} L q_x \\ \\ \frac{\partial p}{\partial r} - \lambda_2 \beta T \left[\frac{1}{r} \frac{\partial}{\partial r} \left(r \frac{\partial q_r}{\partial r} \right) - \frac{q_r}{r^2} \right] = 0 \\ \\ \frac{\partial T}{\partial r} - \lambda_2 \beta^2 T^3 \left[\frac{1}{r} \frac{\partial}{\partial r} \left(r \frac{\partial q_r}{\partial r} \right) - \frac{q_r}{r^2} \right] = -\frac{K}{\zeta} L q_r \end{cases} \tag{3.5}$$

where we have put $\mathbf{q} = q_x \mathbf{i} + q_r \mathbf{u}$, with $\mathbf{i}$ and $\mathbf{u}$ the unit vectors in the axial and the radial directions.

3.2 Heat flux profile in longitudinal cylindrical counterflow

For the sake of simplicity we consider the liquid helium II subject to a longitudinal cylindrical counterflow $\mathbf{q} \parallel \mathbf{i}$, i.e. $\mathbf{q} = \mathbf{i} q$. The normal component flows in one direction (from hot to cold ends) and the superfluid component flows in the opposite direction. We assume that we are far from the wall where the superfluid is being heated, i.e. we are far from the so-called entrance region studied in the next chapter. In this case equations (3.5_a), (3.5_d) and (3.5_e) lead to:

$$q = q(r), \qquad p = p(x), \qquad T = T(x). \tag{3.6}$$

We look for solutions of the heat flux equation (3.5_c), which is

$$\frac{\partial T}{\partial x} - \frac{\eta}{TS^2}\frac{1}{r}\frac{\partial}{\partial r}\left(r\frac{\partial q}{\partial r}\right) = -\frac{KL}{\zeta}q, \tag{3.7}$$

where we have used $\beta = -1/(ST^2)$, and we have identified the coefficient λ_2 with the viscosity of the fluid η.

First of all, we consider the counterflow in the absence of vortices (namely $L = 0$). Later, we consider the counterflow situation under an homogeneous value of the vortex line density $L(x, r) = L_0$. In Chapter 5 we will also consider inhomogeneous values of L, dependent on $\mathbf{q}$.

3.2.1 Velocity profile in absence of vortices

In absence of vortices ($L = 0$), the linearized equation for the heat flux in the stationary state, obtained from (3.7), is

$$\frac{\partial T}{\partial x} - \frac{\eta}{TS^2}\frac{1}{r}\frac{\partial}{\partial r}\left(r\frac{\partial q}{\partial r}\right) = 0, \tag{3.8}$$

where the right-hand term vanishes because $L = 0$. We will search for solutions of this equation in the region $x \in \mathbb{R}$ and $r \in [0, R]$, with the boundary condition (3.2), assuming η/TS^2 constant. With condition (3.6), we obtain $\partial T/\partial x =$ constant, and

$$q(r) = -\frac{1}{4}\frac{TS^2}{\eta}\frac{\partial T}{\partial x}(R^2 - r^2), \tag{3.9}$$

that is a parabolic profile of q, like the Poiseuille flow for the velocity of a viscous fluid in a straigh cylindrical tube. In this case, from equation (3.4) we get

$$\frac{\partial p}{\partial x} = S\frac{\partial T}{\partial x}, \tag{3.10}$$

from which we see that a temperature difference between the two ends of the channel corresponds to a pressure difference, driving the helium flow.

3.2.2 Homogeneous presence of vortices

Let's consider now a homogeneous stationary distribution of vortex lines everywhere in the channel, whose length per unit volume is L_0 (except in the entrance region where can be $L = L(x)$), and look for the profile of $\mathbf{q}$ in this situation. We will assume that the condition (2.12) remains valid also in the presence of a homogeneous vortex tangle. In fact in (Ardizzone et al., 2009, 2011) this condition was generalized to the case in which a inhomogeneous vortex tangle is present, obtaining

$$v_t + \frac{1}{TS}\left(1 - \nu\mu_L\right) q_t = 0, \tag{3.11}$$

where μ_L is the chemical potential of vortex line and ν a parameter that links the flux of vortex line to the heat flux (see equation (2.25)). Also this new condition implies $q_t = 0$ when $\mathbf{v} = 0$ inside the channel. Because of the hypotheses made in the introduction of this section, see (3.6), we look for a solution of the equation (3.7), with $T = T(x)$ and $q = q(r)$. We will still assume $\eta/(TS^2)$ constant for the sake of mathemathical simplicity. In this hypothesis, writing

$$\frac{\eta}{TS^2}\frac{1}{r}\frac{\partial}{\partial r}\left(r\frac{\partial q}{\partial r}\right) - \frac{KL_0}{\zeta}q(r) = \frac{\partial T(x)}{\partial x} = H, \tag{3.12}$$

one deduces that H must be a numerical constant, because the left-hand side only depends on r, and the right-hand side only depends on x.

We look for solutions of this equation with the boundary condition $q(R) = 0$,

$$\frac{\partial^2 q}{\partial r^2} + \frac{1}{r}\frac{\partial q}{\partial r} - KL_0\frac{TS^2}{\eta\zeta}q = \frac{TS^2}{\eta}H. \tag{3.13}$$

Let's denote:

$$A = \frac{TS^2}{\eta} = \frac{T\rho^2 s^2}{\eta} \qquad \text{and} \qquad B = \frac{K}{\zeta} = \frac{\kappa B_{HV}}{3\zeta}. \tag{3.14}$$

Both A and B are positive constants, as it follows from the restrictions of the second law. Then (3.13) can be rewritten

$$\frac{\partial^2 q}{\partial r^2} + \frac{1}{r}\frac{\partial q}{\partial r} - ABL_0 q = AH. \tag{3.15}$$

This equation has the particular solution $q = -\frac{1}{BL_0}H$. The remaining homogeneous equation is

$$\frac{\partial^2 q}{\partial r^2} + \frac{1}{r}\frac{\partial q}{\partial r} - ABL_0 q = 0. \tag{3.16}$$

This is a zero-order modified Bessel equation, whose solutions are the modified Bessel functions $I_0(y)$ and $K_0(y)$, where $y = r\sqrt{ABL_0}$. The general solution of (3.15) is

$$q(r) = -\frac{1}{BL_0}H + c_1 I_0\left(r\sqrt{ABL_0}\right) + c_2 K_0\left(r\sqrt{ABL_0}\right), \tag{3.17}$$

where c_1 and c_2 are numerical constants which depend on the boundary conditions. $K_0(y)$ diverges for $y = 0$, and hence $c_2 = 0$ is required. Imposing the boundary condition, $q(R) = 0$, we can determine c_1 from:

$$q(R) = -\frac{1}{BL_0}H + c_1 I_0\left(R\sqrt{ABL_0}\right) = 0.$$

Then, remembering that $H = \frac{\partial T}{\partial x}$, the general solution is

$$q(r) = -\frac{1}{BL_0}\left(1 - \frac{I_0\left(r\sqrt{ABL_0}\right)}{I_0\left(R\sqrt{ABL_0}\right)}\right)\frac{\partial T}{\partial x}, \tag{3.18}$$

where $\frac{\partial T}{\partial x}$ is negative in the direction of x.

In order to plot this solution, we needed to evalute the quantity $\frac{\partial T}{\partial x}$. In (Martin and Tough, 1983) the values of the temperature gradient measured in the experiment are not reported, and it is only reported that the temperature differences *"would vary from about* 10^7 *K in laminar flow to about* 10^4 *K in the fully developed T II superfluid turbulent state".* In general terms, the thermal resistance will be composed of the resistance arising from the friction between the viscous component and the quantized vortices of superfluid (which is usually the dominant contribution) and the resistance of the laminar viscous flow of the normal component. In fact, in the fully laminar regime, the normal component contribution is the only contribution, and in the fully developed turbulent regime it is relatively small, but it is not negligible in the transition laminar-to-turbulent regime, as we point out in the following of this section. In the Poiseuille laminar regime, according to the Landau expression, the temperature gradient is given by (Landau, 1941; Landau and Lifshitz, 1987)

$$(\nabla T)^{Landau} = -\frac{8\eta\rho_s}{R^2\rho^2 s}\overline{\mathbf{V}}_{ns} = -\frac{8\eta}{R^2 T\rho^2 s^2}\overline{\mathbf{q}}, \tag{3.19}$$

while in presence of a homogeneous tangle of vortices, it is

$$(\nabla T)^{vort} = \frac{1}{3}\kappa B_{HV}\frac{\rho_n}{\rho s}\overline{\mathbf{V}}_{ns}L_0 \tag{3.20}$$

where $\overline{\mathbf{V}}_{ns} = \overline{\mathbf{v}}_n - \overline{\mathbf{v}}_s$ is the average counterflow velocity over a cross section of the channel. This result is obtained also in the one-fluid model, neglecting the terms in the second derivatives of $\mathbf{q}$ from (2.21). Indeed, we have used the sum of these two contributions (3.19) and (3.20) to plot the solution (3.18). The values of this contribution are reported in Table 3.6 in Section 3.3.1 for $T = 1.7$ K or in Tables 3.12 and 3.13 in Appendix 3.8 for $T = 1.5$ K and $T = 1.6$ K. The values of the constants A and B for different temperatures, obtained from equation (3.14) using data extracted from (Donnelly and Barenghi, 1998), are reported in Table 3.1, while the data of L_0 are extracted from (Martin and Tough, 1983). $\mathbf{q}$ and the other quantities are expressed in the cgs system (cgs units are commonly used in superfluid bibliography). The values of $\frac{\partial T}{\partial x}$ are calculated in detail in Section 3.3.

The plots of solution (3.18) in the laminar regime (absence of vortices), in the two turbulent regimes **TI** and **TII** (corresponding to low and high vortex line densities, respectively), and in the transition between these different regimes, are shown in Figures 3.1 and 3.2, that are analogous to Figures 1, 2, 3 and 4 of (Saluto et al., 2014) where we considered only the thermal resistance due the friction between the viscous component and the quantized vortices of superfluid, i.e. the contribution (3.20), instead of the sum of the two contributions (3.19) and (3.20) considered here.

T K	$A = \frac{TS^2}{\eta}$ cm s^3 K g^{-1}	$\frac{1}{B} = \frac{3\zeta}{\kappa B_{HV}}$ (cm s^3 K)$^{-1}$ g
1.5	$8.3 * 10^{15}$	$1.2 * 10^{16}$
1.6	$1.9 * 10^{16}$	$2.2 * 10^{16}$
1.7	$3.9 * 10^{16}$	$3.3 * 10^{16}$

Table 3.1: Values of the constants A and B, defined in (3.14) at three different temperatures, extracted from the data of (Donnelly and Barenghi, 1998).

Figure 3.1-left shows the profile of heat flux at $T = 1.7$ K in the transition from absence of vortices to the **TI** turbulence regime (low density of vortices), note that in the latter situation the profile is flatter because of the presence of vortices, in contrast to the parabolic profile in the laminar ($L = 0$) situation. Figure 3.1-right shows the profile of heat flux for $T = 1.7$ K and different values of L_0 but the same values of the counterflow velocity, in the transition region between the regimes **TI** and **TII**. Note that different values of L_0 correspond to the same value of the total heat flux, in the transition regions (in the figure we have chosen the smallest and the highest ones correspondent to $V_{ns} = 1.85\,\mathrm{cm/s}$ from Figure 10 of (Martin and Tough, 1983)). Analogous behavior is obtained for different values of the temperature T. It is seen that the higher the value of L_0, the flatter, lower and wider the velocity profile.

Figures 3.2 show the profile of $\mathbf{q}$ at three different temperatures and in different turbulence regimes. In Figure 3.2-left, the vortex line length L_0 is chosen in the first regime of turbulence, **TI**, in the Figure 3.2-right the vortex line length L_0 is chosen in the regime **TII**, and one can observe the progressive flattening of the profile for higher L_0. We point out that the heat flux assumes larger values for higher temperature because terms in T are present in both coefficients of $\mathbf{q}$ and $\nabla^2\mathbf{q}$, in particular the last one is prevalent when L_0 is higher.

As it may be noted in the figures, the solution (3.18) has a profile that depends on the value of L_0. In absence of vortices (namely $L = 0$) and in the turbulent **TI** regime (small values of L_0) $\mathbf{q}$ has a parabolic profile, which assumes maximum value $-\frac{1}{BL_0}\frac{\partial T}{\partial x}$; in the **TII** regime, instead, the profile becomes flat, equal to the maximum value $-\frac{1}{BL_0}\frac{\partial T}{\partial x}$, and falls steeply to zero near the boundary of the channel, as shown in Figures 3.1-right and 3.2-right.

As in equation (3.10), also in this case we see that to a temperature difference between the two ends of the channel corresponds a pressure difference; indeed we have

$$\frac{\partial p}{\partial x} = S\frac{\partial T}{\partial x}\frac{I_0\left(r\sqrt{ABL_0}\right)}{I_0\left(R\sqrt{ABL_0}\right)}. \tag{3.21}$$

Comparing with equation (3.10) we deduce that in the presence of vortices the pressure

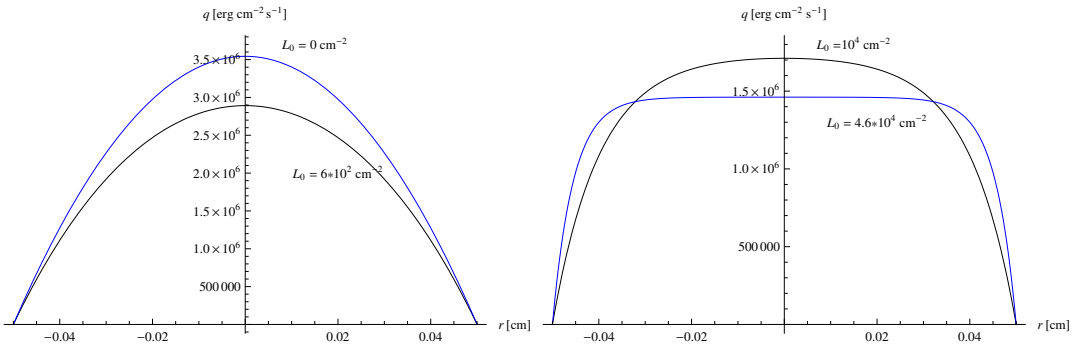

Figure 3.1: Profile of q in terms of r at $T = 1.7\,\mathrm{K}$ in the transition from absence of vortices to **TI** turbulence. In both cases the values of L_0 correspond to $V_{ns} = 1.00$ cm/s (left); and at $T = 1.7\,\mathrm{K}$ in the transition between the regimes **TI** (lower value of L_0) - **TII** (higher value of L_0). In both cases the values of L_0 correspond to $V_{ns} = 1.85\,\mathrm{cm/s}$ (right).

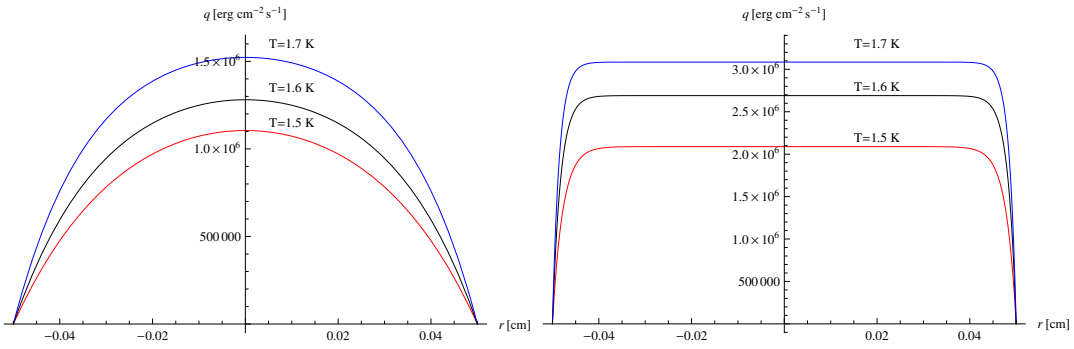

Figure 3.2: Profile of q in terms of r for $L_0 = 4 * 10^3$ cm^{-2} corresponding to $\frac{\partial T}{\partial x} = 1.74 * 10^{-7}\,\mathrm{K/cm}$ at $1.5\,\mathrm{K}$, $\frac{\partial T}{\partial x} = 1.57 * 10^{-7}\,\mathrm{K/cm}$ at $1.6\,\mathrm{K}$ and $\frac{\partial T}{\partial x} = 1.28 * 10^{-7}\,\mathrm{K/cm}$ at $1.7\,\mathrm{K}$ (left); and for $L_0 = 4 * 10^5$ cm^{-2} corresponding to $\frac{\partial T}{\partial x} = 5.19 * 10^{-5}\,\mathrm{K/cm}$ at $1.5\,\mathrm{K}$, $\frac{\partial T}{\partial x} = 4.65 * 10^{-5}\,\mathrm{K/cm}$ at $1.6\,\mathrm{K}$ and $\frac{\partial T}{\partial x} = 3.56 * 10^{-5}\,\mathrm{K/cm}$ at $1.7\,\mathrm{K}$ (right).

gradient is smaller than in the absence of them, because the function $I_0(x)$ is crescent and the term $\frac{I_0(r\sqrt{ABL_0})}{I_0(R\sqrt{ABL_0})}$ is always smaller than 1, for $0 < r < R$.

Furthermore, equation (3.21) implies a dependence of p on r, that would imply in turn a radial heat flux, which has been assumed to be zero at the beginning of this section. Owing to the steady-state condition (3.3_a), namely, $\nabla \cdot \mathbf{q} = 0$, the radial heat flux q_r will be of the order of $(r/l)q_x$, q_x being the longitudinal heat flux. Thus, when the length of the channel is much longer than the radius of the channel, the radial heat flux (and the dependence of the pressure on the radius) may be neglected. Otherwise, the physical (and mathematical) situation becomes much richer and complex, with also radial heat flux besides the longitudinal heat flux, or with the barycentric velocity of the fluid locally different from 0 (in contrast with what we have assumed here). We aim to consider these effects in the future, but since the current analyses of counterflow situations assume *a priori* that the heat flux is longitudinal, we do not deal with this further complicated but interesting topic here.

3.2.3 The normal fluid profile and Reynolds numbers estimation

In the one-fluid model deduced from E.T. it's possible to replace the fields $\mathbf{q}$ and $\mathbf{v}$ with the variables $\mathbf{u}^{(n)}$ and $\mathbf{u}^{(s)}$, introduced in (2.10) and (2.11). In counterflow situation, the velocity of liquid helium is zero, and only the heat flux $\mathbf{q}$ is present. Therefore, in this case the profile of the velocity of the normal component $\mathbf{u}^{(n)}$ is directly linked to the profile of the heat flux by the relation

$$\mathbf{u}^{(n)} = -\beta T \mathbf{q} = \frac{1}{ST}\mathbf{q}. \tag{3.22}$$

The profile of the normal component $\mathbf{u}^{(n)}$ is shown in Figures 3.3, and 3.4, in the various situations considered in the previous section. Also in this case, these figures are analogous to Figures 6, 7, 8 and 9 of (Saluto et al., 2014) where we considered only the thermal resistance due the friction between the viscous component and the quantized vortices of superfluid, i.e. the contribution (3.20), instead of the sum of the two contributions (3.19) and (3.20) considered here.

One sees that, like in Figures 3.2, the profile is parabolic in the regime **TI** and becomes flat in the regime **TII**. Only difference between the profile of $\mathbf{q}$ and $\mathbf{u}^{(n)}$ is that the first has higher values at higher temperatures, while the other one has higher values at lower temperatures. Thus, it is seen that for sufficiently high values of the vortex line density L_0, the velocity profile becomes gradually flatter in the central region. To verify whether this is a dynamical consequence of the resistance of the vortices, or whether it corresponds to a genuine turbulence of the normal component (which is also known to lead to flat profiles at the center), we will analyze the Reynolds numbers derived from

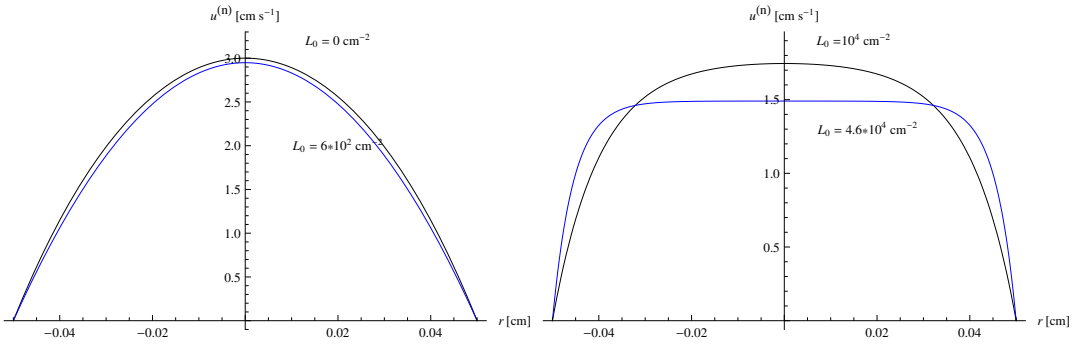

Figure 3.3: Profile of $\mathbf{u}^{(n)}$ in terms of r at $T = 1.7\,\mathrm{K}$ in the transition from absence of vortices to **TI** turbulence, in both cases the values of L_0 correspond to $V_{ns} = 1.00\,\mathrm{cm/s}$ (left); and at $T = 1.7\,\mathrm{K}$ in the transition between the regimes **TI** - **TII**, in both cases the values of L_0 correspond to $V_{ns} = 1.85\,\mathrm{cm/s}$ (right). These figures come from Figure 3.1, by using the relation (3.22) between $\mathbf{u}^{(n)}$ and $\mathbf{q}$.

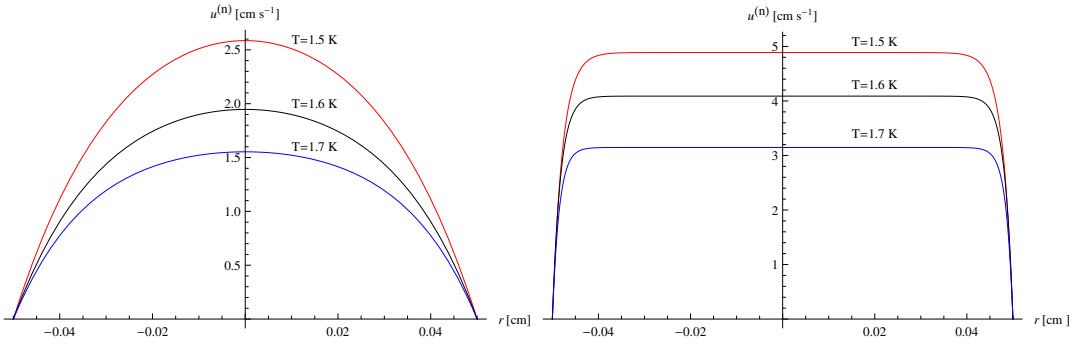

Figure 3.4: Profile of $\mathbf{u}^{(n)}$ in terms of r for $L_0 = 4{*}10^3\,\mathrm{cm}^{-2}$ corresponding to $\frac{\partial T}{\partial x} = 1.74{*}10^{-7}$ K/cm at 1.5 K, $\frac{\partial T}{\partial x} = 1.57 * 10^{-7}\,\mathrm{K/cm}$ at 1.6 K and $\frac{\partial T}{\partial x} = 1.28 * 10^{-7}\,\mathrm{K/cm}$ at 1.7 K (left); and for $L_0 = 4 * 10^5\,\mathrm{cm}^{-2}$ corresponding to $\frac{\partial T}{\partial x} = 5.19 * 10^{-5}\,\mathrm{K/cm}$ at 1.5 K, $\frac{\partial T}{\partial x} = 4.65 * 10^{-5}\,\mathrm{K/cm}$ at 1.6 K and $\frac{\partial T}{\partial x} = 3.56 * 10^{-5}$ K/cm at 1.7 K (right). These figures come from Figure 3.2, by using the relation (3.22) between $\mathbf{u}^{(n)}$ and $\mathbf{q}$.

the velocity profile we have obtained. Since the turbulence of viscous fluids is related to sufficiently high value of the Reynolds number, it is illustrative to compute the value of this number at the center of the channel. The Reynolds number is:

$$Rey = \frac{\rho^{(n)} u_x^{(n)} 2R}{\eta}, \tag{3.23}$$

where η is the viscosity of liquid helium II. The value of $\mathbf{u}_x^{(n)}$ is related to $\mathbf{q}$ by $\mathbf{u}_x^{(n)} = \mathbf{q}(\rho^{(s)} Ts)^{-1}$ as it has been said in Section 2.2.2. In Tables 3.2 we show the Reynolds numbers corresponding to the central value of $\mathbf{q}$ for different temperature and $L_0 = 4{*}10^3$ cm^{-2} in regime **TI** (left) as in Figure 3.2-left, and for $L_0 = 4{*}10^5$ cm^{-2} in regime **TII** (right) as in Figure 3.2-right. In Table 3.3 we show the Reynolds numbers for two values of L_0 in the transition to the **TII** turbulence, as in Figure 3.1-right, related to the same counterflow velocity $V_{ns} = 1.85$ cm/s.

L_0 cm^{-2}	T K	$q(r=0)$ erg / (cm*s)	Rey
$4 * 10^3$	1.5	$4.4 * 10^5$	122
	1.6	$6.8 * 10^5$	191
	1.7	$9.1 * 10^5$	243

L_0 cm^{-2}	T K	$q(r=0)$ erg / (cm*s)	Rey
$4 * 10^5$	1.5	$2 * 10^6$	555
	1.6	$2.6 * 10^6$	730
	1.7	$2.9 * 10^6$	775

Table 3.2: Reynolds numbers estimation for the flow of the normal component for values of L_0 in the regimes **TI** (left) and **TII** (right) at different temperatures.

For $T = 1.7$ K and $V_{ns} = 1.85$ cm/s		
L_0 cm^{-2}	$q(r=0)$ erg / (cm*s)	Rey
10^4	$1.34 * 10^6$	358
$4.6 * 10^4$	$1.37 * 10^6$	366

Table 3.3: Reynolds numbers estimation for the normal component in the transition between the two regimes of turbulence.

It is seen that the normal fluid is expected to be in laminar flow, because its corresponding Reynolds number is much lower than the critical Reynolds numbers for viscous fluids (the critical value of the Reynolds number related to the presence of turbulence in a Poiseuille flow of a Newtonian fluid is of the order of 1500). In this case, the flat profile of the normal component velocity illustrated in Figures 3.1–3.4 is a consequence of the interaction with the vortices, rather than from an intrinsic turbulence of the normal fluid.

3.2.4 Effective thermal conductivity

If the solutions obtained for the heat flux (both in the laminar case or in the presence of vortices) are integrated over the whole transversal section, i.e. from $r = 0$ to $r = R$, one gets the total heat flux Q. Then, we have in the laminar case ($L_0 = 0$, parabolic profile (3.9))

$$Q = \int_\sigma q(r) d\sigma = -2\pi \frac{\Delta T}{l} \int_0^R \frac{1}{4} \frac{TS^2}{\eta} (R^2 - r^2) dr = -\frac{\pi R^4 T S^2}{8\eta} \frac{\Delta T}{l}, \tag{3.24}$$

where ΔT indicates the temperature difference between the two ends of the channel, and l the length of the channel (or, in more general terms, $\Delta T/l$ is the modulus of the temperature gradient). From here one can determine the average heat flux along the channel $q_{average} = \frac{Q}{\pi R^2}$, and one may define an effective thermal conductivity as

$$\lambda_{eff} = \frac{|Q|}{\pi R^2} \frac{l}{\Delta T} = \frac{R^2 T S^2}{8\eta}, \tag{3.25}$$

thus, it vanishes for R going to zero, in contrast with the usual thermal conductivity, which depends on the material, but not on the geometry. Indeed if the radius of the channel goes to zero, equation (3.25) implies also $\mathbf{q} = 0$. In fact, it is known that inside a very thin capillary (superleak) a heat flux must be accompanied by a matter flux in opposite direction.

Instead, in presence of a homogeneous tangles of vortices ($L_0 \neq 0$, Bessel profile (3.18)), we obtain

$$Q = \int_\sigma q(r) d\sigma = 2\pi \frac{\Delta T}{l} \int_0^R \frac{r}{BL_0} \left(1 - \frac{I_0\left(r\sqrt{ABL_0}\right)}{I_0\left(R\sqrt{ABL_0}\right)} \right) dr, \tag{3.26}$$

and the effective thermal conductivity becomes

$$\lambda_{eff} = \frac{Q}{\pi R^2} \frac{l}{\Delta T} = \frac{1}{BL_0} \frac{I_2\left(R\sqrt{ABL_0}\right)}{I_0\left(R\sqrt{ABL_0}\right)}, \tag{3.27}$$

where I_2 indicates the modified Bessel function of first kind and second order.

For $L = 0$ the value of λ_{eff} in (3.27) becomes $\frac{AR^2}{8} = \frac{TS^2}{\eta} \frac{R^2}{8}$ as in (3.25). Increasing L_0, the values of λ_{eff} decrease, as shown in Figure 3.5.

The Figure 3.5 is the logarithmic plot of λ_{eff} vs L_0 given by (3.25) in terms of L_0 in the regime **TI** (left) and given by Eq. (3.27) in the regime **TII** (right). In both figures R is the radius of the channel and it is $R = 0.5$ cm and the values of the constants A and B are taken for $T = 1.7$ K. These plots show as the slope of λ_{eff} in the regime **TII** is in good approximation hyperbolic, $\lambda_{eff} \cong \frac{1}{L^\alpha}$, with $\alpha = 0.9$, with an error from 0.2 to 4.4 per cent. In the regime **TI** the slope of λ_{eff} is fitting by a polynomial of the type: $a + \frac{b}{\sqrt{L}} - \frac{c}{L}$, with an error from 0.2 to 1 per cent, and where $a = -2.2 * 10^{12}$, $b = 4.9 * 10^{14}$ and $c = 5 * 10^{15}$.

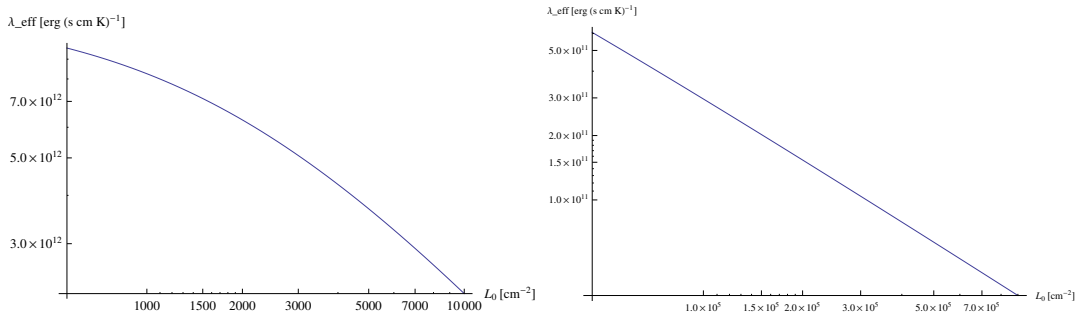

Figure 3.5: Logarithmic plot of the effective thermal conductivity λ_{eff} given by Eq. (3.25) in terms of L_0 in the regime **TI** (left) and given be Eq. (3.27) in the regime **TII** (right).

3.3 Evaluation of the laminar viscous contribution to the thermal resistance

In fully developed turbulence the thermal resistance — in other terms, the total temperature gradient for a given heat flux — is due essentially to the friction between viscous component and the quantized vortices of superfluid (which is usually the dominant contribution), and the contribution of the laminar flow of the normal component to the thermal resistance can be neglected.

In a first analysis it is a good approximation, but for a more detailed comparison between theoretical results and the experimental data, we must take into account also the thermal resistance due to the viscous flow of the normal component, as we did in Section 3.2.2. In this section we do it. Carrying out this analysis, we realized that the contribution of the normal component may in fact become considerably different from the Landau expression, as a consequence of the velocity profile being given by (3.18) instead of the well-known Poiseuille parabolic profile (3.9). Since for a given value of the heat flux $\mathbf{q}$ the thermal resistance is proportional to the corresponding temperature gradient, we will compare the respective temperature gradients obtained from the Landau thermal resistance and from the thermal resistance obtained in this section (Saluto et al., 2015).

As in Section 3.2.2, we can evaluate the temperature gradient in the Poiseuille laminar regime as in (3.19) and the vortex contribution as in (3.20).

From equation (3.7), neglecting in it the term in the second derivative of $\mathbf{q}$ (which gives the laminar contribution to the temperature gradient), as in (3.20), we obtain

$$(\nabla T)^{vort} = -\frac{K}{\zeta}\overline{\mathbf{q}}L_0 = -B\overline{\mathbf{q}}L_0, \tag{3.28}$$

where $\overline{\mathbf{q}} = \langle q(r)\rangle$ is the average value of $q(r)$ in (2.21) and using the relation $\overline{\mathbf{q}} = \rho_s T s \overline{\mathbf{V}}_{ns}$, one sees that equations (3.20) and (3.28) coincide.

By integration of (3.18) over the whole transversal area (i.e. for $0 \leq r \leq R$), we obtain

$$\nabla T = -\frac{\dot{Q}}{\pi R^2} B L_0 \frac{I_0\left(R\sqrt{ABL_0}\right)}{I_2\left(R\sqrt{ABL_0}\right)}, \tag{3.29}$$

being $\dot{Q}$ the total heat flow imposed to the channel, i.e. $\dot{Q} = \overline{\mathbf{q}}\pi R^2$ (where $\overline{\mathbf{q}}$ is the modulus of the average heat flux), whose experimental values can be obtained from the figures of (Martin and Tough, 1983). This expression for the temperature gradient reduces to the Landau form in the limit for $L_0 = 0$, and to (3.28) for very high values of L_0 (i.e. in the regime **TII**).

The total temperature gradient obtained from (3.29) is smaller than that obtained from eq. (3.28) for the vortex contribution, because

$$|\nabla T| = B\overline{q}L_0 < B\overline{q}L_0 \frac{I_0\left(R\sqrt{ABL_0}\right)}{I_2\left(R\sqrt{ABL_0}\right)}. \tag{3.30}$$

Both expressions become equal for high values of L_0 or of R; this is an indication that the right-hand side of (3.30) includes not only the vortex resistance, but also the laminar viscous resistance due to the normal component, which becomes negligible for wide channels.

Now, we aim to compare $(\nabla T)^{Landau}$ obtained from (3.19) with $(\nabla T)^{lam}$ obtained by subtracting from the total ∇T given in (3.29) the pure vortex contribution given by (3.28), namely:

$$(\nabla T)^{lam} = \nabla T - (\nabla T)^{vort} = BL_0 \left[\frac{I_0\left(R\sqrt{ABL_0}\right)}{I_2\left(R\sqrt{ABL_0}\right)} - 1\right] \frac{\dot{Q}}{\pi R^2}. \tag{3.31}$$

In Tables 3.4 and 3.5, the values of V_{ns} and L_0 are extracted from Fig. 10 of (Martin and Tough, 1983). The values for $\dot{Q}$ in the first column are obtained from $\dot{Q} = \overline{\mathbf{q}}\pi R^2$ with $\overline{\mathbf{q}} = \rho_s T s \overline{\mathbf{V}}_{ns}$, the values in the fourth column are obtained from (3.19). These values are calculated for $R = 0.05$ cm (the radius of the channel used in the experiments in (Martin and Tough, 1983)) in Table 3.4, and for $R = 0.025$ cm in Table 3.5. For the other coefficients the values are extracted from (Donnelly and Barenghi, 1998). In the appendix are also given the respective results for $T = 1.5$ K and $T = 1.6$ K. For each value of temperature, the lowest value of V_{ns} is the critical velocity indicated in (Martin and Tough, 1983) as V_{C2} that yields the transition between regimes **TI** and **TII**.

In order to evaluate the viscous contribution of the normal component also in a channel with smaller radius, we have extracted from the Fig. 10 of (Martin and Tough, 1983) the values of the total heat flux imposed (through the values of V_{ns} and relation (1) of (Martin and Tough, 1983)) and we have calculated the corresponding values of V_{ns}

$\dot{Q}$ erg/s	V_{ns} cm/s	L_0 cm^{-2}	$(\nabla T)^{Landau}$ K/cm	$(\nabla T)^{vort}$ K/cm	∇T K/cm	$(\nabla T)^{lam}$ K/cm
$1.13 * 10^4$	1.93	$4.34 * 10^4$	$2.80 * 10^{-7}$	$1.86 * 10^{-6}$	$2.25 * 10^{-6}$	$3.87 * 10^{-7}$
$1.56 * 10^4$	2.67	$1.47 * 10^5$	$3.87 * 10^{-7}$	$8.73 * 10^{-6}$	$9.64 * 10^{-6}$	$9.12 * 10^{-7}$
$1.80 * 10^4$	3.07	$2.03 * 10^5$	$4.46 * 10^{-7}$	$1.39 * 10^{-5}$	$1.51 * 10^{-5}$	$1.27 * 10^{-6}$
$2.45 * 10^4$	4.19	$4.12 * 10^5$	$6.07 * 10^{-7}$	$3.84 * 10^{-5}$	$4.07 * 10^{-5}$	$2.37 * 10^{-6}$
$2.79 * 10^4$	4.78	$5.50 * 10^5$	$6.93 * 10^{-7}$	$5.85 * 10^{-5}$	$6.14 * 10^{-5}$	$2.92 * 10^{-6}$
$3.42 * 10^4$	5.85	$8.17 * 10^5$	$8.49 * 10^{-7}$	$1.14 * 10^{-4}$	$1.18 * 10^{-4}$	$4.53 * 10^{-6}$

Table 3.4: The last column shows the viscous contribution of the normal component to the temperature gradient, for $T = 1.7$ K and $R = 0.05$ cm. The values of V_{ns} and L_0 are extracted from Fig. 10 of (Martin and Tough, 1983) in the regime **TII**. The first value of V_{ns} is the critical velocity indicated in (Martin and Tough, 1983) as V_{C2} yielding the transition between regimes **TI** and **TII**. The values of $(\nabla T)^{Landau}$ and $(\nabla T)^{vort}$ are calculated from Eqs. (3.19) and (3.28) respectively. The values of ∇T are obtained from eq. (3.29).

and L_0 from Eqs. (1) and (18) of (Martin and Tough, 1983). From these values we have calculated the other quantities, as in Table 3.4.

$\dot{Q}$ erg/s	V_{ns} cm/s	L_0 cm^{-2}	$(\nabla T)^{Landau}$ K/cm	$(\nabla T)^{vort}$ K/cm	∇T K/cm	$(\nabla T)^{lam}$ K/cm
$1.13 * 10^4$	7.70	$1.42 * 10^6$	$1.88 * 10^{-6}$	$2.43 * 10^{-4}$	$2.60 * 10^{-4}$	$1.68 * 10^{-5}$
$1.56 * 10^4$	10.67	$2.95 * 10^6$	$2.60 * 10^{-6}$	$7.00 * 10^{-4}$	$7.32 * 10^{-4}$	$3.17 * 10^{-5}$
$1.80 * 10^4$	12.30	$4.05 * 10^6$	$3.00 * 10^{-6}$	$1.11 * 10^{-3}$	$1.15 * 10^{-3}$	$4.22 * 10^{-5}$
$2.45 * 10^4$	16.74	$8.03 * 10^6$	$4.08 * 10^{-6}$	$2.99 * 10^{-3}$	$3.08 * 10^{-3}$	$8.16 * 10^{-5}$
$2.79 * 10^4$	19.11	$1.07 * 10^7$	$4.66 * 10^{-6}$	$4.57 * 10^{-3}$	$4.65 * 10^{-3}$	$8.30 * 10^{-5}$
$3.42 * 10^4$	23.41	$1.67 * 10^7$	$5.70 * 10^{-6}$	$8.68 * 10^{-3}$	$8.86 * 10^{-3}$	$1.73 * 10^{-4}$

Table 3.5: The last column shows the viscous contribution of the normal component to the temperature gradient, for $T = 1.7$ K and $R = 0.025$ cm. We have extracted the values of the total heat flux imposed from Fig. 10 of (Martin and Tough, 1983) in the regime **TII**. From these values we have calculated the values of V_{ns} and L_0 from Eqs. (1) and (18) of (Martin and Tough, 1983). The values of $(\nabla T)^{Landau}$ and $(\nabla T)^{vort}$ are calculated from Eqs. (3.19) and (3.28) respectively. The values of ∇T are obtained from eq. (3.29).

Inspection of total ∇T in the sixth column shows that it is close to $(\nabla T)^{vort}$ of the fifth column in all cases, as it is shown also in Figure 3.3, where the different contributions of ∇T are plotted. This fact is logical, because the friction force of normal component against the vortices is the main contribution to the normal resistance, and the quantity $\frac{I_0\left(R\sqrt{ABL_0}\right)}{I_2\left(R\sqrt{ABL_0}\right)}$ is close to 1 for high values of the argument $R\sqrt{ABL_0}$. However, from the point of view of the behavior of the normal component, which is the main aim of recent studies and of the present work, the relevant aspect is that the

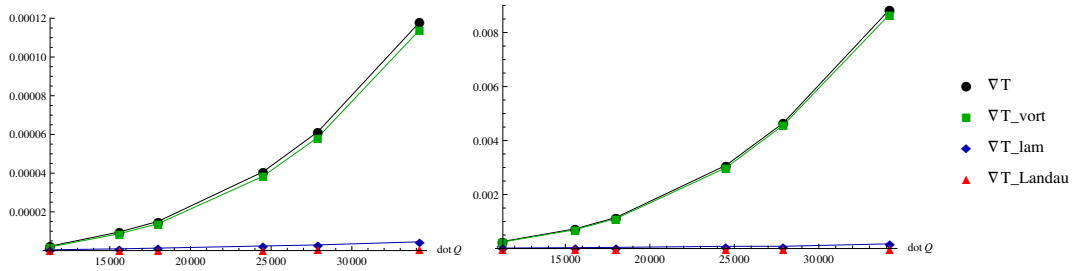

Figure 3.6: Data of Tables 3.4 and 3.5 for the several contributions to the temperature gradient in terms of $\dot{Q}$ for $R = 0.05$ cm (left) and for $R = 0.025$ cm (right).

contribution $(\nabla T)^{lam} = \nabla T - (\nabla T)^{vort}$ of the seventh column (corresponding to the non parabolic profile (3.18)) may be two orders of magnitude higher (in the lowest row of Tables 3.4 and 3.5) than $(\nabla T)^{Landau}$ corresponding to the parabolic profile. Therefore, if one actually wants to get information on the flow of the normal component, a high precision is needed in the measurement of ∇T. In Tables 3.8 and 3.9 in the Appendix 3.7 we give the analogous values to Table 3.4, but for $T = 1.5$ K and $T = 1.6$ K. In Tables 3.10 and 3.11 are the analogous values to Table 3.5. It is seen there that the lower the temperature, the lower the values of the respective laminar contributions; this is logical because the value of the viscosity is also lower (recall that for lower temperatures ρ_n decreases, and ρ_s increases).

3.3.1 Comparison between experimental data and the results of the one-fluid model

Starting from the model proposed in Section 3.2, we can evaluate the average value of $q(r)$, $\overline{\mathbf{q}}$, in a cross section of the channel, using equation (3.18), i.e.

$$\overline{\mathbf{q}} = \frac{1}{BL_0} \frac{I_2\left(R\sqrt{ABL_0}\right)}{I_0\left(R\sqrt{ABL_0}\right)} \nabla T. \tag{3.32}$$

As we did in Section 3.2, we can choose for $\frac{\Delta T}{l}$ the sum of $(\nabla T)^{Landau}$ and $(\nabla T)^{vort}$, see equations (3.19) and (3.20), to evaluate $\overline{\mathbf{U}}_{ns} = U_{ns} = \overline{\mathbf{u}}^{(n)} - \overline{\mathbf{u}}^{(s)}$ from (2.17). As shown in Table 3.6, for $T = 1.7$ K, the values obtained for U_{ns} are quite close to the values of V_{ns} extracted from Fig. 10 of (Martin and Tough, 1983) in the fully developed turbulent regime (as in the last rows).

The value of V_{ns} in the first two rows has been chosen in the transition between **TI**–**TII** regimes: this is the reason why we have for the same velocity two different values of L_0 — the same reported in Fig. 3.1-right or in Fig. 4 of (Saluto et al., 2014)

V_{ns} cm/s	L_0 cm^{-2}	$(\nabla T)^{Landau}$ K/cm	$(\nabla T)^{vort}$ K/cm	$(\nabla T)^{Landau}+(\nabla T)^{vort}$ K/cm	$\overline{\mathbf{q}}$ erg / (cm*s)	U_{ns} cm/s
1.85	10^4	$2.69 * 10^{-7}$	$4.12 * 10^{-7}$	$6.80 * 10^{-7}$	$1.52 * 10^6$	2.04
1.85	$4.60 * 10^4$	$2.69 * 10^{-7}$	$1.89 * 10^{-6}$	$2.16 * 10^{-6}$	$1.31 * 10^6$	1.76
1.93	$4.34 * 10^4$	$2.80 * 10^{-7}$	$1.86 * 10^{-6}$	$2.14 * 10^{-6}$	$1.37 * 10^6$	1.84
2.67	$1.47 * 10^5$	$3.87 * 10^{-7}$	$8.73 * 10^{-6}$	$9.11 * 10^{-6}$	$1.88 * 10^6$	2.52
3.07	$2.03 * 10^5$	$4.46 * 10^{-7}$	$1.39 * 10^{-5}$	$1.43 * 10^{-5}$	$2.17 * 10^6$	2.91
4.19	$4.12 * 10^5$	$6.07 * 10^{-7}$	$3.84 * 10^{-5}$	$3.90 * 10^{-5}$	$2.99 * 10^6$	4.01
4.78	$5.05 * 10^5$	$6.93 * 10^{-7}$	$5.85 * 10^{-5}$	$5.92 * 10^{-5}$	$342 * 10^6$	4.60
5.85	$8.71 * 10^5$	$8.49 * 10^{-7}$	$1.14 * 10^{-4}$	$1.14 * 10^{-4}$	$4.21 * 10^6$	5.65

Table 3.6: This table shown that in the fully developed regime the values of U_{ns} are quite close to that of V_{ns} extracted by experimental data. Here we are reported the values only for $T = 1.7$ K. The values of V_{ns} and L_0 are extracted from Fig. 10 of (Martin and Tough, 1983) in the regime **TII**. The first two row have the same value of V_{ns} because it is chosen in the transition between regimes **TI** and **TII**, and we have chosen two different values of L_0. In the third row the value V_{ns} is the critical velocity indicated in (Martin and Tough, 1983) as V_{C2} yielding the transition between regimes **TI** and **TII**. The values of $(\nabla T)^{Landau}$ and $(\nabla T)^{vort}$ are calculated from Eqs. (3.19) and (3.20). The values for $\overline{\mathbf{q}}$ are calculated from (3.32), and that for U_{ns} from (2.17).

—. In Appendix 3.8 we report tables analogous to Table 3.6 but for $T = 1.5$ K and $T = 1.7$ K.

If we evaluate ∇T from (3.29) — using experimental data for the total heat flow imposed $\dot{Q}$ —, because it depends on L_0, for a fixed value of $\dot{Q}$ or V_{ns} we obtain different value of the temperature gradient corresponding to the different values of L_0. But for the average velocity $\overline{\mathbf{U}}_{ns}$ we obtain the same value of $\overline{\mathbf{V}}_{ns}$. In fact, one has:

$$\overline{\mathbf{U}}_{ns} = \overline{\mathbf{u}}^{(n)} - \overline{\mathbf{u}}^{(s)} = \rho_s T s\, \overline{\mathbf{q}} = \rho_s T s\, \frac{1}{BL_0} \frac{I_2\big(R\sqrt{ABL_0}\big)}{I_0\big(R\sqrt{ABL_0}\big)} \frac{\Delta T}{l_c} = \rho_s T s\, \frac{\dot{Q}}{\pi R^2} = \overline{\mathbf{V}}_{ns}. \quad (3.33)$$

In Figure 3.7 the discontinuous lines correspond to Figure 4 of (Saluto et al., 2014) where the normal component contribution was neglected in the estimation of ∇T; the continous lines are those obtained with ∇T computed from (3.29). The new lines are more realistic, because both the parabolic and the flattened profile yield the same total value for the integrated heat flow $\dot{Q}$.

Because we have chosen the same values for $V_{ns} = 1.85$ cm/s (slightly less than the critical velocity indicated in Fig. 10 of (Martin and Tough, 1983), for $T = 1.7$ K, i.e. $V_{ns} = 1.93$ cm/s), we expect the same values for $\overline{\mathbf{q}}$, calculated for the two different values of L_0, taken in the transition region **TI**–**TII**. Our predictions are supported by the values shown in Table 3.6, obtained using the one-fluid model deduced by E.T.

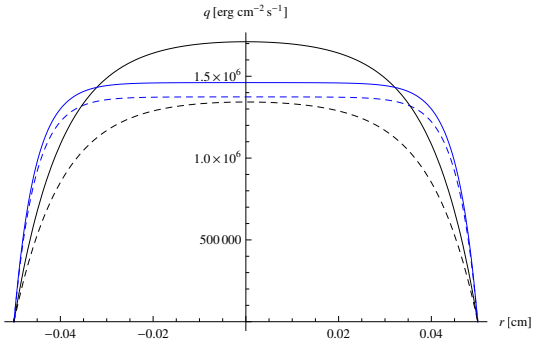

Figure 3.7: Profile of $\mathbf{q}$ in terms of r for $T = 1.7$ K in the transition between the regimes **TI** - **TII**. The values choosen for L_0 correspond to $V_{ns} = 1.85$ cm/s, which is the transition velocity from **TI** to **TII** regime (Martin and Tough, 1983). The parabolic profiles correspond to $L_0 = 10^4$ cm^{-2} in the **TI** regime, the other to $L_0 = 4.6 * 10^4$ cm^{-2} in the **TII** regime.

Thus, a good choice for the thermal resistance is important in the comparison of the two mentioned models. In the case in which the values of ∇T obtained in Section 3.2 are used to estimate $\overline{\mathbf{U}}_{ns}$ (instead of using $(\nabla T)^{Landau} + (\nabla T)^{vort}$), $\overline{\mathbf{U}}_{ns}$ would coincide with $\overline{\mathbf{V}}_{ns}$, as in (3.33).

3.4 Ballistic regime and slip flow along the walls

In Section 3.3 it has been seen that the smaller the radii R, the higher the contribution of the normal component to the normal resistance. But when R becomes very small, comparable to phonon mean free path, the non-slip condition for $\mathbf{v}_n$ at the surface should be modified, by admitting some degree of slip flow, as it is usual in rarefied gas dynamics, for the sake of illustration see (Struchtrup, 2005; Tabeling, 2005), and in phonon hydrodynamics (Alvarez et al., 2010; Dong et al., 2014; Sellitto et al., 2010).

In this section we generalize the results of Section 3.2 to the ballistic region in which the phonon mean free path becomes comparable to the radius of the channel (Saluto et al., 2015). This situation is found at low temperatures (for instance, below $T = 0.7$ K, the mean free path ℓ is longer than $5 * 10^{-7}$ cm) (Greywall, 1981). In such a case, the normal component cannot be longer considered as a usual viscous fluid but as a rarefied fluid. In analogy of the description of the transition from viscous flows to ballistic flows in gases, the non-slip condition $\mathbf{q} = 0$ on the wall must be modified as (Greywall, 1981; Sciacca et al., 2014b)

$$q(r = R) = -Cl \frac{\partial q(r)}{\partial r}_{|r=R}. \tag{3.34}$$

The coefficient C may be interpreted as $C = (2-f)/f$, f being the fraction of phonons which undergo diffusive scattering with the walls, and $(1-f)$ the fraction undergoing specular scattering. Thus, the expected values of C are higher than 1 (Greywall, 1981). We will explore the situation $C = 2$, for the sake of illustration.

With boundary condition (3.34), the solution of (3.7) is no longer (3.18), but

$$q(r) = -\frac{1}{BL_0}\left(1 - \frac{I_0\left(r\sqrt{ABL_0}\right)}{I_0\left(R\sqrt{ABL_0}\right) + Cl\sqrt{ABL_0}\, I_1\left(R\sqrt{ABL_0}\right)}\right)\frac{\partial T}{\partial x}, \tag{3.35}$$

with I_1 the modified Bessel function of first kind and first order. In Figure 3.4, the profile (3.35) is plotted (for $C = 2$). It may be compared to Figure 3.2-right. It is a very flat profile but it lacks the steep velocity gradients near the walls, because the value of $\mathbf{q}$ along the walls is not zero, as in Figure 3.2-right, but given by (3.34). This reduces the viscous contribution to the thermal resistance.

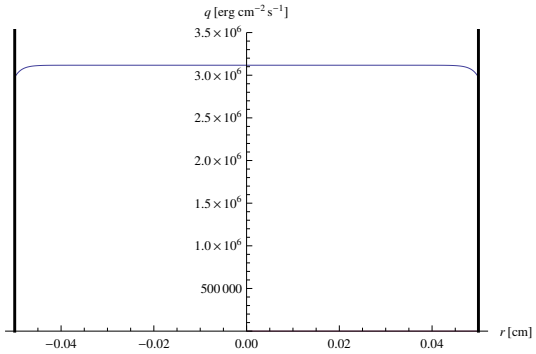

Figure 3.8: Profile of q in terms of r for $T = 1.7$ K and $C = 2$, according to (3.35).

In the limit for $L = 0$, this solution reduces to

$$q(r) = -\frac{1}{4}A(r^2 - R^2 - 2ClR)\frac{\partial T}{\partial x}, \tag{3.36}$$

where the two first terms are the Poiseuille profile and the last one the slip contribution.

From (3.35) by integration from $r = 0$ to $r = R$, we can define the effective thermal conductivity as (Sciacca et al., 2014a,b)

$$\lambda_{eff} = \frac{\dot{Q}}{\pi R^2}\frac{l}{\Delta T} = \frac{1}{BL_0}\left[1 - \frac{2}{R\sqrt{ABL_0}}\frac{I_1\left(R\sqrt{ABL_0}\right)}{I_0\left(R\sqrt{ABL_0}\right) + Cl\sqrt{ABL_0}\, I_1\left(R\sqrt{ABL_0}\right)}\right], \tag{3.37}$$

where ΔT is still the temperature difference at the ends of the channel and l is the

length of the channel. Thus, we obtain

$$\nabla T = -\frac{\dot{Q}}{\pi R^2} B L_0 \left[1 - \frac{2}{R\sqrt{ABL_0}} \frac{I_1\left(R\sqrt{ABL_0}\right)}{I_0\left(R\sqrt{ABL_0}\right) + Cl\sqrt{ABL_0}\, I_1\left(R\sqrt{ABL_0}\right)} \right]^{-1}. \tag{3.38}$$

In Table 3.7, we compare the values of ∇T obtained from (3.38) for $C = 2$, with those obtained from (3.29) (corresponding to non-slip condition $C = 0$), for the value of $\dot{Q}$ and L_0 of the last three rows of Table 3.4. We assume, for the sake of illustration, that $\ell \approx 1.53 * 10^{-2}$ cm at $T = 1.7$ K, estimated by extrapolating the relation $\ell/\ell_{0.7} = (T/0.7)^{-\frac{4}{3}}$ from (Greywall, 1981).

$\dot{Q}$ erg/s	L_0 cm^{-2}	$(\nabla T)_{non-slip}$ K/cm	$(\nabla T)_{slip}$ K/cm
$2.45 * 10^4$	$4.12 * 10^5$	$4.07 * 10^{-5}$	$3.85 * 10^{-5}$
$2.79 * 10^4$	$5.50 * 10^5$	$6.14 * 10^{-5}$	$5.85 * 10^{-5}$
$3.42 * 10^4$	$8.17 * 10^5$	$1.18 * 10^{-4}$	$1.07 * 10^{-4}$

Table 3.7: ∇T evaluated for three different values of $\dot{Q}$ and for $R = 0.05$ cm. The values of $(\nabla T)_{no-slip}$ and $(\nabla T)_{slip}$ (for $C = 2$) are calculated from eqs. (3.29) and (3.38) respectively (the first one is ∇T in Table 3.4).

It is seen that the slip flow condition leads to a lower thermal resistance than the usual non-slip condition. This is logical, because in the non-slip condition it is imposed that the heat flux along the walls is zero, whereas for the slip condition it is higher than zero. In fact, the order of magnitude of the difference between ∇T for $C = 0$ and $C = 2$ is comparable or higher than the laminar contribution for $C = 0$. According to Table 3.7, the difference in thermal resistance between non-slip and slip conditions is of the order of 5% for $C = 2$. Higher values of C would lead to more significant differences.

This may be of special interest for the flow of helium in porous media. A future work of interest would be to compare the effects of this slip flow with an interesting proposal (Fliessbach, 1991; Mongiovì, 2000b; Schäfer and Fliessbach, 1994) related to a possible non-vanishing entropy $\rho_s s_s$ of the superfluid component, but with non-slip condition, i.e. vanishing tangential heat flux on the walls. As in (Mongiovì, 2000b) the total heat flux would be

$$\mathbf{q} = \rho_n s_n T(\mathbf{v}_n - \mathbf{v}) + \rho_s s_s T(\mathbf{v}_s - \mathbf{v}). \tag{3.39}$$

The first part is the usual one, as considered in the discussion in Section 2.1, and along this thesis. The second one is a non-standard proposal. In principle, it is assumed that $s_s \ll s_n$, but in very narrow channels and without slip of the normal component, thus

new term related to s_s would be relevant. Indeed, the tangential heat flow along the walls would be

$$q_t = \rho_n s_n T(\mathbf{v}_n - \mathbf{v})_t + \rho_s s_s T(\mathbf{v}_s - \mathbf{v})_t. \tag{3.40}$$

In usual situations, $v_{nt} = 0$ (non-slip condition), but the superfluid component may have a tangential velocity component along the walls, v_{st}. Then, in counterflow situation, q_t would be

$$q_t = \rho_n s_n T v_{nt} + \rho_s s_s T v_{st} = \rho_s s_s T v_{st}. \tag{3.41}$$

Instead, if one considers that, for very narrow channels (namely, in the ballistic regime with phonon mean free path comparable or larger than the radius of the channel), and one consider $s_s = 0$, the tangential heat flux would be

$$q_t = \rho s_n T v_{nt}. \tag{3.42}$$

We leave for the future the conceptually interesting comparison between (3.41) and (3.42) interpretations. Since q_t is not directly observable, one should consider the flux across the whole (narrow) channel, yielding the total heat flux.

3.5 Stationary counterflow in narrow two-dimensional channel

The present chapter has been devoted to a superfluid flow along a cylindrical channel. In this last section we present, for the sake of a wider generality, the results for the flow in a two-dimensional infinitely wide channel between parallel plates separated at distance $2a$ to describe heat flow along a narrow slit (see Figure 3.5). This is the two-dimensional equivalent of the problem analyzed in Section 3.2 in axial symmetry. Some of the results obtained here will be useful in the next chapter, and are also of interest from a general perspective. Of course, other kinds of channels (triangular, square, rectangular or elliptical cross sections) could be considered, but for the purpose of our analysis, these two paradigmatic flows (axial and plane) are sufficient.

A heat flux is applied in x-direction and we assume that it depends only on y; then the equation for the heat flux from system (3.3), becomes

$$\frac{\partial T}{\partial x} - \frac{1}{A}\frac{\partial^2 q}{\partial y^2} = -BLq, \tag{3.43}$$

where $A = \frac{S^2 T}{\eta}$ and $B = \frac{K}{\zeta}$, as in (3.14).

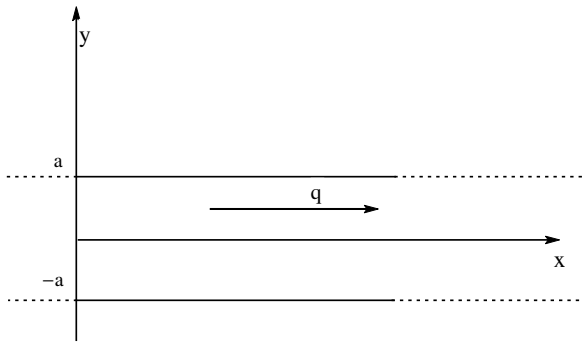

Figure 3.9: An heat flux is applied in x-direction and it depends only on y.

3.5.1 Constant vortex density

A general solution of (3.43) with constant value of L_0 and the non-slip heat flux boundary conditions, $q(\pm a) = 0$, is:

$$q(y) = -\frac{1}{BL_0}\frac{\partial T}{\partial x} + C_1 \mathrm{e}^{y\sqrt{ABL_0}} + C_2 \mathrm{e}^{-y\sqrt{ABL_0}}. \tag{3.44}$$

Imposing the non-slip boundary conditions, namely $\mathbf{q}(\pm a) = 0$, we obtain

$$C_1 = C_2 = \frac{1}{BL_0}\frac{\partial T}{\partial x}\left(\mathrm{e}^{a\sqrt{ABL_0}} + \mathrm{e}^{-a\sqrt{ABL_0}}\right)^{-1}$$

and then

$$q(y) = -\frac{1}{BL_0}\frac{\partial T}{\partial x}\left[1 - \frac{\mathrm{e}^{y\sqrt{ABL_0}} + \mathrm{e}^{-y\sqrt{ABL_0}}}{\mathrm{e}^{a\sqrt{ABL_0}} + \mathrm{e}^{-a\sqrt{ABL_0}}}\right] = -\frac{1}{BL_0}\frac{\partial T}{\partial x}\left[1 - \frac{\cosh\left(y\sqrt{ABL_0}\right)}{\cosh\left(a\sqrt{ABL_0}\right)}\right] \tag{3.45}$$

instead of the $q(r)$ profile in (3.18). By integration from $-a$ to a we obtain the total heat flux, $\int_{-a}^{a} q(y)dy = 2q_0$, i.e.

$$q_0 = -\frac{1}{BL_0}\frac{\partial T}{\partial x} a\left(1 - \frac{\tanh(a\sqrt{ABL_0})}{a\sqrt{ABL_0}}\right). \tag{3.46}$$

The latter equation is the analogous to (3.29), but for thin flat channels. In the limit when $L_0 \to 0$, this goes to

$$q_0 = -\frac{Aa^3}{3}\frac{\partial T}{\partial x}. \tag{3.47}$$

By using (3.46), to express $\frac{\partial T}{\partial x}$ in terms of q_0, the heat flux profile (3.45) may be alternatively rewritten as

$$q(y) = q_0\left(1 - \frac{\cosh(y\sqrt{ABL_0})}{\cosh(a\sqrt{ABL_0})}\right)\left(a - \frac{\tanh(a\sqrt{ABL_0})}{\sqrt{ABL_0}}\right)^{-1}. \tag{3.48}$$

Considering now the total heat flux in a section S of thickness $2a$, we can define an effective thermal conductivity as

$$\lambda_{eff} = \frac{Q}{S}\frac{l}{\Delta T} = \frac{1}{2a}\int_{-a}^{a} q(y)dy\frac{l}{\Delta T} = \frac{1}{BL}\left(1 - \frac{\tanh(a\sqrt{ABL_0})}{a\sqrt{ABL_0}}\right). \tag{3.49}$$

This is the analogous of (3.27) but for a wide plane channel. As well as (3.27), it shows a reduction of λ_{eff} for increasing values of L_0.

3.6 Remarks

In this chapter we used the one-fluid model formulated in (Jou et al., 2002), derived by Extended Thermodynamics, that we presented in the previous chapter, to search the influence of vortices ($L_0 \neq 0$) on the normal component velocity profile.

In Section 3.2 it has been seen that the presence of a sufficiently high vortex line density makes that the velocity profile of the normal component in counterflow turbulence becomes very flat in the central region. In fact, in this model there is not a sudden transition from parabolic to flat profile, but a gradual one, according to the form of the modified Bessel function of the zero order of the first type.

Thus, to ascertain whether a flat velocity profile truly corresponds to a turbulent state, it is necessary to be sure that the vortex line density is not high enough to explain by itself the flat form of the profile.

If the normal component flow in a cylindrical duct is laminar, its velocity profile is expected to have the usual parabolic form of Poiseuille flow. In contrast, if it is turbulent, the velocity profile will be much flatter in the central regions, as it is known from usual turbulence. In order to explain which of these situations is valid, experiments have been carried out with small suspended particles in the fluid, which are expected to visualize the form of the velocity profile (Barenghi, 2010; Galantucci et al., 2011; Galantucci and Sciacca, 2012, 2014; Guo et al., 2010). Experiments showed that the marker particles distributed in a flat profile perpendicular to the flow direction. From this observation, it was inferred that the normal fluid was turbulent in its own. We have pointed out, here, however, that a relatively flat profile of the normal fluid does not necessarily imply that its flow is turbulent. Indeed, we have shown that a simple model for the interaction between the quantized vortices and the normal component leads in a direct way to a velocity profile which significatively differs from the parabolic one and which is considerably flat in the central region. Thus, to assert the turbulent character of the normal component is more demanding than the observation of a flat velocity profile, and requires other further exploration, as those based on the analysis of velocity fluctuations.

Furthermore we reported analogous results for the normal fluid velocity introduced in the one-fluid model by (Mongiovì, 1993). Through the comparison between the experimental data for the relative velocity of the superfluid, i.e. $\mathbf{V}_{ns}$, and the results obtained in our model for the velocity $\mathbf{U}_{ns}$, we show how the results of the one-fluid model well agree with experimental data.

- Some results of Section 3.2 are published in:
  L. Saluto, M. S. Mongiovì and D. Jou, *Longitudinal counterflow in turbulent liquid helium: velocity profile of the normal component*,
  Z. Angew. Math. Phys. **65** 531–548 (2014), DOI 10.1007/s00033-013-0372-7

In Section 3.3 we have shown that the viscous contribution of the normal component of helium II to the thermal resistance in counterflow along a cylindrical channel in the superfluid turbulent regime may be considerably higher than the classical Landau estimation, as seen by comparing $(\nabla T)^{Landau}$ and $(\nabla T)^{lam}$ (Eqs. (3.19) and (3.31)). This is due to the fact that in presence of vortices the normal velocity profile becomes flat at the center and steep near the walls (Saluto et al., 2014), in such a way that it is considerably different than the Poiseuille parabolic profile, which is used to derive the well-known Landau estimation of the helium II thermal resistance. We have seen that, although the viscous contribution is smaller than the vortex contribution, it may be one or two orders of magnitude higher than the expected Landau contribution, in the partially developed **TII** turbulent regime.

The value of this viscous contribution is negligible for wide channels but it increases for decreasing radius — for a same value of the counterflow velocity $\mathbf{V}_{ns}$ —, as it is seen by comparing Table 3.5 (corresponding to $R = 0.025$ cm) and Table 3.4 ($R = 0.05$ cm). To obtain a detailed evaluation of the thermal resistance, the value of L_0 in terms of $\mathbf{q}$ and R is needed. A full self-contained analysis would require an evolution equation for L going beyond the standard Vinen's equation and including the influence of the walls, as that proposed in (Mongiovì and Jou, 2005a; Mongiovì et al., 2007).

The results obtained here are relevant because one could compare the measured thermal resistance with that expected for laminar flow of the normal component, to check whether the normal component is laminar or turbulent. If such a difference were actually observed in such a way that $(\nabla T)^{lam}$ was higher than $(\nabla T)^{Landau}$, one could apparently conclude that the normal component is not flowing in a laminar way. However, we have seen here that such a conclusion requires a detailed knowledge of the expected laminar contribution to the thermal resistance, since such contribution is not that expected from the parabolic velocity profile, but from a more complex profile, which may yield a much higher contribution. If one ignores this fact, one could interpret this enhanced value of thermal resistance as a proof of turbulent flow of the normal component, but we have seen here that this is not necessarily so, because the

modified velocity profile implies such an enhancement even in absence of turbulence of the normal component.

In Section 3.4 we have analized the particular situation in which the radius of the channel becomes comparable or higher than the phonon mean free path. In this case, the non-slip boundary condition for the velocity could break down, and a slip flow along the walls is expected to arise. We have explored the mathematical consequences of this possibility and we have found that this implies a reduction of the thermal resistance. This may be of special interest for the analysis of heat or mass transfer in porous media, where usually the non-slip condition process is considered, for very narrow channels, especially at low temperature, when the phonon mean free path becomes of the order of 500 μm.

- Some results of these two last sections are published in:
  L. Saluto, D. Jou and M. S. Mongiovì, *Contribution of the normal component to the thermal resistance of turbulent liquid helium*,
  Z. Angew. Math. Phys. (2015), DOI 10.1007/s00033-015-0493-2

The hypothesis of no matter flow along the channel is made. This is not an abstract mathematical simplification, but it corresponds to the well characterized and widely studied counterflow situation. For instance, if the channel is closed at both ends, there may be a heat flow but not a matter flow across them. In a following paper this hypothesis will be removed, to better describing the use of superfluid helium as cryogenic refrigerant in industry.

Another interesting situation, to be studied in the future, would be a so-called coflow situation, namely, when the total mass flow is not zero, but the superfluid flows along a channel with warmer walls, taking with it the heat; this situation is especially interesting in refrigeration problems. From a theoretical point of view, the interaction between a radial heat transfer and a longitudinal mass transfer would be especially challenging, because both effects may produce vortex tangles which will interact with each other.

Finally, for the sake of a wider generality, in Section 3.5 we report the solution for the heat flux equation for a flow in a two-dimensional infinitely wide channel between parallel plates to describe heat flow along a narrow slit. Through the essential physical results are similar to those in a cylindrical channel (non-parabolic and flatter velocity profile, effective thermal conductivity decreasing for increasing vortex density), the concrete analytical expressions are different.

3.7 Appendix 3.A: Viscous contribution of the normal component at $T = 1.5$ K and $T = 1.6$ K

For the sake of completeness, in this appendix we give the analogous of Tables 3.4 and 3.5 for two different values of T than that used in Section 3.3 (for $T = 1.7$ K), namely $T = 1.5$ K (Tables 3.8 and 3.10) and $T = 1.6$ K (Tables 3.9 and 3.11), for the radii $R = 0.05$ cm (Tables 3.8 and 3.9) and $R = 0.025$ cm (Tables 3.10 and 3.11)

- In these tables, the last column shows the viscous contribution of the normal component.
- The values of V_{ns} and L_0 for $R = 0.05$ cm are extracted from Fig. 10 of (Martin and Tough, 1983) in the regime **TII**.

  In the tables related to $R = 0.025$ cm we have taken values of V_{ns} of the same order of magnitude as for $R = 0.05$ cm, but the values for L_0 have been derived from the equations (1) and (18) of (Martin and Tough, 1983), giving L_0 in terms of V_{ns} and R.
- In each table, the first value of V_{ns} is the critical velocity indicated in (Martin and Tough, 1983) as V_{C2} yielding the transition between regimes **TI** and **TII**.
- The values of $(\nabla T)^{Landau}$, $(\nabla T)^{vort}$ and ∇T are calculated from equations (3.19), (3.28) and (3.29).

Inspection of the corresponding values indicates that the viscous contribution to the thermal resistance is lower for lower temperatures; this is logical because for lower temperatures ρ_n, the density of the normal component, is strongly reduced, and also its influence on the thermal resistance.

$\dot{Q}$ erg/s	V_{ns} cm/s	L_0 cm^{-2}	$(\nabla T)^{Landau}$ K/cm	$(\nabla T)^{vort}$ K/cm	∇T K/cm	$(\nabla T)^{lam}$ K/cm
$6.84 * 10^3$	2.30	$2.78 * 10^4$	$3.33 * 10^{-7}$	$1.56 * 10^{-6}$	$2.23 * 10^{-6}$	$6.67 * 10^{-7}$
$1.04 * 10^4$	3.48	$1.60 * 10^5$	$5.05 * 10^{-7}$	$1.36 * 10^{-5}$	$1.57 * 10^{-5}$	$2.11 * 10^{-6}$
$1.29 * 10^4$	4.33	$2.67 * 10^5$	$6.29 * 10^{-7}$	$2.83 * 10^{-5}$	$3.15 * 10^{-5}$	$3.23 * 10^{-6}$
$1.49 * 10^4$	5.00	$4.44 * 10^5$	$7.26 * 10^{-7}$	$5.44 * 10^{-5}$	$5.91 * 10^{-5}$	$4.71 * 10^{-6}$
$1.79 * 10^4$	6.00	$5.63 * 10^5$	$8.71 * 10^{-7}$	$8.25 * 10^{-5}$	$8.91 * 10^{-5}$	$6.57 * 10^{-6}$
$1.94 * 10^4$	6.52	$6.40 * 10^5$	$9.46 * 10^{-7}$	$1.02 * 10^{-4}$	$1.09 * 10^{-4}$	$7.24 * 10^{-6}$

Table 3.8: Values for $T = 1.5$ K and $R = 0.05$ cm

$\dot{Q}$ erg/s	V_{ns} cm/s	L_0 cm^{-2}	$(\nabla T)^{Landau}$ K/cm	$(\nabla T)^{vort}$ K/cm	∇T K/cm	$(\nabla T)^{lam}$ K/cm
$9.20 * 10^3$	2.15	$1.85 * 10^4$	$3.12 * 10^{-7}$	$9.68 * 10^{-7}$	$1.37 * 10^{-6}$	$4.05 * 10^{-7}$
$1.27 * 10^4$	2.96	$1.35 * 10^5$	$4.30 * 10^{-7}$	$9.78 * 10^{-6}$	$1.10 * 10^{-5}$	$1.25 * 10^{-6}$
$1.70 * 10^4$	3.96	$2.70 * 10^5$	$5.75 * 10^{-7}$	$2.61 * 10^{-5}$	$2.85 * 10^{-5}$	$2.35 * 10^{-6}$
$1.87 * 10^4$	4.37	$4.10 * 10^5$	$6.34 * 10^{-7}$	$4.36 * 10^{-5}$	$4.68 * 10^{-5}$	$3.15 * 10^{-6}$
$2.11 * 10^4$	4.93	$5.07 * 10^5$	$7.15 * 10^{-7}$	$6.09 * 10^{-5}$	$6.48 * 10^{-5}$	$3.95 * 10^{-6}$
$2.43 * 10^4$	5.67	$5.90 * 10^5$	$8.23 * 10^{-7}$	$8.15 * 10^{-5}$	$8.65 * 10^{-5}$	$5.00 * 10^{-6}$

Table 3.9: Values for $T = 1.6$ K and $R = 0.05$ cm

$\dot{Q}$ erg/s	V_{ns} cm/s	L_0 cm^{-2}	$(\nabla T)^{Landau}$ K/cm	$(\nabla T)^{vort}$ K/cm	∇T K/cm	$(\nabla T)^{lam}$ K/cm
$6.84 * 10^3$	9.19	$1.18 * 10^6$	$5.33 * 10^{-6}$	$2.64 * 10^{-4}$	$2.94 * 10^{-4}$	$2.97 * 10^{-5}$
$1.04 * 10^4$	13.93	$2.98 * 10^6$	$8.09 * 10^{-6}$	$1.02 * 10^{-3}$	$1.09 * 10^{-3}$	$6.91 * 10^{-5}$
$1.29 * 10^4$	17.33	$4.86 * 10^6$	$1.01 * 10^{-6}$	$2.06 * 10^{-3}$	$2.17 * 10^{-3}$	$1.06 * 10^{-4}$
$1.49 * 10^4$	20.00	$6.66 * 10^6$	$1.16 * 10^{-5}$	$3.26 * 10^{-3}$	$3.40 * 10^{-3}$	$1.44 * 10^{-4}$
$1.79 * 10^4$	24.00	$9.92 * 10^6$	$1.39 * 10^{-5}$	$5.82 * 10^{-3}$	$6.04 * 10^{-3}$	$2.16 * 10^{-4}$
$1.94 * 10^4$	26.07	$1.19 * 10^7$	$1.51 * 10^{-5}$	$7.57 * 10^{-3}$	$7.83 * 10^{-3}$	$2.54 * 10^{-4}$

Table 3.10: Values for $T = 1.5$ K and $R = 0.025$ cm

$\dot{Q}$ erg/s	V_{ns} cm/s	L_0 cm^{-2}	$(\nabla T)^{Landau}$ K/cm	$(\nabla T)^{vort}$ K/cm	∇T K/cm	$(\nabla T)^{lam}$ K/cm
$9.20 * 10^3$	8.59	$1.29 * 10^6$	$3.20 * 10^{-6}$	$2.69 * 10^{-4}$	$2.92 * 10^{-4}$	$2.30 * 10^{-5}$
$1.27 * 10^4$	11.85	$2.65 * 10^6$	$4.41 * 10^{-6}$	$7.65 * 10^{-4}$	$8.09 * 10^{-4}$	$4.44 * 10^{-5}$
$1.70 * 10^4$	15.85	$5.07 * 10^6$	$5.90 * 10^{-6}$	$1.96 * 10^{-3}$	$2.04 * 10^{-3}$	$8.07 * 10^{-5}$
$1.87 * 10^4$	17.48	$6.30 * 10^6$	$6.51 * 10^{-6}$	$2.69 * 10^{-3}$	$2.78 * 10^{-3}$	$9.28 * 10^{-5}$
$2.11 * 10^4$	19.70	$8.20 * 10^6$	$7.34 * 10^{-6}$	$3.94 * 10^{-3}$	$4.06 * 10^{-3}$	$1.22 * 10^{-4}$
$2.43 * 10^4$	22.67	$1.11 * 10^7$	$8.44 * 10^{-6}$	$6.16 * 10^{-3}$	$6.31 * 10^{-3}$	$1.47 * 10^{-4}$

Table 3.11: Values for $T = 1.6$ K and $R = 0.025$ cm

3.8 Appendix 3.B: Data for V_{ns} and U_{ns} at $T = 1.5$ K and $T = 1.6$ K

For the sake of completeness, we report here the analogous results obtained in Section 3.3.1, for $T = 1.5$ K and $T = 1.6$ K.

These tables show that in the fully developed regime the values of U_{ns} are quite close to that of V_{ns} extracted by experimental data.

V_{ns} cm/s	L_0 cm^{-2}	$(\nabla T)^{Landau}$ K/cm	$(\nabla T)^{vort}$ K/cm	$(\nabla T)^{Landau} + (\nabla T)^{vort}$ K/cm	$\overline{\mathbf{q}}$ erg / (cm*s)	U_{ns} cm/s
2.30	$2.78 * 10^4$	$3.33 * 10^{-7}$	$1.56 * 10^{-6}$	$1.89 * 10^{-6}$	$7.39 * 10^5$	1.95
3.48	$1.60 * 10^5$	$5.05 * 10^{-7}$	$1.36 * 10^{-5}$	$1.41 * 10^{-5}$	$1.19 * 10^6$	3.13
4.33	$2.67 * 10^5$	$6.29 * 10^{-7}$	$2.83 * 10^{-5}$	$2.89 * 10^{-5}$	$1.51 * 10^6$	3.97
5.00	$4.44 * 10^5$	$7.26 * 10^{-7}$	$5.44 * 10^{-5}$	$5.51 * 10^{-5}$	$1.77 * 10^6$	4.67
6.00	$5.63 * 10^5$	$8.71 * 10^{-7}$	$8.25 * 10^{-5}$	$8.34 * 10^{-5}$	$2.13 * 10^6$	5.63
6.52	$6.40 * 10^5$	$9.46 * 10^{-7}$	$1.02 * 10^{-4}$	$1.03 * 10^{-4}$	$2.33 * 10^6$	6.14

Table 3.12: Values of V_{ns} and U_{ns} in the regime **TII** for $T = 1.5$ K

V_{ns} cm/s	L_0 cm^{-2}	$(\nabla T)^{Landau}$ K/cm	$(\nabla T)^{vort}$ K/cm	$(\nabla T)^{Landau} + (\nabla T)^{vort}$ K/cm	$\overline{\mathbf{q}}$ erg / (cm*s)	U_{ns} cm/s
2.15	$1.85 * 10^4$	$3.12 * 10^{-7}$	$9.68 * 10^{-7}$	$1.28 * 10^{-6}$	$1.09 * 10^6$	2.00
2.96	$1.35 * 10^5$	$4.30 * 10^{-7}$	$9.78 * 10^{-6}$	$1.02 * 10^{-5}$	$1.50 * 10^6$	2.74
3.96	$2.70 * 10^5$	$5.75 * 10^{-7}$	$2.61 * 10^{-5}$	$2.67 * 10^{-5}$	$2.03 * 10^6$	3.72
4.37	$4.10 * 10^5$	$6.34 * 10^{-7}$	$4.36 * 10^{-5}$	$4.43 * 10^{-5}$	$2.25 * 10^6$	4.14
4.93	$5.07 * 10^5$	$7.15 * 10^{-7}$	$6.09 * 10^{-5}$	$6.16 * 10^{-5}$	$2.55 * 10^6$	4.69
5.67	$5.90 * 10^5$	$8.23 * 10^{-7}$	$8.15 * 10^{-5}$	$8.23 * 10^{-5}$	$2.95 * 10^6$	5.40

Table 3.13: Values of V_{ns} and U_{ns} in the regime **TII** for $T = 1.6$ K

Chapter 4

Entrance region: longitudinal and transversal flows

In the previous chapter we have assumed a long infinite channel, with a fully developed flow for the normal component. The aim of the present chapter is to study the so-called entrance flow, i.e. the region from the entrance to the tube to the region where the velocity profile has the fully developed (asymptotic) form. Since in this case the longitudinal component q_x depends not only on r (radial position) but also on x (position along the channel), the steady state condition $\nabla \cdot \mathbf{q} = 0$, namely:

$$\frac{\partial q_x}{\partial x} + \frac{1}{r}\frac{\partial}{\partial r}(r q_r) = 0 \tag{4.1}$$

(for axially symmetric flows independent of the angle θ), implies the existence of a transverse (radial) component $q_r(x, r)$. Therefore this chapter has two new aspects with respect to the previous one: the dependence of the profile along the tube, and the existence of a radial component of the flow.

Flows in the entrance region are a classical topic in fluid mechanics of viscous fluids, but we adapt it here to heat transport in helium II, relating the temperature gradient to the heat flux instead of the pressure gradient to the mass flow, and using more general equations than the viscous fluid equations.

In the case of viscous fluids, the starting situation is easy to understand from a qualitative point of view and is represented in Figure 4.1. At the entry part, the fluid is assumed to have a flat velocity profile (of course, from the mathematical point of view many other kinds of profiles at $x = 0$ are conceivable). However, when it becomes in contact with the walls, a zero velocity — or at least a small velocity — is imposed on them. This implies a steep velocity gradient in that region and, therefore, a high viscous force in the fluid, slowing it down near the wall and increasing its velocity near the centre of the channel. The propagation of this force into the fluid, towards

the axis of the channel, will eventually lead to the parabolic Poiseuille form in the absence of turbulent effects, or to the flattened profile in presence of a constant density of quantized vortices, as it has been seen in Chapter 3 ((3.18) for cylindrical channels and (3.48) for flat channels). These two situations are usually described by assuming that the channel is sufficiently long for the velocity profiles to correspond to a fully developed situation, with vanishing radial flows, and only longitudinal flows. However, for channels with a length shorter than $0.05 ReyD$, with D the diameter of the channel and Rey the Reynolds number ($Rey = \overline{\mathbf{v}} D/\nu$, $\overline{\mathbf{v}}$ being the average velocity of the normal component and $\nu = \eta/\rho$ its kinematic viscosity, with η the bulk viscosity coefficient and ρ the density of the fluid), the velocity profile has not yet arrived to the fully developed regime (Landau and Lifshitz, 1987).

This situation is often found in actual counterflow experiments. As a consequence, a deep analysis of counterflow requires to know whether the channel is longer or shorter than the entrance region. In fact, in this region, temperature gradient at a given heat flux is higher than that in a fully developed regime and therefore this region may contribute essentially strongly to the thermal resistance.

In the classical theory of laminar viscous flow (Landau and Lifshitz, 1987; Lautrup, 2011), the length of the entrance region has the approximate form

$$L_{entrance} = K Rey D, \tag{4.2}$$

with K a numerical constant (of the order of 0.05 (Landau and Lifshitz, 1987)). Thus, at $Rey = 2000$, for instance — more or less the limiting value beyond which turbulence would appear — the length of the entrance region will be $L_e \approx 100D$. For instance, if the diameter of the channel is 2 mm, the length of the entrance region will be 20 cm. But, in actual fact, the length should be considerably longer — let us say, some five or six times longer at least — in order that the dominant profile in most of the length of the channel is the fully developed profile, the entrance region being only a relatively small zone of the total flow. This would lead to a length of the order of 1 m but, in the usual experiments on turbulent counterflow in liquid helium the tubes are shorter than that. In fact, the actual Reynolds number of the normal component of He II is much smaller than 2000, of the order of 400; in this case, the actual entrance lenght will be one order of magnitude smaller, but the influence of the entrance region will be still important.

We are not aware of a previous detailed consideration to this problem in helium II counterflow, which is more complex than in usual laminar viscous flows, because of the presence of vortex lines. An analysis of this problem is needed to interpret the velocity profile of the normal component, for instance, a topic which we have already commented in the previous chapter. This profile is needed, not only on its own, for the sake of theoretical curiosity, but also to obtain the expression for the effective thermal

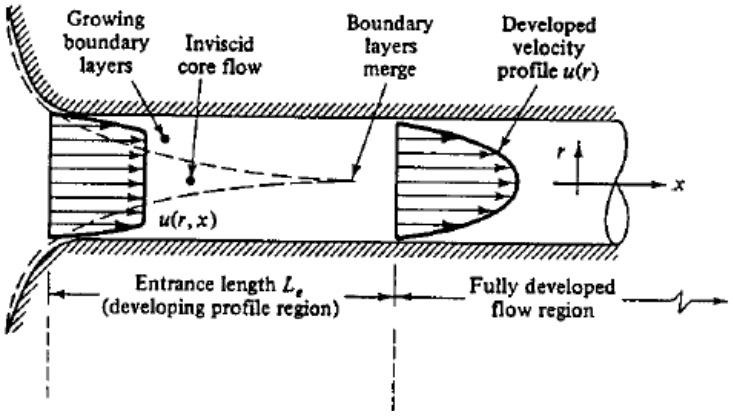

Figure 4.1: Developing velocity profile in the entrance of a duct flow. One can see the entrance region, where the velocity profile evolves from flat to parabolic.

conductivity of the superfluid. In the first section we will deal with this problem in a phenomenological way, as an introduction to the practical interest of the entrance flow in superfluids.

A still more complicated problem would be a channel of finite length l, connecting two wide containers, as for instance a narrow channel through a thin wall separating two containers. In this case, the asymptotic form of the velocity profile would be never achieved, and one should consider also the influence of the "exit region" besides that of the "entrance region".

4.1 Entrance flow and effective heat conductivity of superfluid helium in short channels: laminar situation

The practical aim of this section is to obtain the suitable corrections to the well-known Landau formula for the effective thermal conductivity of superfluid helium in situations where the channel is not long enough to have a fully developed flow. This is relevant from the practical point of view because it is known that, in principle, wide channels are preferable to thin channels for an efficient heat transport (the Landau effective thermal conductivity is proportional to the square of the radius of the channel). However, if the diameter of the channel is of the order or wider than $l/(0.05Rey)$, the Landau formula for the thermal conductivity will not be suitable. For instance, if $Rey = 1000$, this implies that Landau formula will be valid only for $D \ll l/50$. Therefore, an exploration of this topic is needed. We will follow the paper (Lesniewski et al., 1996), but introducing additional comments and details.

In the usual two-fluid model, the calculation of the effective thermal conductivity of helium II in a channel goes along the following lines, already proposed in (Landau, 1941), and briefly reviewed in the previous chapter. Here, we repeat a part of the previous comments but from a more general perspective, including non-linear terms which are specially relevant in the entrance region, but which were neglected in the previous chapter. The velocity $\mathbf{v}_n$ of the normal component is assumed to follow the classical Navier-Stokes equation, namely:

$$\rho \mathbf{v}_n \cdot \nabla \mathbf{v}_n + \nabla p = \eta \nabla^2 \mathbf{v}_n, \tag{4.3}$$

with η the viscosity of the normal component and p the pressure. In the well-developed flow, the non-linear term vanishes, because $\mathbf{v}_n$ does not depend on the axial coordinate, and because the radial component of $\mathbf{v}_n$ is zero. In the one-fluid model we could consider $\mathbf{q}$ instead of $\mathbf{v}_n$, so that the essential results would be analogous to those obtained here. Here we will use $\mathbf{v}_n$ for the sake of close comparison with the bibliography on usual fluids.

According to the Gibbs equation, $dG = -SdT + Vdp$, with vanishing chemical potential, one has

$$\nabla p = \rho s \nabla T, \tag{4.4}$$

with s the entropy per unit mass. This relation allows to express the pressure gradient in terms of the temperature gradient, as was done in (3.10), which is useful in the analysis of heat transfer.

The result of the integration of (4.3) without the first term — i.e. in the fully developed flow region — in a cylindrical channel of radius R and length l and assuming $\mathbf{v}_n = 0$ on the wall (for $r = R$), is

$$\mathbf{v}_n(r) = \frac{\Delta p}{4l\eta} R^2 \left[1 - \frac{r^2}{R^2}\right]. \tag{4.5}$$

This leads, after integration over the cross section from $r = 0$ to $r = R$, to the following expression for the average normal velocity

$$\overline{\mathbf{v}}_n = \frac{R^2}{8\eta} \frac{\Delta p}{l}. \tag{4.6}$$

As said in the previous chapter, the heat flux is given by $\mathbf{q} = \rho s T \mathbf{v}_n$. Thus, using (4.4), the total heat flux across the tube will be

$$\dot{Q} = \rho T s \overline{\mathbf{v}}_n \pi R^2 = \frac{\rho^2 s^2 T \pi R^4}{8\eta} \frac{\Delta T}{l}. \tag{4.7}$$

This leads to the following expression for the effective thermal conductivity (see (3.25))

$$\lambda_{eff} \equiv \frac{\dot{Q}}{\pi R^2} \frac{l}{\Delta T} = \frac{\rho^2 s^2 T R^2}{8\eta}. \tag{4.8}$$

As we commented in the previous chapter, this is not a true thermal conductivity in the classical sense, i.e. as a quantity which only depends on the material, because it also depends on the size of the tube. This feature is well known in heat transport in nanosystems (Alvarez et al., 2010; Sellitto et al., 2010), as for instance nanowires whose radius is comparable or smaller than the phonon mean free path.

The former derivation assumes that the flow of the normal component is well developed, but this is not true in the entrance region. In (Lesniewski et al., 1996) the authors have made a simplified analysis of the influence of the entrance region in usual fluids. Here, we apply their results to helium II, for the sake of illustration and motivation of our further work in this chapter, where we will deal in deeper detail with this topic. In the entrance region, the non-linear terms in the left hand side of (4.3) are different from zero, and they must be taken into account. The mathematical development is complicated, but several approximate solutions or empirical expressions are known for classical viscous fluids.

In (Lesniewski et al., 1996) the authors find that Δp in a tube of length l is given approximately by

$$\Delta p = \frac{\rho U^2}{2}\left[13.74 X^{\frac{1}{2}} + \frac{1.25 + 64X - 13.74X^{\frac{1}{2}}}{1 + 0.00021 X^{-2}}\right], \tag{4.9}$$

with X a dimensionless parameter, given by

$$X = l\frac{\eta}{4R^2\rho U}, \tag{4.10}$$

where U is the average velocity. Note that this parameter may be rewritten in terms of the Reynolds number as $X = \frac{l}{D}\frac{1}{Rey}$, and that when $Rey > 2000$ the flow becomes turbulent. When X is very high (as for instance when l is very long as compared to the radius R times the Reynolds number), corresponding to fully developed parabolic profile, one has

$$\Delta p = \frac{\rho U^2}{2}(1.25 + 64X) \approx \frac{\rho U^2}{2} 64X = 8\eta\frac{Ul}{R^2}, \tag{4.11}$$

which is just the Poiseuille expression (4.6) for Δp, as a function of U, η, l and R. Note that (4.10) and (4.11) may be related to (4.2) by writing (4.10) as

$$L_{entrance} = X' Rey D, \tag{4.12}$$

where X' could be obtained by requiring that $64X' \approx 25$ (in order that the 1.25 in the parenthesis in the second member of (4.11) is less than 5% of the Poiseuille term $64X$); this yields $X' \approx 0.38$, which is considerably larger than the value 0.05 mentioned below (4.2) and which is usually reported in fluid hydrodynamics books (such value would be obtained if we require $64X' \approx 1.25$ instead of 25).

In superfluid helium the total heat flux $\dot{Q}$ is related to the velocity of the normal component by the relation $\dot{Q} = \rho s T \pi R^2 \overline{\mathbf{v}}_n$. Then, taking into account (4.9) instead of (4.6) and making the changes $\Delta p = \rho s \Delta T$ and $\dot{Q}$ in terms of $\mathbf{v}_n$, (4.11) can be rewritten as

$$\Delta T = \frac{\dot{Q}^2}{2\pi^2 R^4 \rho^2 s^3 T^2} \left[13.74 X^{\frac{1}{2}} + \frac{1.25 + 64X - 13.74 X^{\frac{1}{2}}}{1 + 0.00021 X^{-2}} \right]. \tag{4.13}$$

This leads to an effective thermal conductivity $\lambda_{eff} = (\dot{Q}/\pi R^2)(l/\Delta T)$ given by

$$\lambda_{eff} = \frac{\dot{Q}}{\pi R^2} \frac{l}{\Delta T} = \lambda_{Landau} \left[0.214 X^{-\frac{1}{2}} + \frac{0.019 X^{-1} + 1 - 0.214 X^{-\frac{1}{2}}}{1 + 0.00021 X^{-2}} \right]^{-1}, \tag{4.14}$$

where X is written in terms of $\dot{Q}$ as

$$X = \frac{l}{4} \frac{\eta \pi s T}{\dot{Q}}, \tag{4.15}$$

and $\lambda_{Landau} = \frac{\rho^2 s^2 T R^2}{8\eta}$ is the well-known Landau expression for the effective thermal conductivity.

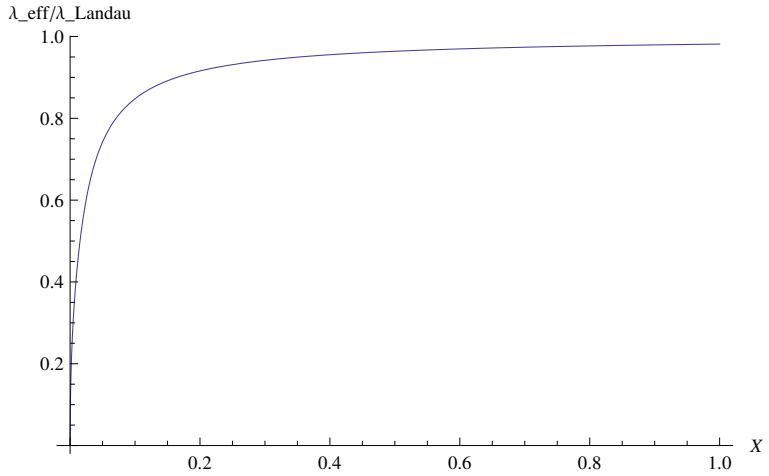

Figure 4.2: $\lambda_{eff}/\lambda_{Landau}$ vs X from equation (4.14), with X defined in (4.15).

When l is long, or $\dot{Q}$ is small ($X \gg 1$), equation (4.14) reduces to (4.8), but for short channels the effective thermal conductivity depends not only on R but also on l and it is lower than the effective conductivity derived in the fully developed regime, i.e. when the profile of the normal component velocity is parabolic. The form of $\lambda_{eff}/\lambda_{Landau}$ is plotted in Figure 4.2 for the interval $0 < X < 1$, where the entrance effects are more

visible. Note that for constant T and $\dot{Q}$, X is proportional to the length l, according to (4.15), and therefore, in these conditions, Figure 4.2 is equivalent to a plot of the dependence of $\lambda_{eff}/\lambda_{Landau}$ with the length. Concerning analytic expressions for the asymptotic behaviour for X high but not infinite, the correction to λ_{eff} will be

$$\lambda_{eff} = \lambda_{Landau}(1 + 0.019X^{-1})^{-1}. \tag{4.16}$$

This correction is only valid for relatively high values of X and it turns to be small; usually, the correction may be important, but the full equation (4.14) will be necessary to account for it. For instance, the difference with respect to (4.8) may be relevant. As an example, for $X = 1/4$, λ_{eff} in the short channel would be $\frac{1}{1.07} \approx 0.94$ times the value predicted by (4.8), and for $X = 1/9$, it would be $\frac{1}{1.17} \approx 0.85$ times the value predicted by (4.8). Thus, in short channels the steady Poiseuille flow has no space enough to be settled, and the flow will be more complicated. This may influence not only the effective thermal conductivity, but also the microscopic details of the vortex tangle in the case that superfluid turbulence were produced. Indeed, a strong gradient in thermal conductivity may also indicate high gradients in the heat flux, which could act as a source of vortices (see Section 5.3 for a discussion).

In fact, the influence of the entrance region may also lead to wrong interpretations of the observed results. For instance, the increase of thermal resistance for increasing values of $\dot{Q}$ could be interpreted as being due to the appearance of some additional vortex lines, instead of attributing it to the effects of the entrance region. Another risk of misinterpretation may be found in the experimental analysis of normal velocity profile: some observations of a relatively flat profile for the normal velocity distribution could in part be due to the fact that the velocity profile has not yet arrived to the asymptotic distribution. This reason could be added to the one analyzed in the previous chapter, namely, that the friction with vortices flattens the velocity profile. Thus, this topic truly deserves a detailed attention.

To be more explicit, we may study the asymptotic expression in the limit of X very small, as obtained from (4.14), which is:

$$\lambda_{eff} \cong \lambda_{Landau} \frac{1}{0.214X^{-\frac{1}{2}} + \frac{0.019}{0.00021}X} \cong \lambda_{Landau} \frac{X^{\frac{1}{2}}}{0.214} \tag{4.17}$$

It is indeed seen that for short l or high $\dot{Q}$, λ_{eff} becomes very small. Furthermore, the relation between ΔT and $\dot{Q}$ is no longer linear, but $\dot{Q}$ becomes

$$\dot{Q} \propto l^{\frac{1}{3}} \left(\frac{\Delta T}{l}\right)^{\frac{2}{3}} = l^{-\frac{1}{3}} \Delta T^{\frac{2}{3}}. \tag{4.18}$$

Note that this dependence is different from that of the Gorter-Mellink law in superfluid turbulence, in which

$$\dot{Q} \propto l^{-\frac{1}{3}} \Delta T^{\frac{1}{3}}. \tag{4.19}$$

Indeed, a dependence of $\log \dot{Q}$ with $\frac{2}{3} \log \Delta T$ has been experimentally observed in (Childers and Tough, 1976).

Of course, the phenomenon analyzed here is very different and it is not expected that the dependence of $\dot{Q}$ with $(\Delta T/l)$ is the same in both cases. It is interesting to note that a marked separation from the linear dependence of $\dot{Q}$ with $(\Delta T/l)$ is found in short channels. This may be understood in Figure 4.3, where it is seen that, for a given mass flow — or heat flow, in our case — the pressure gradient in the entrance region, is higher — in absolute value — than in the fully developed regime. This implies, in our case, a lower thermal conductivity, since a higher temperature gradient is required for a given heat flux. Furthermore, for a given l, a higher value of $\dot{Q}$ will imply a smaller effective thermal conductivity. This reduction is not due to friction with vortices, so that in the presence of vortices, the reduction would still be higher, because one should add the contribution of vortex resistance to the excess resistance related to the entrance region.

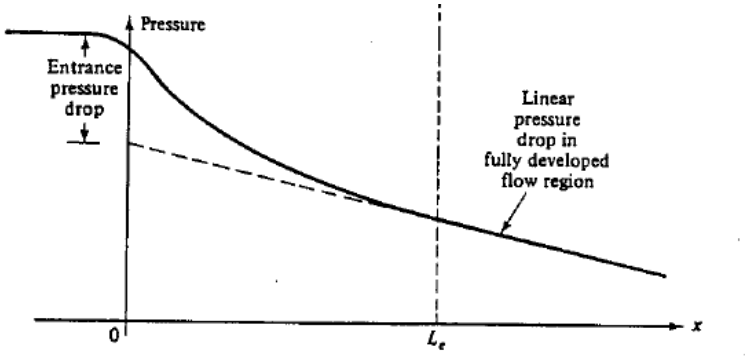

Figure 4.3: Pressure change in the entrance of a duct flow. Note that the pressure gradient is higher in the entrance region than in the fully developed region. This implies, in our model, that the effective thermal conductivity for short channels will be lower than for long channels.

The dependence found in (4.18) follows after the detailed analysis leading to (4.14), the exponents appearing in (4.18) are not obvious. Instead, from a naive dimensional analysis of equation (4.3), for instance, one could have assumed, in the entrance region, a behaviour of the form $\rho v_n (v_n/l)$ proportional to $-\nabla p$; making the relation between the flow of the normal component and the heat flux, and of the pressure gradient with the temperature gradient, one would have been led to v_n^2 proportional to $l(\Delta T/l)$ and, therefore, to $\dot{Q}$ proportional to $l^{\frac{1}{2}}(\Delta T/l)^{\frac{1}{2}}$.

4.2 Entrance flow and effective heat conductivity of superfluid helium in short channels: turbulent situation

The situation considered in the previous section corresponds to a purely laminar situation, both for normal component and for the superfluid component. In this section we briefly analyze the order of magnitude of the parameter X introduced in (4.10) for which turbulence in the superfluid component will arise. This gives a further view on the range of validity of the analysis of the previous section.

As it has been commented above, from the hydrodynamical point of view, the parameter X defined in (4.10) may be expressed in terms of the Reynolds number as $X = \frac{l}{D}\frac{1}{Rey}$. Assume that the critical value of Rey that characterises the appearance of the turbulence in the normal component is $Rey^{(c)} = 2000$; one realises that small values of $\overline{\mathbf{v}}$ could be due to two different situations (or both of them simultaneously), namely, high values of the Reynolds number or small values of l/D. In particular we consider both situations:

a) $Rey < 2000$ but $\frac{l}{2R} < 2000$, implying laminar flow,

b) $Rey > 2000$ and $\frac{l}{2R}$ sufficiently low, implying turbulent flow.

Here we are more interested in the first situation, because we want to focus our attention on turbulence of the normal component. There arises, however, the question about which conditions are required to know wether superfluid turbulence will arise in the entrance region although normal turbulence is not present.

We have seen in Chapter 3 that an usual condition for quantum turbulence is that the quantum Reynolds number is higher than a critical value, i.e. $V_{ns}D/\kappa > Rey_{q_1}$. In counterflow, one has $\mathbf{V}_{ns} = (\rho/\rho_n)\mathbf{v}_n$. Then, we may rewritte X as

$$X = \frac{l\eta}{4R^2\rho\overline{\mathbf{v}}} = \frac{1}{Rey_q}\frac{l}{D}\frac{\nu}{\kappa}, \tag{4.20}$$

with $\nu \equiv \frac{\eta}{\rho_n}$ being the kinematic viscosity of the normal component. Assume that $Rey_{q_{critical}}$ is of the order 200 (in fact it depends on T) (Martin and Tough, 1983). Then, to have, for instance, $X \approx 10^{-2}$ and still being laminar flow, we need that $XRey_q \lesssim 2$ and therefore

$$\frac{l}{D}\frac{\nu}{\kappa} < 2, \qquad \text{or} \qquad \frac{l}{D} < 2\frac{\kappa}{\nu}. \tag{4.21}$$

The quantum of vorticity κ does not depends on T and has value of the order of 10^{-3} cm^2/s. At $T = 1,5$ K, the value of ν is $2.786{*}10^{-3}$. Then, to have $X = 10^{-2}$ but without quantum turbulence nor normal turbulence, one should have $\frac{l}{D} < \frac{2}{2.79} \sim 0.71$.

Thus, it is unrealistic to consider the situation of small X without superfluid turbulence, whereas to avoid normal fluid turbulence we need for $X \approx 20$ and therefore

$$\frac{l}{D} \lesssim 20 \tag{4.22}$$

Note that this is a very short length. Rather than to a channel or a pore across a thick wall it could correspond to a circular hole through a very thin wall.

In summary, high values of X usually imply turbulence, at least in usual fluids. Therefore, it is logical to ask how quantum turbulence effects can be included in a description of entrance flows. This is the aim of the next section.

4.3 Influence of vortices on the entrance heat flow: turbulent situation, cylindrical channels

We consider now a semi-infinite pipe of radius R, filled with He II and subject to a longitudinal heat flux (i.e. counterflow situation), in order to search how the entry length, i.e. the point where the central velocity has reached 99% of its terminal value, is affected by the presence of vortices. In more general terms, one is interested in the evolution profile (or the heat flux profile $q_x(0,r)$, where x indicates the position along the channel) at the entrance of the channel at $x = 0$ to the fully developed profile $v_x(r)$ independent of x. Usually one assume a flat profile $v_x(0,r)$ =constant at $x = 0$. One usually may to describe the entrance flow is to assume $v_x(x,r) = f(x)v_x[\overline{\omega}(x)r]$; with $f(x)$ and $\overline{\omega}(x)$ determined in such a way that the total volume flow is independent of x, and that $f(x) \to 1$ and $\overline{\omega}(x) \to 1$ for $x \to \infty$, and $f(0)v_x[\overline{\omega}(0)r]$ approximates sufficiently well the imposed velocity profile at $x = 0$.

Here, we will follow the *Addenda* of the book (Lautrup, 2011), but using the variable used in the previous chapters of this thesis. We can indifferently use the variable $\mathbf{q}$ of the one-fluid model or the variable $\mathbf{v}_n$ of the two-fluid model, but to a greater analogy with the work of Lautrup we use the second one, taking in mind that it is always possible make the change $\mathbf{q} = ST\mathbf{v}_n$ (in the following for a simplest notation we will use $\mathbf{v}^{(n)}$ instead of $\mathbf{v}_n$).

Under particular boundary conditions, as those proposed by Lautrup, and assuming that the pressure only depends on x, the Navier-Stokes equation (4.3) for the longitudinal velocity of the flow $v_x^{(n)}$ of the normal component in cylindrical coordinates, becomes a Prandtl equation, i.e.

$$v_x^{(n)}\frac{\partial v_x^{(n)}}{\partial x} + v_r^{(n)}\frac{\partial v_x^{(n)}}{\partial r} = G(x) + \frac{\overline{\nu}}{r}\frac{\partial}{\partial r}(r\frac{\partial v_x^{(n)}}{\partial r}) - \overline{\eta}L(x)v_x^{(n)} \tag{4.23}$$

where $G(x) = -\frac{1}{\rho}\nabla p$, x is the direction along the axis of the pipe, L is the vortex line density, $\overline{\nu}$ and $\overline{\eta}$ parameters whit dimensions (length)^2/time.

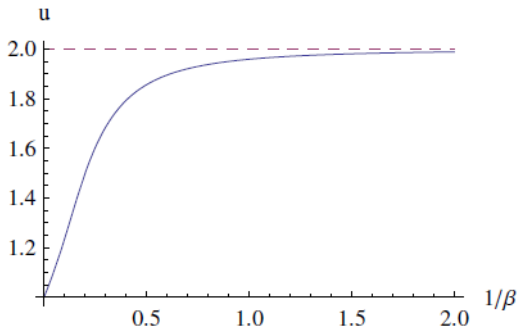

Figure 4.4: Central flow velocity as a function of $1/\beta$. It reaches 99% of the terminal value ($u = 2$ cm/s) for $\beta = \beta_{99} = 0.699861$, or $1/\beta_{99} = 1.42885$ (dotted line). This figure is Figure 1-right of the *Addenda: Pipe Entrance Flow* of (Lautrup, 2011), in which $\beta = \overline{\omega}$.

The friction term in $L(x)$ has not been considered in previous works, but it will play a central role in our analysis, because it describes the frictional effects between the quantized vortices and the flow of the normal component.

An approximate solution can be found, defining a function $H(x)$ as

$$H(x) = v_x^{(n)} \frac{\partial v_x^{(n)}}{\partial x} + v_r^{(n)} \frac{\partial v_x^{(n)}}{\partial r} - \overline{\nu\omega}^2 v_x^{(n)} + \overline{\eta} L(x) v_x^{(n)}, \tag{4.24}$$

where $\overline{\omega} = \overline{\omega}(x)$ is an unknown function of x, to be determined below, that is a parameter of tension length with dimensions $(\text{length})^{-1}$. In terms of H the equation (4.23) becomes

$$\overline{\nu} \left(\frac{\partial^2 v_x^{(n)}}{\partial r^2} + \frac{1}{r} \frac{\partial v_x^{(n)}}{\partial r} \right) = \overline{\nu\omega}^2 v_x^{(n)} + H(x) - G(x). \tag{4.25}$$

Provided H only depends on x, the only solution that is regular for $r \to 0$, because of the symmetry of the steady flow in a cylindrical channel, is

$$v_x^{(n)}(x, r) = \frac{G(x) - H(x)}{\overline{\nu\omega}^2} + F(x) I_0(\overline{\omega} r), \tag{4.26}$$

where $F(x)$ is an arbitrary function of x. It is determined by the boundary condition $v_x^{(n)} = 0$ for $r = \pm R$, and we find

$$v_x^{(n)}(x, r) = \frac{G(x) - H(x)}{\overline{\nu\omega}^2} \left[1 - \frac{I_0(\overline{\omega} r)}{I_0(\overline{\omega} R)} \right]. \tag{4.27}$$

Introducing the average value $q_{x0}(x)$ of $q_x(x, r)$ across a section of the pipe

$$\int_0^R q_x(x, r) 2\pi r dr = \pi R^2 q_{x0}(x), \qquad \Rightarrow \qquad \int_0^R v_x^{(n)}(x, r) 2\pi r dr = \pi R^2 v_{x0}^{(n)}(x) \tag{4.28}$$

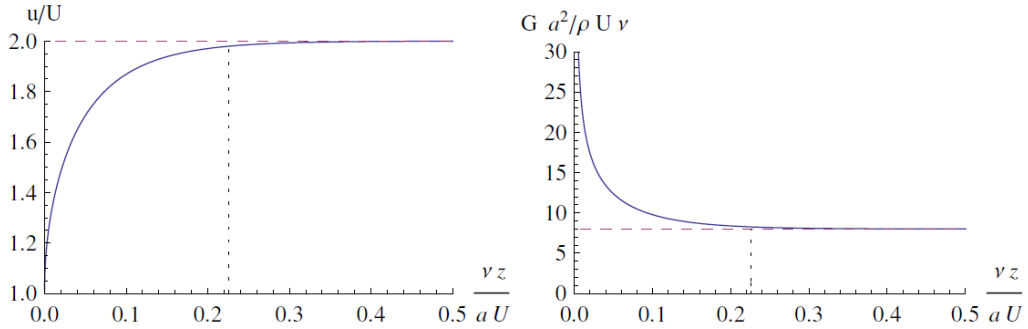

Figure 4.5: Central velocity (left) and central pressure gradient (right) as function of x. The dashed lines are the asymptotic approximations. The vertical dotted line is the 99% asymptotic point, that indicates the end of the entrance region. This figure is the same as Figure 2 of the *Addenda: Pipe Entrance Flow* of (Lautrup, 2011).

from which, assuming constant the product ST and recalling that in counterflow it is $\mathbf{q} = ST\mathbf{v}^{(n)}$, we get

$$\frac{G(x) - H(x)}{\overline{\nu\omega}^2} = v_{x0}^{(n)} \frac{I_0(\overline{\omega}R)}{I_2(\overline{\omega}R)}. \tag{4.29}$$

So that:

$$v_x^{(n)}(x,r) = \frac{v_{x0}^{(n)}}{I_2(\overline{\omega}R)} \left[I_0(\overline{\omega}R) - I_0(\overline{\omega}r)\right], \tag{4.30}$$

which for small $\overline{\omega}$ and $\overline{\omega}r$ becomes

$$v_x^{(n)}(x,r) = 2v_{x0}^{(n)} \left(1 - \frac{r^2}{R^2}\right), \tag{4.31}$$

which corresponds to the Poiseuille parabolic profile.

The solution (4.27) corresponds to (3.18) that we found in Section 3.2 for the flow of He II along a cylindrical channel, that in terms of $v_x^{(n)}$ in stationary counterflow situation is written

$$v_x^{(n)}(r) = -\frac{1}{ST}\frac{1}{BL_0}\left(1 - \frac{I_0\left(r\sqrt{ABL_0}\right)}{I_0\left(R\sqrt{ABL_0}\right)}\right)\frac{\partial T}{\partial x}, \tag{4.32}$$

but in the actual analysis it is intuitive to guess that L is not homogeneous along the channel, but depends on x, in contrast with the assumptions of Chapter 3. However, we have assumed that most vortices are already produced in a thin very inhomogeneous region close to the entrance plane (see Chapter 5) so that the hypothesis of L to depend on x only in a mild form may be reasonable on a physical basis.

The central velocity of the normal component is now obtained by setting $r = 0$ in equation (4.30), i.e.

$$v_x^{(n)}(x,0) \equiv u(x) = \frac{v_{x0}^{(n)}}{I_2(\overline{\omega}R)} \left[I_0(\overline{\omega}R) - 1 \right]. \tag{4.33}$$

High values of $\overline{\omega}$ correspond to velocity profile close to a flat profile, i.e. close to the entrance region, whereas small values of $\overline{\omega}$ correspond to a parabolic profile.

The dependence of $\overline{\omega}$ on x must now be searched. Following Lautrup, we look rather for the inverse function, namely $x = x(\overline{\omega})$, which is easier to be obtained. To do so, one starts from (4.23) and the energy balance equation, that in stationary counterflow situation is $\nabla \cdot \mathbf{q} = 0$. Recall that in counterflow it is $\mathbf{q} = ST\mathbf{v}^{(n)}$, assuming ST constant, the condition on $\nabla \cdot \mathbf{q}$ leads to $\nabla \cdot \mathbf{v}^{(n)} = 0$, i.e.

$$\frac{\partial v_x^{(n)}}{\partial x} + \frac{1}{r}\frac{\partial (r v_r^{(n)})}{\partial r} = 0. \tag{4.34}$$

By combining (4.23) and (4.34), one obtains

$$\frac{\partial}{\partial x}\left((v_x^{(n)}) \right)^2 + \frac{1}{r}\frac{\partial}{\partial r}\left(r v_x^{(n)} v_r^{(n)} \right) = G(x) + \frac{\overline{\nu}}{r}\frac{\partial}{\partial r}\left(r \frac{\partial v_x^{(n)}}{\partial r} \right) - \overline{\eta} L(x) v_x^{(n)}. \tag{4.35}$$

As boundary conditions we use:

$$\begin{cases} v_x^{(n)} = v_{x0}^{(n)}(\overline{\omega}, L) & v_r^{(n)} = 0 \quad (x = 0, \quad 0 \le r \le R) \\ v_x^{(n)} = v_{x0}^{(n)}(\overline{\omega}, L)\frac{[I_0(\overline{\omega}R) - I_0(\overline{\omega}r)]}{I_2(\overline{\omega}R)} & v_r^{(n)} = 0 \quad (x = \infty, \quad 0 \le r \le R) \\ \frac{\partial v_x^{(n)}}{\partial r} = 0 & v_r^{(n)} = 0 \quad (0 \le x \le \infty, \quad r = 0) \\ v_x^{(n)} = 0 & v_r^{(n)} = 0 \quad (0 \le x \le \infty, \quad r = R) \end{cases} \tag{4.36}$$

where $v_{x0}^{(n)}$ is the average velocity (that depends on $\overline{\omega}$ and L) and R is the radius of the pipe.

Thus, by integrating (4.35) over $0 \le r \le R$, one obtains

$$\frac{1}{\pi R^2}\frac{\partial}{\partial x}\int_0^R \left(v_x^{(n)}(x,r) \right)^2 2\pi r dr = G(x) + \frac{2\overline{\nu}}{R^2}\left[r \frac{\partial v_x^{(n)}(x,r)}{\partial r} \right]_{r=R} - \overline{\eta} L(x) v_{x0}^{(n)}. \tag{4.37}$$

The pressure gradient $G(x)$ may be eliminated from (4.23) setting $r = 0$, and taking into account the non-slip boundary conditions, one gets

$$G(x) = u(x)\frac{\partial u}{\partial x} - \overline{\nu}\left[\frac{1}{r}\frac{\partial}{\partial r}\left(r \frac{\partial v_x^{(n)}(x,r)}{\partial r} \right) \right]_{r=0} + \overline{\eta} L(x) u(x), \tag{4.38}$$

where $u(x) = v_x^{(n)}(x,0)$.

Combining (4.37) and (4.38), the global momentum balance equation becomes

$$\frac{\partial}{\partial x}\left(\langle (v_x^{(n)})^2\rangle - \frac{1}{2}u^2\right) = \frac{2\overline{\nu}}{R^2}\left[r\frac{\partial v_x^{(n)}}{\partial r}\right]_{r=R} - \overline{\nu}\left[\frac{1}{r}\frac{\partial}{\partial r}\left(\frac{\partial v_x^{(n)}}{\partial r}\right)\right]_{r=0} - \overline{\eta}L(x)\left(v_{x0}^{(n)} - u(x)\right) \tag{4.39}$$

with

$$\langle (v_x^{(n)})^2\rangle = \frac{1}{\pi R^2}\int_0^R (v_x^{(n)})^2 2\pi r dr \tag{4.40}$$

being the average squared velocity in a cross section.

Using (4.30) and (4.33) for $v_x(x,r)$ and $u(x)$ in (4.39), we obtain

$$f_1(\overline{\omega}R) = \langle (v_x^{(n)})^2\rangle - \frac{1}{2}u^2 = \frac{4I_0(\overline{\omega}R)I_2(\overline{\omega}R) - 2I_1^2(\overline{\omega}R) - I_0^2(\overline{\omega}R) + 2I_0(\overline{\omega}R) - 1}{2I_2^2(\overline{\omega}R)}, \tag{4.41}$$

and

$$g_1(\overline{\omega}R) = \left(\frac{v_{x0}^{(n)}}{\overline{\nu\omega}^2 - \overline{\eta}L}\right)^{-1}\frac{2\overline{\nu}}{R^2}\left[r\frac{\partial v_x^{(n)}}{\partial r}\right]_{r=R} - \overline{\nu}\left[\frac{1}{r}\frac{\partial}{\partial r}\left(\frac{\partial v_x^{(n)}}{\partial r}\right)\right]_{r=0} - \overline{\eta}L(x)\left(v_{x0}^{(n)} - u(x)\right) = \frac{I_0(\overline{\omega}R) - I_2(\overline{\omega}R) - 1}{I_2(\overline{\omega}R)}, \tag{4.42}$$

then, equation (4.39) can be written in a more compact form, i.e.

$$\frac{df_1(\overline{\omega}R)}{dx} = -\frac{v_{x0}^{(n)}}{\overline{\nu\omega}^2 - \overline{\eta}L}g_1(\overline{\omega}R). \tag{4.43}$$

In the entrance region of the channel, and especially in a relatively thin longitudinal region just behind the entrance, as compared with the total entry length (see for instance Figure 4.3 and 4.4), the temperature gradient is much higher than in the fully developed region. Also the velocity gradients are higher in this region. Thus, it may be expected that many vortices may appear there and that we can consider that beyond this short length, most of vortices are present and we can consider L constant in good approximation. In the next chapter we will discuss with more detail the possible influence of the velocity gradients as sources of vortices, so that we refer the reader to Section 5.1.

Then, if consider $L(x) = L$, differentiating the expression (4.43) with respect to $\overline{\omega}R$, one finds

$$\frac{dx}{d(\overline{\omega}R)} = -\frac{v_{x0}^{(n)}}{\overline{\nu\omega}^2 - \overline{\eta}L}h_1(\overline{\omega}R), \tag{4.44}$$

with $h_1(\overline{\omega}R) = \frac{f_1'(\overline{\omega}R)}{g_1(\overline{\omega}R)}$. (Note that $\overline{\nu\omega}^2$ and $\overline{\eta}L$ have dimensions (time)$^{-1}$ and then $v_{x0}^{(n)}/(\overline{\nu\omega}^2 - \overline{\eta}L)$ has dimensions of length as x, while $(\overline{\omega}R)$ and $h_1(\overline{\omega}R)$ are dimensionless). Integrating this last expression we can obtain implicitly x as a function of $\overline{\omega}$ and L.

To have a first glimpse of a solution, we provisionally begin by considering the simplest situation of small $\overline{\eta}L/\overline{\nu}$ and small $\overline{\omega}$, although we will see below that $\overline{\eta}L/\overline{\nu}$ small is unrealistic in many situations. In any case, in this hypothetical situation one has, for $\overline{\omega}R \to 0$, that $h_1(\overline{\omega}R)$ can be approximated with

$$h_1(\overline{\omega}R) = \frac{5}{36}\overline{\omega}R, \tag{4.45}$$

introducing this expression into (4.44) and integrating, one gets

$$\overline{\nu}x = -\frac{5}{36}v_{x0}^{(n)}R^2 \log\left(\sqrt{\frac{\overline{\nu\omega}^2 - \overline{\eta}L}{C}}\right), \tag{4.46}$$

where $C = mv_{x0}^{(n)}/R$, with m a numerical constant.

Note that $\overline{\omega}^2$, although being small, is expected to be higher than $\overline{\eta}L$, because for short lengths $\overline{\omega}$ is high. Thus, it is reasonable to assume that in (4.46) the square root is well defined. Note that for $L = 0$ one gets $\overline{\omega} \to 0$ for $x \to \infty$. In this case, as seen before, (4.30) yields the parabolic profile (4.31).

Below we consider a more general situation. The expression (4.46) is valid for high values of x. In the limit of high values of x, the quantity in the root must vanish, and we are led to $\overline{\omega} = \sqrt{\overline{\eta}L/\overline{\nu}}$. Then, the fully developed velocity profile becomes, by introducing this value of $\overline{\omega}$ into (4.30),

$$v_x^{(n)}(x,r) = \frac{v_{x0}^{(n)}}{I_2\left(R\sqrt{\overline{\eta}L/\overline{\nu}}\right)}\left[I_0\left(R\sqrt{\overline{\eta}L/\overline{\nu}}\right) - I_0\left(r\sqrt{\overline{\eta}L/\overline{\nu}}\right)\right]. \tag{4.47}$$

When L tends to zero, this expression tends to the usual parabolic profile (4.31). In general, it coincides with (3.18).

As an application of (4.46), assume that the length of the channel is finite, but long. Instead of $\overline{\omega} = \sqrt{\overline{\eta}L/\overline{\nu}}$ we will have

$$\overline{\nu\omega}^2 - \overline{\eta}L = B\mathrm{e}^{-x/x^*}, \tag{4.48}$$

where

$$x^* = \frac{5}{72}\frac{v_{x0}^{(n)}R^2}{\overline{\nu}} = \frac{5}{288}DRey, \tag{4.49}$$

with $Rey = \frac{v_{x0}^{(n)}2R}{\overline{\nu}}$ and $D = 2R$ the diameter of the pipe. Then:

$$\overline{\omega}^2 = \frac{1}{\overline{\nu}}\left(\overline{\eta}L + B\mathrm{e}^{-x/x^*}\right). \tag{4.50}$$

We can consider the characteristic length x^* as an *entrance length* in the presence of $L \neq 0$, comparable with (4.2).

The solution (4.46) is only valid for $\overline{\omega}$ small and $\overline{\eta}L/\overline{\nu}$ small; but it allows us to see that one may expect that the fully developed flow profile will be like (4.47) instead of a parabolic Poiseuille profile, as it was derived in (4.31).

Expression (4.50) has more information than the fully developed value (4.47). For instance, for $x = 0$, (4.50) yields $\overline{\omega}^2 = (\overline{\eta}L + B)/\overline{\nu}$. Thus, at the entrance the turbulent flow will behave like (4.47) but as if it had an effective vortex line density $L_{eff} = L + (B/\overline{\eta})$; logically this implies that the thermal resistance at the entrance region will be higher than in the fully developed region, not only in usual viscous fluids, but also in turbulent superfluids.

The thermal resistance along a tube of length l will be

$$\Delta T = \int_0^l K L_{eff}(x) q_x dx = \int_0^l K \left(L + \frac{B}{\overline{\eta}} \mathrm{e}^{-x/x^*} \right) q_x dx, \tag{4.51}$$

with L the true vortex density and L_{eff} the apparent vortex density; this yields to

$$\Delta T = KLq_x l + K\frac{B}{\overline{\eta}} q_x x^* \left(1 - \mathrm{e}^{-l/x^*} \right). \tag{4.52}$$

If $x^* \ll l$, this yields to $\Delta T = KLq_x l$, a different value. Thus, the actual value of L will be $\Delta T/Kq_x l$ only when $l \gg x^*$. This is not always so in the experiments.

Finally, let us note that when $\overline{\eta}L/\overline{\nu}$ is not small, but $\overline{\omega}$ becomes close to the value $\sqrt{\overline{\eta}L/\overline{\nu}}$, $h_1(\overline{\omega}R)$ in (4.44) can be approximated with

$$h_1(\overline{\omega}R) = -A_0 + A_1 R \left(\overline{\omega} - \sqrt{\frac{\overline{\eta}L}{\overline{\nu}}} \right), \tag{4.53}$$

where A_0 and A_1 are positive constants (see Appendix 4.7). Introducing this expression into (4.44) and integrating, one gets

$$\begin{aligned} \overline{\nu}x \;=\; & v_{x0}^{(n)} A_0 \sqrt{\frac{\overline{\nu}}{\overline{\eta}L}} \mathrm{arctanh} \left(\overline{\omega} \sqrt{\frac{\overline{\nu}}{\overline{\eta}L}} \right) + \\ & v_{x0}^{(n)} R A_1 \mathrm{arctanh} \left(\overline{\omega} \sqrt{\frac{\overline{\nu}}{\overline{\eta}L}} \right) + v_{x0}^{(n)} R A_1 \log \sqrt{\overline{\nu}\overline{\omega}^2 - \overline{\eta}L} + H. \end{aligned} \tag{4.54}$$

From here it is seen that for $x \to \infty$, $\overline{\omega}$ tends to $\sqrt{\overline{\eta}L/\overline{\nu}}$, and the asymptotic velocity profile is again (4.47). However, the relation between $\overline{\omega}$ and x, for long but finite x will be different — and more complicated — than in (4.48). Expression (4.54) may be expressed in other ways that we give here for sake of completeness, and for possible future use.

$$\begin{aligned}
&\overline{\nu}x = v_{x0}^{(n)} A_0 \sqrt{\tfrac{\overline{\nu}}{\overline{\eta}L}} \operatorname{arctanh}\left(\overline{\omega}\sqrt{\tfrac{\overline{\nu}}{\overline{\eta}L}}\right) + v_{x0}^{(n)} R A_1 \log\left(\overline{\omega} + \sqrt{\tfrac{\overline{\eta}L}{\overline{\nu}}}\right) + H \\
&\text{or} \\
&\overline{\nu}x = v_{x0}^{(n)} A_0 \sqrt{\tfrac{\overline{\nu}}{\overline{\eta}L}} \log\left(\frac{\sqrt{1-\frac{\overline{\nu}\overline{\omega}^2}{\overline{\eta}L}}}{1-\overline{\omega}\sqrt{\frac{\overline{\nu}}{\overline{\eta}L}}}\right) + v_{x0}^{(n)} R A_1 \log\left(\overline{\omega} + \sqrt{\tfrac{\overline{\eta}L}{\overline{\nu}}}\right) + H.
\end{aligned} \tag{4.55}$$

4.4 Influence of vortices on the entrance heat flow: turbulent situation, flat channels

Following the same steps of the previous section, we will consider here the Navier-Stokes equation for the flow in a plane semi-infinite channel for $y \in [-a, a]$ and $x \in [0, +\infty)$, under suitable particular boundary condition. The reader may skip this section, which is analogous to Section 4.3, but we have preferred to keep it for the sake of completeness.

The Navier-Stokes equation for $v_x^{(n)}$ becomes a Prandtl equation, i.e.

$$v_x^{(n)} \frac{\partial v_x^{(n)}}{\partial x} + v_y^{(n)} \frac{\partial v_x^{(n)}}{\partial y} = G(x) + \overline{\nu} \frac{\partial^2 v_x^{(n)}}{\partial y^2} - \overline{\eta} L(x) v_x^{(n)} \tag{4.56}$$

where $G(x) = -\frac{1}{\rho}\nabla p$, x is the direction along the axis of the channel, y the direction orthogonal to the walls and L is the vortex line density. The component $v_y^{(n)}$ is related to $v_x^{(n)}$ by the continuity equation, i.e.

$$\frac{\partial v_x^{(n)}}{\partial x} + \frac{\partial v_y^{(n)}}{\partial y} = 0. \tag{4.57}$$

When the flow is fully developed, $v_y^{(n)}$ tends to zero and $v_x^{(n)}$ does not depend on x. As a consequence, and for $L = 0$, (4.56) reduces to $\nabla p = \eta \frac{\partial^2 v_x^{(n)}}{\partial^2 y}$, which leads to the usual Poiseuille parabolic profile.

As in previous section we can define a function $H(x)$ as

$$H(x) = v_x^{(n)} \frac{\partial v_x^{(n)}}{\partial x} + v_y^{(n)} \frac{\partial v_x^{(n)}}{\partial y} - \overline{\nu\omega}^2 v_x^{(n)} + \overline{\eta} L(x) v_x^{(n)}, \tag{4.58}$$

where $\overline{\omega} = \overline{\omega}(x)$ is an unknown function of x (with dimensions $(\text{length})^{-1}$).

As made in previous section, we impose the symmetry of the solution under $y \to -y$ and the non-slip boundary condition $v_x^{(n)} = 0$ for $y = \pm a$, then we find the solution

$$v_x^{(n)}(x, y) = \frac{G(x) - H(x)}{\overline{\nu\omega}^2} \left(1 - \frac{\cosh(\overline{\omega} y)}{\cosh(\overline{\omega} a)}\right). \tag{4.59}$$

Imposing the energy balance equation, we get

$$\frac{G(x)-H(x)}{\overline{\nu}\overline{\omega}^2} = v_{x0}^{(n)}\left(1-\frac{\tanh(\overline{\omega}a)}{\overline{\omega}a}\right)^{-1}, \tag{4.60}$$

where $v_{x0}^{(n)}$ is the average value of $v_x^{(n)}$ across the thickness of the channel, now so that

$$v_x^{(n)}(x,y) = v_{x0}^{(n)}\left[1-\frac{\cosh(\overline{\omega}y)}{\cosh(\overline{\omega}a)}\right]\left[1-\frac{\tanh(\overline{\omega}a)}{\overline{\omega}a}\right]^{-1}. \tag{4.61}$$

This solution is analogous to (3.48) that we found in Section 3.5 for the flow of He II along a narrow slit, in stationary counterflow situation, i.e. in term of the velocity $v_x^{(n)}$ is written

$$v^{(n)}(y) = \frac{v_{x0}^{(n)}}{ST}\left[1-\frac{\cosh(y\sqrt{ABL})}{\cosh(a\sqrt{ABL})}\right]\left[a-\frac{\tanh(a\sqrt{ABL})}{\sqrt{ABL}}\right]^{-1}. \tag{4.62}$$

The central velocity $v_x^{(n)}(x,0) \equiv u(x)$ is now obtained by setting $y=0$ in equation (4.61)

$$u(x) = v_{x0}^{(n)}\left[1-\operatorname{sech}(\overline{\omega}a)\right]\left[1-\frac{\tanh(\overline{\omega}a)}{\overline{\omega}a}\right]^{-1}. \tag{4.63}$$

Also in this case, high values of $\overline{\omega}$ correspond to velocity profile close to a flat profile, i.e. close to the entrance region, whereas small values of $\overline{\omega}$ correspond to a parabolic profile.

In order to search the dependence of $\overline{\omega}$ on x we proceed as in the previous section, combining (4.56) and (4.57), and choosing as boundary conditions:

$$\begin{cases} v_x^{(n)} = v_{x0}^{(n)}(\overline{\omega},L) & v_y^{(n)} = 0 \quad (x=0, \quad 0\le y\le a) \\ v_x^{(n)} = v_{x0}^{(n)}(\overline{\omega},L)\dfrac{\left[1-\frac{\cosh(y\sqrt{ABL})}{\cosh(a\sqrt{ABL})}\right]}{\left[a-\frac{\tanh(a\sqrt{ABL})}{\sqrt{ABL}}\right]} & v_y^{(n)} = 0 \quad (x=\infty, \quad 0\le y\le a) \\ \dfrac{\partial v_x^{(n)}}{\partial y} = 0 & v_y^{(n)} = 0 \quad (0\le x\le\infty, \quad y=0) \\ v_x^{(n)} = 0 & v_y^{(n)} = 0 \quad (0\le x\le\infty, \quad y=a) \end{cases} \tag{4.64}$$

where $v_{x0}^{(n)}$ is the average velocity (that depend on $\overline{\omega}$ and L) and $2a$ is the distance between the walls. Thus we obtain

$$\frac{1}{a}\frac{\partial}{\partial x}\int_0^a v_x^{(n)}(x,y)^2 dy = G(x) + \frac{\overline{\nu}}{a}\left[\frac{\partial v_x^{(n)}(x,y)}{\partial y}\right]_{y=a} - \overline{\eta}L(x)v_{x0}^{(n)}. \tag{4.65}$$

In analogous way as in the previous section, we can write the global momentum balance equation in the form

$$\frac{\partial}{\partial x}\left(\langle (v_x^{(n)})^2\rangle - \frac{1}{2}u^2\right) = \frac{\overline{\nu}}{a}\left[\frac{\partial v_x^{(n)}(x,y)}{\partial y}\right]_{y=a} - \overline{\nu}\left[\frac{\partial^2 v_x^{(n)}(x,y)}{\partial y^2}\right]_{y=0} - \overline{\eta}L(x)v_{x0}^{(n)} + \overline{\eta}L(x)u, \tag{4.66}$$

with

$$\langle (v_x^{(n)})^2 \rangle = \frac{1}{a}\int_0^a \left[v_x^{(n)}\right]^2 dy, \tag{4.67}$$

being the average squared velocity along x. Using (4.61) and (4.63) for $v_x^{(n)}(x,y)$ and $u(x)$, we obtain

$$f_2(\overline{\omega}a) = \langle \left[v_x^{(n)}\right]^2 \rangle - \frac{1}{2}u^2 = \left[1 - \frac{\tanh(\overline{\omega}a)}{\overline{\omega}a}\right]^{-1}\left[\frac{3}{2} + \frac{\mathrm{sech}(\overline{\omega}a) - 1}{1 - \frac{\tanh(\overline{\omega}a)}{\overline{\omega}a}}\right], \tag{4.68}$$

and

$$\begin{aligned} g_2(\overline{\omega}a) = \frac{\overline{\nu}}{a}\left[\frac{\partial v_x^{(n)}(x,y)}{\partial y}\right]_{y=a} - \overline{\nu}\left[\frac{\partial^2 v_x^{(n)}(x,y)}{\partial y^2}\right]_{y=0} - \overline{\eta}L(x)v_{x0}^{(n)} \\ + \overline{\eta}L(x)u = \left[1 - \frac{\tanh(\overline{\omega}a)}{\overline{\omega}a}\right]^{-1}\left[\frac{\tanh(\overline{\omega}a)}{\overline{\omega}a} - \mathrm{sech}(\overline{\omega}a)\right], \end{aligned} \tag{4.69}$$

then, equation (4.66) can be written in a more compact form, i.e.

$$\frac{df_2(\overline{\omega}a)}{dx} = -\frac{v_{x0}^{(n)}}{\overline{\nu}\overline{\omega}^2 - \overline{\eta}L}g_2(\overline{\omega}a). \tag{4.70}$$

Differentiating the resulting expression with respect to $\overline{\omega}a$, one finds

$$\frac{dx}{d(\overline{\omega}a)} = -\frac{v_{x0}^{(n)}}{\overline{\nu}\overline{\omega}^2 - \overline{\eta}L}h_2(\overline{\omega}a), \tag{4.71}$$

with $h_2(\overline{\omega}a) = \frac{f_2'(\overline{\omega}a)}{g_2(\overline{\omega}a)}$.

As in Section 4.3 we provisionally begin by considering the simplest situation of small $\overline{\eta}L/\overline{\nu}$ and small $\overline{\omega}$, in this hypothetical situation and for $\overline{\omega}a \to 0$, $h_2(\overline{\omega}a)$ can be approximated with:

$$h_2(\overline{\omega}a) = \frac{73}{700}\overline{\omega}a, \tag{4.72}$$

introducing this expression into (4.71) and integrating, one gets

$$\overline{\nu}x = -\frac{73}{700}v_{x0}^{(n)}a^2 \log\left(\sqrt{\frac{\overline{\nu}\overline{\omega}^2 - \overline{\eta}L}{\overline{C}}}\right), \tag{4.73}$$

where $\overline{C} = cv_{x0}^{(n)}/a$, with c a numeric constant.

Note that $\overline{\omega}^2$, although being small, is expected to be higher than $\overline{\eta}L$, because for short lengths $\overline{\omega}$ is high. Thus, it is reasonable to assume that in (4.73) the square root is well defined. Note that for $L = 0$ one gets $\overline{\omega} \to 0$ for $x \to \infty$. In this case (4.61) yields the parabolic profile.

Below we consider a more general situation. The expression (4.73) is valid for high values of x. In the limit of high values of x, the quantity in the root must vanish, and we are led to $\overline{\omega} = \sqrt{\overline{\eta}L/\overline{\nu}}$. Then, the fully developed velocity profile becomes, by introducing this value of $\overline{\omega}$ into (4.61),

$$v_x^{(n)}(x,y) = \left[1 - \frac{\tanh\left(a\sqrt{\overline{\eta}L/\overline{\nu}}\right)}{a\sqrt{\overline{\eta}L/\overline{\nu}}}\right]^{-1} \left[1 - \frac{\cosh\left(y\sqrt{\overline{\eta}L/\overline{\nu}}\right)}{\cosh\left(a\sqrt{\overline{\eta}L/\overline{\nu}}\right)}\right]. \tag{4.74}$$

When L tends to zero, this expression tends to the usual parabolic profile. In general, it coincides with (3.45).

As an application of (4.73), assume that the length of the channel is finite, but long. Instead of $\overline{\omega} = \sqrt{\overline{\eta}L/\overline{\nu}}$ we will have

$$\overline{\nu\omega}^2 - \overline{\eta}L = \overline{C}\mathrm{e}^{-x/x^*}, \tag{4.75}$$

where

$$x^* = \frac{73}{1400}\frac{v_{x0}^{(n)}a^2}{\overline{\nu}} = \frac{73}{5600}DRey, \tag{4.76}$$

with $Rey = \frac{v_{x0}^{(n)}2a}{\overline{\nu}}$ and $D = 2a$ the distance between the walls. Then:

$$\overline{\omega}^2 = \frac{1}{\overline{\nu}}\left(\overline{\eta}L + \overline{C}\mathrm{e}^{-x/x^*}\right). \tag{4.77}$$

As in (4.49) we can consider the characteristic length x^* as an *entrance length* in the presence of $L \neq 0$, comparable with (4.2).

The solution (4.73) is only valid for $\overline{\omega}$ small and $\overline{\eta}L/\overline{\nu}$ small; but it allows us to see that one may expect that the fully developed flow profile will be like (4.74) instead of a parabolic Poiseuille profile, as it was derived in Section 3.5. Expression (4.77) has more information than the fully developed value (4.74). For instance, for $x = 0$, (4.77) yields $\overline{\omega}^2 = (\overline{\eta}L + \overline{C})/\overline{\nu}$. Thus, at the entrance the turbulent flow will behave, like (4.74) but as if it had an effective vortex line density $L_{eff} = L + (\overline{C}/\overline{\eta})$; logically this implies that the thermal resistance at the entrance region will be higher than in the fully developed region, not only in usual viscous fluids, but also in turbulent superfluids.

Finally, let us note that when $\overline{\eta}L/\overline{\nu}$ is not small, but $\overline{\omega}$ becomes close to the value $\sqrt{\overline{\eta}L/\overline{\nu}}$, $h_2(\overline{\omega}a)$ in (4.71) can be approximated with

$$h_2(\overline{\omega}a) = -B_0 + B_1 a\left(\overline{\omega} - \sqrt{\frac{\overline{\eta}L}{\overline{\nu}}}\right), \tag{4.78}$$

where B_0 and B_1 are positive constants (see Appendix 4.7). Introducing this expression into (4.71) and integrating, one gets

$$\begin{aligned}\overline{\nu}x &= v_{x0}^{(n)} B_0 \sqrt{\frac{\overline{\nu}}{\overline{\eta}L}} \operatorname{arctanh}\left(\overline{\omega}\sqrt{\frac{\overline{\nu}}{\overline{\eta}L}}\right) \\ &\quad + v_{x0}^{(n)} a B_1 \operatorname{arctanh}\left(\overline{\omega}\sqrt{\frac{\overline{\nu}}{\overline{\eta}L}}\right) + v_{x0}^{(n)} a B_1 \log\sqrt{\overline{\nu}\overline{\omega}^2 - \overline{\eta}L} + H \end{aligned} \tag{4.79}$$

From here it is seen that for $x \to \infty$, $\overline{\omega}$ tends to $\sqrt{\overline{\eta}L/\overline{\nu}}$, and the asymptotic velocity profile is again (4.74). However, the relation between $\overline{\omega}$ and x, for long but finite x will be different — and more complicated — than in (4.75). Expression (4.79) may be expressed in other ways that we give here for sake of completeness, and for possible future use.

$$\begin{aligned}&\overline{\nu}x = v_{x0}^{(n)} B_0 \sqrt{\tfrac{\overline{\nu}}{\overline{\eta}L}} \operatorname{arctanh}\left(\overline{\omega}\sqrt{\tfrac{\overline{\nu}}{\overline{\eta}L}}\right) + v_{x0}^{(n)} a B_1 \log\left(\overline{\omega} + \sqrt{\tfrac{\overline{\eta}L}{\overline{\nu}}}\right) + H \\ &\text{or} \\ &\overline{\nu}x = v_{x0}^{(n)} B_0 \sqrt{\tfrac{\overline{\nu}}{\overline{\eta}L}} \log\left(\frac{\sqrt{1-\frac{\overline{\nu}\overline{\omega}^2}{\overline{\eta}L}}}{1-\overline{\omega}\sqrt{\frac{\overline{\nu}}{\overline{\eta}L}}}\right) + v_{x0}^{(n)} a B_1 \log\left(\overline{\omega} + \sqrt{\tfrac{\overline{\eta}L}{\overline{\nu}}}\right) + H\end{aligned} \tag{4.80}$$

4.5 Stationary heat flux profile in turbulent helium II in a semi-infinite cylindrical channel

In the present section we explicitly solve the equations for the heat flux profile in a semi-infinite channel (from $x = 0$ to $x = \infty$) instead of the infinite channel of the Section 3.2 (from $x = -\infty$ to $x = +\infty$). In contrast to the assumption $q(r)$ made in Section 3.2, here it is possible to have $q(x, r)$.

The analysis is different from that in Section 4.3 in two main aspects: the equations for the heat flux components used in Chapter 3 are used, instead of the analogous of the Navier-Stokes equation, and the boundary conditions on the temperature along the walls of the channels are different, as it will be commented later on.

Under the assumption of axial symmetry around the axis of the duct and assuming the fluid at rest (i.e. $\mathbf{v} = 0$), the equations for q_x and q_r from system (3.5) are:

$$\frac{\partial T}{\partial x} - \lambda_2 \beta^2 T^3 \nabla^2 q_x = -\frac{K}{\zeta} L q_x \tag{4.81}$$

$$\frac{\partial T}{\partial r} - \lambda_2 \beta^2 T^3 \nabla^2 q_r = -\frac{K}{\zeta} L q_r \tag{4.82}$$

The other equations of system (3.5) give us some compatibility conditions on the solutions that will be obtain below, as that for ∇p, i.e. (3.4).

In this section we search for solutions of q_x and q_r, which in turn depend on x and r, under the simplifying hypothesis that the temperature $T = T(x, r)$ inside the channel is known and, in particular, that along the walls is constant. This means that the superfluid flows along the tube in contact with an homogeneous system from which it is extracting some heat.

Note that this is different from the assumption we have made in Section 3.4, where T was not assumed to depend on r, but it was assumed to vary linearly along the walls, in the same way as the temperature of the fluid, consequently, the solutions will be different from those of Section 3.4, and the heat flux will have a radial component it had not in Section 3.4.

4.5.1 Longitudinal components of q and ∇p

We start our analysis looking for a solution of the equation for the longitudinal heat flux, that is written as

$$\lambda_2 \beta^2 T^3 \left(\frac{\partial^2 q_x}{\partial x^2} + \frac{\partial^2 q_x}{\partial r^2} + \frac{1}{r} \frac{\partial q_x}{\partial r} \right) - \frac{K}{\zeta} L_0 q_x = \frac{\partial T}{\partial x}, \tag{4.83}$$

where L_0 is a constant value of L. This equation must satisfy the following boundary conditions:

- $q_x(0, r) = q_0(r)$
- $q_x(x, R) = 0$
- $lim_{x \to \infty} q_x(x, r) < +\infty$

Furthermore, we assume that the temperature T is constant along the walls of the cylinder:

$$T(x, R) = T_0 \qquad \Rightarrow \qquad \frac{\partial T}{\partial x}(x, R) = 0. \tag{4.84}$$

Equation (4.83) has the particular solution $q_0(x, r) = -\frac{\zeta}{K L_0} \frac{\partial T}{\partial x}$, that satisfies the boundary condition $q_x(x, R) = 0$, because of equation (4.84). It remains to solve the following homogeneous equation

$$\lambda_2 \beta^2 T^3 \left(\frac{\partial^2 q_1}{\partial x^2} + \frac{\partial^2 q_1}{\partial r^2} + \frac{1}{r} \frac{\partial q_1}{\partial r} \right) - \frac{K}{\zeta} L_0 q_1 = 0, \tag{4.85}$$

with the boundary conditions:

- $q_1(0, r) = q_0(r) - \frac{\zeta}{K L_0} \frac{\partial T}{\partial x}(0, r) = q_1^{(0)}(r)$
- $q_1(x, R) = -\frac{\zeta}{K L_0} \frac{\partial T}{\partial x}(x, R) = 0$

- $lim_{x\to\infty} q_1(x,r) < +\infty$

where $q_1(x,r)$ indicates the solution of (4.85) and then the solution of equation (4.83) will be the sum of $q_0(x,r)$ and $q_1(x,r)$.

Let us introduce the positive quantity $C_0 = \frac{KL_0}{\lambda_2 \beta^2 T^3 \zeta}$, whose dimensions are $(\text{length})^{-2}$ (as L_0) and that coincides with the quantity ABL_0 of the Section 3.2, with A and B defined in (3.14) under the hypothesis $\beta = -1/(ST^2)$.

As in Section 3.2, we assume C_0 constant; then the last equation can be written

$$\frac{\partial^2 q_1}{\partial x^2} + \frac{\partial^2 q_1}{\partial r^2} + \frac{1}{r}\frac{\partial q_1}{\partial r} - C_0 q_1 = 0. \tag{4.86}$$

Now we look for a solution of this equation, in the form of separation of variables, i.e.

$$q_1(x,r) = P(x)Q(r).$$

By substituting this expression in equation (4.86), we obtain the following two equations, one depending only on x and the other one depending only on r. Then both equations must be equal to a constant M with dimension $(\text{length})^{-2}$

$$\frac{P''}{P} - C_0 = M, \tag{4.87}$$

$$\frac{Q''}{Q} + \frac{1}{r}\frac{Q'}{Q} = -M. \tag{4.88}$$

We will suppose first, $M = 0$; in this situation the solution of the equation (4.88) that satisfy the boundary condition $Q(R) = 0$ is $Q(r) = 0$ and we have the solution $q_1(x,r)$ identically null.

Let's define the new dimensionless variable $y := \sqrt{|M|}r$ in the equation (4.88), it becomes a zero-order Bessel equation for the new quantity $\tilde{Q}(y)$ (dependent on the sign of M)

$$\tilde{Q}'' + \frac{1}{y}\tilde{Q}' \pm \tilde{Q} = 0, \tag{4.89}$$

with the boundary condition, for $r = R$, $\tilde{Q}\left(\sqrt{|M|}R\right) = 0$.

If $M < 0$ then equation (4.89) is a zero-order modified Bessel, whose solutions are the Bessel function $I_0(y)$ and $K_0(y)$, and the general solution of the equation (4.89) is:

$$\tilde{Q}(y) = c_1 I_0(y) + c_2 K_0(y), \tag{4.90}$$

but $K_0(y)$ goes to infinite for $y = 0$, and hence $c_2 = 0$ is required. Moreover, $I_0(y)$ is not zero for all y and the boundary conditions are satisfied only for $c_1 = 0$. In conclusion M has to be necessarily positive.

In this way equation (4.88) is a zero-order Bessel equation, and its solutions are the Bessel function $J_0(y)$ e $Y_0(y)$. Again, $Y_0(y)$ goes to infinite for $y = 0$, and thus the solution is:

$$\tilde{Q}(y) = c_1 J_0(y). \tag{4.91}$$

For the solution (4.91), the boundary conditions are verified for any y_i, zero of the function J_0, so that we have the following eigenvalues for M

$$M_i = \left(\frac{y_i}{R}\right)^2. \tag{4.92}$$

Now we consider equation (4.87), for any egenvalue M_i, in the form

$$P'' - (C_0 + M_i)P = 0, \tag{4.93}$$

since $(C_0 + M_i) > 0$, the general solution of equation (4.93) is:

$$P_i(x) = c_1 \mathrm{e}^{-x\sqrt{C_0+M_i}} + c_2 \mathrm{e}^{x\sqrt{C_0+M_i}}. \tag{4.94}$$

By assuming $c_2 = 0$, the solution does not diverge and goes to zero for large x, i.e.

$$\lim_{x\to\infty} P_i(x) = 0, \tag{4.95}$$

whereas the boundary condition, for $x = 0$, must be verified by the general solution of the equation (4.86). The most general separate solution of the equation (4.86) is:

$$q_1^{(i)}(x, r) = cJ_0(\sqrt{M_i}r)\mathrm{e}^{-x\sqrt{C_0+M_i}}, \tag{4.96}$$

for any value of M_i depending on the zeros of the Bessel function J_0, and for $x = 0$ this solution must correspond to $q_1^{(0)}(r)$, that is:

$$q_1^{(i)}(0, r) = cJ_0\left(\frac{y_i}{R}r\right) = q_1^{(0)}(r).$$

Note that the decaying exponential contains interesting information on how $q_1(x, r)$ decays to zero, i.e. how steeply the solution $q_0(x, r)$ is approached as the fluid separates from $x = 0$. In other words, it yields information on the length of the entrance region, in analogy with (4.49) (cylindrical channels) and (4.49) (flat channels) but for different lateral boundary conditions.

If the function $q_1^{(0)}(r)$ is not a Bessel function then we look for a solution in the form

$$q_1(x, r) = \sum_{i=1}^{\infty} c_i q_1^{(i)} = \sum_{i=1}^{\infty} c_i J_0\left(\frac{y_i}{R}r\right) \mathrm{e}^{-x\sqrt{C_0+(\frac{y_i}{R})^2}}, \tag{4.97}$$

where the coefficients c_i are found by expanding $q_1^{(0)}(r)$ in a Fourier-Bessel series, whenever it is possible (see for details (Watson, 1922)), i.e.

$$q_1^{(0)}(r) = \sum_{i=1}^{\infty} c_i J_0\left(\frac{y_i}{R} r\right),$$

and

$$c_i = \frac{2}{R^2 J_1^2(y_i)} \int_0^R r q_1^{(0)}(r) J_0\left(\frac{y_i}{R} r\right) dr.$$

Finally, we get

$$q_x(x,r) = q_0(x,r) + q_1(x,r) = -\frac{\zeta}{KL_0}\frac{\partial T}{\partial x} + \sum_{i=1}^{\infty} c_i J_0\left(\frac{y_i}{R} r\right) \mathrm{e}^{-x\sqrt{C_0+(\frac{y_i}{R})^2}} \tag{4.98}$$

and from equation (3.4), we obtain that the pressure gradient has to satisfy the following condition

$$\frac{\partial p}{\partial x} = -\frac{1}{\beta T^2}\left(\frac{\partial T}{\partial x} + \frac{K}{\zeta} L_0 q_x\right) = -\frac{KL_0}{\zeta \beta T^2} \sum_{i=1}^{\infty} c_i J_0\left(\frac{y_i}{R} r\right) \mathrm{e}^{-x\sqrt{C_0+(\frac{y_i}{R})^2}}. \tag{4.99}$$

The second term on the right hand of (4.98), i.e. $q_1(x,r)$, is shown in Figure 4.6 and the plot is achieved by choosing a particular function $q_1^{(0)}(r) = 10^9[-r^2 + (0.05)^2]$ and setting the constants C and L_0 according to the experimental data.

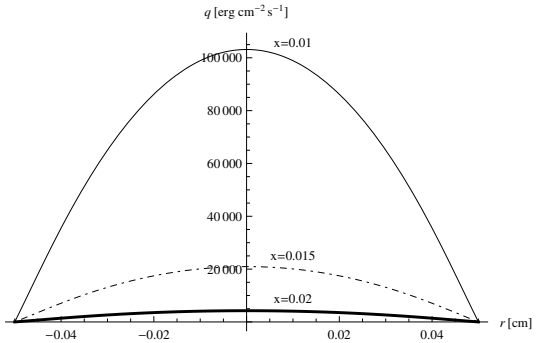

Figure 4.6: Profile of $q_1(x,r)$ for $q_1^{(0)}(r) = 10^9[-r^2 + (0.05)^2]$ and for different values of x.

It is evident that it goes quickly to zero and hence the function $q_x(x,r)$ becomes proportional to the gradient of the temperature T, as also shown in the Table 4.1 (in which the order of magnitude of $q_1(x,r)$ and $\frac{\partial p}{\partial x}$ for $r = 0$ are shown). Furthermore the value of $\frac{\partial p}{\partial x}$ goes very quickly to zero.

x	[cm]	0	0.01	0.015	0.02	0.05	0.1	0.5
$q_1(x,0)$	[erg/(cm^2 s)]	10^6	10^6	10^5	10^3	10^{-1}	10^{-8}	10^{-63}
$\frac{\partial p}{\partial x}(x,0)$	[g/(cm^2 s^2)]	1	1	10^{-1}	10^{-3}	10^{-7}	10^{-14}	10^{-69}

Table 4.1: Approximated values of $q_1(x,0)$ and $\frac{\partial p}{\partial x}$ with respect to x.

4.5.2 Transversal components of q and ∇p

Now we will look for the solution for q_r. The radial components of the heat flux are an important ingredient in entrance flows but here they still have an additional relevance, because the boundary conditions chosen here, which imply a thermal contact and heat exchange with the lateral walls. This may be the case, for instance, in heat exchangers, where lateral heat flow is especially relevant. In these situations, an equation for $q_r(x,R)$ will be needed to describe the lateral heat exchange across the wall. This consideration makes the analysis of superfluid counterflow more realistic than in the more usual situations in which it is assumed that the lateral wall is adiabatic.

The solution for q_r must satisfy the relation (3.4), i.e.

$$\frac{\partial p}{\partial r} = -\frac{1}{\beta T^2}\left(\frac{\partial T}{\partial r} + \frac{K}{\zeta} L_0 q_r\right). \tag{4.100}$$

Furthermore, they must be compatible with the solution (4.98) and (4.99) obtained for $q_x(x,r)$ and $\partial p/\partial x$. Whenever the function $q_1^{(0)}(r)$ admits the differentiability of its Fourier-Bessel expansion, we can differentiate equation (4.99) with respect to r and (4.100) with respect to x, under the hypothesis βT^2 constant, and we obtain

$$\frac{\partial q_x}{\partial r} = \frac{\partial q_r}{\partial x},$$

from which

$$\frac{\partial q_r(x,r)}{\partial x} = -\frac{\zeta}{KL_0}\frac{\partial}{\partial x}\frac{\partial T}{\partial r} - \sum_{i=1}^{\infty} c_i \frac{y_i}{R} J_1\left(\frac{y_i}{R} r\right) \mathrm{e}^{-x\sqrt{A+(\frac{y_i}{R})^2}}, \tag{4.101}$$

because $J_0'(\alpha\xi) = \alpha J_1(\xi)$, where $J_1(\xi)$ is the Bessel function of order 1.

By integrating eq.(4.101) with respect to x (from x_0 to x) the following expression is obtained

$$q_r(x,r) = q_r(x_0,r) - \frac{\zeta}{KL_0}\frac{\partial}{\partial r}T(x,r) + \frac{\zeta}{KL_0}\frac{\partial}{\partial r}T(x_0,r) +$$

$$+\sum_{i=1}^{\infty} c_i \frac{y_i}{R} J_1\left(\frac{y_i}{R} r\right)\left[\frac{\mathrm{e}^{-x\sqrt{A+(\frac{y_i}{R})^2}} - \mathrm{e}^{-x_0\sqrt{A+(\frac{y_i}{R})^2}}}{\sqrt{A+(\frac{y_i}{R})^2}} + f(r)\right], \tag{4.102}$$

where the values of $f(r)$, $q_r(x_0,r)$ and $T(x_0,r)$ will depend on the physics of the problem.

Finally we get

$$\frac{\partial p}{\partial r} = -\frac{1}{\beta T^2}\left(\frac{\partial T}{\partial r} + \frac{K}{\zeta} L_0 q_r\right) = -\frac{K L_0}{\zeta \beta T^2}\left(q_r(x_0, r) + \frac{\zeta}{K L_0}\frac{\partial}{\partial r} T(x_0, r) + \right.$$

$$\left. + \sum_{i=1}^{\infty} c_i \frac{y_i}{R} J_1\left(\frac{y_i}{R} r\right)\left[\frac{\mathrm{e}^{-x\sqrt{A+(\frac{y_i}{R})^2}} - \mathrm{e}^{-x_0\sqrt{A+(\frac{y_i}{R})^2}}}{\sqrt{A+(\frac{y_i}{R})^2}} + f(r)\right]\right). \tag{4.103}$$

The functions $T(x, r)$ and $f(r)$ will be chosen using the boundary conditions on T and p.

4.6 Remarks

In this chapter we have explored in detail some additional aspects that are relevant for the estimation of the effective thermal conductivity of superfluid helium in relatively short cylindrical channels, i.e. the effects of the *entrance region*, where there are strong inhomogeneiteis in the longitudinal heat flow which imply, in turn, the presence of radial heat flow. One of the relevant aspects is the transition from a flat velocity profile at $x = 0$ to a fully developed profile at the end of the entrance region. In particular, we have seen that for short channels (much shorter than the entry length) the heat flow Q is proportional to $R^2 l^{\frac{1}{3}} (\Delta T/l)^{\frac{2}{3}}$. Note that this is different from the dependence in $(\Delta T/l)^{\frac{1}{3}}$ in fully developed turbulence of the Görter-Mellink expression.

Since the topic of the modifications of Landau expression for thermal conductivity in short channels is not very well known, we have examined the situation in order to complement the phenomenological Lesniewski study (Lesniewski et al., 1996). In practical situations, in order that the effects of the entrance region on the thermal conductivity may be neglected and Landau formula be valid, it is needed that the length of the tube is at least some 10 or 20 times the entrance length, in order that the well developed region truly dominates over the entrance region. Thus, the strict validity of the Landau formula requires considerably long tubes.

- Some results of the first part of this chapter are published in:
  L. Saluto and D. Jou, *Effective thermal conductivity of superfluid helium in short channels*,
  Bolettino di Matematica Pura e Applicata **Vol. VI** 153–163 (2013), Aracne Ed.

- Some results of the last section are published in:
  L. Saluto, *Stationary heat flux profile in turbulent helium II in a semi-infinite cylindrical channel*,
  Bollettino di Matematica Pura e Applicata **Vol. V** 133–144 (2012), Aracne Ed.

In the future, we plan to study the interaction between entrance effects and superfluid turbulence, namely, how the strong gradient in velocity found in the entrance region may act as a supplementary source of vortex lines.

In Section 4.3 and 4.4, the flow in the entrance region has been studied in detail, following the Lautrup approach but incorporating to it the influence of the vortices. We have assumed that the vortices are generated in the strongly steep region close to $x = 0$, at that from where L may be considered as independent of x.

Finally, in Section 4.5 we have also studied the problem of entrance region but with two main differences with respect to Section 4.3 and 4.4, because the basic equations were different from the modified Navier-Stokes equations, and because the boundary conditions assumed temperature constant along the walls. In particular, we have determined some particular stationary solutions of the heat flux equation in counterflow experiments in a semi-infinite cylindrical channel filled with turbulent superfluid helium.

The solution obtained for the longitudinal component of q in (4.98) depends on ∇T and on the data $q_1^{(0)}(r)$ at $x = 0$, but as shown in Table 4.1 the transition solution $q_1(x, r)$ goes quickly to zero and the solution obtained depends essentially on ∇T. For the transversal component it is necessary particularizing the functions $f(r)$, $q_r(x_0, r)$ and $T(x, r)$ to analyze the solutions obtained. The chosen boundary conditions (constant temperature and zero heat flux on the lateral walls of the channel) simulate a channel, filled with superfluid helium, contained in a sample at constant temperature. The arbitrary functions mentioned above can be determined imposing additional boundary conditions to describe a particular experiment. Such particular situations could be the comparison between an insulating lateral wall or a well-conducting lateral wall; the first situation may be of special theoretical interest for the analysis of the counterflow turbulent tangle of quantized vortices, and the microscopic mechanisms of vortex breaking and recombination, whereas the second one will be much more realistic in heat exchangers.

Some topics for future research could be, for instance, whether the critical velocity for instability of the laminar state, could be different in the entrance region than in the asymptotic region; or whether some vortices could be formed there, but which would disappear in the asymptotic region. These are left for the future because of their mathemathical complexity.

4.7 Appendix 4.A

In this appendix we give the results for the coefficients A_0, and A_1 in (4.53) and for B_0, and B_1 in (4.78). In each of these let $b = \sqrt{\overline{\eta}L/\overline{\nu}}$.

The coefficient A_0 and A_1 in equation (4.53) are:

$$\begin{aligned} A_0 &= h_1\left(R\sqrt{\overline{\eta}L/\overline{\nu}}\right) = h_1(Rb) = \\ &= \left\{I_1(Rb)\left[I_1^2(Rb)\left(\frac{8}{R^2b^2}+2\right) - 3I_0^2(Rb) + \frac{4}{Rb}I_1(Rb)\left(I_0(Rb)-1\right)+1\right] + \right. \\ &\quad \left. I_3(Rb)\left[I_0^2(Rb) + 2I_1^2(Rb) - 2I_0(Rb)\left(I_2(Rb)+1\right)+1\right]\right\} \cdot \\ &\quad \left[2I_2^2(Rb)\left(I_0(Rb) - I_2(Rb) - 1\right)\right]^{-1} \end{aligned} \tag{4.104}$$

$$\begin{aligned} A_1 &= h_1\left(R\sqrt{\overline{\eta}L/\overline{\nu}}\right) = h_1'(Rb) = \\ &= \left\{-4R^4b^4I_0^5(Rb) + 2R^3b^3I_0^4(Rb)\left[R^3b^3 + 14I_1(Rb) - Rb\right] + \right. \\ &\quad R^2b^2I_0^3(bR)[R^4b^4 + 8I_1(Rb)\left(3Rb - 2I_1(Rb)\left(R^2b^2+5\right)\right)] + \\ &\quad 2RbI_1^2(Rb)\left[Rb\left(R^2b^2+1\right)\left(R^2b^2+4\right) + I_1(Rb)\left[-5R^4b^4 - 24R^2b^2 + \right.\right. \\ &\quad \left.\left. 2\left(R^2b^2+2\right)I_1(Rb)\left[Rb\left(R^2b^2+8\right) - 2I_1(Rb)\left(R^2b^2+7\right)\right] - 24\right]\right] + \\ &\quad RbI_0^2(Rb)\left[R^2b^2I_1(Rb)\left(5R^2b^2-12\right) - 2RbI_1^2(Rb)\left(3R^4b^4 + 25R^2b^2 + 36\right) + \right. \\ &\quad \left. 8I_1^3(Rb)\left(R^4b^4 + 8R^2b^2 + 14\right) - R^3b^3\left(R^2b^2-2\right)\right] + I_0(Rb)I_1(Rb) \\ &\quad \left[I_1(Rb)\left[-R^6b^6 + 10R^4b^4 + 48R^2b^2 + 4I_1(Rb)\left[I_1(Rb)\left(R^2b^2+2\right)\right.\right.\right. \\ &\quad \left.\left.\left.\left(3R^2b^2-8\right) + Rb\left(R^4b^4 + 13R^2b^2 + 16\right)\right]\right] - R^3b^3\left(3R^2b^2+8\right]\right]\right\} \cdot \\ &\quad \left\{R^6b^6I_2^3(Rb)\left[I_0(Rb) - I_2(Rb) - 1\right]^2\right\}^{-1} \end{aligned} \tag{4.105}$$

The coefficient B_0 and B_1 in equation (4.78) are:

$$\begin{aligned} B_0 &= h_2\left(a\sqrt{\overline{\eta}L/\overline{\nu}}\right) = h_2(ab) = \\ &= \left\{\operatorname{sech}^3(ab)\left[\cosh(ab) - 4\right] - \frac{\tanh^2(ab)}{(ab)^2}\left[2a^2b^2\operatorname{sech}(ab) + 3\right] + \right. \\ &\quad \left. \frac{\tanh(ab)}{ab}\left[\operatorname{sech}(ab)\left(2a^2b^2 + 3\operatorname{sech}(ab) + 4\right) - 1\right]\right\} \cdot \\ &\quad \left[2ab\left(\frac{1-\tanh(ab)}{ab}\right)^2\left(\operatorname{sech}(ab) - \frac{\tanh(ab)}{ab}\right)\right]^{-1} \end{aligned} \tag{4.106}$$

$$
\begin{aligned}
B_1 &= h_2'\left(a\sqrt{\overline{\eta}L/\overline{\nu}}\right) = h_2(ab) = \\
&= \Big\{\operatorname{sech}(ab)\Big[-7a^2b^2 + \operatorname{sech}(ab)\Big[\big(2ab\sinh(ab)\left(a^2b^2+6\right)+5\big)+ \\
&\quad \frac{\tanh(ab)}{ab}\left(13-2a^2b^2\right)+\operatorname{sech}^3(ab)\left(13a^2b^2+11\right)+\operatorname{sech}^2(ab) \\
&\quad \left(\frac{\tanh(ab)}{ab}\left(6a^4b^4-a^2b^2-6\right)+2a^4b^4+a^2b^2-4\right)- \\
&\quad \operatorname{sech}(ab)\left(\frac{\tanh(ab)}{ab}\left(3a^4b^4+9a^2b^2+1\right)+7a^2b^2+19\right)\Big]+ \\
&\quad \frac{\tanh(ab)}{ab}+8\Big]-7\frac{\tanh(ab)}{ab}-1\Big\}\cdot \\
&\quad \left[2(ab)^4\left(1-\frac{\tanh(ab)}{ab}\right)^3\left(\operatorname{sech}(ab)-\frac{\tanh(ab)}{ab}\right)^2\right]^{-1}
\end{aligned}
\tag{4.107}
$$

Chapter 5

Radial counterflow and vortex diffusion and production

In this chapter we focus our attention on pure radial flows and flows in convergent channels, where inhomogeneity of the heat flux and of the vortex line density have a special relevance. Our aim here is to study the role of these inhomogeneities. Radial flow between two concentric cylinders, where a central heat source supplies heat to helium and is carried out along the radial direction from the internal to the external cylinder, is the simplest model of inhomogeneous flow, because heat flux has a single component, the radial one, and depends on a single coordinate, the radial one. A second aspect of this chapter is the emphasis on the vortex dynamics, whereas in Chapter 3 and 4 the vortex density has been assumed as a given quantity and the interest has been focused on the heat flow.

A salient feature of radial flows (and of some other flows as for instance the flow in divergent-convergent channels) is that the average speed of the normal component (and also that of the superfluid component) changes along the axis (or with the distance to the heat source). This adds a new complexity to our analysis and, in particular, we are led to ask what is the influence of the mentioned acceleration on vortex production and destruction, and on the structure of the vortex tangle. One may also ask, furthermore, whether helium counterflow in convergent - divergent channels could also yield some heat rectification.

Another appealing aspect of radial flow is that the dependence of $\mathbf{V}_{ns}$ with the position allows one to have the several regimes of turbulence **TII** or **TI** and laminar flow simultaneously in the same experiment (see Figure 5.2-right) and that the radial dependence of $\mathbf{V}_{ns}$ is relatively simple. A second aspect of interest concerns the definition of the quantum (and the classical) Reynolds number, because here there is not a single well-defined spatial scale as in cylindrical or plane channels: one can use the external radius or the local radius to define the Reynolds numbers. A third aspect

comes from the inhomogeneity which allows the possibility of analyzing the role of a velocity gradient (or, alternatively, the superfluid acceleration) as an additional source of vorticity and the role of vortex diffusion.

One could guess as a formal but reasonable illustration, an evolution equation for the vortex line density of the tentative form

$$\frac{dL}{dt} = \alpha_V \mathbf{V}_{ns} L^{\frac{3}{2}} + \alpha' \mathbf{V}_{ns} \cdot \nabla L + \alpha'' \mathbf{V}_{ns} \cdot \nabla T - \beta_V \kappa L^2 + D\nabla^2 L, \tag{5.1}$$

with α' and α'' dimensionless parameter. In Section 5.6 a much more general expression will be examined, but here we write this simple version for the sake of a concrete illustration. The last term in (5.1) corresponds to vortex diffusion, which was previously considered in (Tsubota et al., 2003), from computer dynamic simulations, and found that, at T close to 0 K, $D \approx 10^{-1}\kappa$ (note indeed that the quantum of vorticity $\kappa = h/m$ has dimension of (length)^2(time)$^{-1}$, which are the dimensions of the diffusion coefficient). Also Nemirovskii has computed D in (Nemirovskii, 2010), using a kinetic model and an equation for the evolution of L in which only the diffusive term appears. He found the coefficient $D \approx 2.2\kappa$ at zero temperature, a value higher than that found by Tsubota, probably because Nemirovskii considered a pure diffusive situation (results for D at higher temperatures are not yet available, to our knowledge). A simple form of equation (5.1), with $\alpha' = \alpha'' = 0$, has also been considered by Nemirovskii to analyze the propagation of turbulence fronts in (Nemirovskii, 2011), adding a term of the form $\nabla(LV_L)$, where V_L is the drift velocity of the vortex front (see below eq.(5.49)). In (Nemirovskii, 2010) also the evolution and decay of inhomogeneous superfluid turbulence are studied.

5.1 Thermodynamic approach to vortex production and diffusion in inhomogeneous superfluid turbulence

Recent experimental and numerical results lead us to consider inhomogeneous and anisotropic tangles (Nemirovskii, 2010, 2011, 2013), with special emphasis on the role of vortex diffusion. Here we will consider inhomogeneous situations, where the tangle may still be described by L, but L may change from point to point in the volume of the tangle. In this case, the evolution equation for L must be written taking explicitly into account the contributions of inhomogeneity, as for instance a diffusion flux of vortices (already considered by some authors), or an additional contribution to vortex formation or destruction (not considered up to now).

This may be especially relevant in studies of strongly inhomogeneous flows, as for instance radial flows or flows in convergent or divergent channels (Castiglione et al., 1995; Kafkalidis et al., 1994a; Klinich III et al., 1997; Murphy et al., 1993), in the dif-

fusion contribution to the decay of vortex tangles in narrow channels (Kondaurova and Nemirovskii, 2012) or in the entrance region to channels. The description of anisotropic situations would require to use a tensor instead of a scalar — see (Jou et al., 2011b) —, as mentioned in Chapter 2 to take into account the different properties of vortices in the different spatial directions, and we will not consider it here.

Non-equilibrium thermodynamic methods have been used to describe the constitutive equations of homogeneous superfluid turbulence (Ardizzone et al., 2009; Geurst, 1989, 1992; Jou et al., 2002; Jou and Mongiovì, 2005; Mongiovì and Jou, 2007). In recent papers several non-homogeneous effects were already considered in the equation for L (Ardizzone et al., 2009; Mongiovì and Jou, 2007). Here, we reexamine the thermodynamical derivation of those equations from a more general perspective, allowing for the explicit role of inhomogeneities. Since inhomogeneities in the heat flux are expected to be deeply coupled with those in vortex density, the aim of building a model with both kinds of inhomogeneities seems well-motivated in radial flows and in channels with non-homogeneous cross-section. For instance, several observations in some of these channels (Castiglione et al., 1995; Kafkalidis et al., 1994a) show for the vortex line density some features which cannot be described by a local form of the Vinen's equation, because they depend not only on the modulus of the heat flux but also on its relative orientation with respect to the direction of convergent (or divergent) cross-section. Then, the roles of ∇L and their relative direction with respect to $\mathbf{q}$, as well as that of $\nabla \mathbf{q}$ itself, should be incorporated into a wider, more inclusive formalism.

5.1.1 Balance Equations

The basic variables we will use are internal energy E (per unit volume), vortex line density L, and heat flux density $\mathbf{q}$. The barycentric velocity $\mathbf{v}$ is assumed to be zero (counterflow situation) and the mass density ρ is assumed to stay constant (otherwise, both ρ and $\mathbf{v}$ should be included as independent variables, as in the model recalled in Chapter 2, in particular in Section 2.4). In these hypotheses, system (2.22) reduces to:

$$\begin{cases} \dot{E} + \nabla \cdot \mathbf{q} = 0 \\ \dot{\mathbf{q}} + \nabla \cdot \mathbf{J}^{\mathbf{q}} = \sigma^{\mathbf{q}} \\ \dot{L} + \nabla \cdot \mathbf{J}^{L} = \sigma^{L} \end{cases} \tag{5.2}$$

where the upper dot indicates the time derivatives, $\mathbf{J}^{\mathbf{q}}$ being the flux of the heat flux, and $\mathbf{J}^{L}$ the flux of vortex line density; $\sigma^{\mathbf{q}}$ and σ^{L} are the net production of heat flux and of vortices per unit time and volume, respectively.

We start our analysis from an entropy S and an entropy flux $\mathbf{J}^S$ of the form

$$S = S(E, L, \mathbf{q}, \nabla E, \nabla L, \nabla \mathbf{q}), \tag{5.3}$$

$$\mathbf{J}^S = \mathbf{J}^S(E, L, \mathbf{q}, \nabla E, \nabla L, \nabla \mathbf{q}). \tag{5.4}$$

The motivation to include the gradients is to describe non-local effects. In fact, we may exclude the terms in ∇E, ∇L and $\nabla \mathbf{q}$ from S, because we are not looking for an evolution equation for the gradients themselves, and it is known (Cimmelli, 2009; Cimmelli and Frischmuth, 2007) that in this case the entropy does not depend on the gradients, as shown in Section 1.1.2 (see equation (1.13)). This result allows us to simplify our presentation and to focus directly on the purely non-local contributions to the transport equations, which are known to be deeply related to the entropy flux (Cimmelli, 2009; Cimmelli and Frischmuth, 2007; Jou et al., 2010; Muller and Ruggeri, 1998) rather than to the entropy itself. Restrictions on the constitutive equations for the fluxes $\mathbf{J}^{\mathbf{q}}$ and $\mathbf{J}^L$ can be obtained imposing the validity of the second law of thermodynamics, as we did in Section 2.4.2.

As a consequence of the material objectivity principle (Muller and Ruggeri, 1998) the expressions of the fluxes, $\mathbf{J}^{\mathbf{q}}$ and $\mathbf{J}^L$, are:

$$\mathbf{J}^{\mathbf{q}} = -\beta_2(\nabla \cdot \mathbf{q})\mathbf{U} - \xi_2\langle \nabla \mathbf{q} \rangle, \tag{5.5}$$

$$\mathbf{J}^L = \nu \mathbf{q} + \nu_2 \nabla E + \nu_3 \nabla L, \tag{5.6}$$

where ν is a function of E and L, while β_2, ξ_2, ν_2 and ν_3 are supposed constants. These are the simplest vector and tensor depending on $\mathbf{q}$, E and L and their first-order derivatives (higher-order terms, for instance $\nabla\nabla E$, $\nabla\nabla L$ or $\nabla^2\nabla E$, $\nabla^2\nabla L$, could contribute to the fluxes, but they are beyond the first-order local effects we are considering here).

As production terms in the equations for the heat flux $\mathbf{q}$ and vortex line density L, we choose the following expressions, more general than those proposed in Section 2.4.5 (see equations (2.87) and (2.88))

$$\sigma^{\mathbf{q}} = -\frac{1}{\tau_1}\mathbf{q} - N_1 L \mathbf{q} + N_2 L^{3/2}\frac{\mathbf{q}}{|\mathbf{q}|} + \tilde{\alpha}_1 \nabla E + \tilde{\alpha}_2 \nabla L, \tag{5.7}$$

$$\sigma^L = \gamma_1 L^{3/2}|\mathbf{q}| - \gamma_2 L^2 + \tilde{\alpha}_3\, \mathbf{q} \cdot \nabla E + \tilde{\alpha}_4\, \mathbf{q} \cdot \nabla L. \tag{5.8}$$

The latter expression, neglecting the terms dependent on the gradients, is the well-known Vinen expression for the vortex production-destruction rates (Barenghi et al., 2001; Donnelly, 1991; Nemirovskii, 2013; Nemirovskii and Fiszdon, 1995; Tsubota et al., 2012; van Sciver, 2012), with γ_1 and γ_2 being coefficients related to the rate of vortex creation and destruction per unit volume (see below equation (5.17)). They are linked to Vinen's coefficients α_V and β_V by the relations $\gamma_1 = \alpha_V(\rho_s T s)^{-1}$ and $\gamma_2 = \beta_V \kappa$. The terms independent of the gradients in equation (5.7) were derived in a previous

thermodynamic analysis in (Mongiovì and Jou, 2007), where these terms describe the friction between vortices and the normal component, but here they are taken as macroscopic hypotheses, with τ_1 the relaxation time of the heat flux, and N_1 and N_2 being friction coefficients depending on temperature. The terms in N_1 and N_2 depend on $\mathbf{q}$ in two different ways: the former is proportional to the heat flux, while the second one, depends only on the direction of $\mathbf{q}$, but not on its value. The new terms considered in this chapter are those in $\tilde{\alpha}_1$, $\tilde{\alpha}_2$, $\tilde{\alpha}_3$ and $\tilde{\alpha}_4$ in (5.7) and (5.8). Note that the last two terms in expression (5.8) could be written in the form of the terms in α' and α'' in (5.1) by expressing $\mathbf{q}$ in terms of $\mathbf{V}_{ns}$ and ∇E in terms of ∇T and ∇L.

5.1.2 Second law restrictions

To exploit the restriction imposed by the second law of thermodynamics, as in the previous chapters, we consider the equations (5.2) as constraints for the entropy inequality to hold. Taking these constraints into account, one obtains the following inequality, which must be satisfied for arbitrary values of the field variables,

$$\partial_t S+\nabla\cdot\mathbf{J}^S-\Lambda^E\left[\dot{E}+\nabla\cdot\mathbf{q}\right]-\Lambda^{\mathbf{q}}\cdot[\dot{\mathbf{q}}+\nabla\cdot\mathbf{J}^{\mathbf{q}}-\sigma^{\mathbf{q}}]-\Lambda^L\left[\dot{L}+\nabla\cdot\mathbf{J}^L-\sigma^L\right]\geq 0. \quad (5.9)$$

We choose for S and $\mathbf{J}^S$ expression like (2.26) and (2.27) of Section 2.4.2, and suppose that S depends on $\mathbf{q}$ only through its modulus. Following the Liu procedure of Lagrange multipliers, as in Section 2.4.2, we obtain the following expression for the entropy flux density

$$\mathbf{J}^S=(\Lambda^E+\Lambda^L\nu)\mathbf{q}+\Lambda^L(\nu_2\nabla E+\nu_3\nabla L)+\lambda\mathbf{q}(-\beta_2\nabla\cdot\mathbf{q}-\xi_2\langle\nabla\mathbf{q}\rangle), \quad (5.10)$$

and from (5.9) it remains the following inequality

$$\phi_3(\nabla\cdot\mathbf{q})^2+\phi_4\langle\nabla\mathbf{q}\rangle:\langle\nabla\mathbf{q}\rangle+\lambda\mathbf{q}\cdot\sigma^{\mathbf{q}}+\Lambda^L\sigma^L\geq 0. \quad (5.11)$$

This inequality is valid for any value of fields and of their spatial derivatives and its positiveness requires $\phi_3>0$ and $\phi_4>0$. Furthermore, in situations with homogeneous values of $\mathbf{q}$ (i.e. vanishing gradients of $\mathbf{q}$), it also requires that:

$$\lambda\mathbf{q}\cdot\sigma^{\mathbf{q}}+\Lambda^L\sigma^L\geq 0, \quad (5.12)$$

that coincides with (2.48). This last inequality may be written explicitly by taking into account the form (5.7) and (5.8) for the production terms, and one has

$$\begin{aligned}-\lambda\left[\frac{1}{\tau_1}+N_1L\right]\mathbf{q}^2+\lambda N_2L^{\frac{3}{2}}|\mathbf{q}|+\lambda\tilde{\alpha}_1\mathbf{q}\cdot\nabla E+\lambda\tilde{\alpha}_2\mathbf{q}\cdot\nabla L\\ +\Lambda^L\left[\gamma_1L^{\frac{3}{2}}|\mathbf{q}|-\gamma_2L^2+\tilde{\alpha}_3\mathbf{q}\cdot\nabla E+\tilde{\alpha}_4\mathbf{q}\cdot\nabla L\right]\geq 0. \quad (5.13)\end{aligned}$$

We have just seen in Section 2.4.2 that $\Lambda^L < 0$ and $\lambda < 0$. Therefore, the first term of the first line and the second term of the second line will be always positive provided $\tau_1 > 0$, $N_1 > 0$ and $\gamma_2 > 0$. Further, the sum of the terms in λN_2 and $\Lambda^L \gamma_1$ will also be positive if $\lambda N_2 + \Lambda^L \gamma_1 > 0$, because $L^{\frac{3}{2}}|\mathbf{q}|$ is positive. Being γ_1 positive, as it describes vortex formation in the Vinen's equation, N_2 ought to be negative. The remaining terms could be positive or negative, and therefore they cannot contribute to the entropy production and should vanish identically. This requires that:

$$\lambda\tilde{\alpha}_1 + \Lambda^L\tilde{\alpha}_3 = 0, \qquad \lambda\tilde{\alpha}_2 + \Lambda^L\tilde{\alpha}_4 = 0. \tag{5.14}$$

The coefficients $\tilde{\alpha}_3$ and $\tilde{\alpha}_4$ are linked to $\tilde{\alpha}_1$ and $\tilde{\alpha}_2$, but their concrete signs do not follow from (5.14). We will keep on the discussion on their physical meaning in Section 5.2.

5.2 Field equations accounting for non-local effects

In order to predict the behavior of the observable fields E (related to the temperature), $\mathbf{q}$ and L, we must take into account the expressions for the fluxes in their evolution equations.

Substituting the constitutive relations (5.5) and (5.6) for the fluxes and the expressions of the source terms (5.7) and (5.8) in the evolution equations (5.2), and assuming $E = E(T, L)$ and $\nu = \nu(T, L)$, we obtain

$$\rho c_V \dot{T} + \frac{\partial E}{\partial L}\dot{L} = -\nabla \cdot \mathbf{q}, \tag{5.15}$$

$$\dot{\mathbf{q}} - \beta_2 \nabla(\nabla \cdot \mathbf{q}) - \xi_2 \nabla^2 \mathbf{q} = -\frac{1}{\tau_1}\mathbf{q} - N_1 L \mathbf{q} + N_2 L^{\frac{3}{2}} \frac{\mathbf{q}}{|\mathbf{q}|} + \tilde{\alpha}_1 \rho c_V \nabla T + X \nabla L, \tag{5.16}$$

$$\dot{L} = \gamma_1 L^{\frac{3}{2}}|\mathbf{q}| - \gamma_2 L^2 + D\nabla^2 L - \nu \nabla \cdot \mathbf{q} - \nu_2 \rho c_V \nabla^2 T + Y' \mathbf{q} \cdot \nabla T + X' \mathbf{q} \cdot \nabla L, \tag{5.17}$$

where c_V is the constant-volume specific heat, and

$$X = \tilde{\alpha}_1 \frac{\partial E}{\partial L} + \tilde{\alpha}_2, \qquad X' = \tilde{\alpha}_4 + \tilde{\alpha}_3 \frac{\partial E}{\partial L} - \frac{\partial \nu}{\partial L}, \qquad Y' = \tilde{\alpha}_3 \rho c_V - \frac{\partial \nu}{\partial T}. \tag{5.18}$$

Here $D = -\nu_2 \frac{\partial E}{\partial L} - \nu_3$ is the diffusion coefficient of vortex lines. The coefficients β_2 and ξ_2 may also be written in terms of the viscosity and the entropy of the normal component, but we do not need it now (Saluto et al., 2014).

Equations (5.16) and (5.17) are the evolution equations of $\mathbf{q}$ and L. Simpler forms of (5.16) and (5.17) have just been used in this thesis, taking $\tau_1 = \infty$, $N_2 = 0$, $\tilde{\alpha}_1 \neq 0$ and $X = 0$ in (5.16) and $D = 0$, $\nu = 0$, $\tilde{\alpha}_3 = 0$ and $X' = 0$ in (5.17). The terms in τ_1, D, ν and $\tilde{\alpha}_i$ are clearly related to inhomogeneity, whereas the terms in N_i follow from a thermodynamic analysis as in (Mongiovì and Jou, 2007).

The coefficient ν_2 in (5.17) plays a role analogous to the so called thermal-diffusion coefficient in the Soret effect in matter diffusion. Indeed, if we take $\nu = 0$ (for the sake of simplicity), expression (5.6) for the vortex diffusion may be written as

$$\mathbf{J}^L = \nu_2 \rho c_V \nabla T - D \nabla L. \tag{5.19}$$

The term in ∇T in this equation expresses a coupling between temperature field and vortex density field, analogous to the coupling between ∇T and the diffusion flux of matter in thermodiffusion.

In steady states, and according to (5.15), one must have $\nabla \cdot \mathbf{q} = 0$. In this case, the equations (5.16) and (5.17) reduce to

$$-\xi_2 \nabla^2 \mathbf{q} = -\frac{1}{\tau_1}\mathbf{q} - N_1 L \mathbf{q} + N_2 L^{\frac{3}{2}} \frac{\mathbf{q}}{|\mathbf{q}|} + \tilde{\alpha}_1 \rho c_V \nabla T + X \nabla L, \tag{5.20}$$

$$\gamma_1 L^{\frac{3}{2}} |\mathbf{q}| - \gamma_2 L^2 + D \nabla^2 L - \nu_2 \rho c_V \nabla^2 T + Y' \mathbf{q} \cdot \nabla T + X' \mathbf{q} \cdot \nabla L = 0. \tag{5.21}$$

We pay close attention to these equations below.

5.2.1 Equation for the heat flux

If the term $X \nabla L$ in equation (5.20) is neglegible with respect to the other terms (this is exactly true for homogeneous vortex tangles in which $\nabla L = 0$), then equation (5.20) becomes

$$\frac{1}{\tau_1}\mathbf{q} + N_1 L \mathbf{q} - N_2 L^{\frac{3}{2}} \frac{\mathbf{q}}{|\mathbf{q}|} = \tilde{\alpha}_1 \rho c_V \nabla T + \xi_2 \nabla^2 \mathbf{q}, \tag{5.22}$$

that is a generalization of the equations studied in Chapter 3. In a linear approximation and in absence of vortices and neglecting inhomogeneities in $\mathbf{q}$, one must obtain the Fourier's law, i.e. $\mathbf{q}$ proportional to ∇T with a negative coefficient, then recalling the meaning of the thermal conductivity k, we have:

$$-\frac{k}{\tau_1} = \tilde{\alpha}_1 \rho c_V. \tag{5.23}$$

It follows $\tilde{\alpha}_1 < 0$. The term in $N_1 L \mathbf{q}$ is related to the friction between the tangle and the normal component of the fluid and, in well developed conditions, it is proportional to $|\mathbf{q}|^3$, because L is proportional to $|\mathbf{q}|^2$. The term in N_2 is another frictional contribution, and it is also proportional to $|\mathbf{q}|^3$. Thus the heat flux $\mathbf{q}$ across the tangle is proportional to $(\nabla T)^{1/3}$, because the frictional term becomes dominant (this correspond to so-called Gorter-Mellink regime in heat transport in He II).

In Chapter 3 we have considered a homogeneous L, but here we are interested in a more general analysis allowing L to depend on the position. Therefore we must considering also the term $X \nabla L$ in equation (5.20) obtaining

$$\frac{1}{\tau_1}\mathbf{q} + N_1 L \mathbf{q} - N_2 L^{\frac{3}{2}} \frac{\mathbf{q}}{|\mathbf{q}|} = -\frac{k}{\tau_1} \nabla T + X \nabla L + \xi_2 \nabla^2 \mathbf{q}. \tag{5.24}$$

One sees that the heat flux has contributions from a term in ∇T, corresponding to the energy carried out by the fluid itself, and from a term in ∇L, which could be interpreted as the energy carried out by the tangle itself, i.e. by the vortices which go from higher to lower L, in a separate way from the ∇T contribution. We pay further attention on it in Section 5.2.3.

5.2.2 Equation for the vortex line density

Now we comment the new terms in $\tilde{\alpha}_3$ and $\tilde{\alpha}_4$, through X' and Y', appearing in equation (5.21) describing the evolution of L, in order to identify some of their possible observable consequences.

According to (5.14)

$$\tilde{\alpha}_3 = -\frac{\lambda}{\Lambda^L}\tilde{\alpha}_1 = \frac{\lambda}{\Lambda^L}\frac{k}{\tau_1}\frac{1}{\rho c_V} = -\frac{1}{\Lambda^L T^2}\frac{1}{\rho c_V}, \tag{5.25}$$

where we have taken into account the identification (5.23) of k and (2.81) of λ. Since $\Lambda^L < 0$, it follows that $\tilde{\alpha}_3 > 0$.

Introducing the last expression for $\tilde{\alpha}_3$ in (5.18), equation (5.17) becomes

$$\dot{L} = \gamma_1 L^{3/2}|\mathbf{q}| - \gamma_2 L^2 + PL|\mathbf{q}|^2 + D\nabla^2 L + X'\mathbf{q}\cdot\nabla L + Y'\mathbf{q}\cdot\nabla T, \tag{5.26}$$

where $P = -\frac{\tau_1}{k}N_1\left(-\frac{1}{\Lambda^L T^2} - \frac{\partial\nu}{\partial T}\right)$. The two last terms come from the new coupled effects relating ∇T and $\mathbf{q}$. In (5.26) we have assumed a very high thermal conductivity and we have simply taken

$$\nabla T = -\left(\frac{\tau_1}{k}N_1 L\right)\mathbf{q}. \tag{5.27}$$

From this we get

$$\nabla^2 T = -\left(\frac{\tau_1}{k}N_1\right)\left(\nabla L\cdot\mathbf{q} + L\nabla\cdot\mathbf{q}\right). \tag{5.28}$$

In steady-state, it must be $\nabla\cdot\mathbf{q} = 0$, and then equation (5.26) becomes

$$\gamma_1 L^{3/2}|\mathbf{q}| - \gamma_2 L^2 + PL|\mathbf{q}|^2 = -D\nabla^2 L - X''\mathbf{q}\cdot\nabla L, \tag{5.29}$$

where $X'' = X' + \frac{\nu_2}{\tilde{\alpha}_1}N_1 = \tilde{\alpha}_4 + \tilde{\alpha}_3\frac{\partial E}{\partial L} - \frac{\partial\nu}{\partial L} + \frac{\nu_2}{\tilde{\alpha}_1}N_1$.

The term in $\mathbf{q}\cdot\nabla L$ in (5.26) is especially appealing because it indicates that a vortex density gradient could contribute not only to vortex diffusion, but also to vortex creation (or destruction), in inhomogeneous vortex tangles. We illustrate this aspect in Section 5.2.3.

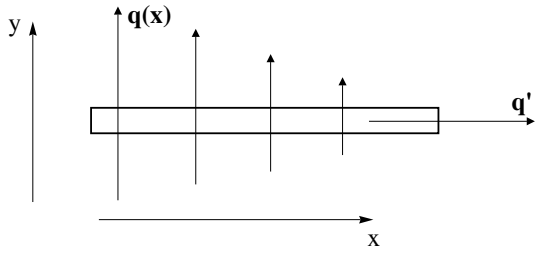

Figure 5.1: Channel filled with superfluid He II; perpendicular to the channel, in direction y, a heat flux $\mathbf{q}(\mathbf{x})$ which depends on x is imposed. This implies that L, proportional to q^2, will also depend on x. According to (5.24), this inhomogeneity of L should contribute to the heat transfer along x, although T is constant along x.

5.2.3 Proposal of experiment

We propose here an experiment to check the physical effects of the new terms proposed in the evolution equations (5.24) for the heat flux and (5.29) for the vortex line density.

In order to study the effects of the term in ∇L in (5.24), we propose the following experiment. Take a parallelepipedic channel filled of He II, with its elongated site in direction x, as in Figure 5.1. Perpendicular to the channel, in direction y, we impose a heat flux whose intensity depends on x: $\mathbf{q}(x) = q(x)\hat{\mathbf{j}}$. According to the two first terms in (5.8) or in (5.21), corresponding to Vinen's equation, this will produce along the channel an $L(x)$ profile proportional to the local value of $|\mathbf{q}|^2$. The experiment must be made in such a way that the He II temperature T is constant along the channel, i.e. it does not depend on x. Now, according to (5.24), one should have a heat flux $\mathbf{q}' = q'\hat{\mathbf{i}}$ along the x-axis as a consequence of the inhomogeneity of L; this term, proportional to ∇L, would be absent in homogeneous tangles. This could allow to explore the energy carried by the vortices which migrate from higher to lower L.

This flow would correspond to a diffusion flux of vortices, carrying vortex energy from regions of high L to those of low L. Then, this experiment would allow to measure the vortex diffusion coefficient D as well, appearing in equation (5.21) (note that in this situation the last term in (5.21) is negligible, because the dominant heat fluxes are perpendicular to ∇L, indeed, also the term in $\nabla^2 T$ is negligible because of (5.28)). Then, equation (5.21) reduces to:

$$\gamma_1 L^{\frac{3}{2}}|\mathbf{q}| - \gamma_2 L^2 + D\nabla^2 L + Y'\mathbf{q}\cdot\nabla T = 0. \tag{5.30}$$

Still another experiment could be settled along the lines of a situation examined in (Kondaurova and Nemirovskii, 2012), where the authors have studied the influence of vortex diffusion in the decay of vortex tangles in relatively narrow channels. After

suddenly switching off the heat flow, a part of the vortices annihilated by mutual interaction amongst them but another part annihilated on the walls. This produced an inhomogeneity leading more vortices towards the walls, in such a way that diffusion considerably contributed to the decay. In fact, they observed that in finite boxes the escape process is not purely diffusive, but it has also a ballistic contribution, namely, a direct flow from the bulk to the walls, without loop collisions inside the bulk, but only on the walls. In the situation studied by them, our additional terms in (5.17), especially the two latter terms, would not contribute to the decay, because $\mathbf{q}$ would be set to 0. However, if $\mathbf{q}$ was suddenly reduced to a non-vanishing value (instead of 0), the last term in (5.17) would imply a further contribution to the decay. In particular, since ∇L points from the walls to the interior of the container, the last term in (5.17) would imply a different rate of decay in the walls parallel to $\mathbf{q}$ (for which the term in $\mathbf{q}\cdot\nabla L$ would be zero), than in the walls perpendicular to $\mathbf{q}$ (where the mentioned term would be different from zero, and would have a different sign in the wall where the heat flux enters into the container and the wall through which it would exit from it).

5.3 Radial counterflow

Here we consider a radial counterflow from a cylindrical wall of radius r_0 at temperature T_0 to another concentric cylinder of radius r_1 at temperature T_1. This is a classical situation in heat management. For instance, in the context of Fourier's law, and for constant thermal conductivity k, the heat removed from the internal cylinder per unit time and unit cylinder length is:

$$\dot{Q} = \frac{2\pi k}{\frac{k}{r_0 h_0} + \frac{k}{r_1 h_1} + ln(\frac{r_1}{r_0})}(T_0 - T_1), \tag{5.31}$$

where h_0 and h_1 are the corresponding heat transfer coefficients between the fluid and the walls. However, our situation is much more complicated because we assume that the space between r_0 and r_1 is filled with superfluid helium — in a cryogenic device, for instance —. An analogous situation has been studied in (Campbell, 1987) where superfluid ^4He is in a rotating annulus driven by a radial counterflow. As in (Campbell, 1987) we obtain an heat flux dependent only on r.

Though our inspiration comes from a practical situation, our motivation is basically theoretical, and it is focused on the role of quantum superfluid turbulence in heat transport.

Recall that, according to Vinen equation, the vortex-line density L depends on the local value of $q(r)$ (for $q > q_{crit}$) as

$$L^{\frac{1}{2}}(q) = \frac{\alpha_V}{\beta_V \kappa}|\mathbf{V}_{ns}| = \frac{\alpha_V}{\beta_V \kappa}\frac{|q|}{\rho_s T s} = \frac{\gamma_1}{\gamma_2}|q|, \tag{5.32}$$

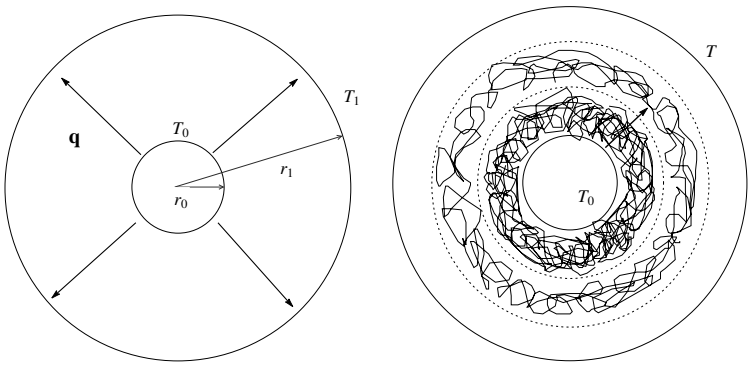

Figure 5.2: **Left:** Heat flows axially from the inner cylinder (the hotter one), at fixed temperature T_0, to the outer colder one. The radial temperature profile $T(r)$ depends on the heat flow and the vortex density radial distribution. **Right:** Example of vortex inhomogeneity. Since the heat flow is higher near the center, the vortex line density will also be higher there, and it will decrease towards the borders; thus, one can observe simultaneously several regimes of turbulence in the same experiment. As a consequence of the inhomogeneity, vortex diffusion will arise.

this expression comes from (5.1) with $\alpha' = \alpha'' = 0$ and $D = 0$ (or from equation (5.29) with $P = 0$, $D = 0$ and $x'' = 0$), and implies

$$\frac{\partial L}{\partial r} = 2\frac{\gamma_1}{\gamma_2} L^{\frac{1}{2}} \frac{\partial q}{\partial r}. \tag{5.33}$$

Then we can write the equation for the radial component of the heat flux from equation (5.24), taking in mind the relation (5.23) between k and τ_1,

$$\frac{\partial T}{\partial r} - \overline{\xi}\left(\frac{\partial^2 q_r}{\partial r^2} + \frac{1}{r}\frac{\partial q_r}{\partial r} - \frac{q_r}{r^2}\right) = -\frac{KL}{\zeta} q_r - \frac{1}{k} q_r + 2\overline{X}\frac{\gamma_1}{\gamma_2} L^{\frac{1}{2}} \frac{\partial q_r}{\partial r}, \tag{5.34}$$

here the coefficient $\overline{\xi}$ is linked to ξ_1, the coefficient $\overline{X}$ to X, and the coefficient $\frac{K}{\zeta}$ is linked to N_1 and N_2.

In steady-state situations, the heat flux $\mathbf{q}$ must have the form $\mathbf{q} = q_r \hat{\mathbf{r}}$, where

$$q_r = q(r) = \Gamma / r, \tag{5.35}$$

with Γ a constant. This follows from the condition $\nabla \cdot \mathbf{q} = 0$ of energy balance equation in steady-state, and it may be intuitively understood because the total heat flowing radially away from the internal cylinder must satisfy the relation $2\pi r q(r) = 2\pi\Gamma = cost$ equal to the total heat flow supplied by the internal cylinder per unit length. This gives the physical meaning of Γ.

In this case the Laplacian of $q(r)$, i.e. the terms in parenthesis in equation (5.34), is equal to 0 (from (5.35)), and $\frac{\partial q}{\partial r} = -\Gamma/r^2$. Then, taking in mind equation (5.33), equation (5.34) becomes

$$\frac{\partial T}{\partial r} = \left(-\frac{KL}{\zeta} - \frac{1}{k} - 2\overline{X}\frac{\gamma_1}{\gamma_2}\frac{L^{\frac{1}{2}}}{r} \right) q(r), \tag{5.36}$$

this last expression reduces to the Fourier's law in absence of vortices, i.e. when $L = 0$.

We will take the expression (5.32) for L as a reference for comparison with situation in which non local terms are taken into account as in (5.1). The strategy we will apply is the following one: we impose a value of Γ and obtain the local values of $\mathbf{q}$ and the temperature radial gradient $\frac{\partial T}{\partial r}$, in order to obtain the full heat profile as a function of r. From here, and given values of the heat transfer coefficients h_0 and h_1, of the internal and external cylindrical surface, we obtain $T(r)$ and, in particular, T at the external surface $T_1(r_1)$. Since we know Γ, the heat extracted from internal cylinder per unit length of the cylinder and unit time will be $\dot{Q} = 2\pi\Gamma$; since we know the corresponding temperature T_1 we will be able to calculate $\dot{Q}$ as a function of $T_0 - T_1$. This could do numerically.

The result will be different if we use a generalization of the Vinen equation, adding non local terms. For example if the gradient of $\mathbf{V}_{ns}$ or of $\mathbf{q}$ also contributes as an additional source of vortices, as commented in (5.1), namely if:

$$\frac{dL}{dt} = \gamma_1 q L^{\frac{3}{2}} - \gamma_2 L^2 + \overline{\alpha}\left|\frac{dq}{dr}\right| L, \tag{5.37}$$

one will have for the steady state:

$$\gamma_2 L - \gamma_1 q L^{\frac{1}{2}} - \overline{\alpha}\left|\frac{dq}{dr}\right| = 0, \tag{5.38}$$

in Section 5.6 the term in $\overline{\alpha}|d\mathbf{q}/dr|L$ will be written in the more general invariant form, $\alpha'(\nabla\mathbf{q} : \nabla\mathbf{q})^{\frac{1}{2}}L$, but here $d\mathbf{q}/dr$ is the only nonvanishing component of $\nabla\mathbf{q}$.

Since $q = \Gamma/r$, $|dq/dr| = \Gamma/r^2$, L would depend on r as

$$L^{\frac{1}{2}} = \frac{\gamma_1}{2\gamma_2} q \left[1 + \sqrt{1 + \frac{4\gamma_2}{\gamma_1^2 q^2}\overline{\alpha}\left|\frac{dq}{dr}\right|} \right] = \frac{\gamma_1 \Gamma}{2\gamma_2 r} \left[1 + \sqrt{1 + \frac{4\gamma_2\overline{\alpha}}{\gamma_1^2\Gamma}} \right]. \tag{5.39}$$

Thus, the dependence of L with the radius would be the same as for $\overline{\alpha} \neq 0$, but the coefficient would be different, implying a higher value of L. This would be one of the consequences of the assumption that a gradient of $\mathbf{q}$ acts as an additional source of vortices.

5.4 Vortex diffusion and hysteresis cycle in radial quantum turbulence

In this section we study the influence of vortex diffusion (described by the last term of equation (5.1)) in radial counterflow between two concentric cylinders at different temperatures.

In this case, L is no longer homogeneous but depends on the radial distance r to the axis, and, as a consequence, vortex diffusion plays a role (Nemirovskii, 2010, 2011; Tsubota et al., 2003) which, in turn, influences the temperature profile. The origin of inhomogeneity of vortex-line density is the inhomogeneity of the heat flux itself. Because of the geometry of the flow, the heat flux is maximum near the center and decreases towards the external wall. The source of vortices is everywhere (corresponding to the source term of the local Vinen's equation), but more intense in the inner region.

5.4.1 Hydrodynamical model

Also in this section, as in the previous, we use as fundamental fields the temperature T, the vortex line density L, and the heat flux $\mathbf{q}$. In these conditions, the system is described by equations (5.15)–(5.17), in the simplified form:

$$\rho c_V \dot{T} = -\nabla \cdot \mathbf{q} \tag{5.40}$$

$$\dot{\mathbf{q}} = -\frac{\zeta}{k}\mathbf{q} - N_1 L \mathbf{q} + N_2 L^{\frac{3}{2}} \frac{\mathbf{q}}{|\mathbf{q}|} - \zeta \nabla T - \chi \nabla L \tag{5.41}$$

$$\dot{L} = \gamma_1 L^{\frac{3}{2}} |\mathbf{q}| - \gamma_2 L^2 + D\nabla^2 L + \nabla \cdot (\nu \mathbf{q}) \tag{5.42}$$

with k thermal conductivity, k/ζ the relaxation time of the heat flux, i.e. τ_1 in (5.16), γ_1 and γ_2 the rates of vortex formation and destruction, respectively, χ a coupling coefficient between heat flux and the gradient of L, and the other coefficients have the same meaning as in (5.15)–(5.17). Here, we will pay a special attention to diffusion effects in inhomogeneous vortex tangles arising in radial counterflow.

5.4.2 Application to radial counterflow

Here we apply equations (5.40)–(5.42) to a steady-state counterflow of He II between two concentric cylindrical walls at different temperatures. The inner cylinder (the hotter one) is at fixed temperature T_0 (Figure 5.2-left). The temperature profile $T(r)$ between both cylinders will depend on heat flux, thermal conductivity, and the vortex line density profile $L(r)$.

The steady state situation requires $\nabla \cdot \mathbf{q} = 0$ according to (5.40). Since we can consider an axial symmetry for the problem, the heat flux has only a radial component q_r (which will be called here as q), this implies that $q = \Gamma/r$, as mentioned in (5.35).

Here we will study the behavior of $L(r)$, which could be obtained experimentally from the attenuation coefficient of second sound. Introduction of $q = \Gamma/r$ in (5.42) and assuming ν constant, allows to obtain $L(r)$ from

$$\gamma_1 \frac{\Gamma}{r} L^{\frac{3}{2}} - \gamma_2 L^2 + D\nabla^2 L = 0. \tag{5.43}$$

If the temperature gradients are small, γ_1, γ_2 and D (which in principle depend on temperature) may be taken as constant. In this case, one sees easily that equation (5.43) admits the solutions:

$$L(r) = 0 \qquad \text{and} \qquad L(r) = \overline{\gamma}^2 \frac{\Gamma^2}{r^2}, \tag{5.44}$$

with

$$\overline{\gamma} = \frac{\gamma_1}{2\gamma_2} \left(1 + \sqrt{1 + \frac{16 D \gamma_2}{\gamma_1^2 \Gamma^2}} \right). \tag{5.45}$$

If $D = 0$ one recovers the result $\overline{\gamma} = \frac{\gamma_1}{\gamma_2}$, of the usual Vinen equation, i.e.

$$L(r) = \frac{\gamma_1^2}{\gamma_2^2} \frac{\Gamma^2}{r^2}. \tag{5.46}$$

If we compare the different expression of L obtained above, i.e. (5.39) (corresponding to increased heat production but with vanishing diffusion) and (5.44)–(5.45) (corresponding to diffusion, but without an increase in the vortex production) with expression (5.32), we note that in the first two cases the value of L is increased with respect to (5.32). It is interesting to note that the dependence of the additional terms as a function of Γ is different in both situations: it changes as Γ^{-1} if the excess of L is due to a source of vortices proportional to the gradient of the heat flux in (5.39), and as Γ^{-2} if it is due to diffusion in (5.45). Thus, a comparison of the results for L with different values of Γ could allow us to separate both kinds of contributions.

Equation (5.45) shows that the diffusion of vortices increases the local values of L as compared with the situation with $D = 0$, especially at relatively low values of the heat flux. The diffusion contribution will be specially relevant when γ_1/γ_2 is small (as compared to $D/\gamma_1\Gamma^2$, or in other terms when D is higher than $\gamma_2/\gamma_1\Gamma^2$) because in that case the second term inside the root will be high. This increase may be intuitively understood as the result of a diffusive flow of vortices from the inner cylinder (where $\mathbf{q}$ is higher and therefore the vortex production is higher) to the outer cylinder, where they will disappear when colliding against the external wall. Thus, the term in $\gamma_1\Gamma$ accounts for the "native" vortices, as meaning that they were produced in the same point being considered, in contrast with the term in D, which accounts for the "visiting" or "migrating" vortices in that point. For small heat flux or high diffusion, the "migrating" vortex population is higher than the native vortex population.

When vortex diffusion effects become dominating, the vortex line density profile (5.44) takes the form

$$L(r) = \frac{4D}{\gamma_2 r^2}. \tag{5.47}$$

In this regime, L is independent of the heat flux, but it keeps the same dependence $1/r^2$ on the radius than in (5.44) for $D = 0$. Thus, the influence of the vortex diffusion is focused on the local values of $L(r)$ rather than on the form of the spatial steady distribution. In the limit of low Γ, (5.43) with $D = 0$ would lead to $L = 0$, but for $D \neq 0$ it leads for L to (5.47).

5.4.3 Possible hysteresis cycle

The remark (5.45) of the different values of L in the presence or absence of diffusion suggests the possibility of hysteresis when the heat flux is increased from zero to some maximum value, at a rate sufficiently higher than the diffusion rate, and is subsequently lowered to zero, at a rate sufficiently lower than the diffusion rate. In the first case, diffusion will not have time to act during the process, so that L will be given by (5.44)–(5.45) with $D = 0$ (the "native" population will predominate), i.e. $L(r) = \frac{\gamma_1^2}{\gamma_2^2}\frac{\Gamma^2}{r^2}$. In contrast, in the slow process, diffusion will always act and L will be described by (5.44)–(5.45) with $D \neq 0$.

The situation is presented in Figure 5.3, where we have considered the dimensionless quantities Lr^2, $\overline{\gamma}_0\Gamma$ and $\tilde{D}$, defined by the following relations:

$$\begin{aligned} &\overline{\gamma}_0 \equiv \tfrac{\gamma_1}{2\gamma_2}, \\ &\tilde{\gamma}_0 = \overline{\gamma}_0 \left[1 + \sqrt{1 + \tilde{D}\tfrac{1}{(\overline{\gamma}_0\Gamma)^2}}\right], \\ &\tilde{D} \equiv \tfrac{4D}{\gamma_2}. \end{aligned} \tag{5.48}$$

In this notation, for $D = 0$, one has, from (5.46) $Lr^2 = 4(\overline{\gamma}_0\Gamma)^2$.

The initial situation of the cycle corresponds to $L = 0$ and $\Gamma = 0$ (state A). The quick increase of Γ produces the corresponding increase of L (from A to B). From B to C the heat flux is no longer changed and diffusion plays a central role. As in (Nemirovskii, 2011), one can see that, if one considers the drift velocity of the vortex front, in equation (5.42), i.e.

$$\frac{\partial L}{\partial t} + \nabla(LV_L) = \gamma_1 L^{\frac{3}{2}}|\mathbf{q}| - \gamma_2 L^2 + D\nabla^2 L + \nabla\cdot(\nu\mathbf{q}) \tag{5.49}$$

a locally increase of the value of L corresponds to the propagation of a vortex front, from the inner to the outer regions, with a speed proportional to $q\sqrt{D\gamma_1^2/\gamma_2}$ (see Section 5.5). When Γ slowly decreases (from C to D), the final value of L will be given by (5.47),

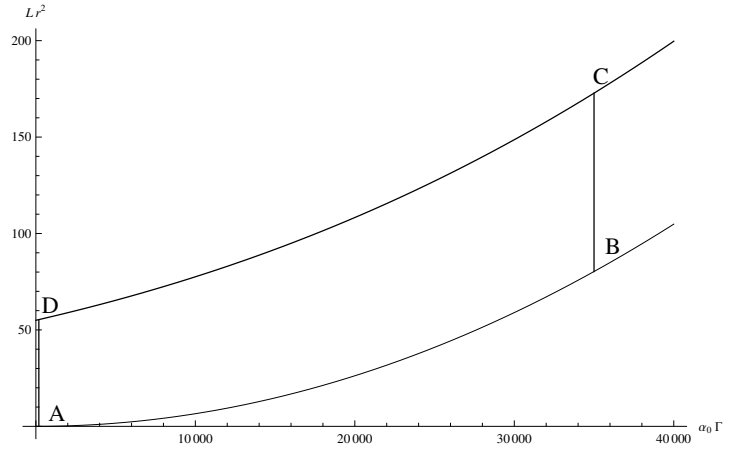

Figure 5.3: Hysteresis cycle. The value of Lr^2 (vertical axis) as a function of the dimensionless expression for the heat flux $\overline{\gamma}_0\Gamma$. The value of L for fastly increasing heat flux (A to B), corresponding to eq. (5.46), is different from that for slowly decreasing heat flux (C to D), corresponding to eqs. (5.44)-(5.45) with $D \neq 0$. The values of $\overline{\gamma}_0 = 1.28 * 10^{-4}$ s^3/(cm*g) for $T = 1.5$ K and $D = 2.2\kappa$ cm^2/s have been taken from (Nemirovskii, 2010) for D, from (Sciacca et al., 2008a) for γ_2, and from (Martin and Tough, 1983) for the ratio γ_1/γ_2.

i.e. $Lr^2 = \tilde{D}$. Of course, this value will not last very much, because in the absence of the driving heat flux, L will decay as

$$\frac{dL}{dt} = -\gamma_2 L^2 + D\nabla^2 L. \tag{5.50}$$

This decay process corresponds to stage D to A.

The paths followed by the vortex line density during increase and decrease of the heat flux will not be the same, which is the defining feature of hysteresis. From B to C the heat flux is no longer changed and diffusion plays a central role, by locally increasing the value of L through the propagation of a vortex front from the inner to the outer regions. From D to A (in the absence of the heat flux, i.e. for $\Gamma = 0$) turbulence decays and tangle disappears, in this stage the energy of the tangle decrease because it is turned into heat or, that is the same, internal energy of the fluid. This hysteresis cycle is analogous to those arising in magnetic systems, in which magnetization for increasing magnetic fields is different from that for decreasing magnetic fields. The role of the motion of magnetic domain walls, one of the reasons of magnetic hysteresis, would be played in our case by the propagation of a vortex front during the stage B to C. Along this stage, the region with higher L near the inner cylinder would propagate towards the outer cylinder as a finite-speed front.

The characteristic time τ_D of the diffusion process is of the order of $\tau_D^{-1} = D(\Delta r)^{-2}$,

with $\Delta r \equiv r_1 - r_0$, the separation between both cylinders of respective radii r_1 and r_0. Then the rate of increase of the heat flux (or of Γ) from A to B, should be faster than $\dot{\Gamma}/\Gamma = D(\Delta r)^{-2} \equiv \tau_D^{-1}$ in order that diffusion has no time enough to act, and the decrease of the heat flux from C to D should be sufficiently slower than this rate (in absolute value) for diffusion to have time enough to act.

A more realistic description of this possible hysteresis cycle should take into account that in order to go from the initial laminar regime (with $L = 0$) to the turbulent regime ($L \neq 0$), Γ should overcome a threshold value (in analogy with what is observed in counterflow along cylindrical tubes), instead of setting directly at $\Gamma = 0$, as in Figure 5.3.

The existence of such a threshold for Γ could be obtained from a more general equation than (5.42) as for instance:

$$\frac{dL}{dt} = \gamma_1 |\mathbf{q}| L^{\frac{3}{2}} - \gamma_2 L^2 - \frac{\gamma_3}{(\Delta r)^2} L + D\nabla^2 L + \nabla \cdot (\nu \mathbf{q}). \tag{5.51}$$

The third term has been added here in analogy with the extension of Vinen's equation proposed in (Mongiovì and Jou, 2005a) to account for a threshold in heat flux for transition to laminar-to-turbulent transition in counterflow along cylindrical tubes. From (5.50), the critical value of the heat flux required to go from laminar ($L = 0$) to turbulent ($L \neq 0$) situation is:

$$q^2 = \frac{\Gamma_{critic}^2}{r^2} = \frac{4\gamma_2\gamma_3}{\gamma_1^2 (\Delta r)^2}. \tag{5.52}$$

Because Γ_{critic} is proportional to r, it is higher at large distances from the hotter cylinder. From this follows, for instance, that vortices will fill the region where r is sufficiently small, i .e. for r smaller than Γ_{critic}/q. If this value of r is higher than the radius of the external cylinder, all the regions between the cylinders will be filled with vortices; if this value of r is intermediate between the radii of the internal and the external cylinders, only the region between the internal cylinder and this value of r will be filled with vortices.

This threshold would slightly modify the curves of Figure 5.3 by giving an horizontal part to the lower line from $\Gamma = 0$ to $\Gamma = \Gamma_{critic}$. For $\Gamma > \Gamma_{critic}$, the lower curve would generically increase as the curve AB in Figure 5.3. However, this would not essentially modify the generic possibility of the hysteresis cycle pointed out here.

5.4.4 Behaviour of the temperature profile

The temperature profile is another relevant quantity of the situation we are considering. The expression for $T(r)$ may be obtained by introducing in (5.41) the expressions for $q(r)$ and $L(r)$ found above. When the dependence of T is taken into account, the L

and T profiles become strongly coupled quantities, because the several coefficients in equations (5.41) and (5.42) depend on temperature. If, anyway, the gradients are small and the coefficients may be considered as approximately constant, the profile for T may be obtained from (5.41), which, for $\frac{\partial q}{\partial t} = 0$, takes the form

$$\zeta \frac{\partial T}{\partial r} = -\chi \frac{\partial L}{\partial r} - \frac{\zeta}{k} q - N_1 L q + N_2 L^{\frac{3}{2}}. \tag{5.53}$$

The terms with the coefficients N_1 and N_2 correspond to the friction between the normal component and the vortices. The term in $\chi \partial L/\partial r$ may be interpreted as the energy transported by the vortices which move from regions of higher L to those of lower L. Some of these vortices are destroyed in the latter regions and their energy becomes internal energy of the fluid. This would be the energetic aspect of vortex diffusion. We will not consider this problem in detail, because at this moment we will focus only on the simpler situation, but solving it is relevant for an understanding of heat transfer between both cylinders.

Since the thermal conductivity k is very high, the second term on the right-hand side may be neglected. Taking in mind equation (5.44), i.e. $L(r) = \overline{\gamma}^2 \frac{\Gamma^2}{r^2}$ with $\overline{\gamma}$ expressed by (5.45), and assuming that the heat flux $q = \Gamma/r$ goes from the inner cylinder to the outer one (see Figure 5.2-left), equation (5.53) becomes

$$\frac{\partial T}{\partial r} = \frac{\Gamma^3}{r^3} \left(-2 \frac{\chi}{\zeta} \frac{\overline{\gamma}^2}{\Gamma} - \frac{N_1}{\zeta} \overline{\gamma}^2 + \frac{N_2}{\zeta} \overline{\gamma}^3 \right), \tag{5.54}$$

in accordance with the properties of the heat transport in stationary He II, described by the well-known Gorter-Mellink law, $\partial T/\partial r \propto \frac{\Gamma^3}{r^3} = q^3$. Observe that the quantity in parenthesis depend on $\overline{\gamma}$, that assumes different values in the paths A-B and C-D in the Figure 5.3. This implies that to the hysteresis cycle in the line density L corresponds a hysteresis cycle for the temperature.

Note that in the linearized version of (5.53), the temperature profile would depend on r as r^{-2}, analogously to $L(r)$. This dependence is different from the one expected from Fourier's law; in this case, one would have $-k\frac{\partial T}{\partial r} = q$ and since $q = \Gamma/r$, a temperature profile of the form

$$T(r) = T(r_0) + \frac{\Gamma}{k} \log \left(\frac{r_0}{r} \right), \tag{5.55}$$

with r_0 the radius of the internal cylinder. Instead, the dominating influence of the friction terms in N_1 and N_2 in (5.53) leads to a much steeper decrease of T for increasing values of the radius r. This makes that, in a further analysis, the temperature dependence of the coefficients appearing in (5.43) and in (5.53) should be explicitly considered, leading to more complicated equations.

5.5 Vortex front propagation

In this section we study the propagation of a discontinuous vortex front as a consequence of vortex diffusion and vortex production. The concrete motivation is to study the fragment B-C of the hysteresis cycle presented in Section 5.4.3.

Consider the mentioned flow between two concentric cylinders. After a relatively fast process from A to B in Figure 5.3, one has everywhere the vortex density profile (5.46). From now on the heat flux is kept unchanged, and we want to study the transition from the profile (5.46) to the diffusion-influenced profile (5.44)–(5.45). We assume that the corresponding process is the propagation of a vortex front from the internal cylinder (highest contribution) to the external one (see Figure 5.2-right). Accordingly, the time to go from states B to C would correspond to such propagation process. Then, for $r < r_f(t)$, we consider L given by (5.44) whereas for $r > r_f(t)$, it is given by (5.46), with $r_f(t)$ being the position (radius) of the front. We want to describe how $r_f(t)$ evolves with time from $r_{internal}$ to $r_{external}$.

5.5.1 Propagation velocity

In one dimensional case, i.e. when the front propagates along the x-axis, the equation for the vortex line density has the form (Nemirovskii, 2011)

$$\frac{\partial L(x,t)}{\partial t} + \frac{\partial}{\partial x}(L(x,t)V_L) = D\frac{\partial^2 L(x,t)}{\partial x^2} + F(L(x,t)) \tag{5.56}$$

where the second term on the left-hand side is related to the drift of the vortex tangle as a whole due to polarization of vortex loops, and it was introduced for the first time in (van Beelen et al., 1988) and further explored in (Nemirovskii, 2011). The first term in the right-hand side is due to the diffusion of the vortices and the second one is the source term.

In the more simple situation, $F(L)$ must have the form of the source term in the classical Vinen's equation, i.e.

$$F(L) = \alpha_V |\mathbf{V}_{ns}| L^{\frac{3}{2}} - \beta_V \kappa L^2, \tag{5.57}$$

but it could be different (for instance, if velocity gradient terms act as a supplementary vortex source). The propagation velocity of the front will depend on the form of $F(L)$.

In principle, the quantity V_L is a very complicated functional of the whole vortex filaments configuration, independent of the vortex line density $L(x,t)$, however for slow hydrodynamic processes, it is routinely accepted that the equilibrium is established and all characteristics of the vortex tangles depends on the instantaneous value of the vortex line density $L(x,t)$, or, which is equally, on the relative velocity $\mathbf{V}_{ns}$. In particular a simple expression for V_L is:

$$V_L = \mathbf{v}_s + c_L I_L \mathbf{V}_{ns}, \tag{5.58}$$

where c_L and I_L are the so-called structure parameters of the vortex tangle, obtained (for counterflow turbulence) in (Schwarz, 1988). In (Sciacca et al., 2008b) the authors give a more general expression for V_L, that takes into account that the velocity of the vortices is not exact collinear with the counterflow velocity, but we use here the simple expression (5.58).

Following (Nemirovskii, 2011) one can look for a solution of (5.56) in a form of a steady propagating profile, i.e.

$$L(x,t) = L(x - Vt) = L(\eta), \tag{5.59}$$

with V the velocity of the front, we can write (5.56) as

$$-(V - V_L)\frac{\partial L}{\partial \eta} = D\frac{\partial^2 L}{\partial \eta^2} + F(L). \tag{5.60}$$

In a first moment one can consider $V = V - V_L$ and add the drift velocity in the final result and assume that far before the front (formally $\eta = \infty$) the vortices are absent, i.e. $L = 0$, and behind the front there is well developed turbulence and the vortex line density takes its equilibrium value.

In (Nemirovskii, 2011) was found numerically an eigenvalue for V, that is:

$$V = 0.8|\mathbf{V}_{ns}|\sqrt{D\frac{\alpha_V^2}{\beta_V \kappa}} = 0.8\sqrt{\frac{D}{\tau}}, \tag{5.61}$$

where τ has dimensions of time, and it characterizes the rate of change of the vortex line density. Reintroducing the drift velocity, one obtains

$$V = \left(-\frac{\rho_n}{\rho} + c_L I_L\right)|\mathbf{V}_{ns}| \pm 0.8|\mathbf{V}_{ns}|\sqrt{D\frac{\alpha_V^2}{\beta_V \kappa}}. \tag{5.62}$$

This last expression for V shows how to determine the speed of propagation of the front with the use of the characteristics of superfluid turbulence in the counterflowing helium II. This would be the propagation speed of the vortex front, in such a way that the characteristic time from state B to state C in Figure 5.3 would be given by the separation betwen the internal and the external cylinders divided by the average value of (5.62). These results can be extended to other cases, for example, rotating helium.

5.6 Non-local generalizations of Vinen equation and application to convergent channel

In this section we aim to generalize the evolution equation for L by including in it terms in $\nabla \mathbf{q}$, which, to our knowledge, have not been considered before by other authors.

The intuitive idea is that a gradient of the heat flux, and not only the heat flux, could contribute to the vortex production (or destruction). A generic possibility is to write

$$\frac{\partial L}{\partial t} + \nabla \cdot [L V_L] = \gamma_1 q L^{\frac{3}{2}} - \gamma_2 L^2 + \gamma' \mathbf{q} \cdot \nabla L + \gamma'' \mathcal{F}(\nabla \mathbf{q}) L + D \nabla^2 L, \tag{5.63}$$

where γ_1, γ_2, γ', γ'' and D are coefficients with suitable dimensions, while $\mathcal{F}(\nabla \mathbf{q})$ is a scalar functional of $\nabla \mathbf{q}$, as for instance $[(\nabla \mathbf{q}) : (\nabla \mathbf{q})]^{\frac{1}{2}}$ or $\hat{\mathbf{u}} \cdot (\nabla \mathbf{q}) \cdot \hat{\mathbf{u}}$, with $\hat{\mathbf{u}}$ the unit vector in a given direction, i.e. that of the heat flux $\mathbf{q}$ or that of the Schwarz vector $\mathbf{I}$, a characteristic vector introduced in (Schwarz, 1988), defined as in (2.101). As it is known, in Schwarz derivation of Vinen equation, the first term in the right hand size of equation (5.63) is substituted with $\gamma \mathbf{q} \cdot \mathbf{I} L^{\frac{3}{2}} = \gamma I_0 q L^{\frac{3}{2}}$ (Schwarz, 1988). From a mathematical point of view, the presentation in terms of $\mathbf{I} \cdot \mathbf{q}$ rather than in terms of the modulus of $\mathbf{q}$ is more elegant, and it is more convenient as a starting point for our analysis in this section.

The diffusion term in D and the term in γ' were just considered above from a thermodynamic point of view. In this section we focus our attention on the term in γ'', that describes the role of the heat gradient as vortex source. In the well known Vinen equation, the vortex source is considered to be related to heat flux modulus $|\mathbf{q}| = q$ but independent of heat gradients (which in the two fluid model are related to gradients of the counterflow velocity). However the heat flux gradients are expected to act as natural source of vorticity, and therefore of vortex lines, in addition to the usual term in γ_1.

In this section we consider several different ways of generalizing Schwarz-Vinen equation with diffusion effects, namely:

$$\frac{dL}{dt} = \tilde{\alpha} \mathbf{V}_{ns} \cdot \mathbf{I} L^{\frac{3}{2}} - \beta_V \kappa L^2 + D \nabla^2 L \tag{5.64}$$

in the presence of $\nabla \mathbf{V}_{ns}$ and ∇L. Here we use the counterflow speed $\mathbf{V}_{ns}$ rather than $\mathbf{q}$ (that has been introduced in (5.63)) because it is more well known, in the context of two-fluid model of turbulence. In the one-fluid model, using $\mathbf{q}$ instead of $\mathbf{V}_{ns}$ seems more natural and more closely related to observational quantities. Anyway, since in counterflow $\mathbf{q} = \rho_s s T \mathbf{V}_{ns}$, going from one formalism to the other is not difficult. In the following of this section we will use $\mathbf{V}$ rather than $\mathbf{V}_{ns}$ for the sake of simplicity.

Diffusion effects are the most direct and intuitive non-local contribution to the dynamics of the vortices, but other non-local effects may appear, related to the production or destruction of vortices, as seen in (5.63). We will proceed our exploration in a systematic way. First, we will expand up to second order in $L^{-1/2}$ (the average distance among vortex lines) the production and destruction terms in Vinen equation. Second, we will incorporate other possible terms following from dimensional analysis.

We assume, for the sake of simplicity, that the effects of the temperature gradient are much less than the effects of the gradients of $\mathbf{V}$ and L, so that they can be neglected.

5.6.1 Series expansion of the production and destruction terms

Taking into account that the average separation δ between vortex lines in the tangle is of the order of $L^{-\frac{1}{2}}$, it may be expected that the creation and destruction processes will be affected by inhomogeneities of $\mathbf{V}$ and L, because vortices from $x-\delta$ and from $x+\delta$ will collide with vortices at x, and, therefore, their effects should be considered, instead of considering only the interactions of vortices already at x. The non-local contributions will be specially relevant for small values of L, where the mean free path $\delta = L^{-\frac{1}{2}}$ is long.

The expansion up to second order in $d\mathbf{x} = L^{-1/2}\hat{\mathbf{u}}$ (with $\hat{\mathbf{u}}$ an arbitrary unit vector) of the creation term $\tilde{\alpha}\mathbf{V}_{ns}\cdot\mathbf{I}L^{\frac{3}{2}}$ of (5.64) is given by:

$$\begin{aligned}\left[\frac{\partial L}{\partial t}\right]_{prod} &= \tilde{\alpha}\Big\{\mathbf{V}\cdot\mathbf{I}L^{\frac{3}{2}} + L\hat{\mathbf{u}}\cdot[(\nabla\mathbf{V})\cdot\mathbf{I} + \mathbf{V}\cdot(\nabla\mathbf{I})] \\ &+ \frac{1}{2}L^{\frac{1}{2}}\hat{\mathbf{u}}\cdot[(\nabla(\nabla\mathbf{V}))\cdot\mathbf{I} + 2\nabla\mathbf{V}:\nabla\mathbf{I} + \mathbf{V}\cdot(\nabla(\nabla\mathbf{I}))]\cdot\hat{\mathbf{u}} \\ &+ (\mathbf{V}\cdot\mathbf{I})\left[\frac{3}{2}\hat{\mathbf{u}}\cdot\nabla L + \frac{3}{8}L^{-\frac{3}{2}}|\nabla L|^2 + \frac{3}{4}L^{-\frac{1}{2}}\nabla^2 L\right] \\ &+ \frac{3}{2}L^{-\frac{1}{2}}[\mathbf{I}\cdot(\nabla\mathbf{V})\cdot\nabla L + \mathbf{V}\cdot(\nabla\mathbf{I})\cdot\nabla L]\Big\}. \end{aligned} \tag{5.65}$$

On the other side the destruction term $\beta_V\kappa L^2$ of (5.64) is approximated by:

$$\left[\frac{\partial L}{\partial t}\right]_{destr} = \beta_V\kappa\left\{L^2 + 2L^{\frac{1}{2}}\hat{\mathbf{u}}\cdot\nabla L + L^{-1}|\nabla L|^2 + \nabla^2 L\right\}. \tag{5.66}$$

Thus, a non local extension of (5.64) is obtained substituting to Schwarz-Vinen original production and destruction terms the expressions (5.65) and (5.66).

Assuming $\mathbf{V}$ and $\mathbf{I}$ collinear and $\mathbf{I}$ constant, a non-local hydrodynamical extension of equation (5.64) would be

$$\begin{aligned}\frac{\partial L}{\partial t} &= \tilde{\alpha}I\left[VL^{\frac{3}{2}} + L\hat{\mathbf{u}}\cdot(\nabla\mathbf{V})\cdot\hat{\mathbf{u}} + \frac{1}{2}L^{\frac{1}{2}}\hat{\mathbf{u}}\cdot[\nabla(\nabla\mathbf{V})]\cdot\hat{\mathbf{u}}\right. \\ &+ \left.\frac{3}{2}V\hat{\mathbf{u}}\cdot\nabla L + V\left(\frac{3}{8}L^{-\frac{3}{2}}|\nabla L|^2 + \frac{3}{4}L^{-\frac{1}{2}}\nabla^2 L\right) + \frac{3}{2}L^{-\frac{1}{2}}\hat{\mathbf{u}}\cdot\nabla\mathbf{V}\cdot\nabla L\right] \\ &- \beta_V\kappa\left[L^2 + 2L^{\frac{1}{2}}\hat{\mathbf{u}}\cdot\nabla L + L^{-1}|\nabla L|^2\right] + (D - \beta_V\kappa)\nabla^2 L. \end{aligned} \tag{5.67}$$

Here, we want to consider situations where the heat flux has approximately only one component and depends only on one coordinate. This is the case of radial flows, in an exact sense, and of convergent channels in an approximate sense. In this simplified

situation one is $\mathbf{V} = V\hat{\mathbf{x}}$, $\mathbf{I} = I\hat{\mathbf{x}}$, the previous equation becomes

$$\begin{aligned}\frac{\partial L}{\partial t} &= \tilde{\alpha} I \left\{ V L^{\frac{3}{2}} + \frac{\partial V}{\partial x} L + \frac{1}{2} L^{\frac{1}{2}} \frac{\partial^2 V}{\partial x^2} + \frac{3}{2} L^{-\frac{1}{2}} \frac{\partial V}{\partial x} \frac{\partial L}{\partial x} \right. \\ &+ \left. V \left[\frac{3}{2} \frac{\partial L}{\partial x} + \frac{3}{8} L^{-\frac{3}{2}} \left(\frac{\partial L}{\partial x} \right)^2 + \frac{3}{4} L^{-\frac{1}{2}} \frac{\partial^2 L}{\partial x^2} \right] \right\} \\ &- \beta_V \kappa \left[L^2 + 2L^{1/2} \frac{\partial L}{\partial x} + L^{-1} \left(\frac{\partial L}{\partial x} \right)^2 \right] + (D - \beta_V \kappa) \frac{\partial^2 L}{\partial x^2}. \end{aligned} \tag{5.68}$$

To these terms still other terms could be added in principle. Note that a much simpler equation than this one was proposed by Gueurst in (Geurst, 1989, 1992; Geurst and van Beelen, 1994), by incorporating only the term in $L^{-1}(\partial L/\partial x)^2$ and the diffusion term in $D(\partial^2 L/\partial x^2)$ as additional contributions to the Vinen equation. Our expression is more general and systematic.

Thus, equation (5.68) is a simple and direct implementation of an evolution of L starting from Vinen equation, but other kinds of term not coming from such a non-local extension may also contribute, in principle, to such non-local extension.

Dimensional analysis and additional non-local terms

On dimensional grounds one may directly incorporate to (5.64) terms depending on ∇L and on $\nabla \mathbf{V}$, up to second order, and requiring that they have the correct physical dimensions. Later on, one must consider their physical meaning, their compatibility with the second law of thermodynamics, their agreement or lack of agreement with experimental observations, and their microscopic bases.

Up to this order, a simple generalization is:

$$\frac{dL}{dt} = \alpha_V V L^{\frac{3}{2}} - \beta_V \kappa L^2 + D\nabla^2 L - \chi_1 \mathbf{V}\cdot\nabla L - \chi_2 \frac{V^2}{\kappa L} |\nabla L|^2 - \chi_3 L \left[(\nabla \mathbf{V}) : (\nabla \mathbf{V}) \right]^{\frac{1}{2}}, \tag{5.69}$$

where we have put $\tilde{\alpha} I = \alpha_V$, and where we have chosen, for the functional $\mathcal{F}(\nabla \mathbf{V})$, the expression $\chi_3 L \left[(\nabla \mathbf{V}) : (\nabla \mathbf{V}) \right]^{\frac{1}{2}}$. This term will be a production term (if $\chi_3 < 0$) or a destruction term (if $\chi_3 > 0$) and it is due to the inhomogeneity of the flow and in $\mathbf{V}$. When it is expressed in terms of $\mathbf{q}$, it plays a role analogous to the term in γ'' in

(5.63). Thus, a possible generalized non-local equation should be

$$\begin{aligned}
\frac{\partial L}{\partial t} &= \alpha_V V L^{\frac{3}{2}} - \beta_V \kappa L^2 - 2\beta_V \kappa L^{\frac{1}{2}} \hat{\mathbf{u}} \cdot \nabla L \\
&+ \left(D - \beta_V \kappa + \frac{3}{4} \alpha_V V L^{-\frac{1}{2}} \right) \nabla^2 L \\
&- \left(\beta_V \kappa \frac{1}{L} - \chi_2 \frac{V^2}{\kappa L} + \frac{3}{8} \alpha_V V L^{-\frac{3}{2}} \right) |\nabla L|^2 \\
&+ \left(\frac{3}{2} V \hat{\mathbf{u}} - \chi_1 \mathbf{V} \right) \cdot \nabla L + \frac{3}{2} L^{-\frac{1}{2}} \hat{\mathbf{u}} \cdot \nabla \mathbf{V} \cdot \nabla L \\
&- \chi_3 \left[(\nabla \mathbf{V}) : (\nabla \mathbf{V}) \right]^{\frac{1}{2}} L + \alpha_V L \hat{\mathbf{u}} \cdot (\nabla \mathbf{V}) \cdot \hat{\mathbf{u}} \\
&+ \frac{1}{2} \alpha_V L^{\frac{1}{2}} \hat{\mathbf{u}} \cdot [\nabla (\nabla \mathbf{V})] \cdot \hat{\mathbf{u}}. \qquad (5.70)
\end{aligned}$$

5.6.2 Application to averaged one-dimensional description of convergent channels

The situation that we are considering, is represented in Figure 5.4. A constant heat flow $\dot{Q}$ is imposed in the direction of x-axis, r indicates the width of the channel and it depends on the position x, while the thickness h of the channel is considered constant.

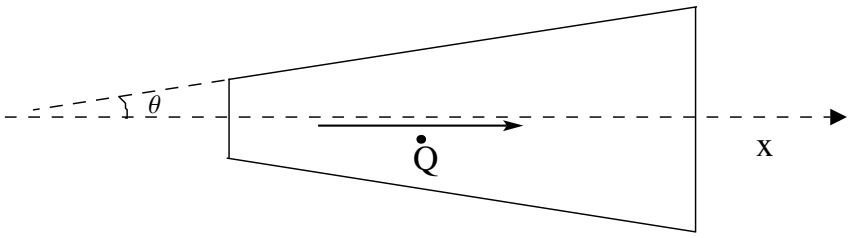

Figure 5.4: A constant heat $\dot{Q}$ is imposed in the x-direction. The channel has a constant height h, and a variable width $r(x) = \theta x$, where θ is the slope of the walls with respect to the axis of the channel. Then $\dot{Q} = \frac{Q_1 r_1}{r(x)}$.

In this situation, one has from the energy balance equation

$$q(x) h r(x) = \overline{A} \dot{Q}, \qquad (5.71)$$

with $\overline{A}$ constant, and therefore

$$q(x) = \frac{\overline{A} \dot{Q}}{h r(x)} = \frac{A'}{r(x)}, \qquad (5.72)$$

where $A' = \frac{\overline{A}\dot{Q}}{h}$ is constant. Because in counterflow it is $q = \rho_s T s V$ we obtain also

$$V(x) = \frac{\overline{B}}{r(x)}, \tag{5.73}$$

where $\overline{B} = A'/(\rho_s T s)$.

Since in (5.70) there are many terms, we begin by considering them independently: we will separately consider term in ∇L, in $\nabla L \cdot \nabla L$, in $\nabla^2 L$, and terms containing $\nabla \mathbf{V}$, $\nabla(\nabla \mathbf{V})$ and $\nabla \mathbf{V} \cdot \nabla L$, in order to understand their physical consequences in a given physical situation, which is a necessary step to propose suitable experiments to check the equations. According with Vinen equation, line density L, at each point x, should be given by:

$$L(x) = \left(\frac{\alpha_V}{\beta_V \kappa}\right)^2 V^2(x), \tag{5.74}$$

with the local counterflow velocity $V(x)$ dependent on x as in (5.73). Local perturbations, due to the presence of these terms, with respect to Vinen's prediction shall be analyzed in detail. In particular, we will assume that the opening angle θ is relatively small, and determine the several terms that must be added to the classical expression (5.74) for L, in terms of θ and x (or θ and r).

Different contributions of additional terms one by one

In the following we consider some of the additional terms in the equation (5.70) one by one.

- *Only a term in* ∇L

  We will start with a term in ∇L (ignoring all the other terms), as in the following expression,

  $$\frac{\partial L}{\partial t} = \alpha_V V L^{\frac{3}{2}} - \beta_V \kappa L^2 - \chi_1 \mathbf{V} \cdot \nabla L. \tag{5.75}$$

  In the steady state, if one considers a perturbation L' of the homogeneous solution of (5.75), L_h given by $L_h = (\alpha_V/\beta_V\kappa)^2 V^2(x)$, namely $L = L_h(x) + L'$, one would have, from the linearized version of (5.75),

  $$\frac{3}{2}\alpha_V V L_h^{\frac{1}{2}} L' - 2\beta_V \kappa L_h L' = \pm \chi_1 V \frac{\partial L_h}{\partial x}, \tag{5.76}$$

  where for sake of simplicity we have assumed L' independent of x. Note that the sign of the term in the right-hand side will depend on whether heat flux goes to the right of Figure 5.4 (positive sign) or it goes to the left (negative sign).

Then, one obtains

$$L' = \pm 2\frac{\chi_1}{\alpha_V V}\frac{\beta_V\kappa}{\alpha_V}\frac{\partial}{\partial x}\left[\left(\frac{\alpha_V}{\beta_V\kappa}\right)^2 V^2\right] = \pm 4\frac{\chi_1}{\beta_V\kappa}\frac{\partial V}{\partial x} = \mp 4\frac{\chi_1}{\beta_V\kappa}\frac{\overline{B}\theta}{r^2}, \tag{5.77}$$

where from Figure 5.4 we have found $\frac{\partial V}{\partial x} = -\frac{\overline{B}\theta}{r^2}$.

- *Only a term in* $|\nabla L|^2$

  A second contribution in order to modify Vinen equation can be the following

$$\frac{\partial L}{\partial t} = \alpha_V V L^{\frac{3}{2}} - \beta_V\kappa L^2 - \chi_2\frac{V^2}{\kappa L}|\nabla L|^2. \tag{5.78}$$

  In this case, one obtains

$$L' = -8\frac{\chi_2}{\beta_V\kappa^2}\left(\frac{\partial V}{\partial x}\right)^2 = -8\frac{\chi_2}{\beta_V\kappa^2}\frac{\overline{B}^2\theta^2}{r^4}. \tag{5.79}$$

- *Only a term in* $\nabla^2 L$

  Adding only a term proportional to $\nabla^2 L$, one has

$$\frac{\partial L}{\partial t} = \alpha_V V L^{\frac{3}{2}} - \beta_V\kappa L^2 + D\nabla^2 L, \tag{5.80}$$

  and then:

$$L' = 4\frac{D}{\beta_V\kappa}\frac{1}{V^2}\left[\left(\frac{\partial V}{\partial x}\right)^2 + V\frac{\partial^2 V}{\partial x^2}\right] = 4\frac{D}{\beta_V\kappa}\frac{3\theta^2}{r^2}. \tag{5.81}$$

- *Only a term in* $[\nabla\mathbf{V} : \nabla\mathbf{V}]^{\frac{1}{2}}$

  Adding only the term in $[\nabla\mathbf{V} : \nabla\mathbf{V}]^{\frac{1}{2}}$, or equivalently the term in $\hat{\mathbf{x}} \cdot (\nabla\mathbf{V}) \cdot \hat{\mathbf{x}}$, that in this case leads to the same result, one has

$$\frac{\partial L}{\partial t} = \alpha_V V L^{\frac{3}{2}} - \beta_V\kappa L^2 - \chi_3 L[\nabla\mathbf{V} : \nabla\mathbf{V}]^{\frac{1}{2}}, \tag{5.82}$$

  and then:

$$L' = -2\frac{\chi_3}{\beta_V\kappa}\frac{\partial V}{\partial x} = 2\frac{\chi_3}{\beta_V\kappa}\frac{\overline{B}\theta}{r^2}. \tag{5.83}$$

- *Only the term in* $\hat{\mathbf{x}} \cdot [\nabla(\nabla\mathbf{V})] \cdot \hat{\mathbf{x}}$

  Adding only the term in $\hat{\mathbf{x}} \cdot [\nabla(\nabla\mathbf{V})] \cdot \hat{\mathbf{x}}$, one has

$$\frac{\partial L}{\partial t} = \alpha_V V L^{\frac{3}{2}} - \beta_V\kappa L^2 + \frac{1}{2}\alpha_V L^{\frac{1}{2}}\hat{\mathbf{x}} \cdot [\nabla(\nabla\mathbf{V})] \cdot \hat{\mathbf{x}}, \tag{5.84}$$

  and then:

$$L' = \frac{1}{V}\frac{\partial}{\partial x}\left(\frac{\partial V}{\partial x}\right) = 2\frac{\theta^2}{r^2}. \tag{5.85}$$

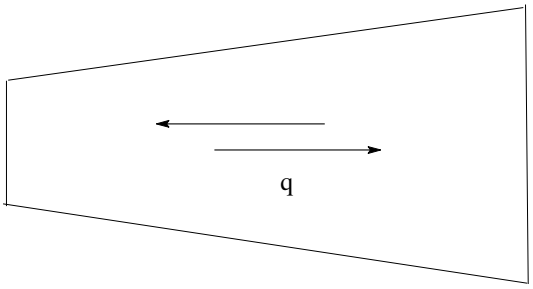

Figure 5.5: Heat flux along x-axis in a channel with varying transversal section. In steady states, the change in the transversal area implies a corresponding change of the average heat flux across the section.

- *Only the term in* $\hat{\mathbf{x}} \cdot \nabla \mathbf{V} \cdot \nabla L$

  Adding only the term in $\hat{\mathbf{x}} \cdot \nabla \mathbf{V} \cdot \nabla L$, one has

$$\frac{\partial L}{\partial t} = \alpha_V V L^{\frac{3}{2}} - \beta_V \kappa L^2 + \frac{3}{2} L^{-\frac{1}{2}} \hat{\mathbf{x}} \cdot \nabla \mathbf{V} \cdot \nabla L, \tag{5.86}$$

  and then:

$$L' = \frac{6}{\alpha_V V^2} \left(\frac{\partial V}{\partial x} \right)^2 = 6 \frac{\theta^2}{\alpha_V r^2}. \tag{5.87}$$

Final result

The final result of this analysis would be that the perturbation with respect to Vinen's solution would have the form

$$L' = \pm 4 \frac{\chi_1}{\beta_V \kappa} \frac{\overline{B}\theta}{r^2} - 8 \frac{\chi_2}{\beta_V \kappa^2} \frac{\overline{B}^2 \theta^2}{r^4} + 4 \frac{D}{\beta_V \kappa} \frac{3\theta^2}{r^2} + 2 \frac{\chi_3}{\beta_V \kappa} \frac{\overline{B}\theta}{r^2} + 2 \frac{\theta^2}{r^2} + 6 \frac{\theta^2}{\alpha_V r^2}. \tag{5.88}$$

Other terms can be added choosing other different additional terms.

Note the possible signs of the first term, which could lead heat rectification in convergent or divergent channels. Since $\overline{B}$ depends in $\dot{Q}$ and h, and r depends on x, we have obtained $L'(\dot{Q}, h, \theta, x)$. The parameter β_V is known from steady-state homogeneous situations. Coefficients χ_1, χ_2, χ_3, α_V and β_V may be obtained and checked.

In particular, we can observe in Figure 5.5 (where we have represented the longitudinal section of a channel) that the heat flux density $\mathbf{q}$ will be higher in the narrow transversal section than in the wide transversal section, since the total heat flow in the steady state must be homogeneous.

5.7 Remarks

In this chapter we have generalized a previous thermodynamic derivation of non-local effects in inhomogeneous vortex tangles (Mongiovì and Jou, 2007). The two main contributions have been the incorporation of non-local terms in the evolution equation (5.16) for the heat flux (namely, the terms in β_2 and ξ_2) and in the evolution equation for vortex line density (5.17).

In Section 5.2.3 we have proposed an experiment in which the contribution of ∇L to the heat flux could be checked and observed. This would be a typical effect of inhomogeneous vortex tangles and, to our knowledge, has not yet been searched for. Thus, it is seen that inhomogeneous vortex tangles may exhibit new physical effects which have not received attention up to now, but which could clarify the role of vortices in energy transfer.

In Sections 5.3–5.4 we have focused our attention on radial turbulent counterflows in He II between two concentric cylindrical walls, a situation which, up to now, has not yet received experimental attention, in contrast to the turbulence between two concentrical walls at the same temperature but with different rotation speeds. The situation studied here is characterized by inhomogeneous heat flux, dependent on the radius, and therefore provides a simple and promising situation for the analysis of inhomogeneous tangles. We have considered that inhomogeneities in L may contribute not only to vortex diffusion but also to vortex creation.

Furthermore we have shown vortex diffusion to increase the local values of vortex line density, because of a diffusive vortex flow from hotter to colder cylinder. Here we have focused our attention on the behavior of L described by (5.42), under a steady heat flux, described by equation (5.40). The influence of D on the L profile has been explicitly shown in (5.45). In particular, in Section 5.4.3 we have explored the possibility of hysteresis under a relative fast increase of heat flux followed by a slow decrease of it. To our knowledge, the physical situation considered here has not yet been explored experimentally. It would be an interesting situation for the analysis of vortex diffusion, easier than in a flow along a cylindrical channel from a practical point of view.

In Section 5.6 we have generalized in a systematic way the Vinen equation up to second-order in non-local terms, in order to identify all possible contributions. We have applied such equation to the analysis of vortex-density distribution in helium flow along convergent channels in terms of the total heat flow, the opening angle, and the position along the channel.

In the future we aim to compare our theoretical predictions (5.88) to the experimental observations carried our some years ago in convergent (or divergent) channels (Castiglione et al., 1995; Kafkalidis et al., 1994a,b; Klinich III et al., 1997; Tough et al., 1994); this would allow to obtain information on the several coefficients appearing in

(5.88). In fact, to identify in detail such coefficients one should enlarge the mentioned experiments by considering channels with different opening angles, and with different width and thickness. It would also be interesting to explore whether heat rectification effects are observed in convergent channels. On the other side, it would be interesting to implement the microscopic analysis by Kondaurova and Nemirovskii (Kondaurova and Nemirovskii, 2012) for the decay of a vortex tangle by vortex diffusion to the walls to the situation mentioned here, where vortices appear in one wall and disappear in the opposite wall.

Some results of this chapter are published in:

- L. Saluto, D. Jou and M. S. Mongiovì, *Thermodynamic approach to vortex production and diffusion in inhomogeneous superfluid turbulence*,
  Physica A **406** 272–280 (2014), DOI 10.1016/j.physa.2014.03.062
- L. Saluto, M. S. Mongiovì and D. Jou, *Vortex diffusion and vortex-line hysteresis in radial quantum turbulence*,
  Physica B **440C** 99–103 (2014), DOI 10.1016/j.physb.2014.01.041
- L. Saluto and M. S. Mongiovì, *Inhomogeneous vortex tangles in superfluid turbulence: flow in convergent channels*,
  submitted to CAIM, Special Session: Constitutive Equations for Heat Conduction in Nanosystems and Non-equilibrium Processes.

Conclusions

At the end of each chapter we have discussed in detail the respective results. Here, we will summarize the ten main results, from a general perspective. We will also point out the open problems suggested by this thesis and will recall the publications that have stemmed from it.

Main results

- In Chapter 1, we have build up a *macroscopic model to describe the behaviour of liquid ^{4}He above and below the lambda-transition line, under pressure and in the presence of heat flux.* We have worked in a non-equilibrium thermodynamic framework, choosing as fundamental fields the heat flux $\mathbf{q}$ in addition to the mass, momentum and energy densities, and introducing as a new internal variable a scalar function f, linked to the modulus of the wave function of the condensate by the equation (1.2) and which is the geometrical mean between the total density of the fluid and that of the superfluid component and is used as the order parameter of this transition. The original aspect is considering the effect of $\mathbf{q}$ on the transition, and, reciprocally, the influence of the transition on the thermal conductivity and the heat flux relaxation time.

- In Chapter 2 we recalled the *basic equations for the study of superfluid helium in presence of turbulence* in the two frameworks of the two-fluid model and the one-fluid model, comparing the two models. The main contributions have been the *incorporation of non-local terms* in the evolution equation for the heat flux, and a detailed discussion of the physical meaning of the several terms, also from a microscopic point of view.

- In Chapter 3 it has been seen that *the presence of a sufficiently high vortex line density makes that the velocity profile of the normal component in counterflow turbulence becomes very flat in the central region.*

  Thus, to ascertain whether a flat velocity profile truly corresponds to a turbulent state, it is necessary to be sure that the vortex line density is not high enough to explain by itself the flat form of the profile.

  Furthermore we reported analogous results for the normal fluid velocity introduced in the one-fluid model. Through the comparison between the experimental data for the relative velocity of the superfluid, i.e. $\mathbf{V}_{ns}$, and the results obtained in our model for the velocity $\mathbf{U}_{ns}$, we show how the results of the one-fluid model agree with experimental data.

- In Section 3.3 we have shown that *the viscous contribution of the normal component of helium II to the thermal resistance in counterflow along a cylindrical channel* in the superfluid turbulent regime *may be considerably higher than the classical Landau estimation.* This is due to the fact that in presence of vortices the normal velocity profile becomes flat at the center and steep near the walls, in such a way that it is considerably different than

the Poiseuille parabolic profile, which is used to derive the well-known Landau estimation of the helium II thermal resistance. It may be one or two orders of magnitude higher than the expected Landau contribution, in the partially developed **TII** turbulent regime.

- In Section 3.4 we have analized *the particular situation in which the radius of the channel becomes comparable or smaller than the phonon mean free path.* In this case, the non-slip boundary condition for the velocity could break down, and *a slip flow along the walls is expected to arise. This implies a reduction of the thermal resistance.* This may be of special interest for the analysis of heat or mass transfer in porous media, with very thin channels or at low temperatures, because below 1 K the phonon mean free path becomes of the order of 100 μm.

- In Chapter 4 we have explored in detail the main physical features of the so-called *entrance region*, i.e. the region where the heat flux profile or the velocity profile has not yet reached the asymptotic form independent of the position along the channel. Furthermore, we have estimated *the relative influence of this region on the effective thermal conductivity of helium II in relatively short channels.* In these situations, the radial heat flow cannot be neglected, besides the longitudinal heat flow.

  We have determined some particular stationary solutions of the heat flux equation in a semi-infinite cylindrical channel filled with turbulent superfluid helium, under several boundary conditions, as for instance constant temperature and zero heat flux on the lateral walls of the channel, in order to simulate a channel, filled with superfluid helium, contained in a vessel with constant homogeneous temperature on the lateral walls.

- In Chapter 5 we have reexamined and generalized a previous thermodynamic derivation of *non-local effects in inhomogeneous vortex tangles.* In particular, we have considered *three main effects: vortex diffusion, the coupling of a gradient in vortex line density with the heat flux, and the influence of non-local terms on the vortex production rate.* The two latter effects have been considered here for the first time. We have proposed an experiment in which the contribution of ∇L to the heat flux could be checked and observed. This would be a typical effect of inhomogeneous vortex tangles.

- In Sections 5.3–5.4 we have focused our attention on *radial turbulent counterflows* in He II between two concentric cylindrical walls, a situation which, up to now, has not yet received experimental attention, in contrast to the turbulence between two concentrical walls at the same temperature but with different rotation speeds. The situation studied here is characterized by *inhomogeneous heat flux, dependent on the radius*, and therefore provides a useful benchwork for the analysis of inhomogeneous tangles. Furthermore, we have shown that the influence of diffusion contribution to the steady-state vortex line distribution has a different dependence on the heat flux that the influence of non-local contribution to vortex production.

- In *radial turbulent counterflow vortex diffusion is shown to increase the local values of vortex line density*, because of a diffusive vortex flow from hotter to colder cylinder. We have considered the *possibility of hysteresis* under a relative fast increase of heat flux followed by a slow decrease of it. To our knowledge, the physical situation considered here has not yet been explored experimentally.

- We have *generalized the Vinen equation in a systematic way to incorporate all possible second-order non-local contributions*, and we have applied it to radial heat flows and to heat flow in convergent (or divergent) channels. In particular, the relative direction of

the heat flux with respect to the narrowing direction could have an influence on the vortex line density; this could lead to so-called heat rectification in such geometries, thus allowing to extend the ideas of the so-called "phononics" to superfluid helium. Finally, we have analized the several physical consequences of the generalized equation to the vortex density distribution of helium flow in *convergent channels*, in terms of the divergence angle, the value of the total heat flow, and the position along the channel.

Main open problems

Our thesis has been a first detailed exploration of the normal velocity profile and heat flux profile. However, the problem is much wider and complex than the situations we have been able to deal with. From this point of view, the main drawback of our thesis has been to consider situations with constant (homogeneous) vortex line density in Chapters 3 and 4, and studying its influence on heat flux profile. This is of course interesting and non-trivial, but it is much desirable to go beyond this and to consider the detailed coupling between inhomogeneous vortex line densities and inhomogeneous heat fluxes. To some extent, we have already begun this approch in the last chapter, especially in radial heat flows.

In science, every limitation of one work is a source of inspiration for future works. This is a stimulus to mention some of the future works that could be done as a future prolongation of this thesis.

- Concerning the role of a heat flux on the superfluid transition, would be of interest to generalize the model presented in Chapter 1, to describe also phenomena as the vortex formation when the imposed heat flux is sufficiently high and the successive establishment of superfluid turbulence. It is known indeed that a sufficiently high value of the heat flux q destroys superfluidity, i.e. determines a shift of the transition, by creating a high number of quantized vortices, in analogy with what happens in a superconductor when a magnetic field higher than a critical value H_c is applied.

  Another factor which could modify the superfluid transition is a rotation of the fluid. If helium I is in a cylindrical container rotating with angular velocity Ω, the *lambda*-temperature would also be lowered. In fact, there is a strong analogy between Ω in a superfluid and H in a superconductor (even stronger than the analogy between $\mathbf{q}$ and H), because Ω produces ordered vortices. An analogous analysis to that carried out here in the presence of $\mathbf{q}$ could be carried out for Ω.

- The hypothesis of no matter flow along the channel has been made. This is not an abstract mathematical simplification, but it corresponds to the well characterized and widely studied counterflow situation. For instance, if the channel is closed at both ends, there may be a heat flow but not a matter flow along it. This hypothesis should be removed, to better describing the use of superfluid helium as cryogenic refrigerant in industry, by means of the flow of helium along tubes through the system that should be refrigerated. From a theoretical point of view, the interaction between a radial heat transfer and a longitudinal mass transfer would be especially challenging, because both effects may produce vortex tangles which will interact with each other.

- Though the laminar and the fully developed regimes are well known, the transition between them is still an open topic. In particular, the topic of the modifications of Landau expression for thermal conductivity in short channels is not very well known. In practical situations, in order that the effects of the entrance region on the thermal conductivity may be neglected and Landau formula be valid, it is needed that the length of the tube

is at least some 10 or 20 times the *entrance length*, in order that the well developed region truly dominates over the entrance region. Thus, the strict validity of the Landau formula requires considerably long tubes. This happens not only for the laminar regime, but also for the turbulent regime. The analysis of the so-called "entrance region" is a difficult mathemathical and physical problem. However, its study is unavoidable, because in many actual counterflow experiments the length of the channels is only twice or three times the length of the entrance regions. Despite of this, all the theoretical analyses we are aware of ignore the effects of the entrance region and assume that the asymptotic regime is valid everywhere along the channel.

In the future, we also plan to study the interaction between entrance effects and superfluid turbulence, namely, how the strong gradient in velocity found in the entrance region may act as a supplementary source of vortex lines.

- Some other topics for future research could be, for instance, whether the critical velocity for instability of the laminar state, could be different in the entrance region than in the asymptotic region; or whether some vortices could be formed there, but which would disappear in the asymptotic region. Furthermore, the analysis of situations where the flow of the normal components becomes also turbulent is a relevant open topic. To analize the interaction between classical turbulence of normal component and quantum turbulence of superfluid component is an experimental and theoretical challenge.

- Comparison with experiments should include analysis of the convergent and divergent flows. We have found a very general equation for vortex line density including the several different kinds of second-order admissible term. The consistency with experiments and with the second law of thermodynamics should be checked.

- Comparison of mechanical and hydrodynamical effects of quantum superfluid vortices in Helium with quantum electromagnetic vortices in superconductors would be another interesting topic in the future. Instead of the quantization of vorticity, one has quantization in the magnetic flux. These vortices are often pinned at the walls of superconductor layers. One could then take a thin layer of supefluid He II between two parallel walls; make it rotate to produce an array of vortices perpendicular to the layer; and study their effects on the flow of superfluid, in analogy to previous works on the mechanical effects on electromagnetic vortices. (Maruszewski, 2007, 2008a; Maruszewski et al., 2007, 2012).

The publications have been:

- L. Saluto, M. S. Mongiovì and D. Jou, *Longitudinal counterflow in turbulent liquid helium: velocity profile of the normal component*,
Z. Angew. Math. Phys. **65** 531–548 (2014), DOI 10.1007/s00033-013-0372-7

- M.S. Mongiovì and L. Saluto, *A model of λ transition in liquid ^4He*,
Meccanica **49** 2125–2137 (2014), DOI 10.1007/s11012-014-9922-0

- L. Saluto, D. Jou and M. S. Mongiovì, *Thermodynamic approach to vortex production and diffusion in inhomogeneous superfluid turbulence*,
Physica A **406** 272–280 (2014), DOI 10.1016/j.physa.2014.03.062

- L. Saluto, M. S. Mongiovì and D. Jou, *Vortex diffusion and vortex-line hysteresis in radial quantum turbulence*,
Physica B **440C** 99–103 (2014), DOI 10.1016/j.physb.2014.01.041

- L. Saluto, D. Jou and M. S. Mongiovì, *Contribution of the normal component to the thermal resistance of turbulent liquid helium*,
  Z. Angew. Math. Phys. (2015), DOI 10.1007/s00033-015-0493-2
- L. Saluto, *Stationary heat flux profile in turbulent helium II in a semi-infinite cylindrical channel*,
  Bollettino di Matematica Pura e Applicata **Vol. V** 133–144 (2012), Aracne Ed.
- L. Saluto and D. Jou, *Effective thermal conductivity of superfluid helium in short channels*,
  Bollettino di Matematica Pura e Applicata **Vol. VI** 153–163 (2013), Aracne Ed.
- L. Saluto, *Nonlocal model of Superfluid Turbulence: Constitutive Theory*,
  Bollettino di Matematica Pura e Applicata **Vol. VI** 165–175 (2013), Aracne Ed.
- L. Ardizzone and L. Saluto, *Propagation of plane and cylindrical waves in turbulent superfluid helium*,
  Bollettino di Matematica Pura e Applicata **Vol. VII** 61–69 (2014), Aracne Ed.
- L. Saluto and M. S. Mongiovì, *Inhomogeneous vortex tangles in superfluid helium turbulence: flow in convergent channels*,
  submitted to CAIM, Special Session: Constitutive Equations for Heat Conduction in Nanosystems and Non-equilibrium Processes.

The results of this thesis have been presented at:

- First Joint International Meeting RSME-SCM-SEMA-SIMAI-UMI
  Special Session: Constitutive Equations for Heat Conduction in Nanosystems and Non-equilibrium Processes. Bilbao 30 June–4 July 2014.
- International Study Days on Non-conventional Thermodynamical Models of Complex Media. Messina 27–28 Ottobre 2014.

Appendix A

Bessel functions

A.1 Definitions

In mathematics, Bessel functions are special functions, which are solutions of a particular type of linear differential equations of the second order, known as *Bessel equation*. The expressions, identities and properties of the Bessel functions reported in this appendix can be found more in details in (Abramowitz and Stegun, 1972) and (Bowman, 1958).

The ordinary Bessel equation has the form

$$x^2 \frac{d^2y}{dx^2} + x\frac{dy}{dx} + (x^2 - n^2)y = 0, \tag{A.1}$$

or equivalently, dividing by x^2,

$$\frac{d^2y}{dx^2} + \frac{1}{x}\frac{dy}{dx} + \left(1 - \frac{n^2}{x^2}\right) y = 0. \tag{A.2}$$

In these equations n indicates the order of the solution, because of the Bessel differential equation is second-order, so there must be two classes of solution, usually called the *Bessel function of the first kind* $J_n(x)$ and *Bessel function of the second kind* $Y_n(x)$ (a Bessel function of third kind, more commonly called a Hankel function, is a special combination of the first and second kinds). Bessel equation has a regular singularity at 0 and an irregular singularity at ∞. Several related functions are also defined by slightly modifying the defining equations.

Another type of Bessel differential equation is the *modified Bessel equation*, i.e.

$$x^2 \frac{d^2y}{dx^2} + x\frac{dy}{dx} - (x^2 + n^2)y = 0, \tag{A.3}$$

or equivalently, dividing by x^2,

$$\frac{d^2y}{dx^2} + \frac{1}{x}\frac{dy}{dx} - \left(1 + \frac{n^2}{x^2}\right) y = 0. \tag{A.4}$$

Also in this case n indicates the order of the solution and we have two class of solution, usually called the *modified Bessel function of the first kind* $I_n(x)$ and *modified Bessel function of the second kind* $K_n(x)$.

The argument of these functions can be real or complex.

If $n = 0$, the modified Bessel differential equation (A.3) becomes

$$x^2 \frac{d^2y}{dx^2} + x\frac{dy}{dx} - x^2 y = 0, \tag{A.5}$$

which can also be written as

$$\frac{d}{dx}\left(x\frac{dy}{dx}\right) = xy. \tag{A.6}$$

A.2 The Bessel function of first kind $J_n(x)$

Any Bessel function can be defined in different ways, in terms of the generating function, or by the contour integral, or still in terms of a confluent hypergeometric function of the first kind, or by its Taylor series expansion.

Let's define now the Bessel function of the first kind $J_n(x)$ by its Taylor series expansion around $x = 0$ and then we express the other functions in terms of $J_n(x)$. Then:

$$J_n(x) = \sum_{m=0}^{\infty} \frac{(-1)^m}{m!\Gamma(n+m+1)} \left(\frac{x}{2}\right)^{2m+n}, \tag{A.7}$$

where Γ is the *Gamma function*, a shifted generalization of the factorial function to non-integer values, i.e. $\Gamma(n) = (n-1)!$ for any n non-integer.

- Asymptotic forms for the Bessel functions are:

$$J_m(x) \approx \frac{1}{\Gamma(m+1)} \left(\frac{x}{2}\right)^m \tag{A.8}$$

  for $x \ll 1$ or

$$J_m(x) \approx \sqrt{\frac{2}{\pi X}} \cos(x - \frac{m\pi}{2} - \frac{\pi}{4}) \tag{A.9}$$

  for $x \gg |m^2 - \frac{1}{4}|$.

- A derivative identity is:

$$\frac{d}{dx}(x^m J_m(x)) = x^m J_{m-1}(x). \tag{A.10}$$

- An integral identity is:

$$\int_0^u u' J_0(u')du' = uJ_1(u). \tag{A.11}$$

- Some sum identities are:

$$\begin{aligned} &\Sigma_{k=-\infty}^{\infty} J_k(x) = 1 \\ &(J_0(x))^2 + 2\Sigma_{k=1}^{\infty}(J_k(x))^2 = 1 \end{aligned} \tag{A.12}$$

For particular values of n the function $J_n(x)$ becomes a trigonometric function. For instance, the Bessel functions of order $\pm 1/2$ defined as:

$$J_{1/2}(x) = \sqrt{\tfrac{2}{\pi x}}\sin x,$$
$$J_{-1/2}(x) = \sqrt{\tfrac{2}{\pi x}}\cos x,$$

so that the general solution for $n = \pm 1/2$ is:

$$y = a_0 J_{-\frac{1}{2}}(x) + a_1 J_{\frac{1}{2}}(x). \tag{A.13}$$

Indeed, the function $J_n(x)$ has some particular properties as the trigonometric function, for any value of n, one has:

$$\begin{aligned} &J_{-n}(x) = (-1)^n J_n(x) \\ &J_0'(x) = -J_1(x) \\ &J_n'(x) = \tfrac{J_{n-1}-J_{n+1}}{2} \qquad \text{for} \quad x \neq 0 \end{aligned} \tag{A.14}$$

A.2.1 The other Bessel functions in terms of $J_n(x)$

The other Bessel functions in terms of J_n are expressed as:

$$Y_n(x) = \frac{J_n(x)\cos n\pi - J_{-n}(x)}{\sin n\pi} \tag{A.15}$$
$$I_n(x) = \mathrm{i}^{-n} J_n(\mathrm{i}x) \tag{A.16}$$
$$K_n(x) = \frac{\pi}{2}\frac{I_{-n}(x) - I_n(x)}{\sin n\pi} = \frac{\pi \mathrm{i}^n}{2}\frac{J_n(\mathrm{i}x) - (-1)^n J_{-n}(\mathrm{i}x)}{\sin n\pi} \tag{A.17}$$

A.3 Some properties and identities for the modified Bessel functions of first kind

Here some of the properties and identities used in Chapter 3 and 4 for the modified Bessel function of first kind $I_n(x)$ are recalled. The first one is:

$$\frac{d}{dx}I_n(x) = I_{n-1}(x) - \frac{n}{x}I_n(x) = \frac{n}{x}I_n(x) + I_{n+1}(x). \tag{A.18}$$

In particular, for $n = 0$ and $n = 1$, one has:

$$\begin{aligned} \frac{d}{dx}I_0(x) &= I_1(x), \\ \frac{d}{dx}I_1(x) &= I_0(x) - \frac{1}{x}I_1(x) = \frac{1}{x}I_1(x) + I_2(x). \end{aligned}$$

Another identity is:

$$I_n(x) = \frac{2(n+1)}{x} I_{n+1}(x) + I_{n+2}(x) = I_{n-2}(x) - \frac{2(n-1)}{x} I_{n-1}(x). \tag{A.19}$$

In particular, we have used the following:

$$xI_0(x) = 2I_1(x) + xI_2(x),$$

$$xI_2(x) = xI_0(x) - 2I_1(x).$$

A.4 Plots of the different kinds of Bessel functions

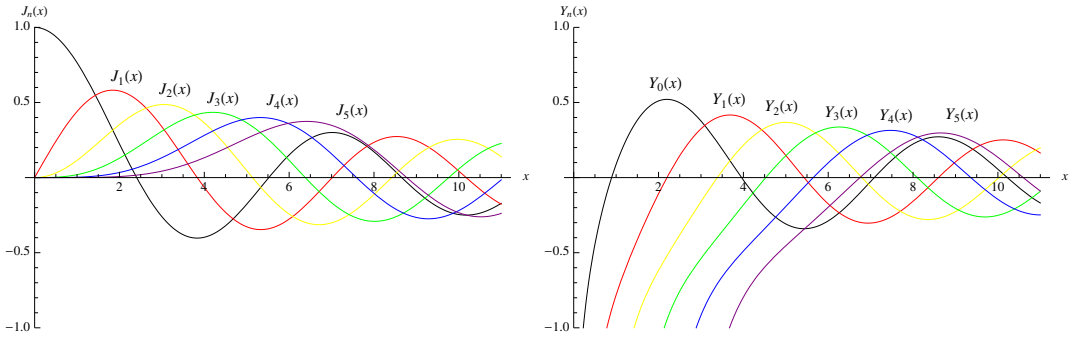

Figure A.1: Bessel functions of first -$J_n(x)$- and second kind -$Y_n(x)$- for $n = 0, 1, 2, 3, 4$ and 5.

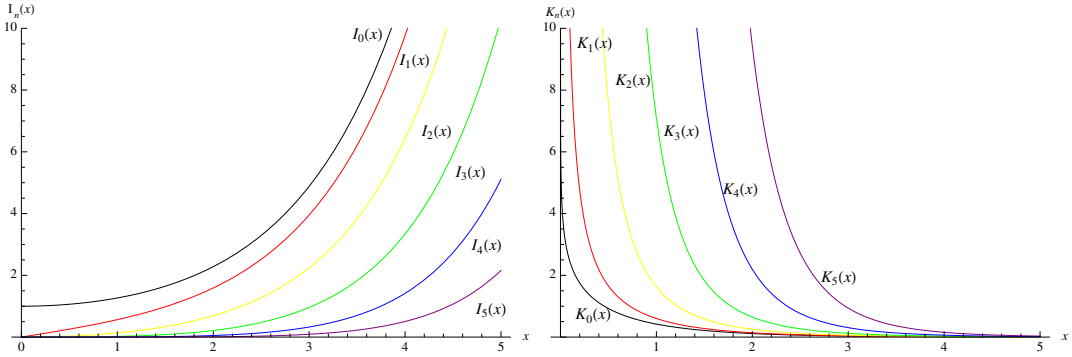

Figure A.2: Modified Bessel functions of first -$I_n(x)$- and second kind -$K_n(x)$- for $n = 0$, 1, 2, 3, 4 and 5.

Bibliography

Abramowitz, M. and Stegun, I. A. (1972). *Handbook of Mathematical Functions*. Dover, New York.

Abrikosov, A. A. (1957). The magnetic properties of superconducting alloys. *J. Phys. Chem. Solids*, 2(3):199–208. DOI:10.1016/0022-3697(57)90083-5.

Alvarez, F. X., Jou, D., and Sellitto, A. (2010). Pore-size dependence of the thermal conductivity of porous silicon: a phonon hydrodynamic approach. *Appl. Phys. Lett.*, 97:33103 (3 pages). DOI:10.1063/1.3462936.

Ardizzone, L., Gaeta, G., and Mongiovì, M. S. (2009). A Continuum Theory of Superfluid Turbulence based on Extended Thermodynamics. *J. Non-Equilib. Thermodyn.*, 34:277–297. DOI:10.1515/JNETDY.2009.015.

Ardizzone, L., Gaeta, G., and Mongiovì, M. S. (2011). Propagation of Fourth Sound in Turbulent Superfluids via Extended Thermodynamics. *J. Non-Equilib. Thermodyn.*, 36:179–201. DOI:10.1515/JNETDY.2011.012.

Ardizzone, L., Gaeta, G., and Mongiovì, M. S. (2013). Wave propagation in anisotropic turbulent superfuids. *Z. Angew. Math. Phys.*, 64:1571–1586. DOI:10.1007/s00033-013-0308-2.

Barenghi, C. F. (2010). Laminar, turbulent, or doubly turbulent? *Physics*, 3. DOI:10.1103/Physics.3.6.

Barenghi, C. F., Donnelly, R. J., and Vinen, W. F. (2001). *Quantized Vortex Dynamics and Superfluid Turbulence*. Springer, Berlin.

Berti, A. and Berti, V. (2013). A thermodynamically consistent Ginzburg-Landau model for superfluid transition in liquid helium. *Z. Angew. Math. Phys.*, 64:1387–1397. DOI:10.1007/s00033-012-0280-2.

Berti, A., Berti, V., and Grandi, D. (2013). A thermodynamic approach to isotropic-nematic phase transitions in liquid crystals. *Meccanica*, 48:983–991. DOI:10.1007/s11012-012-9647-x.

Berti, V. and Fabrizio, M. (2007a). A non-isothermal Ginzburg-Landau model in superconductivity: Existence, uniqueness and asymptotic behaviour. *Nonlinear Anal.*, 66:2565–2578. DOI:10.1016/j.na.2006.03.039.

Berti, V. and Fabrizio, M. (2007b). Existence and uniqueness for a non-isothermal dynamical Ginzburg-Landau model of superconductivity. *Math. Comp. Modelling*, 45:1081–1095. DOI:10.1016/j.mcm.2006.09.010.

Bowman, F. (1958). *Introduction to Bessel functions*. Dover Publications Inc., New York.

Campbell, L. J. (1987). Driven, dissipative superfluids: Radial counterflow of rotating ^{4}He. *Phys. Rev. B*, 36:6773–6781. DOI:10.1103/PhysRevB.36.6773.

Castiglione, J., Murphy, P. J., Tough, J. T., Mayot, F., and Pomeau, Y. (1995). Propagating and stationary superfluid turbulent fronts. *Phys. B*, 100:575–595. DOI:10.1007/BF00751526.

Childers, R. K. and Tough, J. T. (1976). Helium II thermal counterflow: temperature and pressure-difference data and analysis in terms of the Vinen theory. *Phys. Rev. B*, 13-3:1040–1055. DOI:10.1103/PhysRevB.13.1040.

Cimmelli, V. A. (2009). Different thermodynamic theories and different heat conduction laws. *J. Non-Equilib. Thermodyn.*, 34:299–333. DOI:10.1515/JNETDY.2009.016.

Cimmelli, V. A. and Frischmuth, K. (2007). Gradient generalization to the extended thermodynamic approach and diffusive hyperbolic heat conduction. *Physica B*, 400:257–265. DOI:10.1016/j.physb.2007.07.019.

de Groot, S. R. and Mazur, P. (1962). *Nonequilibrium thermodynamics*. North Holland, Amsterdam.

Domínguez-Cascante, R. and Jou, D. (1998). Entropy flux and Lagrange multipliers: Information theory and thermodynamics. *Open Sys. & Information Dyn.*, 5:319–331. DOI:10.1023/A:1009639816325.

Dong, Y., Cao, B.-Y., and Guo, Z.-Y. (2014). Size dependent thermal conductivity of Si nanosystems based on phonon gas dynamics. *Physica E*, 56:256–262. DOI:10.1016/j.physe.2013.10.006.

Donnelly, R. J. (1991). *Quantized vortices in helium II*. Cambridge University Press, Cambridge.

Donnelly, R. J. and Barenghi, C. F. (1998). The Observed Properties of Liquid Helium at the Saturated Vapor Pressure. *J. Phys. Chem.*, 27:1217–1274.

Dreyer, W. (1987). Maximisation of the entropy in non-equilibrium. *J. Phys. A*, 20:6505–6517. DOI:10.1088/0305-4470/20/18/047.

Fabrizio, M. (2010). A Ginzburg-Landau model for the phase transition in Helium II. *Z. Angew. Math. Phys.*, 61:329–340. DOI:10.1007/s00033-009-0011-5.

Fabrizio, M. and Mongiovì, M. S. (2013a). Phase transition and λ line in liquid helium. *J. Non-Equil. Thermodyn.*, 38(2):185–200. DOI:10.1515/jnetdy-2013-004.

Fabrizio, M. and Mongiovì, M. S. (2013b). Phase transition in liquid ^{4}He by a mean field model. *J. Thermal Stresses*, 36:135–151. DOI:10.1080/01495739.2012.720477.

Fliessbach, T. (1991). A model for the λ-transition of helium. *Nuovo Cimento*, D 13:211–231. DOI:10.1007/BF02463998.

Galantucci, L., Barenghi, C. F., Sciacca, M., Quadrio, M., and Luchini, P. (2011). Turbulent Superfluid Profiles in a Counterflow Channel. *J. Low Temp. Phys.*, 162:354–360. DOI:10.1007/s10909-010-0266-4.

Galantucci, L. and Sciacca, M. (2012). Turbulent Superfluid Profiles in a Counterflow Channel. *Acta Appl. Math.*, 122:407–418. DOI:10.1007/s10440-012-9752-9.

Galantucci, L. and Sciacca, M. (2014). Non-classical velocity statistics in counterflow quantum turbulence. *Acta Appl. Math.*, 132:273–281. DOI:10.1007/s10440-014-9902-3.

Geurst, J. A. (1989). Hydrodynamics of quantum turbulence in He II: Vinen's equation derived from energy and impulse of vortex tangle. *Physica B*, 154:327–343. DOI:10.1016/0921-4526(89)90167-1.

Geurst, J. A. (1992). Hydrodynamic theory of superfluid turbulence in He II and Schwarz's vortex modelling. *Physica A*, 183:279–303. http://EconPapers.repec.org/RePEc:eee:phsmap:v:183:y:1992:i:3:p:279-303.

Geurst, J. A. and van Beelen, H. (1994). Hydrodynamics of superfluid turbulence in He II: three-dimensional theory. *Physica A*, 206:58–92. http://EconPapers.repec.org/RePEc:eee:phsmap:v:206:y:1994:i:1:p:58-92.

Ginzburg, V. L. and Landau, L. D. (1950). On the theory of superconductivity. *Zh. Eksp. Teor. Fiz.*, 20:1064–1082. English translation in: L. D. Landau, Collected papers (Oxford: Pergamon Press, 1965) p. 546.

Ginzburg, V. L. and Pitaevskii, L. P. (1958). On the theory of superfluidity. *Zh. Eksp. Teor. Fiz.*, 34:1240–1247. Sov. Phys. JETP 7:858–861.

Greywall, D. S. (1981). Thermal-conductivity measurement in liquid ^4He below 0.7 K. *Phys. Rev. B*, 23(5):2152–2168. DOI:10.1103/PhysRevB.23.2152.

Guo, W., Cahn, S. B., Nikkel, J. A., Vinen, W. F., and McKinsey, D. N. (2010). Visualization study of counterflow in superfluid Helium-4 using metastable helium molecules. *Phys. Rev. Lett.*, 105:45301 (5 pages). DOI:10.1103/PhysRevLett.105.045301.

Hall, H. E. and Vinen, W. F. (1956). The rotation of liquid helium II. the theory of mutual friction in uniformly rotating helium II. *Proc. Roy. Soc.*, A238:215–234. DOI:10.1098/rspa.1956.0215.

Jou, D., Casas-Vàzquez, J., and Criado-Sancho, M. (2011a). *Thermodynamics of fluids under flow.* Springer, Berlin.

Jou, D., Casas-Vàzquez, J., and Lebon, G. (2010). *Extended Irreversible Thermodynamics.* Springer-Verlag, Berlin, Heidelberg, fourth edition.

Jou, D., Lebon, G., and Mongiovì, M. S. (2002). Second sound, superfluid turbulence and intermittent effects in liquid helium II. *Phys. Rev. B*, 66:224509 (9 pages). DOI:10.1103/PhysRevB.66.224509.

Jou, D., Lebon, G., Mongiovì, M. S., and Peruzza, R. A. (2004). Entropy Flux in Non-Equilibrium Thermodynamics. *Physica A*, 338:445–457. DOI:10.1016/j.physa.2004.02.011.

Jou, D. and Mongiovì, M. S. (2004). Phenomenological description of counterflow superfluid turbulence in rotating containers. *Phys. Rev. B*, 69(9):94513 (7 pages). DOI:10.1103/PhysRevB.69.094513.

Jou, D. and Mongiovì, M. S. (2005). Non-Equilibrium Thermodynamics in Counterflow and Rotating Situations. *Phys. Rev. B*, 72:144517 (11 pages). DOI:10.1103/PhysRevB.72.144517.

Jou, D. and Mongiovì, M. S. (2006). Description and evolution of anisotropy in superfluid vortex tangles with counterflow and rotation. *Phys. Rev. B*, 74:54509 (11 pages). DOI:10.1103/PhysRevB.74.054509.

Jou, D., Mongiovì, M. S., and Sciacca, M. (2011b). Hydrodynamic equations of anisotropic, polarized and inhomogeneous superfluid vortex tangles. *Physica D*, 240:249–258. DOI:10.1016/j.physd.2010.09.001.

Jou, D. and Restuccia, L. (2013). Non-equilibrium temperatures in system with internal variables. *in Proceedings of the 12th Joint European Thermodynamics Conference , JETC 2013*, pages 43–48.

Jou, D., Sciacca, M., and Mongiovì, M. S. (2008). Vortex dynamics in rotating counterflow and plane couette and poiseuille turbulence in superfluid helium. *Phys. Rev. B*, 78:24524 (12 pages). DOI:10.1103/PhysRevB.78.024524.

Kafkalidis, J. F., Klinich III, G., and Tough, J. T. (1994a). Superfluid turbulence in a nonuniform rectangular channel. *Rep. Prog. Phys.*, 50:15909 (20 pages). DOI:10.1103/PhysRevB.50.15909.

Kafkalidis, J. F., Klinich III, G., and Tough, J. T. (1994b). The vortex line density in nonuniform superfluid turbulence. *Physica B*, 194–196:717–718. DOI:10.1016/0921-4526(94)90688-2.

Khalatnikov, I. M. (1989). *An Introduction to the Theory of Superfluidity*. Addison-Wesley, Redwood City, California.

Klinich III, G., Kafkalidis, J. F., and Tough, J. T. (1997). Superfluid Turbulence in Converging and Diverging Rectangular Channels. *J. Low Temp. Phys.*, 107:327–346. DOI:10.1007/BF02397461.

Kondaurova, L. and Nemirovskii, S. K. (2012). Numerical study of decay of vortex tangles in superfluid helium at zero temperature. *Phys. Rev. B*, 86:134506 (13 pages). DOI:10.1103/PhysRevB.86.134506.

Landau, L. D. (1941). Theory of the superfluidity of Helium II. *Phys. Rev.*, 60:356–358. DOI:10.1103/PhysRev.60.356.

Landau, L. D. and Lifshitz, E. M. (1987). *Fluid Mechanics*. Pergamon Press, Oxford.

Lautrup, B. (2011). *Physics of Continuous Matter, Second Edition: Exotic and Everyday Phenomena in the Macroscopic World*. CRC Press–Taylor & Francis Group, Boca Raton–Florida, second edition. http://www.lautrup.nbi.dk/continuousmatter2/index.html.

Lebon, G., Jou, D., and Casas-Vàzquez, J. (2008). *Understanding non-equilibrium thermodynamics*. Springer-Verlag, Berlin.

Lesniewski, T. K., Frederking, T. H. K., and Yuan, S. W. K. (1996). On He II inertia effects in short narrow ducts: entrance effects associated with boundary layer development. *Cryogenics*, 36(3):203–207. DOI:10.1016/0011-2275(96)81613-4.

Lipa, J. A., Nissen, J. A., Stricker, D. A., Swanson, D. R., and Chui, T. C. P. (2003). Specific Heat of Liquid Helium in Zero Gravity very near the Lambda Point. *Phys. Rev. B*, 68:174518 (25 pages). DOI:10.1103/PhysRevB.68.174518.

Liu, I. (1972). Method of Lagrange multipliers for exploitation of the entropy principle. *Arch. Rat. Mech. Anal.*, 46(2):131–148. DOI:10.1007/BF00250688.

London, F. (1954). *Superfluid Helium II*. Wiley, New York.

Luzzi, R., Vasconcellos, A. R., and Ramos, J. G. (2001). *Statistical Foundations of Irreversible Thermodynamics*. Teubner, Leipzig.

Luzzi, R., Vasconcellos, A. R., and Ramos, J. G. (2002). *Predictive Statistical Mechanics: A Non-equilibrium Ensemble Formalism*. Kluver, Drdrecht.

Martin, K. P. and Tough, J. T. (1983). Evolution of superfluid turbulence in thermal counterflow. *Phys. Rev. B*, 27(5):2788–2799. DOI:10.1103/PhysRevB.27.2788.

Maruszewski, B. T. (2007). On a nonclassical thermoviscomechanical stress in the vortex field in the type-II superconductor. *Phys. Stat. Solidi (b)*, 244(3):919–927. DOI:10.1002/pssb.200572711.

Maruszewski, B. T. (2008a). On nonlinear kinetic effects in the vortex array in superconductors. *J. Mech. Mater. Struct.*, 3(6):1105–1111. DOI:10.2140/jomms.2008.3.1105.

Maruszewski, B. T. (2008b). A stress field in the vortex lattice in the type ii superconductors. *Atti dellAccademia Peloritana dei Pericolanti, Classe di Scienze Fisiche, Matematiche e Naturali*, LXXXVI-C1S0801014:1–12. DOI:10.1478/C1S0801014.

Maruszewski, B. T., Drzewiecki, A., and Starosta, R. (2007). Anomalous features of the thermomagnetoelastic field in a vortex array in a superconductor. propagation of loves waves. *J. Thermal Stresses*, 30:1049–1065. DOI:10.1080/01495730701572630.

Maruszewski, B. T., Drzewiecki, A., and Starosta, R. (2012). Electromagnetic waves in a vortex layer of a superconductor. *J. Mech. Mater. Struct.*, 7:297–307.

Maruszewski, B. T. and Restuccia, L. (1999). Mechanics of a vortex lattice in superconductors: phenomenological approach. *Trends in continuum physics, Proc. Int. Symp. TRECOP'98*, pages 220–330.

Maynard, J. (1976). Determination of the thermodynamics of He II from sound-velocity data. *Phys. Rev. B*, 14(9):3869–3891. DOI:10.1103/PhysRevB.14.3868.

Mendelsohn, K. (1956). *Liquid Helium*, volume XV. Springer, Berlin.

Mongiovì, M. S. (1991). Superfluidity and entropy conservation in extended thermodynamics. *J. Non-Equilib. Thermodyn.*, 16:225–240. DOI:10.1515/jnet.1991.16.3.225.

Mongiovì, M. S. (1993). Extended irreversible thermodynamics of liquid Helium II. *Phys. Rev. B*, 48:6276–6283. DOI:10.1103/PhysRevB.48.6276.

Mongiovì, M. S. (1994). A Monofluid Flow Mathematical Model of liquid Helium II based on Extended Non-equilibrium Thermodynamics. *Meccanica*, 29:223–238. DOI:10.1007/BF01461437.

Mongiovì, M. S. (2000a). Nonlinear extended thermodynamics of a non-viscous fluid, in the presence of heat flux. *J. Non-Equil. Thermod.*, 25:31–47. DOI:10.1515/JNETDY.2000.003.

Mongiovì, M. S. (2000b). Proposed measurements of the small entropy carried by the superfluid component in liquid helium II. *Phys. Rev. B*, 63:12501 (4 pages). DOI:10.1103/PhysRevB.63.012501.

Mongiovì, M. S. (2001). Extended irreversible thermodynamics of liquid Helium II: Boundary condition and propagation of fourth sound. *Physica A*, 292:55–74. DOI:10.1016/S0378-4371(00)00537-9.

Mongiovì, M. S. and Jou, D. (2005a). Generalization of Vinen's equation including transition to superfluid turbulence. *J. Phys.*, 17:4423–4440. http://stacks.iop.org/0953-8984/17/i=28/a=003.

Mongiovì, M. S. and Jou, D. (2005b). Nonlocal effects in superfluid turbulence: Application to the low-density to high-density-state transition and to vortex decay. *Phys. Rev. B*, 71(9):94507 (7 pages). DOI:10.1103/PhysRevB.71.094507.

Mongiovì, M. S. and Jou, D. (2005c). Superfluid turbulence in rotating containers: Phenomenological description of the influence of the wall. *Phys. Rev. B*, 72(10):104515 (8 pages). DOI:10.1103/PhysRevB.72.104515.

Mongiovì, M. S. and Jou, D. (2007). Thermodynamical derivation of a hydrodynamical model of inhomogeneous superfluid turbulence. *Phys. Rev. B*, 75:24507 (14 pages). DOI:10.1103/PhysRevB.75.024507.

Mongiovì, M. S., Jou, D., and Sciacca, M. (2007). Energy and Temperature of Superfluid Turbulent Vortex Tangles. *Phys. Rev. B*, 75:214514 (10 pages). DOI:10.1103/PhysRevB.75.214514.

Mongiovì, M. S. and Saluto, L. (2014). A model of λ transition in liquid ^{4}He. *Meccanica*, 49:2125–2137. DOI:10.1007/s11012-014-9922-0.

Muller, I. and Ruggeri, T. (1993). *Extended Thermodynamics*. Springer-Verlag, New York.

Muller, I. and Ruggeri, T. (1998). *Rational Extended Thermodynamics*. Springer-Verlag, New York.

Murphy, J. P., Castiglione, J., and Tough, J. T. (1993). Superfluid turbulence in a nonuniform circular channel. *J. Low Temp. Phys.*, 92:307–334. DOI:10.1007/BF00682294.

Nemirovskii, S. K. (2010). Diffusion of inhomogeneous vortex tangle and decay of superfluid turbulence. *Phys. Rev. B*, 81:64512 (10 pages). DOI:10.1103/PhysRevB.81.064512.

Nemirovskii, S. K. (2011). Propagation of a Turbulent Fronts in Quantum Fluids. *J. Low Temp. Phys.*, 162:347–353. DOI:10.1007/s10909-010-0252-x.

Nemirovskii, S. K. (2013). Quantum turbulence: Theorethical and numerical problems. *Phys. Rep.*, 524:85–202. DOI:10.1016/j.physrep.2012.10.005.

Nemirovskii, S. K. and Fiszdon, W. (1995). Chaotic quantized vortices and hydrodynamic processes in superfluid helium. *Rev. Mod. Phys.*, 67:37–84. DOI:10.1103/RevModPhys.67.37.

Saluto, L., Jou, D., and Mongiovì, M. S. (2015). Contribution of the normal component to the thermal resistance of turbulent liquid helium. *Z. Angew. Math. Phys.* DOI:10.1007/s00033-015-0493-2.

Saluto, L., Mongiovì, M. S., and Jou, D. (2014). Longitudinal counterflow in turbulent liquid helium: velocity profile of the normal component. *Z. Angew. Math. Phys.*, 65:531–548. DOI:10.1007/s00033-013-0372-7.

Schäfer, R. and Fliessbach, T. (1994). The two-fluid model with superfluid entropy. *Nuovo Cimento*, D 16:373–394. DOI:10.1007/BF02451645.

Schwarz, K. W. (1985). Three-dimensional vortex dynamics in superfluid He 4: Line-line and line-boundary interactions. *Phys. Rev. B*, 31:5782–5804. DOI:10.1103/PhysRevB.31.5782.

Schwarz, K. W. (1988). Three-dimensional vortex dynamics in superfluid He 4: Homogeneous superfluid turbulence. *Phys. Rev. B*, 38:2398–2417. DOI:10.1103/PhysRevB.38.2398.

Sciacca, M. and Galantucci, L. (2015). aaa. *submitted to Communications in Applied and Industrial Mathematics (CAIM).*

Sciacca, M., Jou, D., and Mongiovì, M. S. (2014a). Effective thermal conductivity of helium II: from landau to GorterMellink regimes. *Z. Angew. Math. Phys.* DOI:10.1007/s00033-014-0479-5.

Sciacca, M., Mongiovì, M. S., and Jou, D. (2008a). Alternative Vinen equation and its extension to rotating counterflow superfluid turbulence. *Physica B*, 4038:2215–2224. DOI:10.1016/j.physb.2007.12.001.

Sciacca, M., Mongiovì, M. S., and Jou, D. (2008b). A mathematical model of counterflow superfluid turbulence describing heat waves and vortex-density waves. *Math. Comput. Modelling*, 48:206–221. DOI:10.1016/j.mcm.2007.09.007.

Sciacca, M., Sellitto, A., and Jou, D. (2014b). Transition to ballistic regime for heat transport in helium II. *Phys. Lett. A*, 378:2471–2477. DOI:10.1016/j.physleta.2014.06.041.

Sellitto, A., Alvarex, F. X., and Jou, D. (2010). Second law of thermodynamics and phonon-boundary conditions in nanowires. *J. Appl. Phys.*, 107:64302 (7 pages). DOI:10.1063/1.3309477.

Struchtrup, H. (2005). *Macroscopic transport equations for rarefied gas flows.* Springer, Berlin.

Tabeling, P. (2005). *Introduction to microfluidics.* Oxford University Press, Oxford.

Tilley, D. R. and Tilley, J. (1990). *Superfluidity and Superconductivity.* IOP Publishing Ltd., Bristol.

Tinkham, M. (1996). *Introduction to Superconductivity.* Oxford University Press, NewYork.

Tisza, L. (1938). Transport phenomena in He II. *Nature*, 141:913 (1 page). DOI:10.1038/141913a0.

Tough, J. T., Kafkalidis, J. F., Klinich, G., Murphy, P. J., and Castiglione, J. (1994). Stationary superfluid turbulent fronts. *Physica B: Condensed Matter*, 194–196:719–720. DOI:10.1016/0921-4526(94)90689-0.

Tsubota, M., Araki, T., and Vinen, W. F. (2003). Diffusion of an Inhomogeneous Vortex Tangle. *Physica B*, 224:329–330. DOI:10.1016/S0921-4526(02)01968-3.

Tsubota, M., Kobayashi, M., and Takeuchi, H. (2012). Quantum hydrodynamics. *Phys. Rep.*, 522:191–238. DOI:10.1016/j.physrep.2012.09.007.

Van, P. (2003). Weakly nonlocal irreversible thermodynamics. *Ann. Phys.*, 12(3):146–173. DOI:10.1002/andp.200310002.

van Beelen, H., van Joolingen, W., and Yamada, K. (1988). On a balance equation for superfluid vorticity in capillary flow of helium II. *Physica B*, 153:248–253. DOI:10.1016/0921-4526(88)90053-1.

van Sciver, S. (2012). *Helium cryogenics*. Springer, Berlin, second edition.

Vinen, W. F. (1957). Mutual friction in a heat current in liquid helium II - III. theory of the mutual friction. *Proc. Roy. Soc. London*, A240:493–515. DOI:10.1098/rspa.1957.0191.

Vinen, W. F. and Niemela, J. (2002). Quantum turbulence. *J. Low Temp. Phys.*, 128:167–231. DOI:10.1023/A:1019695418590.

Wang, R. T., Swanson, C. E., and Donnelly, R. J. (1987). Anisotropy and drift of a quantum vortex tangle. *Phys. Rev. B*, 36:5240–5244. DOI:10.1103/PhysRevB.36.5240.

Watson, G. N. (1922). *A treatise on the theory of Bessel functions*. Cambridge Univ. Press., Cambridge, second edition. reprinted 1996.

Weichman, P. B., Harter, A. W., and Goodstein, D. L. (2001). Criticality and superfluidity in liquid ^{4}He under nonequilibrium conditions. *Rev. Mod. Phys.*, 73:1–15. DOI:10.1103/RevModPhys.73.1.